Evolutionary Conservation of Endocrine-Mediated Development in the Direct-Developing Frog, Eleutherodactylus coqui

Evolutionary conservation of endocrine-mediated development in the direct-developing frog, *Eleutherodactylus coqui*

A dissertation presented

by

Mara Laslo

to

The Department of Organismic and Evolutionary Biology

in partial fulfillment of the requirements

for the degree of

Doctor of Philosophy

in the subject of

Biology

Harvard University

Cambridge, Massachusetts

July, 2019

Dissertation Advisor: James Hanken Mara Laslo

Evolutionary conservation of endocrine-mediated development in the direct-developing frog, *Eleutherodactylus coqui*

Abstract

Direct development, a life history mode wherein the free-living larval stage is bypassed, has independently evolved multiple times in amphibians. Direct-developing frogs, such as the Puerto Rican coquí (*Eleutherdactylus coqui*), hatch from terrestrial eggs as miniature adults. Although they lack both an aquatic tadpole and post-hatching metamorphosis, *E. coqui* undergoes morphological changes in the egg that mimic metamorphosis: adult features, such as limbs, form and grow while larval-specific features, such as gills and tail, resorb. In metamorphosing frogs, the timing of these changes is dependent on endocrine signaling. In particular, two hormones, thyroid hormone (TH) and corticosterone (CORT), have been shown to be important in regulating developmental timing in amphibians. In this dissertation, I investigate the degree of evolutionary conservation of TH and CORT signaling components in the direct-developing frog, *Eleutherdactylus coqui*.

In Chapter 1, I find that dynamics of whole body TH content and thyroid hormone receptor mRNAs throughout development are conserved relative to metamorphosing frogs. Additionally, I measured TH in unfertilized oocytes and early *E. coqui* embryos. Thyroid hormones detected prior to development of the embryonic thyroid gland are likely maternal in origin. Altogether, these data suggest that limb development and tail resorption are mediated by conserved components of the hypothalamus-pituitary-thyroid axis, and that maternal TH could facilitate limb development prior to embryonic thyroid gland formation. In Chapter 2, I find that whole body CORT content increases at hatching and that CORT and TH treatment induces changes in TH-response gene expression in the

tail. These data suggest that CORT and TH together promote rapid tail resorption after hatching through increased TH signaling. In Chapter 3, I use an RNA-seq approach to compare limb development modules and TH-signaling genes in the hind limb of *E. coqui* and the metamorphosing frog *Xenopus tropicalis*. One third of all orthologous genes and one third of TH-signaling genes have the same expression pattern throughout development in the hind limbs of both species. Altogether, these data suggest that several key features of hormonal control of tail resorption and limb development are evolutionarily conserved in the direct-developing frog *E. coqui*.

TABLE OF CONTENTS

ACKNOWLEDGEMENTS

This dissertation could not have been completed without the advice and technical and emotional support of so many people.

Thank you to the Department of Organismic and Evolutionary Biology for funding my graduate studies. Two other funding sources gave me the freedom to pursue scientific questions that were interesting to me: a Graduate Women in Science Fellowship and a Doctoral Dissertation Improvement Grant from NSF. A grant from the Harvard Graduate Student Council allowed me to travel to Lake Louise in Banff, Canada and to share my research. Finally, several Miyata and Goelet travel awards from the Museum of Comparative Zoology were essential to my dissertation. With the funding from these grants, I took four wonderful trips to Hawaii to collect *E. coqui* frogs.

I would also like to thank my committee. Jim, thank you for taking me on as a graduate student and encouraging me to sculpt my own project. I appreciated your calming presence and your expertise in navigating collaborations. Thank you also for your support of my teaching and the opportunity to update the herpetology labs. David, thank you for welcoming me as an honorary lab member and helping me remember that it is important to be a whole person. Cassandra, thank you for your detailed experimental advice, and for letting me join your lab community. Bob, thank you for committing so much time and energy to this project and to my graduate career. I have learned much from all of you about writing, experimental design, and different ways to be an academic scientist.

I was lucky to have many wonderful collaborators throughout my thesis. I would like to thank Bill Mautz and Stephanie Gayle for their help in Hawaii. Bill, thank you for introducing me to Stephanie, for being an expert frog catcher, for showing me around Hilo, and for inviting me to Easter dinner. Stephanie, thank you for all the fun times you helped me catch frogs! Thank you to

Didem Sarikaya, Jenni Austiff, and Sam Church for being excellent and fun field assistants and frog catchers.

I would also like to thank Gwenneg Kerdivel, Nicolas Buisine, Laurent Sachs, Dan Rokhsar, and Richard Harland for sharing unpublished RNA-seq and genome sequence data. These data made Chapters 1 and 3 possible. In particular, I would like to thank Austin Mudd for his generosity in sharing *E. coqui* genome data and helping me to understand bioinformatics! Austin, your enthusiasm made trouble-shooting fun. I need to thank Kumar Subramani for his expertise in processing samples and measuring CORT in *E. coqui* embryos. Thank you also to Adam Freedman for helping navigate the computing cluster.

I can't say how valuable the Hanken Lab community has been throughout my Ph.D. Zach Lewis, Liz Sefton, Jenni Austiff, Matt Gage, Caroline DeVane, Cory Hahn, Brent Hawkins (a.k.a. Brunt a.k.a. the Duke), and Sam Royle - thank you for the experimental advice, hype sessions, yelling at UPS for me, taking such good care of the frogs, and believing in me.

Thank you to the Bauer Core staff for endless hours of technical help: Claire Reardon, Charles Vidoudez, Sunia Trauger, Patrick Dennett, Nicole El-Ali, Christian Daly.

Teaching and outreach have made my graduate student life much richer and emotionally rewarding. Susan Johnson, Marty Samuels, Jennifer Peterson, Amy Gunzelmann, and Wendy Derjue-Holzer: thank you for supporting my teaching and outreach activities at the museum. Joseph Martinez and José Rosado, thank you for your teaching and herpetology expertise and for letting me borrow endless herp specimens.

Thank you to my cohort who made being a graduate student so much fun. Brianna McHorse, Kari Taylor-Burt, Shayla Salzman, Phil Grayson, Jake Cohen, Zach Morris- thank you for being my friends and sharing in the trials and tribulations of graduate school.

Thank you to the scientists that welcomed me as a peer and built me up as scientist. I have returned often to your words of encouragement at many points. Dave Angelini, Allison Shultz, Ambika Kamath, Claire Dufour, Sofia Prado-Irwin, Glenna Clifton, Jen Kotler, Masha Reider, and Dawn Truong. Caren Helbing and Emily Koide, thank you for enthusiastic collaboration and for showing me that my work had an interested audience!

The support of my friends and family throughout my Ph.D. was invaluable. Thank you to the friends outside of academia that have supported me: Abby Granger, Catie Collins, Shilpa Durbal, Alessandra Ferzoco, Julia Stevens, and James Heggie. Mike, thank you for your loving support and patience, for your experimental advice, and for being such a good bunny parent. Finally, thank you to my family, for supporting me my whole life. Tutu, Bubbe, and Dad, I have carried you with me on this journey and I wouldn't be here without your guidance and encouragement.

I dedicate this work to my family near and far: Mom, Dad, Joe and Greg.

INTRODUCTION

Amphibians are known for their incredible life history variation. Amphibian life history can include external or internal fertilization, oviparity or viviparity, and numerous types of parental care (Crump, 2009). This diversity in life history strategies extends to embryonic and postembryonic development as well (Elinson and del Pino, 2012). Developmental timing is a primary axis of diversity among amphibians, as the time to adult form varies markedly among and within species. For example, the Puerto Rican coquí frog takes 17–19 days to develop from oviposition to juvenile adult form, whereas American bullfrogs take at least one year and often longer (Townsend and Stewart, 1985). Phylogenetic analysis suggests that metamorphosis, a condensed period of postembryonic development, is a shared primitive characteristic of all living amphibians (Reiss 2006). Additionally, the existence of fossilized larvae suggest that the ancestral life history mode for Lissamphibia included a free-living larval stage (Schoch and Fröbisch, 2006; Schoch, 2009). However, a number of frog species have evolved direct development, a strategy that can be viewed as an extreme shift in developmental timing. Direct-developing frogs bypass the free-living tadpole stage, recapitulate a type of "metamorphosis" in the egg, and hatch as miniature terrestrial adults (Elinson, 2013). This life history mode has evolved multiple times independently (Feng *et al.*, 2017). A similar situation is present in echinoderms: direct development has evolved multiple times independently (Raff, 1987). Similarly to early studies in direct-developing amphibians, studies in echinoderms have described a similar loss of larval features and an acceleration of the development of adult features (Wray and Raff, 1991). Application of molecular biology techniques has advanced research in direct-developing echinoderms in the past decade; applying similar techniques to studies of direct-developing frogs can highlight commonalities in developmental mechanisms of direct development. Understanding the mechanistic basis of direct development is critical to understanding

the repeated evolution of this developmental strategy and, more broadly, the evolution of amphibian life history diversity.

Thyroid and glucocorticoid hormones mediate development across the animal kingdom

Two hormones are the primary regulators of development in amphibians: thyroid hormone (TH) and the glucocorticoid hormone corticosterone (CORT). However, the evolutionary origins of TH and glucocorticoid signaling pathways predate the origin of amphibians. Thyroid hormone and CORT bind to the thyroid hormone receptor (TR) and glucocorticoid receptor (GR), respectively. Both of these receptors are nuclear receptors (NRs). Because NRs are found in all major metazoan groups except sponges (Escriva *et al.*, 1997; Srivastava *et al.*, 2010), the first NR likely appeared between 800 and 1000 million years ago (Owen and Zelent, 2000). While plants also synthesize steroid hormones (the larger hormone class to which glucocorticoids belong) that affect development (López-Bucio *et al.*, 2006), these hormones influence transcription via membrane receptors or alternate mechanisms of protein-protein interactions (Lumba, Cutler and Mccourt, 2010; Vriet, Russinova and Reuzeau, 2013).

Thyroid hormone signaling appears to have an older evolutionary origin than glucocorticoid signaling. Thyroid hormone receptor orthologs are present in all major dueterostome and protostome groups except ecdysozoans (summarized in Holzer, Roux and Laudet, 2017). Although TRs have been lost in ecdysozoans (Bertrand *et al.*, 2004), NRs still mediate metamorphosis in this group (Henrich and Brown, 1995). Thyroid hormone and TH-like compounds influence development in many metazoan groups, including echinoderms (Heyland, Reitzel and Hodin, 2004; Heyland *et al.*, 2006; Johnson and Cartwright, 2019), cephalochordates (Paris *et al.*, 2010), and tunicates (Patricolo, Ortolani and Cascio, 1981; Patricolo, Cammarata and Agati, 2001). The influence of TH on metazoan development and the presence of TR orthologs across the animal

kingdom suggest an origin of TH signaling at the base of Metazoa. Molecular analysis of GR sequences suggests that glucocorticoid signaling has a more recent evolutionary origin (Bridgham, Carroll and Thornton, 2006). Differentiated tissue capable of producing corticosteroids is present in living cartilaginous and bony fishes, suggesting that the ancestor of these vertebrates could produce corticosteroids. Because hormonal control of development is so widespread throughout the animal kingdom, it comes as no surprise that TH and CORT have important roles in amphibian development.

Hormonal control of development in metamorphosing amphibians

The two endocrine axes that produce TH and CORT are primary mediators of amphibian developmental timing: the hypothalamus-pituitary-thyroid (HPT) and the hypothalamus-pituitary-interrenal (HPI) axes (Denver, 2013). These two axes are linked in tadpoles of metamorphosing species: Corticotropin-releasing hormone (CRH) released by the hypothalamus stimulates both thyrotropes and corticotropes in the anterior pituitary to produce thyroid-stimulating hormone (TSH) and adrenocorticotropic hormone (ACTH), respectively (Denver, 2009, 2013). Thyroid-stimulating hormone and ACTH stimulate the peripheral thyroid gland and interrenal glands to produce TH and corticosteroids (including CORT), respectively (Denver, 2013). Thyroid hormone and CORT circulate throughout the body and act on target tissues. Corticosterone is the primary corticosteroid produced in amphibians (Jaffe, 1981; Krain and Denver, 2004).

Within an individual, target tissues have diverse responses to TH, due in part to different temporal dynamics of deiodinase enzymes and thyroid hormone receptors (TRs, designated alpha and beta). Deiodinase enzymes metabolize TH (primarily thyroxine or T_4) into more active (triiodothyronine or T_3) or biologically inactive (rT_3, and T_2) iodothyronines. For example, the tadpole tail is protected from premature resorption by high levels of deiodinase type III (dio3)

enzyme, which metabolizes TH into inactive iodothyronines. At metamorphic climax, dio3 activity decreases and T_3 activates the tail resorption program (Nakajima, Fujimoto and Yaoita, 2012). In contrast, the deiodinase type II (dio2) converts T_4 into T_3. Early target tissues of TH, including the hind limbs, express constitutive high levels of *dio2* mRNA (Cai and Brown 2004). High *dio2* mRNA levels suggests that the hind limb grows and differentiates in response to low TH levels prior to metamorphic climax (Cai and Brown, 2004).

Thyroid hormone receptor expression also influences tissue sensitivity to T_3. Thyroid hormone receptors are nuclear receptors that, when bound to T_3, promote or repress transcription (Cheng, Leonard and Davis, 2010). In several amphibian species, T_3 and CORT administered together increase *thyroid hormone receptor beta* (*thrb*) and *dio2* mRNA levels but decrease *dio3*, thus increasing intracellular T_3 and sensitivity to T_3 (Galton, 1990; Darras *et al.*, 2002; Kühn *et al.*, 2005; Bonett, Hoopfer and Denver, 2010). Moreover, CORT and T_3 together can activate transcription of T_3-response genes in a synergistic manner to promote TH signaling (Bonett *et al.*, 2009; Kulkarni and Buchholz, 2012; Bagamasbad *et al.*, 2015).

Hormonal control of development in direct-developing frogs

While hormone-regulated development has been studied in detail in metamorphosing frogs, little is known about the HPI and HPT axes in direct-developing frogs. Among the multiple examples of direct development in frogs, the most extensively studied group is the genus *Eleutherodactylus* (family Eleutherodactylidae). These frogs are nested within the group Terrarana, a supergroup of ~800 direct-developing species endemic to Central and South America (Hedges 2008). Because of its ability to breed in captivity, the common Puerto Rican coquí, *Eleutherodactylus coqui*, was an early model for the study of direct development (Elinson, Pino and Townsend, 1990). During embryogenesis, direct-developing frogs, including *E. coqui*, undergo a number of

morphological changes similar to those that occur during metamorphosis. These morphological changes include development of adult features such as limbs and resorption of larval features such as the tail. However, a number of characters that typify larval amphibians, such as gills and larval-specific cranial cartilages (Hanken *et al.*, 1992; Kerney, Gross and Hanken, 2010) are very reduced or totally absent in some direct-developing species (Adamson *et al.*, 1960; Townsend and Stewart, 1985), while adult features such as cranial musculature appear initially in mid-metamorphic configuration (Hanken *et al.*, 1992).

Despite evolutionary conservation of many morphological changes, hormonal control of development may differ between direct-developing frogs and metamorphosing frogs. Corticotropin-releasing hormone regulates development of adult features in *E. coqui* (Kulkarni, Singamsetty and Buchholz, 2010), suggesting that CRH has a conserved role in controlling pituitary TSH in *E. coqui* relative to metamorphosing frogs. However, metamorphosis in indirect-developing species is entirely dependent on TH, while embryogenesis in *E. coqui* appears to be a mosaic of TH-dependent and independent processes.

Initial observations suggested development in direct-developing frogs was primarily TH-independent (Lynn, 1936). Later studies using a TH-synthesis inhibitor showed that endogenous T_3 is necessary for tail resorption and terminal stages of limb development (Lynn, 1948; Lynn and Peadon, 1955; Callery and Elinson, 2000), although treatment with exogenous T_3 does not accelerate limb development (Elinson, 1994). However, by the time thyroid follicles are visible in *E. coqui* (about two-thirds of the way through development; Jennings and Hanken, 1998), limb differentiation and digit formation have already occurred. This observation suggests that TH is not involved in early limb development. Thus, limb development in *E. coqui* comprises two periods: limb bud differentiation and paddle and digit morphogenesis, which precede formation of the thyroid gland and thus appear to be TH independent; and limb growth and elongation, which follow thyroid

gland formation and are TH dependent. However, the fact that thyroid follicles are not present in early embryonic stages does not necessarily mean these stages are TH-independent. It is possible that maternal TH deposited in the yolk may influence the early period of limb development. Additionally, thyroid hormone receptor mRNAs are present in mature unfertilized oocytes (Callery and Elinson, 2000), further suggesting that early *E. coqui* embryos could utilize maternally deposited TH.

In this dissertation, I investigated the evolutionary conservation of the HPT and HPI axes in the direct-developing frog, *Eleutherodactylus coqui*. In Chapter 1, I show that developmental profiles of TR and deiodinase mRNA levels in the limb and tail and whole-body TH content in *E. coqui* resemble those seen in metamorphosing frogs. Additionally, *E. coqui* limb tissue is capable of mounting a robust gene expression response to exogenous T_3 comparable to that observed in the metamorphosing frog *Xenopus tropicalis*. Moreover, I demonstrate that maternal iodothyronines are present in both unfertilized oocytes and early embryos of *E. coqui*. Altogether, these data suggest that limb development and tail resorption in *E. coqui* are mediated by the same components of the HPT axis as those deployed in metamorphosing frogs. Additionally, these data suggest that maternal TH may facilitate limb development prior to thyroid gland formation in *E. coqui*. In Chapter 2, I measured whole-body CORT content, which increased significantly at hatching in *E. coqui*. Treatment with exogenous CORT and T_3 together induced significant changes in mRNA levels of TH-response genes. These data suggest that increased CORT production promotes rapid tail resorption after hatching at least partly through increased TH signaling. In Chapter 3, I used an RNA-seq approach to compare gene expression patterns in the hind limbs of *E. coqui* and *X. tropicalis*, with a focus on TH-signaling genes. Of all orthologous genes identified in both species, one third of these genes are expressed in the same pattern in the hind limbs of both species. Of genes that are regulated by exogenous T_3 in metamorphosing species, one third of these genes share

expression patterns in the hind limbs of both species. Gene expression patterns are consistent with muscle differentiation and growth, and with the end of pattern specification processes in the developing hind limb of both *E. coqui* and *X. tropicalis*.

Altogether, these data suggest that several key components of hormonal control of tail resorption and limb development, including TR and deiodinase mRNA expression dynamics and whole body TH and CORT content, are evolutionarily conserved in the direct-developing frog *E. coqui* relative to metamorphosing frogs. Additionally, experiments with exogenous TH suggest that TRs in the *E. coqui* limb and tail regulate transcription of some of the same TH-response genes as in metamorphosing frog tissue. Although most orthologous genes do not display the same expression pattern in the developing hind limbs of *E. coqui* and *X. tropicalis*, data in this dissertation suggest that at least the core mechanism of transcriptional regulation is the same in *E. coqui* and metamorphosing frogs. Data presented here also suggest that endocrine control of development is highly modular. Developmental modularity facilitates evolution of diverse morphological forms (Carroll 2001) and could enable the repeated independent evolutions of direct development. Endocrine-mediated developmental modules may additionally facilitate shifts in developmental timing in amphibians. For example, a TH-controlled limb development module could be expressed at a different time during ontogeny due to evolutionary changes in timing of TH secretion or tissue sensitivity to TH.

REFERENCES

Adamson, L., Harrison, R. G. and Bayley, I. (1960) 'The development of the whistling frog *Eleutherodactylus martinicensis* of Barbados', *Proceedings of the Zoological Society of London*, 133(3), pp. 453–469.

Bagamasbad, P. D. *et al.* (2015) 'Deciphering the regulatory logic of an ancient, ultraconserved nuclear receptor enhancer module', *Molecular Endocrinology*, 29(6), pp. 856–872. doi: 10.1210/me.2014-1349.

Bertrand, S. *et al.* (2004) 'Evolutionary genomics of nuclear receptors: From twenty-five ancestral genes to derived endocrine systems', *Molecular Biology and Evolution*, 21(10), pp. 1923–1937. doi: 10.1093/molbev/msh200.

Bonett, R. M. *et al.* (2009) 'Stressor and glucocorticoid-dependent induction of the immediate early gene krüppel-like factor 9: implications for neural development and plasticity', *Endocrinology*, 150(4), pp. 1757–65. doi: 10.1210/en.2008-1441.

Bonett, R. M., Hoopfer, E. D. and Denver, R. J. (2010) 'Molecular mechanisms of corticosteroid synergy with thyroid hormone during tadpole metamorphosis', *General and Comparative Endocrinology*, 168(2), pp. 209–19. doi: 10.1016/j.ygcen.2010.03.014.

Bridgham, J. T., Carroll, S. M. and Thornton, J. W. (2006) 'Evolution of hormone-receptor complexity by molecular exploitation', *Science*, 312(5770), pp. 97–102.

Cai, L. and Brown, D. D. (2004) 'Expression of type II iodothyronine deiodinase marks the time that a tissue responds to thyroid hormone-induced metamorphosis in *Xenopus laevis*', *Developmental Biology*, 266(1), pp. 87–95. doi: 10.1016/j.ydbio.2003.10.005.

Callery, E. M. and Elinson, R. P. (2000) 'Thyroid hormone-dependent metamorphosis in a direct developing frog', *Proceedings of the National Academy of Sciences of the United States of America*, 97(6), pp. 2615–20. doi: 10.1073/pnas.050501097.

Cheng, S.-Y., Leonard, J. L. and Davis, P. J. (2010) 'Molecular aspects of thyroid hormone actions', *Endocrine reviews*, 31(2), pp. 139–70. doi: 10.1210/er.2009-0007.

Crump, M. L. (2009) 'Amphibian diversity and life history', in Dodd, C. K. (ed.) *Amphibian Ecology and Conservation: A Handbook of Techniques*. 1st edn. New York: Oxford Univsersity Press, pp. 3–20.

Darras, V. M. *et al.* (2002) 'Effects of dexamethasone treatment on iodothyronine deiodinase activities and on metamorphosis-related morphological changes in the axolotl (*Ambystoma mexicanum*)', *General and Comparative Endocrinology*, 127(2), pp. 157–164.

Denver, R. J. (2009) 'Stress hormones mediate environment-genotype interactions during amphibian development', *General and Comparative Endocrinology*, 164(1), pp. 20–31. doi: 10.1016/j.ygcen.2009.04.016.

Denver, R. J. (2013) 'Neuroendocrinology of amphibian metamorphosis', in Shi, Y. (ed.) *Current Topics in Developmental Biology*. 1st edn. Burlington: Elsevier Inc., pp. 195–227. doi: 10.1016/B978-0-12-385979-2.00007-1.

Elinson, R. P. (1994) 'Leg development in a frog without a tadpole (*Eleutherodactylus coqui*)', *The Journal of Experimental Zoology*, 270(2), pp. 202–10. doi: 10.1002/jez.1402700209.

Elinson, R. P. (2013) 'Metamorphosis in a frog that does not have a tadpole', in Shi, Y.-B. (ed.) *Current Topics in Developmental Biology*. 1st edn. Elsevier Inc., pp. 259–76. doi: 10.1016/B978-0-12-385979-2.00009-5.

Elinson, R. P. and del Pino, E. M. (2012) 'Developmental diversity of amphibians', *Wiley Interdisciplinary Reviews: Developmental Biology*, 1(3), pp. 345–369. doi: 10.1002/wdev.23.

Elinson, R., Pino, E. Del and Townsend, D. (1990) 'A practical guide to the developmental biology of terrestrial-breeding frogs', *The Biological Bulletin*, 179, pp. 163–177.

Escriva, H. *et al.* (1997) 'Ligand binding was acquired during evolution of nuclear receptors', *Proceedings of the National Academy of Sciences of the United States of America*, 94(13), pp. 6803–6808.

Feng, Y.-J. *et al.* (2017) 'Phylogenomics reveals rapid, simultaneous diversification of three major clades of Gondwanan frogs at the Cretaceous–Paleogene boundary', *Proceedings of the National Academy of Sciences of the United States of America*, 114(29), pp. E5864–E5870. doi: 10.1073/pnas.1704632114.

Galton, V. A. (1990) 'Mechanisms underlying the acceleration of thyroid hormone-induced tadpole metamorphosis by corticosterone', *Endocrinology*, 127(6), pp. 2997–3002.

Hanken, J. *et al.* (1992) 'Cranial ontogeny in the direct-developing frog, *Eleutherodactylus coqui* (Anura: Leptodactylidae), analyzed using whole-mount immunohistochemistry.', *Journal of Morphology*, 211(1), pp. 95–118. doi: 10.1002/jmor.1052110111.

Henrich, V. C. and Brown, N. E. (1995) 'Insect nuclear receptors: A developmental and comparative perspective', *Insect Biochemistry and Molecular Biology*, 25(8), pp. 881–897.

Heyland, A. *et al.* (2006) 'Thyroid hormone metabolism and peroxidase function in two non-chordate animals', *Journal of Experimental Biology*, 306(6), pp. 551–566. doi: 10.1002/jez.b.

Heyland, A., Reitzel, A. M. and Hodin, J. (2004) 'Thyroid hormones determine developmental mode in sand dollars (Echinodermata: Echinoidea)', *Evolution & Development*, 6, pp. 382–392. doi: 10.1111/j.1525-142X.2004.04047.x.

Holzer, G., Roux, N. and Laudet, V. (2017) 'Evolution of ligands, receptors and metabolizing enzymes of thyroid signaling', *Molecular and Cellular Endocrinology*., 459, pp. 5–13. doi: 10.1016/j.mce.2017.03.021.

Jaffe, R. C. (1981) 'Plasma concentration of corticosterone during *Rana catesbeiana* tadpole metamorphosis', *General and Comparative Endocrinology*, 44(3), pp. 314–318. doi: 10.1016/0016-6480(81)90007-1.

Jennings, D. H. and Hanken, J. (1998) 'Mechanistic basis of life history evolution in anuran amphibians: thyroid gland development in the direct-developing frog, *Eleutherodactylus coqui*', *General and Comparative Endocrinology*, 111(2), pp. 225–32. doi: 10.1006/gcen.1998.7111.

Johnson, L. G. and Cartwright, C. M. (2019) 'Thyroxine-accelerated larval development in the crown-of-thorns starfish, *Acanthaster planci*', *Biological Bulletin*, 190(3), pp. 299–301.

Kerney, R., Gross, J. B. and Hanken, J. (2010) 'Early cranial patterning in the direct-developing frog *Eleutherodactylus coqui* revealed through gene expression', *Evolution & Development*, 12(4), pp. 373–82. doi: 10.1111/j.1525-142X.2010.00424.x.

Krain, L. P. and Denver, R. J. (2004) 'Developmental expression and hormonal regulation of glucocorticoid and thyroid hormone receptors during metamorphosis in *Xenopus laevis*', *The Journal of Endocrinology*, 181(1), pp. 91–104.

Kühn, E. R. *et al.* (2005) 'Corticotropin-releasing hormone-mediated metamorphosis in the neotenic axolotl *Ambystoma mexicanum*: Synergistic involvement of thyroxine and corticoids on brain type II deiodinase', *General and Comparative Endocrinology*, 143, pp. 75–81. doi: 10.1016/j.ygcen.2005.02.022.

Kulkarni, S. S. and Buchholz, D. R. (2012) 'Beyond synergy: Corticosterone and thyroid hormone have numerous interaction effects on gene regulation in *Xenopus tropicalis* tadpoles', *Endocrinology*, 153(11), pp. 5309–5324. doi: 10.1210/en.2012-1432.

Kulkarni, S. S., Singamsetty, S. and Buchholz, D. R. (2010) 'Corticotropin-releasing factor regulates the development in the direct developing frog, *Eleutherodactylus coqui*', *General and Comparative Endocrinology*, 169(3), pp. 225–30. doi: 10.1016/j.ygcen.2010.09.009.

López-Bucio, J. *et al.* (2006) 'Novel signals for plant development', *Current Opinion in Plant Biology*, 9(5), pp. 523–529. doi: 10.1016/j.pbi.2006.07.002.

Lumba, S., Cutler, S. and Mccourt, P. (2010) 'Plant nuclear hormone receptors: A role for small molecules in protein-protein interactions', *Annual Review of Cell and Developmental Biology*, 26, pp. 445–469. doi: 10.1146/annurev-cellbio-100109-103956.

Lynn, W. G. (1936) 'A study of the thyroid in embryos of *Eleutherodactylus nubicola*', *The Anatomical Record*, 64, pp. 525–535, 2 plates.

Lynn, W. G. (1948) 'The effects of thiourea and phenylthiourea upon the development of *Eleutherodactylus ricordii*', *Biological Bulletin*, 94(1), pp. 1–15.

Lynn, W. G. and Peadon, A. M. (1955) 'The role of the thyroid gland in direct development in the Anuran, *Eleutherodactylus martinicensis*', *Growth*, 19, pp. 263–286.

Nakajima, K., Fujimoto, K. and Yaoita, Y. (2012) 'Regulation of thyroid hormone sensitivity by differential expression of the thyroid hormone receptor during *Xenopus* metamorphosis', *Genes to Cells*, 17(8), pp. 645–659. doi: 10.1111/j.1365-2443.2012.01614.x.

Owen, G. I. and Zelent, A. (2000) 'Origins and evolutionary diversification of the nuclear receptor superfamily', *Cellular and Molecular Life Sciences*, 57, pp. 809–827.

Paris, M. *et al.* (2010) 'Active metabolism of thyroid hormone during metamorphosis of amphioxus', *Integrative and Comparative Biology*, 50(1), pp. 63–74. doi: 10.1093/icb/icq052.

Patricolo, E., Cammarata, M. and Agati, P. D. (2001) 'Presence of thyroid hormones in ascidian larvae and their involvement in metamorphosis', *Journal of Experimental Zoology*, 430(May), pp. 426–430.

Patricolo, E., Ortolani, G. and Cascio, A. (1981) 'The effect of L-thyroxine on the metamorphosis of *Ascidia malaca*', *Cell and Tissue Research*, 214, pp. 289–301.

Raff, R. A. (1987) 'Constraint, flexibility, and phylogenetic history in the evolution of direct devleopment in sea urchins', *Developmental Biology*, 119, pp. 6–19.

Reiss, J. O. (2006) 'The phylogeny of amphibian metamorphosis', *Zoology*, 105(2002), pp. 85–96.

Schoch, R. R. (2009) 'Evolution of life cycles in early amphibians', *Annual Review of Earth and Planetary Sciences*, 37(May), pp. 135–62. doi: 10.1146/annurev.earth.031208.100113.

Schoch, R. R. and Fröbisch, N. B. (2006) 'Metamorphosis and neoteny: Alternative pathways in an extinct amphibian clade', *Evolution*, 60(7), pp. 1467–1475.

Srivastava, M. *et al.* (2010) 'The *Amphimedon queenslandica* genome and the evolution of animal complexity', *Nature*, 466(7307), pp. 720–726. doi: 10.1038/nature09201.

Townsend, D. and Stewart, M. (1985) 'Direct development in *Eleutherodactylus coqui* (Anura: Leptodactylidae): a staging table', *Copeia*, 1985(2), pp. 423–436.

Vriet, C., Russinova, E. and Reuzeau, C. (2013) 'From squalene to brassinolide: The steroid metabolic and signaling pathways across the plant kingdom', *Molecular Plant*, 6(6), pp. 1738–1757. doi: 10.1093/mp/sst096.

Wray, G. A. and Raff, R. A. (1991) 'The evolution of developmental strategy in marine invertebrates', *Trends in Ecology and Evolution*, 6(2), pp. 45–50.

Chapter 1: Evolutionary Conservation of Thyroid Hormone Receptor and Deiodinase Expression Dynamics *in ovo* in a direct-developing frog, *Eleutherodactylus coqui*

Reprinted with permission from:

Laslo M., Denver R.J., Hanken J. (2019) 'Evolutionary Conservation of Thyroid Hormone Receptor and Deiodinase Expression Dynamics *in ovo* in a direct-developing frog, *Eleutherodactylus coqui*', *Frontiers in Endocrinology*, 10, pp. 1-14. doi:10.3389/fendo.2019.00307.

frontiers in Endocrinology

ORIGINAL RESEARCH
published: 24 May 2019
doi: 10.3389/fendo.2019.00307

Evolutionary Conservation of Thyroid Hormone Receptor and Deiodinase Expression Dynamics *in ovo* in a Direct-Developing Frog, *Eleutherodactylus coqui*

Mara Laslo[1]*, *Robert J. Denver*[2] *and James Hanken*[1]

[1] *Department of Organismic and Evolutionary Biology, and Museum of Comparative Zoology, Harvard University, Cambridge, MA, United States,* [2] *Departments of Molecular, Cellular and Developmental Biology, and Ecology and Evolutionary Biology, University of Michigan, Ann Arbor, MI, United States*

OPEN ACCESS

Edited by:
Marco António Campinho, Center of Marine Sciences (CCMAR), Portugal

Reviewed by:
Paula Duarte-Guterman, University of British Columbia, Canada
Salvatore Benvenga, University of Messina, Italy

***Correspondence:**
Mara Laslo
mlaslo@g.harvard.edu

Specialty section:
This article was submitted to Thyroid Endocrinology, a section of the journal Frontiers in Endocrinology

Received: *05 February 2019*
Accepted: *29 April 2019*
Published: *24 May 2019*

Citation:
Laslo M, Denver RJ and Hanken J (2019) Evolutionary Conservation of Thyroid Hormone Receptor and Deiodinase Expression Dynamics in ovo in a Direct-Developing Frog, Eleutherodactylus coqui. Front. Endocrinol. 10:307. doi: 10.3389/fendo.2019.00307

Direct development is a reproductive mode in amphibians that has evolved independently from the ancestral biphasic life history in at least a dozen anuran lineages. Most direct-developing frogs, including the Puerto Rican coquí, *Eleutherodactylus coqui*, lack a free-living aquatic larva and instead hatch from terrestrial eggs as miniature adults. Their embryonic development includes the transient formation of many larval-specific features and the formation of adult-specific features that typically form postembryonically—during metamorphosis—in indirect-developing frogs. We found that pre-hatching developmental patterns of thyroid hormone receptors alpha (*thra*) and beta (*thrb*) and deiodinases type II (*dio2*) and type III (*dio3*) mRNAs in *E. coqui* limb and tail are conserved relative to those seen during metamorphosis in indirect-developing frogs. Additionally, *thra, thrb,* and *dio2* mRNAs are expressed in the limb before formation of the embryonic thyroid gland. Liquid-chromatography mass-spectrometry revealed that maternally derived thyroid hormone is present throughout early embryogenesis, including stages of digit formation that occur prior to the increase in embryonically produced thyroid hormone. *Eleutherodactylus coqui* embryos take up much less 3,5,3′-triiodothyronine (T_3) from the environment compared with *X. tropicalis* tadpoles. However, *E. coqui* tissue explants mount robust and direct gene expression responses to exogenous T_3 similar to those seen in metamorphosing species. The presence of key components of the thyroid axis in the limb and the ability of limb tissue to respond to T_3 suggest that thyroid hormone-mediated limb development may begin prior to thyroid gland formation. Thyroid hormone-dependent limb development and tail resorption characteristic of metamorphosis in indirect-developing anurans are evolutionarily conserved, but they occur instead *in ovo* in *E. coqui*.

Keywords: embryo, direct development, thyroid hormone, amphibians, evolution, metamorphosis, maternal effects, life history

INTRODUCTION

Direct development, a distinctive life-history mode in amphibians and other animals, has evolved in anurans multiple times from the ancestral biphasic life history; it characterizes many hundreds of living species (1). Even though direct-developing frogs typically lack both a free-living aquatic larval stage and a discrete, post-hatching metamorphosis, many species display a cryptic metamorphosis before hatching: adult-specific features, such as limbs, form precociously in the egg, and numerous tadpole-specific features are present initially but then are lost [**Figure 1**; (2, 3)]. Because such changes in frogs with indirect development are mediated by thyroid hormone (TH), the primary regulator of metamorphosis (4), evolutionary change in thyroid axis function and timing may underlie the numerous heterochronies observed between direct-developing and indirect-developing species (5–9). Yet, there have been few attempts to precisely delineate the role of this or other pertinent physiological mechanisms.

Embryonic development of direct-developing frogs, as seen in the Puerto Rican coquí, *Eleutherodactylus coqui*, appears to comprise a mosaic of TH-independent and TH-dependent features. We use the term "embryonic" to describe all *in ovo* development in *E. coqui*, although this period encompasses both the initial formation of major organ systems as well as the patterning, morphogenesis and growth that follows. Many of the latter events correspond to metamorphic changes in biphasic anurans. It was once thought that embryonic development in direct-developing species was primarily TH-independent (5). However, subsequent studies with exogenous T_3 and with TH-synthesis inhibitors suggested at least a partial role for TH in terminal stages of limb development as well as tail resorption (6, 10). In *E. coqui*, for example, treatment with exogenous T_3 causes precocious tail resorption but has little to no effect on limb elongation (11). Similarly, treatment with methimazole, a TH-synthesis inhibitor, inhibits only tail resorption and late stages of limb elongation but does not affect early limb differentiation or digit formation (8). The apparent TH-independence of early stages of limb development is correlated with the fact that limb bud, paddle and digit formation occur prior to formation of the embryonic thyroid gland [**Figure 1**; (12, 13)]. Thus, limb development in *E. coqui* comprises two periods: limb bud differentiation and paddle and digit morphogenesis, which precede formation of the thyroid gland and may be TH independent; and limb growth and elongation, which follow thyroid gland formation and are TH dependent. Experiments with TH-synthesis inhibitors, however, can only address the role of TH in the second period. The presumed TH independence of the first period remains to be verified experimentally.

All organs in the body are exposed to roughly the same concentration of circulating TH, primarily in the form of thyroxine (T_4) and lower concentrations of 3,5,3′-triiodothyronine [T_3; (14, 15)]. Hereafter, we use the term TH to refer to both T_4 and T_3. However, tissue-specific differences in uptake, metabolism, and action provide for diverse effects of TH in different tissues. Thus, tissue-specific changes in TH metabolism and action likely contribute to the heterochrony of developmental events observed in direct-developing anurans relative to biphasic species. Alternatively, the principal locus of change in hormonal control may involve a shift in the source of THs and when they are present in the embryo. Maternally derived TH is present at early developmental stages of all vertebrates examined so far. In most vertebrates, maternal TH is in the yolk; in most mammals, maternal TH can pass from mother to fetus via the placenta or milk. Yet, the role of maternally derived TH in amphibian embryos is poorly understood (16–18). If maternally derived THs are present in early embryos of *E. coqui*, they could influence limb development prior to formation of the embryonic thyroid gland. Finally, three different deiodinase enzymes control cellular metabolism of T_4 in target tissues. In amphibians, two types of deiodinases play major roles during development. Deiodinase enzyme type II (Dio2) converts T_4 into T_3, which has at least 10 times greater affinity for TH receptors (TRs) than T_4. Deiodinase type III (dio3) converts T_4 to both T_2 and reverse triiodothyronine (rT_3), which are unable to bind TRs in most species. Thyroid hormones act by binding to two TR subtypes, designated alpha (α) and beta (β), to activate or repress transcription of TH target genes. Contrasting expression patterns of TRs and deiodinases may in part underlie the diverse, tissue-specific effects of TH in *Xenopus* species (19–26), and it is likely that changes in the temporal or spatial expression of deiodinases or TRs influence TH competence and action in target tissues in *E. coqui*.

Here we tested the hypothesis that developmental changes in TR and deiodinase mRNAs in developing *E. coqui* limb and tail, and in whole body TH content are conserved relative to those seen during metamorphosis in indirect-developing frogs. We also investigated whether *E. coqui* tissues are capable of responding directly to T_3 action by mounting gene regulation responses similar to those seen in metamorphosing species. Taken together, our data support the hypothesis that limb development and tail resorption in *E. coqui* (8, 12) are mediated by conserved components of TH signaling. Additionally, our results suggest that maternal TH could facilitate limb development prior to formation of the embryonic thyroid gland.

MATERIALS AND METHODS

Animal Care

Live adult *Eleutherodactylus coqui* were field-collected from introduced populations in Hilo, Hawaii, with the permission of the U.S. Fish and Wildlife Service (permits EX-14-06, EX-16-07, and EX-17-11). They were brought to Harvard University and maintained as a breeding colony in the Hanken laboratory (IACUC protocol #99-09-03); embryos were obtained following spontaneous matings. Following removal of the overlying chorion with watchmaker forceps in 2% cysteine (pH 8.5) in 10% Holtfreter solution, embryos were reared in 10% Holtfreter solution in Petri dishes at 22.5°C. Embryos were staged according to the normal table of Townsend & Stewart (TS; 1985), which defines 15 stages from fertilization (1) to hatching (15). Following internal fertilization, the adult female deposits embryos at TS stage 1.

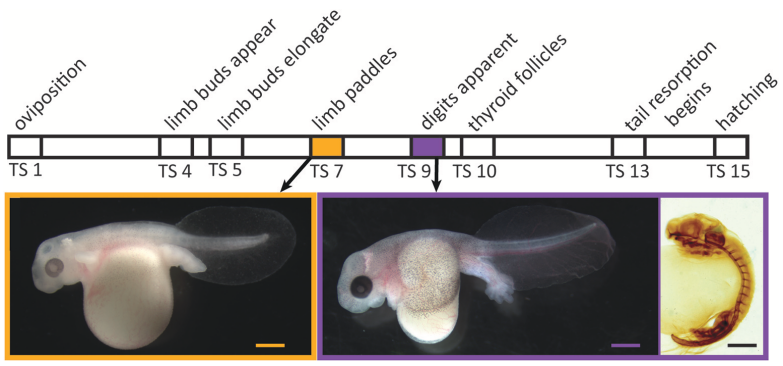

FIGURE 1 | Relative timing of several developmental events during embryogenesis in *Eleutherodactylus coqui*. Images depict live TS stage 7 **(Left)** and stage 9 **(Middle)** embryos removed from overlying egg membranes, and a TS stage 9 embryo **(Right)** stained for type II collagen, which reveals the cartilaginous skeleton and notochord. Scale bars, 1 mm.

Molecular Cloning and Sequence Validation

Partial cDNAs for *dio2*, *dio3*, *thra*, *thrb*, *ribosomal protein L8* (*rpL8*), *thyroid hormone induced bZip protein* (*thibz*), and *alpha-actinin 4* (*actn4*) (Genbank accession numbers MK784754, MK784753, MK784748, MK784749, MK784751, MK784750, MK784755) were isolated by PCR with exact primers (**Table 1**) using cDNA generated from RNA isolated from whole TS stage 13 embryos, and the resultant DNA fragments were subcloned into the pCR II plasmid. Exact primers for *dio2*, *dio3*, *thra*, *thrb*, *rpL8*, and *thibz* were designed from predicted full-length cDNA sequences provided by L. Sachs, N. Buisine, and G. Kerdivel (personal communication), while *actn4* primers were designed from genomic sequences provided by A. Mudd, R. Harland, and D. Roksahr (personal communication). We also subcloned a partial cDNA for *krüppel-like factor 9* (*klf9*) by degenerate PCR (oligonucleotide primers designed using CODEhop) using the same cDNA described above (Genbank accession number MK784752). The sequences of the subcloned partial cDNA fragments were confirmed by direct DNA sequencing and by comparing them against the full-length cDNAs provided by the investigators listed above.

Prior to the full-length predicted cDNA sequences becoming available, oligonucleotide primers for SYBR-based reverse transcriptase quantitative PCR (RTqPCR) were designed based on the available mRNA sequences on Genbank for *thra* and *thrb,* and the previously cloned *rpL8* [Genbank accession numbers AF201957.1 and AF201958.1; (8), **Table 1**]. For probe-based quantitative PCR (qPCR), primers and probes for *actn4* were designed from the partial cloned cDNA sequence while *dio2*, *dio3*, *thra*, *thrb*, *rpL8*, *thibz*, and *klf9* were designed based on the full-length sequences from other investigators listed above (Genbank accession numbers MK784763, MK784762, MK784757, MK784756, MK784760, MK784758, MK784759, MK784761).

Whole Body Extraction and Quantification of Iodothyronines Using LC-MS/MS

The iodothyronines T_3, rT_3, T_4, and T_2 were quantified from whole *E. coqui* embryos throughout development. Because embryos were not dissected from the yolk, all measurements include embryo and yolk TH content. Animals at different stages were anesthetized and snap frozen until extraction and LC-MS/MS analysis. Unfertilized oocytes were dissected from the ovaries of a newly sacrificed female and snap frozen. Between 15 and 20 embryos (∼ 600 mg) were pooled to make one biological replicate. Three or four biological replicates were used for each developmental stage. Tissues were extracted for thyroid hormone analysis as described by Denver (27, 28) with the following modifications: stable isotope-labeled T_3 and T_4 ($^{13}C_6$ T_3 and T_4, Sigma) were used as an internal standard to correct for differences in extraction efficiency, and solid phase extraction with a Supel-Select SCX cartridge (60 mg 3 mL, Sigma) was used to further purify the extracted tissue. After conditioning the cartridge with 3 mL methanol (HPLC Grade, Sigma) and equilibrating it with 5 mL of 2% formic acid in water (HPLC Grade, Sigma), the sample was loaded, rinsed first with 3 mL 2% formic acid in water and then with 3 mL methanol, and finally eluted with 2 mL of freshly prepared 5% ammonium hydroxide in methanol. It was then evaporated to dryness under nitrogen flow and resuspended in 100 µl of 0.1% formic acid in methanol. Samples were measured at the Harvard Small Molecule Mass Spectrometry facility by using gradient liquid-chromatography mass-spectrometry (LC-MS/MS). Ten microliters of samples were injected on a C18 column (Kinetex 2.6 µm, 100 Å pore size, 150 × 2.1 mm, Phenomenex) in an Agilent 1290 HPLC coupled with an Agilent 6460 Triple Quad Mass Spectrometer. See **Supplementary Information** for the LC and MS parameters (**Supplementary Tables 1, 2**). Calibration curves were made in 0.1% formic acid in methanol with pure standards and the same amount of internal standard as the samples. Quantification

TABLE 1 | Degenerate PCR, exact PCR, and qPCR primers and probes for *Eleutherodactylus coqui* and *Xenopus tropicalis*.

Gene	Type	Species		Sequence	Probe sequence	Amplicon size (bp)
thibz	qPCR	*E. coqui*	F	GAGGGTCAAACGCCAGTATT	TGAAGGGTGCTATAAAGTAGCTGAT	72
			R	GTCCGGGTCTGTGTAATGTC		
klf9	qPCR	*E. coqui*	F	CAAGTCCTCCCACCTCAAAG	CCCACTACAGAGTGCATACAGGTGA	65
			R	CATGTGCATGGAAATGGACG		
rpL8	qPCR	*E. coqui*	F	CTGGAGGTGGACGTATTGAC	ACCCATTCTGAAGGCAGGTCGT	68
			R	TCTTGGCCTTGTACTTGTGG		
dio2	qPCR	*E. coqui*	F	ACACAGTTACCTCAACAGGG	TGCAATCTGATCTCCCAGGAGCA	87
			R	AACAGTGTGGAACATGCAGA		
dio3	qPCR	*E. coqui*	F	GCAGCCCAGCAGTATTATCA	CGTGGAGGACATGCGTTTAACCC	95
			R	CACATGGGTGGTCTCGTTTA		
thra	qPCR	*E. coqui*	F	ACTACATCAACCACCGCAAA	CCCACTTCTGGCCTAAGCTCCT	81
			R	CAATCATGCGCAAGTCAGTC		
thrb	qPCR	*E. coqui*	F	GCAGCCCAGCAGTATTATCA	TCAAATGTTGTGCCTGCGGCT	95
			R	GTGATCACCATGGGAGATGG		
actn4	qPCR	*E. coqui*	F	AAGCCATCTCTGAAGTCCTC	AGTGCCAGCCTTCCTCAGGTG	80
			R	TTTCACGGCTTGGTGTAACT		
rpL8	qPCR	*E. coqui*	F	GACCAGAGTAAAGCTGCCTTCT	SYBR	95
			R	TTGTCAATACGTCCACCTCCAG		
thra	qPCR	*E. coqui*	F	CGACAAAATCACCCGAAATCAGT	SYBR	78
			R	GACAAGGTCCATTGCCATGC		
thrb	qPCR	*E. coqui*	F	CTTGCGCCTCTTTTCTCTGTTT	SYBR	76
			R	CAGATCTGGTTTTGGATGACAGC		
klf9	Degenerate	*E. coqui*	F	GGSTGTGGCAAAGTYTAYGGSAA		215
			R	TTGGTYAARTGRTCRCTCCTCAT		
rpL8	Exact	*E. coqui*	F	GACATTATCCATGATCCAGGCCG		616
			R	CAGTCTTTGTACCGCGCAGACG		
dio2	Exact	*E. coqui*	F	GAGTGTGGACCTGTTGATCACT		745
			R	TTTCTGTTCCATCCACTGTCGT		
dio3	Exact	*E. coqui*	F	TGCAAACTTCTCAAACAGGTGG		716
			R	TTCCTCAGTTCAGCGATCTTGT		
thra	Exact	*E. coqui*	F	AGAGCCAGATGAAAAGAGGTGG		801
			R	CTGTCAGGATCGTAACGCACA		
thrb	Exact	*E. coqui*	F	CTAGCAGCATGTCAGGGTACAT		779
			R	TACCACCCCTAGTCCTCCATTT		
actn4	Exact	*E. coqui*	F	GAAACAGCAGCGGAAGACTTTC		619
			R	CTTCTTATCAGGACGAGCGGTG		
thibz	Exact	*E. coqui*	F	CTCCATGATTCAACTCCACCCA		961
			R	CGTAGTGAGGGTGAGACAACAA		
thibz	qPCR	*X. tropicalis*	F	AAGAGACGCAAGAACAACGA	AGAAGCGCCGGGCGGGGGA	111
			R	GAGTCGGGCATTCTCTTCAA		
klf9	qPCR	*X. tropicalis*	F	AGTCTTCCCACCTTAAAGCC	ACGCCCTTTTCCGTGTACGTGGCCT	106
			R	GTCAACTCATCGGAACGAGA		
eef1a1	qPCR	*X. tropicalis*	F	CTTGACTGCATTTTGCCACC	AGCCTCTGCGTCTGCCTCTGCAGG	112
			R	GTCTCCACACGACCAACTG		
dio3	qPCR	*X. tropicalis*	F	CGGTGCCTACTTTGAGAGAC	TACCAGGGAGGGCGGGGGCC	94
			R	CCGAGATCTTGTAGCCTTCC		
thrb	qPCR	*X. tropicalis*	F	TTGATGATACCGAAGTCGCC	TCGCCCTGGCCTCACTAGTGTGGAGA	102
			R	AACCTTCCTGGCACTTTTCT		
actn1	qPCR	*X. tropicalis*	F	CAAAGTGCTGGCTGTCAATC	AGCTGGCCAGTGATCTGCTGGAGTGG	105
			R	TCTAACCAAGGGATTGTGCG		

results with a signal-to-noise (S/N) ratio >10 were used for the statistical analysis. Results with a ratio between 3 and 10 (purple type; **Supplementary Table 3**) were included in the graph (**Figure 2**) but not used in the statistical analysis; those with a ratio below 3 were not used (red type; **Supplementary Table 3**). We normalized iodothyronine content to the weight of the tissue extracted.

Quantitative PCR

Dechorionated embryos were anesthetized by immersion in 10% Holtfreter solution with drops of 2% neutral-buffered MS-222 added until the embryos no longer responded to toe pinches (between 30 and 60 s). Limbs and tails were dissected and homogenized in TriZol reagent (Invitrogen) and kept at −20°C until RNA isolation. Total RNA was isolated following the manufacturer's protocol within 3 weeks of homogenization. Because qPCR primers did not span exon-exon boundaries, genomic DNA was removed with an Ambion DNA-*free* kit (cat. #AM1906). Controls with no reverse-transcriptase verified that removal of genomic DNA was complete. Total RNA was quantified with a Qubit Fluorometer 3.0 and checked for purity on a Nanodrop spectrophotometer. For SYBR Green RTqPCR assays, 200 ng of total RNA was used for input for each reaction. For probe-based qPCR, 660 ng of total RNA for each sample was synthesized into cDNA with iScript Reverse Transcriptase Supermix for RT-qPCR (BioRad). Complementary DNA was kept at −20°C until the qPCR assay was performed. mRNA levels were analyzed with either Ssoadvanced Universal Probes Supermix (BioRad) or an iTaq Universal SYBR Green One-Step kit (BioRad) on a CFX384 machine. See **Supplementary Data** for qPCR cycling conditions. Optimal qPCR conditions were determined with temperature gradient and cDNA dilutions for dynamic range of input. Standard curves showed high efficiency of reaction (90–105%), and R^2 was equal to or >0.98 for all primer sets. No template controls showed no amplification. All oligonucleotides are listed in **Table 1**. All SYBR and probe-based qPCR experiments were done in simplex. The relative mRNA levels were determined as described by Schmittgen and Livak (29). For the developmental expression studies, target-gene expression was normalized to the reference gene *rpL8*, which did not show significant variation across development [*rpL8* mRNA values are given in **Supplementary Table 5**; see also (8)]. In the *in vivo* and the tissue explant T_3 response experiments, *E. coqui* target gene mRNA levels were normalized to the reference genes *rpL8* and *actn4*, which was unaffected by T_3 treatment. Small, statistically insignificant changes in reference gene mRNAs could have led to a small underestimation of the effect of T_3 in these experiments.

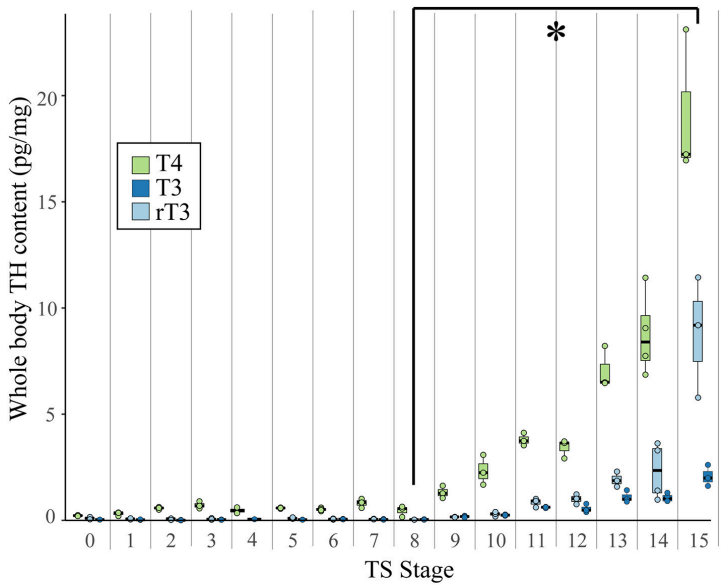

FIGURE 2 | Whole body content of T_4, T_3, and rT_3 in pooled *E. coqui* embryos at TS stages 1–15 and in unfertilized oocytes (TS 0) as quantified by LC-MS/MS. Whole body content of iodothyronines was normalized to sample weight; between 15 and 20 embryos were pooled to generate one biological replicate. Each value depicted in the graph is based on two-to-four replicates. Values based on fewer than three replicates are not included in the statistical analysis. All three iodothyronines increased significantly between TS stages 8 and 15 (*post-hoc* Dunn's test; $p < 0.05$), indicated by the asterisk (*). See **Supplementary Data** for a complete list of significant pairwise differences. Each boxplot represents median and range of the data.

For *Xenopus tropicalis*, qPCR primers and probes for *thrb*, *klf9*, *thibz*, *dio3*, *elongation factor 1 alpha* (*eef1a1*) and *alpha-actinin 1* (*actn1*) were designed from publicly available sequences (Genbank accession numbers XM_012964865.2, NM_001113674.1, XM_018092557.1, NM_001113667.2, NM_001016692.2, and NM_001079198.1). For tissue explant experiments, *X. tropicalis* target gene expression was normalized to *eef1a1* and *actn1*.

Treatment of *E. coqui in vivo*

Eleutherodactylus coqui embryos were dechorionated into 10% Holtfreter solution at least 24 h prior to immersion in T_3. One mM stock T_3 in DMSO or 0.01 N NaOH was diluted to make 50 nM T_3 in 10% Holtfreter solution. We chose 50 nM T_3 because it has been shown to induce tail resorption in *E. coqui* (8), and a 46-h timepoint to allow enough time for induction of T_3 response genes. We chose TS stage 9 embryos because the last third of limb development is TH-dependent (8), but TS stage 9 is still prior to thyroid gland activation. T_3 treatment solutions were refreshed every 8–12 h. After 46 h (n = 12–14 TS-9 embryos), dechorionated embryos were anesthetized as described above and limbs and tails were dissected, from which total RNA was extracted using TriZol reagent.

Measurement of Environmental T_3 Uptake in *X. tropicalis* and *E. coqui*

To determine if *E. coqui* embryos are capable of taking up TH from their surrounding environment, we immersed dechorionated TS stage 9 *E. coqui* embryos or NF 51–55 *X. tropicalis* tadpoles in 30 mL (*E. coqui*) or at least 500 mL (*X. tropicalis*) 10% Holtfreter solution with either 1 nM (n = 4–6 biological replicates/treatment) or 50 nM (n = 3–4 biological replicates/treatment) stable isotope-labeled T_3. We chose TS stage 9 *E. coqui* embryos to match the *in vivo* T_3 treatment experiments and selected *X. tropicalis* tadpoles with developing limbs with similar morphology to *E. coqui* TS stage 9. Approximately twenty *E. coqui* individuals (600 mg tissue) or two tadpoles were pooled were pooled to make one biological replicate. Tadpoles were either ordered from Xenopus1 (Ann Arbor, Michigan, U.S.A.) or derived from the Hanken lab colony. Stock 100 µg/mL stable isotope-labeled T_3 was diluted to either 1 or 50 nM T_3. After either 8 or 24 h in 1 nM labeled T_3 solution or 46 h in 50 nM T_3 solution, *X. tropicalis* tadpoles and *E. coqui* embryos (with yolk removed) were anesthetized with neutral-buffered 2% MS-222, rinsed three times in PBS and snap frozen until extraction. On average, *E. coqui* embryos were more densely packed in T_3 solution (5.9 mg tissue per mL media) than *X. tropicalis* tadpoles (2.0 mg tissue per mL media); however, *E. coqui* embryos are routinely cultured in these conditions with no ill effects. Tissue was extracted as described above. Because we measured whole body content of stable isotope-labeled T_3 as a proxy for T_3 uptake, we used 25 ng of stable isotope-labeled rT_3 as an internal standard to correct for extraction efficiency.

Tissue Explant Culture and T_3 Treatments

To further investigate if thyroid axis components in the *E. coqui* limb and tail are functional, we cultured *E. coqui* and *X. tropicalis* limb and tail explants (30, 31), treated them with T_3, and assayed gene expression. We treated NF stage 52–54 (32) *X. tropicalis* tadpoles and TS stage 9 *E. coqui* embryos with 50 U/mL of penicillin-streptomycin added to aquarium or Petri dish solution for 24 h prior to dissection. Tadpoles and embryos were terminally anesthetized and dipped into 70% ethanol to sterilize the epidermis before dissection. Four *X. tropicalis* and two *E. coqui* individuals were pooled to make a single biological replicate of each species. Tissues were dissected into ice-cold 1:1.5-diluted Leibowitz-15 media (Gibco) containing 50 U/mL penicillin-streptomycin, 50 mg/mL gentamicin and 10 mM HEPES. Prior to T_3 treatment tissues were cultured overnight in media supplemented with insulin (500 ug/mL) on a laboratory bench at room temperature (21°C) with gentle shaking (50 rpm). The next morning, stock T_3 was diluted in 0.01 N NaOH and added to the media to a final concentration of 50 nM. Media and T_3 were changed every 8–12 h. After treatment for 8 or 46 h, limb and tail explants were rinsed three times in phosphate-buffered saline (PBS) and homogenized in TriZol. RNA was isolated according to the manufacturer's protocol.

Statistical Analysis

Statistical analyses of qPCR data were done with RStudio version 1.0.136 and visualized with ggplot2 (https://ggplot2.tidyverse.org/). Developmental timeline qPCR and iodothyronine content data followed a non-normal distribution as determined by Q-Q plots and the Shapiro-Wilk test; Levene's test determined that TH content data additionally had unequal variance. Log_{10}-transformed data were not normally distributed. Therefore, a Kruskal-Wallis test was used to determine if there were significant differences among groups, and a *post-hoc* Dunn's test with the Benjamini and Hochberg (BH) correction was used to identify stages that differ from each other while adjusting for multiple comparisons. We performed a least squares regression on T_4, T_3, and rT_3 data sets to investigate possible differences in iodothyronines kinetics during development. For the developmental timeline qPCR data, statistical tests were performed on data pooled from two independent experiments (see **Supplementary Data** for data from each experiment). For *in vivo* and *in vitro* T_3 treatment experiments, Student's t-test was used to identify significant differences between T_3-treated groups and controls.

RESULTS

Predicted Proteins of Isolated *E. coqui* cDNAs Contain Conserved Domains

Most isolated cDNAs contained functional domains of orthologous proteins. The predicted *E. coqui* TRα and TRβ sequences cover amino acids 11–281 (65%), and amino acids 9–273 (69%) of the orthologous *X. tropicalis* proteins, respectively. Both predicted TR protein sequences contain the DNA-binding domain and most of the ligand-binding domain. Alignments show that the predicted protein sequence of the *E. coqui* TRα DNA-binding domain has 97% identity to the *X. tropicalis* DNA-binding domain, while the TRα ligand-binding domain shared between the predicted *E. coqui* and *X. tropicalis* sequences

are 98% identical. The DNA-binding domain of the predicted *E. coqui* TRβ sequence is 100% identical to the DNA-binding domain in *X. tropicalis* TRβ, and the ligand-binding domain is 95% identical. The predicted partial *E. coqui* Dio2 sequence covers amino acids 2–254 (98%) of *X. tropicalis* Dio2 and the partial *E. coqui* Dio3 sequence covers amino acids 7–252 (90%) of *X. tropicalis* Dio3. Additionally, the predicted protein sequence of both *dio2* and *dio3* isolated cDNAs contain the selenocysteine site and the thioredoxin domain. Both thioredoxin domains share 86% identity with the orthologous *X. tropicalis* thioredoxin domain. The partial predicted amino acid sequence of *E. coqui Klf9* covers amino acids 194–264 (25%) of *X. tropicalis Klf9* and contains the three characteristic zinc-finger domains (100% identity) in the C-terminus of *X. tropicalis Klf9*. The isolated *E. coqui thibz* sequence covers amino acids 159–335 (53%) of *X. tropicalis* NFIL3-like (synonym for *thbzip*) and lacks the highly conserved basic leucine zipper domain. Even without the highly conserved basic leucine zipper domain, the predicted *E. coqui* protein sequence still clusters with other orthologous NFIL3-like proteins, rather than with other proteins with the basic leucine zipper domain (NFIL3 and CREB1) in maximum likelihood trees of these three orthologous vertebrate proteins (data not shown). Similarly, the other partial predicted *E. coqui* sequences cluster with other orthologous genes rather than with other closely related proteins containing similar domains (data not shown). We confirmed all isolated *E. coqui* cDNAs against the full-length transcript provided by investigators listed in the methods. Finally, we also performed BLASTx and BLASTn searches with the isolated *E. coqui* cDNA sequences. All cloned sequences have high similarity to predicted orthologous genes in frog species and other vertebrates (**Supplementary Table 4**).

Changes in Whole Body Iodothyronine Content During Embryonic *E. coqui* Development

Using LC-MS/MS, we detected the iodothyronines T_4, T_3, and rT_3 in unfertilized oocytes and at every stage of development (**Figure 2**). Thyroxine content (pg/mg body weight) was highest, followed by rT_3 and then T_3. We detected T_2 only at TS stages 14 and 15, when hatching occurs, and at this point, T_2 content was less than all other iodothyronine content and ranged between 0.04 and 0.78 pg/mg body weight (**Supplementary Table 3**). The three quantifiable iodothyronines were low and relatively constant up to TS stage 8, after which stage they showed statistically significant increases [T_3: Kruskal-Wallis rank sum test, $X^2 = 43.2$ (df = 15), $p < 0.001$; T_4: Kruskal-Wallis rank sum test, $X^2 = 43.7$ (df = 15), $p < 0.001$; rT_3: Kruskal-Wallis rank sum test, $X^2 = 39.7$ (df = 14), $p < 0.001$]. Whole body content of all three iodothyronines showed statistically significant increases between stages 8 and 13 (*post-hoc* Dunn's test; $p = 0.048, 0.033, 0.035$ for T_3, T_4, and rT_3, respectively). The velocity of change was slower for rT_3 and T_3 compared with T_4. Stage was a significant predictor for all three iodothyronines [T_3: $F = 70.8$ (df = 45), $p < 0.001$; T_4: $F = 54.2$ (df = 46) $p < 0.001$; rT_3: $F = 23.7$ (df = 43), $p < 0.001$]. Although all iodothyronines are positively correlated with stage, the velocity of change was slower for rT_3 and T_3 (slope of least squares regression (LSR) line, b = 0.2964 and 0.1009, respectively) compared to T_4 (LSR, b = 0.7984). Tissue content of all three iodothyronines was highest at TS 15. Note also that oocytes and early embryos (TS 0–5) of *E. coqui* have large yolk deposits, which may increase the S/N ratio and cause an underestimation of iodothyronine content in the embryo and yolk at these stages.

Changes in Thyroid Hormone Receptor and Deiodinase mRNA Levels in the Embryonic Tail

Both *thra* and *thrb* mRNAs in the *E. coqui* tail showed statistically significant changes during development [**Figure 3A**; *thra*: Kruskal-Wallis rank sum test, $X^2 = 20.18$ (df = 4), $p < 0.001$; *thrb*: Kruskal-Wallis rank sum test, $X^2 = 26.78$ (df = 4), $p < 0.001$]. *Thyroid hormone receptor α* and *thrb* mRNA in the tail bud are approximately equal at TS stage 5 (**Figure 3A**). *Thyroid hormone receptor α* mRNA in the tail at hatching is between 2.1- and 4-fold higher than the early tail (TS stages 5 and 7, *post-hoc* Dunn's test, $p = 0.002$ and 0.03, respectively). *Thyroid hormone receptor β* mRNA follows a similar pattern—it increased 4-fold between the onset of tail resorption (TS 13) and hatching (TS 15)—although *thra* increased only 1.8-fold over the same interval (**Figure 3A**). *Thyroid hormone receptor β* mRNA at hatching (TS 15) is between 18- and 47-fold higher than in the early tail (TS stage 5 and TS stage 7, *post-hoc* Dunn's test, $p < 0.001$ and $p = 0.002$, respectively).

Deiodinase type II and *dio3* mRNAs significantly changed during tail development (**Figure 3B**; *dio2*: Kruskal-Wallis rank sum test, $X^2 = 17.37$ (df = 4), $p = 0.002$; *dio3*: Kruskal-Wallis rank sum test, $X^2 = 26.11$ (df = 4), $p < 0.001$). Patterns of deiodinase mRNA in the developing tail were essentially the opposite of those seen in the limb. *Deiodinase type II* mRNA was low throughout tail development and resorption but rose almost 10-fold as hatching neared (TS 15; **Figure 3B**). At hatching (TS 15), *dio2* mRNA was higher than at TS 5, 7 and 13 (*post-hoc* Dunn's test, $p = 0.001$, 0.029, and 0.031, respectively). *Deiodinase type III* mRNA increased 27-fold between TS 5 and 13 (*post-hoc* Dunn's test, $p < 0.001$) and then decreased steeply (11-fold) between the onset of tail resorption and hatching (*post-hoc* Dunn's test, $p = 0.007$). Repeated experiments demonstrate the similar patterns of *thra*, *thrb*, *dio2*, and *dio3* expression (**Supplementary Figure 1**).

Changes in Thyroid Hormone Receptor and Deiodinase mRNA Levels in the Embryonic Hind Limb

Both *thra* and *thrb* mRNAs in the *E. coqui* hind limb showed statistically significant changes during development (**Figure 4A**; *thra*: Kruskal-Wallis rank sum test, $X^2 = 20.66$ (df = 4), $p < 0.001$; *thrb*: Kruskal-Wallis rank sum test, $X^2 = 25.36$ (df = 4), $p < 0.001$). The level of *thra* mRNA was greater than *thrb* mRNA in the limb bud until TS 10, when the *thra* mRNA level began to decrease and continued to decline through hatching (**Figure 4A**). The peak *thra* mRNA level at TS 10 coincides with the appearance of thyroid follicles (13); *thra* mRNA in the hind

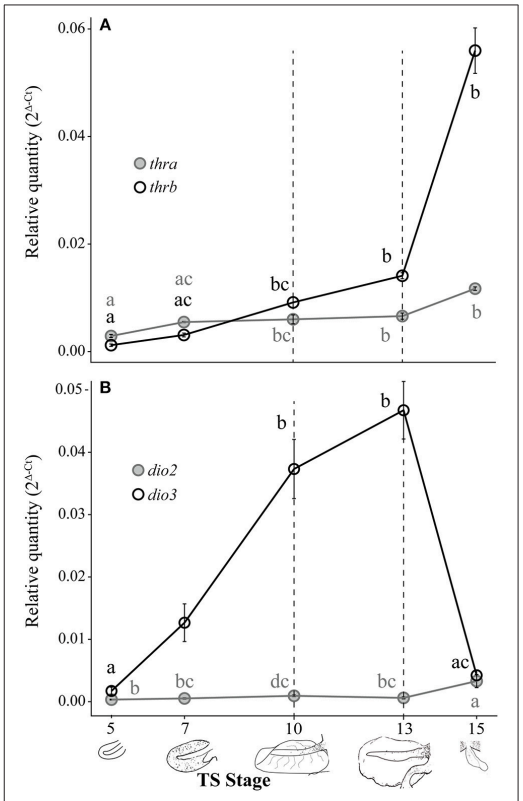

FIGURE 3 | Relative *thra* and *thrb* mRNA levels **(A)** and *dio2* and *dio3* mRNA levels **(B)** in the pre-hatching tail of *E. coqui*. Dashed vertical line at TS stage 10 marks when thyroid follicles are first visible in histological sections; the line at TS 13 indicates the onset of tail resorption. Drawings on the x-axis depict tail growth and resorption before hatching. Each expression value is represented as a circle centered on the mean of 3–7 individuals ± SE. Lower-case letters in gray (*thra* and *dio2*) and black (*thrb* and *dio3*) indicate significant pairwise differences between groups (*post-hoc* Dunn's test, $p < 0.05$). See **Supplementary Data** for a complete list of pairwise comparisons.

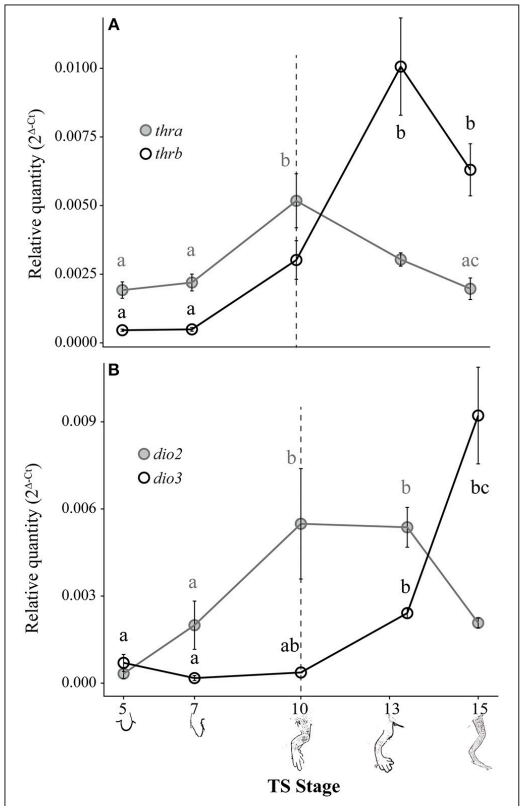

FIGURE 4 | Relative *thra* and *thrb* mRNA levels **(A)** and *dio2* and *dio3* mRNA levels **(B)** in the pre-hatching hind limb of *E. coqui*. Dashed vertical line at TS stage 10 marks when thyroid follicles are first visible in histological sections. Drawings on the x-axis depict sequential formation of the limb. Each expression value is represented as a circle centered on the mean of 5–7 hind limb pairs ± SE. Lower-case letters in gray (*thra* and *dio2*) and black (*thrb* and *dio3*) indicate significant pairwise differences between groups (*post-hoc* Dunn's test, $p < 0.05$). See **Supplementary Data** for a complete list of pairwise comparisons.

limb at this stage was significantly higher than in the limb bud at TS 5 (*post-hoc* Dunn's test, $p = 0.001$), in the limb paddle at TS stage 7 ($p = 0.009$) and in the fully formed froglet limb at TS 15 (*post-hoc* Dunn's test, $p = 0.002$). At hatching, *thra* mRNA level was lower than *thrb* mRNA levels. Between paddle (TS 7) and toepad formation (TS 13), *thrb* mRNA rose ∼21-fold to a peak at TS 13. At TS 13, *thrb* expression was significantly higher than in the limb bud and paddle (**Figure 4A**; TS 5 and 7; *post-hoc* Dunn's test, $p < 0.001$ and p = 0.001, respectively). *Thyroid hormone receptor β* mRNA drops almost 1.5-fold between TS 13 and hatching.

Deiodinase type II and *dio3* mRNAs both showed statistically significant but contrasting patterns throughout limb development [**Figure 4B**; *dio2*: Kruskal-Wallis rank sum test, $X^2 = 18.65$ (df = 4), $p < 0.001$; *dio3*: Kruskal-Wallis rank sum test, $X^2 = 25.76$ (df = 4), $p < 0.001$]. *Deiodinase type II* mRNA increased 16-fold between limb bud (TS 5) and digit formation (TS 10) and remained at this level through subsequent limb growth (TS 13; *post-hoc* Dunn's test, $p = 0.007$ and $p < 0.001$, respectively). *Deiodinase type II* mRNA decreased 2.6-fold between TS 13 and hatching to the level originally present in the newly formed limb bud (e.g., TS 5). *Deiodinase type III* mRNA remained low throughout most of limb development, but it increased 25-fold between the initial formation of thyroid follicles (TS 10) and hatching (TS 15; *post-hoc* Dunn's test, $p = 0.001$). Repeated experiments show the same general

contrasting mRNA expression patterns for *dio2*, *dio3*, *thra*, and *thrb* (**Supplementary Figure 2**).

Exogenous T_3 Induced Gene Expression Responses in the TS 9 *E. coqui* Tail, but Not the Limb

To determine if *E. coqui* tissues are capable of mounting a gene regulation response to exogenous T_3, we performed *in vivo* T_3 treatments (**Figure 5A**). Immersion of TS 9 *E. coqui* embryos in 50 nM T_3 for 8 h caused a significant induction of *klf9* (Student's *t*-test, $t = 5.61$ (df = 21.74), $p < 0.001$) and *thibz* (Student's *t*-test, $t = 6.20$ (df = 12.42), $p < 0.001$) in the tail. Immersion in 50 nM T_3 for 46 h additionally significantly induced *thrb* mRNA (**Supplementary Figure 4**). In contrast, the identical treatment significantly increased only *thibz* expression (**Figure 5B**; Student's *t*-test, $t = 3.11$ (df = 18.92), $p = 0.006$) in the limb.

E. coqui Embryos Took up Significantly Less T_3 From the Environment Than Did *X. tropicalis* Tadpoles

Because previous studies suggested that *E. coqui* limbs are insensitive to TH, and because we observed a weak TH response in our *in vivo* experiments, we wanted to confirm that immersion in T_3 increased tissue content of T_3. We quantified stable isotope-labeled T_3 tissue content after immersing *X. tropicalis* tadpoles or *E. coqui* embryos in stable isotope-labeled T_3 solution under three conditions. We chose 50 nM T_3 and 46 h treatment to match the *E. coqui in vivo* T_3 response experiments. We also chose two conditions that represent relevant time points from previous studies of larval *Xenopus* species: (1) treatment with 1 nM T_3 for 8 h is sufficient for *X. tropicalis*' whole body T_3 content to surpass the T_3 concentration in the surrounding media (33), and (2) treatment with 1 nM T_3 for 24 h is sufficient to induce gene expression responses in *X. tropicalis* (31, 34). After immersing *E. coqui* in 1 nM labeled T_3 for 8 and 24 h, we detected endogenous T_3 but not labeled T_3. However, we detected labeled T_3 in *X. tropicalis* tissue at both 8 and 24 h (**Table 2**). We detected stable isotope-labeled T_3 in both *E. coqui* and *X. tropicalis* tissue following 46-h treatment with 50 nM T_3. Total content of labeled T_3 in *X. tropicalis* tissue was ∼63 times that found in *E. coqui* tissues [**Table 2**, Student's *t*-test, $t = -3.20$ (df = 2.00), $p = 0.085$]. Additionally, *X. tropicalis* has ∼ 875 times more stable isotope-labeled T_3 than endogenous T_3 content. In contrast, stable isotope-labeled T_3 in *E. coqui* is approximately equal to endogenous T_3 content.

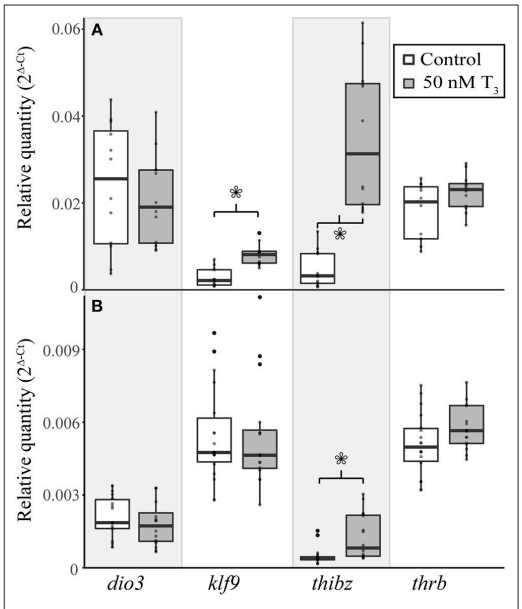

FIGURE 5 | Exogenous treatment with 50 nM T_3 for 8 h induces gene expression in the tail of *E. coqui* embryos at TS stage 9 **(A)**, but not in limbs at the same stage **(B)**. Boxes and whiskers depict the median and range of 12–16 individuals from two independent experiments. Asterisks indicate a significant change in expression (Student's *t*-test, $p < 0.05$).

Exogenous T_3 Strongly Induced T_3 Response Genes in TS Stage 9 *E. coqui* Limb Explants

Treatment with 50 nM T_3 for 8 h significantly increased *dio3* [Student's *t*-test, $t = 8.40$ (df = 4.00), $p = 0.001$), *klf9* (Student's *t*-test, $t = 14.41$ (df = 4.18), $p < 0.001$], *thibz* [Student's *t*-test, $t = 9.64$ (df = 4.01), $p < 0.001$], and *thrb* [Student's *t*-test, $t = 8.26$ (df = 4.39), $p < 0.001$] mRNAs in explants of *X. tropicalis* tail (**Figure 6A**). The same treatment caused a significant increase in *dio3* [Student's *t*-test, $t = 3.49$ (df = 3.00), $p = 0.040$], *klf9* [Student's *t*-test, $t = 13.66$ (df = 3.08), $p < 0.001$], and *thibz* [Student's *t*-test, $t = 21.50$ (df = 2.07), $p = 0.002$] mRNAs in *X. tropicalis* limb explants (**Figure 6B**). Similarly, exogenous T_3 increased *dio3* [Student's *t*-test, $t = 2.56$

TABLE 2 | Nieuwkoop and Faber stage 51–55 *Xenopus tropicalis* tadpoles have more labeled T_3 tissue content than do TS stage 9 *E. coqui* embryos after immersion in labeled T_3 for 8, 24, or 46 h.

Species	Labeled T_3 concentration (nM)	Timepoint (h)	Labeled T_3 pg/mg	T_3 pg/mg
X. tropicalis	1	8	1.079 ± 0.19	0.095 ± 0.02
E. coqui	1	8	0.000 ± 0.00	0.236 ± 0.01
X. tropicalis	1	24	1.371 ± 0.08	0.018 ± 0.01
E. coqui	1	24	0.000 ± 0.00	0.245 ± 0.04
X. tropicalis	50	46	30.436 ± 9.37	0.035 ± 0.01
E. coqui	50	46	0.483 ± 0.27	0.447 ± 0.20

Each value represents the mean of 3–6 individuals ± standard error.

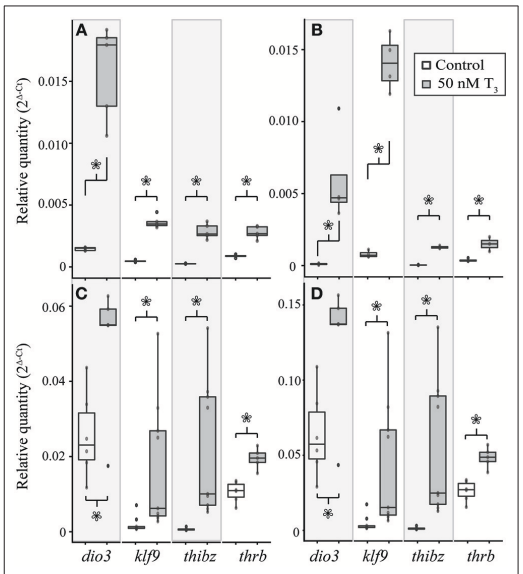

FIGURE 6 | Treatment with 50 nM exogenous T_3 for 8 h induces *deiodinase type III* (*dio3*), *krüppel-like factor 9* (*klf9*), *thyroid hormone induced bZip protein* (*thibz*), and *thrb* expression in NF stage 52–54 *X. tropicalis* tail **(A)** and limb **(B)** explants and in TS stage 9 *E. coqui* tail **(C)** and limb explants **(D)**. Asterisks indicate a significant increase in mRNA levels (Student's *t*-test, $p < 0.05$).

(df = 6.47), $p = 0.040$], *klf9* [Student's *t*-test, $t = 2.67$ (df = 8.22), $p = 0.028$], *thibz* [Student's *t*-test, $t = 3.54$ (df = 8.00), $p = 0.008$], and *thrb* [Student's *t*-test, $t = 5.38$ (df = 8.62), $p < 0.001$] mRNAs in explants of *E. coqui* tail (**Figure 6C**). *Deiodinase type III* [Student's *t*-test, $t = 2.61$ (df = 9.80), $p = 0.027$], *klf9* [Student's *t*-test, $t = 6.11$ (df = 8.05), $p < 0.001$], *thibz* [Student's *t*-test, $t = 6.49$ (df = 8.00), $p < 0.001$], and *thrb* [Student's *t*-test, $t = 7.70$ (df = 8.80), $p < 0.001$] increased after the same treatment in *E. coqui* limb explants (**Figure 6D**).

In both species, the magnitude of increase for all genes was greater in the limb than in the tail (**Table 3**). The same trends were observed after treating tissue explants with 50 nM T_3 for 46 h (**Supplementary Figure 5**). In tail explants, T_3 induced fold changes of a similar order of magnitude for *thibz* (between 42- and 44-fold) and *thrb* (between 1.8- and 3.8-fold), but not for *dio3* and *klf9*; in *E. coqui*, *dio3*, and *klf9* mRNAs increased 2- and 9.9-fold, respectively, while *dio3* and *klf9* mRNAs increased 11.9- and 12.5-fold in *X. tropicalis*. In limb explants, *dio3* and *thibz* mRNA differed by an order of magnitude between species. *Deiodinase type III* mRNA increased 58.8-fold in *X. tropicalis* limb explants, while *dio3* mRNA increased 3.7-fold in *E. coqui* limb tissue. *Thyroid hormone induced bZip protein* mRNA increased only 37-fold in *X. tropicalis* limb explants, while *dio3* mRNA increased 180-fold in *E. coqui* limb explants.

TABLE 3 | Induction of *deiodinase type III* (*dio3*), *krüppel-like factor 9* (*klf9*), *thyroid hormone induced bZip protein* (*thibz*), and *thyroid hormone receptor β* (*thrb*) in tail and limb explants of NF stages 52–54 *Xenopus tropicalis* and TS stage 9 *Eleutherodactylus coqui* after treatment with 50 nM T_3 for 8 h.

		Average fold increase	
Species	**Gene**	**Tail**	**Limb**
X. tropicalis	*dio3*	11.9	58.8
	klf9	12.5	17.8
	thibz	43.8	37.1
	thrb	3.8	4.0
E. coqui	*dio3*	2.0	3.7
	klf9	9.9	21.3
	thibz	42.0	180.0
	thrb	1.8	3.0

Values represent the average fold increase above control (vehicle-treated) levels.

DISCUSSION

In this study we show that the core TH signaling components are evolutionarily conserved in *Eleutherodactylus coqui* limb and tail tissue. We also show that developmental patterns of *thra*, *thrb*, *dio2,* and *dio3* mRNAs, and whole-body TH content in *E. coqui* closely match those reported during metamorphosis of *Xenopus* species. We also find maternal T_4, T_3, and rT_3 in unfertilized eggs and early embryos of *E. coqui*, which may mediate TR signaling prior to embryonic thyroid gland formation. This is the first published report of TH metabolites and maternally derived TH in a direct-developing frog. Additionally, we demonstrate that *E. coqui* tissues show robust gene expression responses to exogenous T_3 similar to those seen in metamorphosing species. *Eleutherodactylus coqui* embryos take up much less T_3 from the environment compared with *X. tropicalis*. This difference likely explains the relatively weak and variable gene expression responses seen *in vivo* in *E. coqui*, and was likely a significant confounding factor for previously published results.

Developmental Profiles of Whole Body Iodothyronine Content

Temporal dynamics of whole-body iodothyronine content in direct-developing *E. coqui* mirror those described for indirect-developing frogs, which retain the ancestral biphasic life history: *Scaphiopus hammondii* (28), *Rana catesbeiana* (35), *Bufo marinus* (36), *Bufo japonicus* (37), and *Xenopus laevis* (33). Anuran metamorphosis comprises three successive stages: premetamorphosis, when little to no TH is present; prometamorphosis, when TH concentrations slowly rise; and a rapid metamorphic climax characterized by a peak in TH concentrations. The temporal profile of TH content in embryonic *E. coqui* similarly defines three successive periods: (1) Low TH content characterizes the first half of development, prior to thyroid follicle formation (TS 1–8). (2) After thyroid follicles appear, TH content gradually rises until tail resorption began (TS 9–12). (3) TH content dramatically increases, with a peak in TH at or just prior to hatching (TS 13–15). In addition to amphibians,

many other vertebrates experience peak concentrations of TH at life history transitions—at hatching in precocial birds (38), at the larval-to-juvenile transition in several fish species (39–41), at ∼14 days post-partum in rats and mice (42, 43), and at birth in humans (44).

Thyroid hormones are present throughout early embryogenesis and the subsequent period of pre-hatching development in *E. coqui* (TS 1–9), beginning up to eight days before thyroid follicles can be detected histologically (13). These hormones are almost certainly maternal in origin. Similarly, T_4 and T_3 have been detected in yolk and gastrulating embryos of four other anuran species—*Bufo marinus* (36), *Rana catesbeiana* (35), *Bombina orientalis* (45), and *Xenopus laevis* (16). Early *Xenopus tropicalis* embryos express key TH signaling components (46). Indeed, TH signaling is also functional in the *Xenopus* tadpole central nervous system (CNS) before thyroid gland formation (16, 18). Maternally derived TH has a conserved role in vertebrate CNS development (47) and embryogenesis (17, 48, 49). Therefore, it seems likely that direct-developing frogs require maternal TH for normal neural development, as do most vertebrate species, although we do not evaluate that hypothesis here.

Maternal TH may regulate limb development occurring before the differentiation of the embryonic thyroid gland in direct-developing frogs. In metamorphosing anurans, TH signaling is required for terminal limb differentiation (22), but the initial stages of limb development are TH-independent. For example, tadpoles immersed in methimazole, a TH-synthesis inhibitor, develop a long limb-bud-like structure (24), and thyroidectomized tadpoles develop calcification centers in the hind limb (50, 51). In *E. coqui*, the limb bud proliferates and digits develop prior to the appearance of embryonic thyroid follicles (TS stages 9–10) [**Figure 3**; (8, 13)]. Two hypotheses could account for this observation: (1) *E. coqui* relies on maternal TH, rather than embryonically produced TH, to regulate early stages of digit patterning and growth (TS 6–9); or (2) paddle and digit formation in *E. coqui* proceed independently of TH. Our data show that requisite components of TH signaling are present at this time. Future investigation should evaluate the functional role of TH during this critical developmental period. A switch from embryonic to maternally synthesized TH for the regulation of early limb development, if it occurred, could explain the heterochronic shift in limb development and would represent an evolutionary novelty in direct-developing species.

Thyroid Hormone Receptor α, thrb, Dio2, and Dio3 mRNA Expression Patterns During Development and T3 Response in the Embryonic Tail

Tail resorption in *Xenopus tropicalis* occurs late in metamorphosis and is mediated by TRβ (52). Because tail resorption in *E. coqui* occurs late in embryogenesis and requires T_3 (8), we expected that *thra, thrb, dio2,* and *dio3* mRNA dynamics in the *E. coqui* tail would mirror those described in *Xenopus*. Our results support this hypothesis: in the *E. coqui* tail, a rise in *thrb* expression coincides with the rise in embryonic TH content, consistent with a role for *thrb* in mediating tail resorption.

Deiodinase type II and *dio3* mRNA expression patterns in the developing *E. coqui* tail are also similar to those described in indirect-developing species in which these deiodinase enzymes are critical for coordinating metamorphosis (20). Elevated *dio3* expression protects the tail from an early apoptotic response to T_3 until metamorphic climax in *Xenopus* (26); *E. coqui* tail resorption also begins at TS 13, when *dio3* expression significantly decreases. Although they serve different functions, the tail serves a critical role in both species: the larval *Xenopus* tail is a critical locomotor organ, whereas the embryonic *E. coqui* tail functions in respiration. In both species, maintenance of the tail is accomplished in part by *dio3* inactivation of T_4 and T_3.

Given the conservation of mRNA dynamics in the *E. coqui* tail, we wanted to determine whether the tissue could respond to exogenous T_3. In *Xenopus* species, treatment with exogenous T_3 induces transcription of direct T_3 response genes *dio3*, *klf9*, *thibz*, and *thrb* (19, 53–56). Exogenous T_3 induces significant increases in the mRNA of three of these T_3 response genes, *klf9*, *thibz*, and *thrb*, supporting the hypothesis that TH signaling components are conserved and mediate tail resorption in *E. coqui*.

Thyroid Hormone Receptor α, thrb, Dio2, and Dio3 mRNA Expression Patterns During Development and T_3 Response in the Embryonic Hind Limb

Thyroid hormone receptor α, thrb, dio2, and *dio3* mRNA expression patterns parallel those described in *Xenopus* species in the period leading up to and during metamorphosis (33, 57). In indirect-developing frogs, TRα has a critical role in controlling post-embryonic developmental timing (58–60) and in promoting proliferation in the hind limb during metamorphosis (61–63). Constitutive *thra* expression supports a proliferative and competence-establishing role for TRα in *E. coqui*. In the *E. coqui* limb, a rise in *thrb* expression coincides with the rise in embryonic TH content, consistent with TRβ autoinduction and tissue sensitization to TH described in *Xenopus* (64).

The tissue-specific patterns of *dio2* and *dio3* underlie the differential sensitivity of limb and tail tissue in metamorphosing frogs. *Deiodinase type II* expression is constitutive in the developing limb of *Xenopus laevis*, causing the limb to be sensitive to small amounts of T_3 produced during premetamorphosis (23). Similarly, elevated *dio2* expression in *E. coqui* limbs throughout most of limb development, including several days prior to formation of the embryonic thyroid gland, supports a role for TH-mediated limb development and growth.

In indirect-developing species, including *Xenopus* and spadefoot toads (*Scaphiopus*), concentrations between 1 and 10 nM T_3 are sufficient to promote precocious metamorphosis, tail resorption, and gene expression responses in limbs and tail (31, 65, 66). However, previous studies report that the

E. coqui limb has no morphological response to high doses of exogenous T_3 (11). Our study is the first to characterize mRNA expression changes in a direct-developing frog species in response to exogenous T_3. Treatment of *E. coqui* embryos with exogenous T_3 prior to formation of the thyroid follicles increases expression of four direct T_3 response genes in the tail, consistent with studies in *Xenopus* species (19, 53–55). However, limbs of the same embryos do not respond to T_3, despite the high dose administered (50 nM T_3). The lack of response previously observed in direct-developing species may be confounded by an inability of T_3 to reach the limb tissue. We observe a weak induction of T_3 response genes in TS stage 7 limbs, a full two days before *E. coqui* begins to produce TH (**Supplementary Figure 3**). It is possible that this response occurs because the adult epidermis is not yet fully formed and T_3 is better able to penetrate into the tissue, or because there is less endogenous T_3 present at TS 7 than at TS 9. In either case, the ability to respond to T_3 prior to thyroid gland formation is similar to biphasic species; tadpoles are also TH competent as soon as they hatch. Finally, the similar robust gene regulation response induced in *E. coqui* and *X. tropicalis* limb explants suggests that the limb tissue itself is similarly competent in both species. Overall, these data support the hypothesis that TH plays a role in *E. coqui* limb development and may do so prior to formation of the embryonic thyroid gland.

Here we support previous claims that later stages of limb development in *E. coqui* are TH-dependent but we additionally show that TH-signaling components are present during earlier stages, and that *E. coqui* limb tissue is sensitive to T_3. *Eleutherodactylus coqui* eggs are provisioned with maternally derived TH, which may mediate organogenesis before differentiation and activity of the embryo's own thyroid gland. Altogether, our data suggest that the TH-mediated molecular module active during post-hatching metamorphosis in indirect-developing frogs has been shifted prior to hatching in direct-developing species.

ETHICS STATEMENT

This study was carried out in accordance with the recommendations of the Harvard Faculty of Arts and Sciences Institutional Animal Care and Use Committee. The protocol was approved by the Harvard Faculty of Arts and Sciences Institutional Animal Care and Use Committee.

AUTHOR CONTRIBUTIONS

ML designed experiments and performed experiments, interpreted data, and wrote the manuscript. RD and JH contributed to experimental design, edited the manuscript, and discussed data interpretation.

FUNDING

This study was supported by a Graduate Women in Science Fellowship and NSF grant IOS 11456115 to RD, an NSF Doctoral Dissertation Improvement Grant #1701591, and Miyata and Goelet Grants from the Museum of Comparative Zoology. Published by a grant from the Wetmore Colles fund of the Museum of Comparative Zoology.

ACKNOWLEDGMENTS

We thank Laurent Sachs, Nicolas Buisine, Gwenneg Kerdivel, Austin Mudd, Richard Harland, and Dan Rokhsar for providing sequences that made this work possible. We also thank Charles Vidoudez for technical help in tissue extraction and TH quantification.

SUPPLEMENTARY MATERIAL

The Supplementary Material for this article can be found online at: https://www.frontiersin.org/articles/10.3389/fendo.2019.00307/full#supplementary-material

REFERENCES

1. Pough FH, Andrews R, Crump M, Savitzky AH, Wells KD, Brandley MC. *Herpetology*. 4th ed. Sunderland, MA: Sinauer Associates, Inc. (2015).
2. Elinson RP, del Pino EM. Developmental diversity of amphibians. *WIREs Dev Biol.* (2012) 1:345–69. doi: 10.1002/wdev.23
3. Hanken J, Klymkowsky MW, Summers CH, Seufert DW, Ingebrigsten N. Cranial ontogeny in the direct-developing frog, *Eleutherodactylus coqui* (Anura: Leptodactylidae), analyzed using whole-mount immunohistochemistry. *J Morphol.* (1992) 211:95–118. doi: 10.1002/jmor.1052110111
4. Denver RJ. Neuroendocrinology of amphibian metamorphosis. In: Shi Y-B, editor. *Current Topics in Developmental Biology*. Burlington: Elsevier Inc. (2013), 195–227.
5. Lynn WG. A Study of the Thyroid in Embryos of *Eleutherodactylus nubicola*. The Anatomical Record, 64, p.525-535, 2 plates.
6. Lynn WG, Peadon AM. The role of the thyroid gland in direct development in the Anuran, *Eleutherodactylus martinicensis*. *Growth.* (1955) 19:263–86.
7. Schlosser G, Roth G. Development of the retina is altered in the directly developing frog *Eleutherodactylus coqui* (Leptodactylidae). *Neurosci Lett.* (1997) 224:153–6. doi: 10.1016/S0304-3940(97)00174-2
8. Callery EM, Elinson RP. Thyroid hormone-dependent metamorphosis in a direct developing frog. *Proc Natl Acad Sci USA.* (2000) 97:2615–20. doi: 10.1073/pnas.050501097
9. Elinson RP. Metamorphosis in a frog that does not have a tadpole. In: Shi Y-B, editor. *Current Topics in Developmental Biology*. Vol. 103. Burlington: Elsevier Inc. (2013), 259–76. doi: 10.1016/B978-0-12-385979-2.00009-5
10. Lynn WG. The effects of thiourea and phenylthiourea upon the development of *Eleutherodactylus ricordii*. *Biol Bull.* (1948) 94:1–15. doi: 10.2307/1538202
11. Elinson RP. Leg development in a frog without a tadpole (*Eleutherodactylus coqui*). *J Exp Zool.* (1994) 270:202–10. doi: 10.1002/jez.1402700209
12. Townsend D, Stewart M. Direct development in *Eleutherodactylus coqui* (Anura: Leptodactylidae): a staging table. *Copeia.* (1985) 1985:423–36. doi: 10.2307/1444854
13. Jennings DH, Hanken J. Mechanistic basis of life history evolution in anuran amphibians: thyroid gland development in the direct-developing frog, *Eleutherodactylus coqui*. *Gen Comp Endocrinol.* (1998) 111:225–32. doi: 10.1006/gcen.1998.7111

14. Rosenkilde P. Thyroid hormone synthesis in metamorphosing and adult *Xenopus laevis*. *Gen Comp Endocrinol.* (1978) 34:95–6.
15. Buscaglia M, Leloup J, De Luze A. The role and regulation of monodeiodination of thyroxine to 3,5,3'-triidothyronine during amphibian metamorphosis. In: Balles M, Bownes M, editors. *Metamorphosis*. Oxford: Clarendon Press. (1985), 273–293.
16. Fini JB, Le Mével S, Palmier K, Darras VM, Punzon I, Richardson SJ, et al. Thyroid hormone signaling in the *Xenopus laevis* embryo is functional and susceptible to endocrine disruption. *Endocrinology.* (2012) 153:5068–81. doi: 10.1210/en.2012-1463
17. Morvan-Dubois G, Fini JB, Demeneix B. A. Is thyroid hormone signaling relevant for vertebrate embryogenesis? In: Shi Y-B, editor. *Current Topics in Developmental Biology*. Vol 103. Burlington: Elsevier Inc (2013), 365–96. doi: 10.1016/B978-0-12-385979-2.00013-7
18. Le Blay K, Préau L, Morvan-Dubois G, Demeneix B. Expression of the inactivating deiodinase, Deiodinase 3, in the pre-metamorphic tadpole retina. *PLoS ONE.* (2018) 13:e0195374. doi: 10.1371/journal.pone.0195374
19. Wang Z, Brown DD. Thyroid hormone-induced gene expression program for amphibian tail resorption. *J Biol Chem.* (1993) 268:16270–8.
20. Becker K, Stephens K. The type 2 and type 3 iodothyronine deiodinases play important roles in coordinating development in *Rana catesbeiana* tadpoles. *Endocrinology.* (1997) 138:2989–97. doi: 10.1210/endo.138.7.5272
21. Galton VA. Iodothyronine 5′-deiodinase activity in the amphibian *Rana catesbeiana* at different stages of the life cycle. *Endocrinology.* (1988) 122:1746–50.
22. Schreiber AM, Das B, Huang H, Marsh-Armstrong N, Brown DD. Diverse developmental programs of Xenopus laevis metamorphosis are inhibited by a dominant negative thyroid hormone receptor. *Proc Natl Acad Sci USA.* (2001) 98:10739–44. doi: 10.1073/pnas.191361698
23. Cai L, Brown DD. Expression of type II iodothyronine deiodinase marks the time that a tissue responds to thyroid hormone-induced metamorphosis in *Xenopus laevis*. *Dev Biol.* (2004) 266:87–95. doi: 10.1016/j.ydbio.2003.10.005
24. Brown DD, Cai L, Das B, Marsh-Armstrong N, Schreiber A, Juste R. Thyroid hormone controls multiple independent programs required for limb development in *Xenopus laevis* metamorphosis. *Proc Natl Acad Sci USA.* (2005) 102:12455–8. doi: 10.1073/pnas.0505989102
25. Buchholz DR, Paul BD, Fu L, Shi Y-B. Molecular and developmental analyses of thyroid hormone receptor function in *Xenopus laevis*, the African clawed frog. *Gen Comp Endocrinol.* (2006) 145:1–19. doi: 10.1016/j.ygcen.2005.07.009
26. Nakajima K, Fujimoto K, Yaoita Y. Regulation of thyroid hormone sensitivity by differential expression of the thyroid hormone receptor during *Xenopus* metamorphosis. *Genes Cells.* (2012) 17:645–59. doi: 10.1111/j.1365-2443.2012.01614.x
27. Denver RJ. Acceleration of anuran amphibian metamorphosis by corticotropin-releasing hormone-like peptides. *Gen Comp Endocrinol.* (1993) 91:38–51. doi: 10.1006/gcen.1993.1102
28. Denver RJ. Hormonal correlates of environmentally induced metamorphosis in the western spadefoot toad, *Scaphiopus hammondii*. *Gen Comp Endocrinol.* (1998) 110:326–36. doi: 10.1006/gcen.1998.7082
29. Schmittgen TD, Livak KJ. Analyzing real-time PCR data by the comparative CT method. *Nat Protoc.* (2008) 3:1101–8. doi: 10.1038/nprot.2008.73
30. Tata JR, Kawahara A, Baker BS. Prolactin inhibits both thyroid hormone-induced morphogenesis and cell death in cultured amphibian larval tissues. *Dev Biol.* (1991) 146:72–80. doi: 10.1016/0012-1606(91)90447-B
31. Bonett RM, Hoopfer ED, Denver RJ. Molecular mechanisms of corticosteroid synergy with thyroid hormone during tadpole metamorphosis. *Gen Comp Endocrinol.* (2010) 168:209–19. doi: 10.1016/j.ygcen.2010.03.014
32. Nieuwkoop P, Faber J. *Normal Table of Xenopus laevis (Daudin).* New York, NY: Garland Publishing Inc. (1994). Available online at: http://www.xenbase.org/anatomy/alldev.do.
33. Krain LP, Denver RJ. Developmental expression and hormonal regulation of glucocorticoid and thyroid hormone receptors during metamorphosis in *Xenopus laevis*. *J Endocrinol.* (2004) 181:91–104. doi: 10.1677/joe.0.1810091
34. Bagamasbad PD, Bonett RM, Sachs L, Buisine N, Raj S, Knoedler JR, et al. Deciphering the regulatory logic of an ancient, ultraconserved nuclear receptor enhancer module. *Molecul Endocrinol.* (2015) 29:856–72. doi: 10.1210/me.2014-1349
35. Fujikara K, Suzuki S. Thyroxine and thyroglobulin in eggs and embryos of bullfrog. *Zool Sci.* (1991) 8:1166.
36. Weber GM, Farrar ES, Tom CKF, Grau EG. Changes in whole-body thyroxine and triiodothyronine concentrations and total content during early development and metamorphosis of the toad *Bufo marinus*. *Gen Comp Endocrinol.* (1994) 94:62–71. doi: 10.1006/gcen.1994.1060
37. Niinuma TM, Hirano T, Kikuyama S. Changes in tissue concentrations of thyroid hormones in metamorphosing toad larvae. *Zool Sci.* (1991) 8:345–50.
38. De Groef B, Grommen SVH, Darras VM. Hatching the cleidoic egg: the role of thyroid hormones. *Front Endocrinol.* (2013) 4:1–10. doi: 10.3389/fendo.2013.00063
39. Brown D. The role of thyroid hormone in zebrafish and axolotl development. *Proc Natl Acad Sci USA.* (1997) 94:13011–6. doi: 10.1073/pnas.94.24.13011
40. De Jesus EGT, Toledo JD, Simpas MS. Thyroid hormones promote early metamorphosis in grouper (*Epinephelus coioides*) larvae. *Gen Comp Endocrinol.* (1998) 112:10–6. doi: 10.1006/gcen.1998.7103
41. Reddy PK, Lam TJ. Role of thyroid hormones in tilapia larvae (*Oreochromis mossambicus*): 1. *Effects of the hormones and an antithyroid drug on yolk absorption, growth and development*. *Fish Physiol Biochem.* (1992) 9:473–85. doi: 10.1007/BF02274228
42. Babu S, Sinha RA, Mohan V, Rao G, Pal A, Pathak A, et al. Effect of hypothyroxinemia on thyroid hormone responsiveness and action during rat postnatal neocortical development. *Exp Neurol.* (2011) 228:91–8. doi: 10.1016/j.expneurol.2010.12.012
43. Hadj-Sahraoui N, Seugnet I, Ghorbel MT, Demeneix B. Hypothyroidism prolongs mitotic activity in the post-natal mouse brain. *Neurosci Lett.* (2000) 280:79–82. doi: 10.1016/S0304-3940(00)00768-0
44. Buchholz DR. More similar than you think: Frog metamorphosis as a model of human perinatal endocrinology. *Dev Biol.* (2015) 408:188–95. doi: 10.1016/j.ydbio.2015.02.018
45. Jennings, D. H. (1997). *Evolution of Endocrine Control of Development in Direct-Developing Amphibians*. Unpublished Ph.D. dissertation. University of Colorado, Boulder.
46. Duarte-Guterman P, Langlois VS, Pauli BD, Trudeau VL. Expression and T3 regulation of thyroid hormone- and sex steroid-related genes during *Silurana (Xenopus) tropicalis* early development. *Gen Comp Endocrinol.* (2010) 166:429–35. doi: 10.1016/j.ygcen.2009.12.008
47. Bernal J. Thyroid hormone receptors in brain development and function. *Nat Clin Pract Endocrinol Metab.* (2007) 3:249–59. doi: 10.1038/ncpendmet0424
48. Havis E, Le Mével S, Morvan Dubois G, Shi D, Scanlan TS, Demeneix B, et al. Unliganded thyroid hormone receptor is essential for *Xenopus laevis* eye development. *EMBO J.* (2006) 25:4943–51. doi: 10.1038/sj.emboj.7601356
49. Morvan Dubois G, Sebillot A, Kuiper GJM, Verhoelst CHJ, Darras VM, Visser TH, et al. Deiodinase activity is present in *Xenopus laevis* during early embryogenesis. *Endocrinology.* (2006) 147:4941–9. doi: 10.1210/en.2006-0609
50. Terry GS. Effects of the extirpation of the thyroid gland upon ossification in *Rana pipiens*. *J Exp Zool.* (1918) 24:567–87. doi: 10.1002/jez.1400240306
51. Allen BM. The results of thyroid removal in the larvae of *Rana pipiens*. *J Exp Zool.* (1983) 24:499–519. doi: 10.1002/jez.1400240303
52. Nakajima K, Tazawa I, Yaoita Y. Thyroid hormone receptor α - and β - knockout *Xenopus tropicalis* tadpoles reveal subtype-specific roles during development. *Endocrinology.* (2017) 159:733–43. doi: 10.1210/en.2017-00601
53. Ranjan M, Wong J, Shi YB. Transcriptional repression of *Xenopus* TRβ gene is mediated by a thyroid hormone response element located near the start site. *J Biol Chem.* (1994) 269:24699–705.
54. Furlow DJ, Kanamori A. The transcription factor basic transcription element-binding protein 1 is a direct thyroid hormone response gene in the frog *Xenopus laevis*. *Endocrinology.* (2002) 143:3295–305. doi: 10.1210/en.2002-220126
55. Das B, Heimeier RA, Buchholz DR, Shi Y-B. Identification of direct thyroid hormone response genes reveals the earliest gene regulation programs during frog metamorphosis. *J Biol Chem.* (2009) 284:34167–78. doi: 10.1074/jbc.M109.066084
56. Helbing CC, Werry K, Crump D, Domanski D, Veldhoen N, Bailey CM. Expression profiles of novel thyroid hormone-responsive genes and proteins in the tail of *Xenopus laevis* tadpoles undergoing precocious metamorphosis. *Molecul Endocrinol.* (2003) 17:1395–409. doi: 10.1210/me.2002-0274

57. Yaoita Y, Brown DD. A correlation of thyroid hormone receptor gene expression with amphibian metamorphosis. *Genes Dev.* (1990) 4:1917–24. doi: 10.1101/gad.4.11.1917
58. Wen L, Shi YB. Unliganded thyroid hormone receptor α controls developmental timing in *Xenopus tropicalis*. *Endocrinology*. (2015) 156:721–34. doi: 10.1210/en.2014-1439
59. Choi J, Suzuki KT, Sakuma T, Shewade L, Yamamoto T, Buchholz D. Unliganded thyroid hormone receptor α regulates developmental timing via gene repression in *Xenopus tropicalis*. *Endocrinology*. (2015) 156:735–44. doi: 10.1210/en.2014-1554
60. Buchholz DR, Shi Y. Dual function model revised by thyroid hormone receptor alpha knockout frogs. *Gen Comp Endocrinol.* (2018) 265:214–8. doi: 10.1016/j.ygcen.2018.04.020
61. Denver RJ. The molecular basis of thyroid hormone-dependent central nervous system remodeling during amphibian metamorphosis. *Compar Biochem Physiol Part C, Pharmacol Toxicol Endocrinol.* (1998) 119:219–28. doi: 10.1016/S0742-8413(98)00011-5
62. Denver RJ, Hu F, Scanlan TS, Furlow DJ. Thyroid hormone receptor subtype specificity for hormone-dependent neurogenesis in *Xenopus laevis*. *Dev Biol.* (2009) 326:155–68. doi: 10.1016/j.ydbio.2008.11.005
63. Choi J, Ishizuya-Oka A, Buchholz DR. Growth, development, and intestinal remodeling occurs in the absence of thyroid hormone receptor a in tadpoles of *Xenopus tropicalis*. *Endocrinology*. (2017) 158:1623–33. doi: 10.1210/en.2016-1955
64. Tata JR. Autoinduction of nuclear hormone receptors during metamorphosis and its significance. *Insect Biochem Mol Biol.* (2000) 30:645–51. doi: 10.1016/S0965-1748(00)00035-7
65. Buckbinder L, Brown DD. Thyroid hormone-induced gene expression changes in the developing frog limb. *J Biol Chem.* (1992) 267:25786–91.
66. Buchholz DR, Hayes TB. Variation in thyroid hormone action and tissue content underlies species differences in the timing of metamorphosis in desert frogs. *Evol Dev.* (2005) 7:458–67. doi: 10.1111/j.1525-142X.2005.05049.x

Conflict of Interest Statement: The authors declare that the research was conducted in the absence of any commercial or financial relationships that could be construed as a potential conflict of interest.

Chapter 2: Corticosterone and thyroid hormone synergistically induce tail resorption and TH-response gene expression in the direct-developing frog, *Eleutherodactylus coqui*

INTRODUCTION

Direct-developing frogs bypass the free-living tadpole stage characteristic of most frogs and hatch as miniature adults. The evolution of direct development is characterized by loss of tadpole-specific morphological traits such as the lateral line, larval mouthparts and a long coiled gut (Callery, Fang and Elinson, 2001). Other highly conserved anuran traits, such as hormonal control of development, appear to be only partially conserved in direct-developing frogs (Callery and Elinson 2000). Two hormones in particular, thyroid hormone (TH) and glucocorticoids (GC), play an important role in regulating development in metamorphosing frogs. Although there have been several studies on the role of TH in direct-developing frogs, far less is known about the role of GC in direct development.

In tadpoles of metamorphosing frogs, two endocrine axes that produce TH and GC (the hypothalamus-pituitary-interrenal axis, HPI; and the hypothalamus-pituitary-thyroid axis, HPT) are linked: the tadpole hypothalamus produces corticotropin-releasing hormone (CRH), which promotes synthesis of TH and GC by the thyroid gland and the interrenal glands, respectively (De Groef *et al.*, 2006; Denver, 2013). Whole-body content of corticosterone (CORT), the major amphibian corticosteroid, parallels the increase in TH levels before metamorphic climax (Jaffe, 1981; Krain and Denver, 2004). This initial observation suggested that GC may promote metamorphosis, although exogenous GC administered alone to premetamorphic tadpoles causes slower or abnormal development (Lorenz *et al.*, 2009; Kulkarni and Gramapurohit, 2016). A wealth of studies now suggest that the timing of GC administration during development is important in predicting its effects: GC administered during premetamorphosis generally inhibit growth while GC administered during prometamorphosis promote metamorphosis (summarized in Denver, 2013).

Eleutherodactylus coqui embryos undergo a TH-dependent cryptic metamorphosis in the egg (Callery and Elinson, 2000). Additionally, injection of ovine corticotropin-releasing hormone (CRH) into *E. coqui* embryos accelerates developmental rate and causes more rapid tail resorption compared to controls (Kulkarni, Singamsetty and Buchholz, 2010). Corticotropin-releasing hormone may accelerate embryonic development in *E. coqui* via induction of thyrotropin-stimulating hormone (TSH) and adrenocorticotropic hormone (ATCH), as has been shown in metamorphosing species.

In metamorphosing species, GC synergize with TH to promote metamorphosis (Galton, 1990; Bonett, Hoopfer and Denver, 2010). Synergy is defined by one hormone having no or minimal effect alone, but both hormones together having a more than additive effect. For example, treatment with 10 nM T_3 or 100 nM CORT does not affect resorption of *X. laevis* tail explants, but treatment with 10 nM T_3 and 100 nM CORT together significantly increases resorption (Bonett, Hoopfer and Denver, 2010).

Synergy is central to the ability of tadpoles to respond to environmental changes by accelerating metamorphosis (Denver, 1998; Boorse and Denver, 2003; Gomez-Mestre, Kulkarni and Buchholz, 2013). Environmental stimuli such as crowding, lack of food, and decreasing water levels are all situations in which it would be advantageous to accelerate metamorphosis. In fact, these scenarios stimulate a physiological stress response resulting in increased stress hormone, or GC, production. For example, decreasing water levels elevates whole body CORT and accelerates development in *Scaphiopus hammondii* (Denver, 1998), while a lack of food resources and crowding increases GC production in *Rana pipiens* tadpoles (Glennemeier and Denver, 2002b). However, much remains to be discovered about how GC function in metamorphosis, and even less is known about how GC function and how GC and TH interact in direct-developing frogs.

Several mechanisms may underlie the interaction of GC and TH in metamorphosing frogs. Glucocorticoids can modulate the timing of development by influencing TH action. They may, for

example, increase tissue sensitivity to T_3. Glucocorticoids increase nuclear binding capacity in tail tissue of *Bufo japonicus* and *Rana catesbeiana* (Niki, Yoshizato and Kikuyama, 1981; Suzuki and Kikuyama, 1983), and CORT and TH administered together at doses that do not normally induce metamorphosis strongly induce *thyroid hormone receptor β* (*thrb*) mRNA levels in *Xenopus laevis* tail tissue (Bonett, Hoopfer and Denver, 2010). Glucocorticoids also influence the amount of T_3 present in target tissues via deiodinase activity. Deiodinase enzyme type II (dio2) converts T_4 into T_3; T_3 has at least 10 times greater affinity for TH receptors (TRs) than does T_4. Deiodinase type III (dio3) converts T_4 to both T_2 and reverse triiodothyronine (rT_3), which are unable to bind TRs in most species. Deiodinase type II activity and mRNA are synergistically increased by TH and GC in axolotl and frog tissues, resulting in increased plasma (Galton, 1990) and intracellular T_3 (Darras *et al.*, 2002; Kühn *et al.*, 2005; Bonett, Hoopfer and Denver, 2010). Altogether, TH and GC increase tissue sensitivity and the amount of biologically active hormone T_3 in target tissue.

Finally, GC could synergize with TH to induce target gene transcription. For example, CORT induces expression of *krüppel-like factor 9*, a direct GC- and T_3-response gene (Bonett *et al.*, 2009), and T_3 and CORT together synergistically up-regulate *klf9* mRNA in *Xenopus* cell lines and brain (Bagamasbad *et al.*, 2015). A cDNA microarray study examining gene expression in *X. tropicalis* tail in response to T_3 alone and to CORT and T_3 in combination found that 22% of significantly regulated genes required both hormones, suggesting that CORT may be necessary for a substantial portion of T_3-induced tail resorption.

Eleutherodactylus coqui embryos develop some of the typical characteristics of tadpoles. One of these characteristics is the tail. However, the tail of *E. coqui* is thin and highly vascularized, in contrast to the muscular tail of tadpoles. While tadpoles use the tail principally for locomotion, it is likely that *E. coqui* uses its tail as a respiratory organ (Townsend and Stewart, 1985). Both direct- and indirect-developing frogs resorb the tail in generating the definitive adult form, and the hallmark of

metamorphic climax in indirect-developing frogs is the onset of tail resorption. Presumably, the tail remnant impedes adult locomotion, and selection favors the rapid resorption of the tail in both direct- and indirect-developing species.

While resorption of the tail in embryonic *Eleutherodactylus coqui* appears to depend on TH (Callery and Elinson 2000), the tissue-specific mechanism of tail resorption is unknown. In this chapter, I tested whether GC and TH can synergistically induce tail resorption and TH target gene expression in *E. coqui*. I find that whole body CORT content increases at hatching, and that CORT and T_3 administered together both increase the rate of *E. coqui* tail resorption and induce T_3-response gene expression to a greater extent than does T_3 alone. Despite differing tail morphology and function in *E. coqui* and metamorphosing frogs, these results suggest that CORT and T_3 synergize to promote tail resorption via induction of T_3-response genes in the *E. coqui* tail as these hormones do in metamorphosing frogs.

METHODS

Animal care

Adult *Eleutherodactylus coqui* were field-collected from introduced populations in Hilo, Hawaii, with the permission of the U.S. Fish and Wildlife Service (permits EX-14-06, EX-16-07 and EX 17-11). Embryos were obtained from spontaneous matings between pairs of these frogs in the Hanken lab breeding colony at Harvard University (IACUC protocol #99-09-03). Embryos were staged according to the normal table of Townsend & Stewart (TS; 1985), which defines 15 stages from fertilization (1) to hatching (15). Following internal fertilization, the adult female deposits embryos at TS stage 1.

Whole body extraction and quantification of corticosterone by enzyme-linked immunosorbant assay

To measure whole body CORT content in *E. coqui*, I collected embryos at TS stages 10, 13 and 15 (hatching) and at 24 hr post-hatching. With assistance from Arasakumar Subramani, a collaborator in the Denver lab at the University of Michigan, I extracted tissue for corticosterone and quantified whole-body corticosterone content with enzyme immunoassay (EIA). Embryos were dechorionated and anesthetized with drops of neutral-buffered 2% MS-222, snap frozen and kept at -80˚C until tissue extraction. Once 50% of a clutch had hatched spontaneously, the remaining embryos were dechorionated and collected as described above. The 24-hr post-hatching time point was determined as 24 hr after 50% of a clutch had spontaneously hatched. Three embryos were pooled for a single biological replicate. Tissue was extracted as described in Denver (1998). For estimation of recoveries, 100 ul of [^{3}H]CORT (approximately 2000 cpm) was added to the extracts and Sephadex LH-20 columns were used to fractionate the extracts. Sephadex LH-20 was prepared by overnight equilibration in methylene chloride. The bottom of the column was packed with 1 cm of glass wool, and the Sephadex slurry was poured after degassing. The final length of the packed column was approximately 20 cm. The column was washed once with 10 mL of methylene chloride:methanol (98:2) and all air bubbles were removed before sample loading. 100 uL sample was loaded on to the column and washed with 14 mL methylene chloride:methanol (98:2) and fractions 15 to 19 containing corticosterone were collected in a glass tube. The collected fractions were then vacuum dried and stored at -80 C. On the day of analysis, samples were resuspended in 110 uL PBS-G. Ten microliters of the sample was read in a scintillation counter to calculate the recovery; the average recorded recovery was 73%. Samples were analyzed by enzyme-linked immunosorbant assay at different dilutions in 25 or 50 ul. The assay was validated with parallelism and standard dilution. Interassay validation was done using a known quality control sample.

Hormonal treatments in vivo

For each hormonal treatment, I split a single clutch of eggs across all treatments to control for genetic background. The egg membrane and chorion of embryos were removed with watchmaker forceps following immersion in 2% cysteine (pH 8.5) in 10% Holtfreter solution at least 24 hr before immersion in either 50 nM T_3, 100 nM CORT, or 50 nM T_3 and 100 nM CORT. Ten-mM corticosterone (CORT; Sigma cat no. 46148) and 2.5 mM T_3 (Sigma cat no. T2877) were diluted to make 100 nM CORT, 500 nM CORT and 50 nM T_3. I chose 50 nM T_3 because this concentration is sufficient to induce tail resorption in *E. coqui* (Callery and Elinson 2000). I initially chose 100 nM CORT and 500 nM CORT because these concentrations have been used in studies of tail resorption in *Xenopus laevis* (Bonett, Hoopfer and Denver, 2010) and to determine what concentration of CORT had little to no effect on *E. coqui* tail resorption alone. Because tail resorption begins at TS stage 13, I chose TS stage 9, prior to embryonic thyroid activation, as the beginning of treatment to test if tail resorption could be accelerated. Hormone solutions were refreshed every 8–12 hr. For the morphological experiments, I stopped treatment when embryos showed several characteristic features of TS stage 15, including adult body pigmentation, eye color and crawling out of the liquid media (between 6 and 8 days of treatment). For qPCR experiments, I chose a 46-hr time point because these timepoints were used in a previous study (Bonett, Hoopfer and Denver, 2010) and to allow enough time for induction of T_3 response genes.

Embryo measurements in ImageJ

Dorsal and ventral photos of terminally anesthetized embryos were taken under a dissecting scope with a Retiga 2000R black-and-white camera. Dissected tails were placed on a slide, covered with a cover slip and photographed. Morphological measurements previously used to describe development (Callery and Elinson 2000) were taken from ventral photographs by using the software

ImageJ (NIH). These measurements included snout-vent length (SVL), ventral width, snout-upper jaw distance, lower jaw-suture distance (see inset in Figure 2.2B), hind limb length and width, tail notochord length, tail length and tail area. Ventral width and the distance between the tip of the snout and the upper jaw decrease as the embryo grows, whereas the distance between the lower jaw and the suture line on the chest of the embryo increases with body size. Because different tail tissues might resorb at different rates, several measures of tail size were taken—tail notochord (the length of the notochord that extends into the tail), tail area and tail length. The notochord is slightly curved, so its total length was measured by adding a series of shorter, straight segments (see inset in 2C). To measure tail length, the distance from the tip of the notochord to the tip of the tail was measured and added to the tail notochord measurement. Tail area was determined by outlining the tail with the polygon function in ImageJ. Because embryos varied in overall size at a given stage, measures of tail size and hind limb length were normalized to SVL.

Quantitative PCR

Partial and predicted cDNA sequences for *ribosomal protein L8* (*rpL8*), *deiodinase type III* (*dio3*), *deiodinase type II* (*dio2*), *krüppel-like factor 9* (*klf9*), *thyroid hormone induced bZip protein* (*thibz*) and *thyroid hormone receptor β* (*thrb*) were obtained as described in Chapter 1 (Laslo *et al.* 2019). Quantitative PCR primers were designed from predicted cDNA sequences (Genbank accession numbers MK784760, MK784762, MK784763, MK784761, MK784758, MK784756 and MK784757).

After hormone treatment, embryos were terminally anesthetized with neutral-buffered 2% MS-222 in 10% Holtfreter solution until they no longer responded to toe pinches (30–60 sec). Total RNA was isolated from dissected tails following the manufacturer's protocol. Because qPCR primers did not span exon-exon boundaries, genomic DNA was removed with an Ambion DNA-*free* kit (cat. #AM1906). Controls with no reverse-transcriptase verified that removal of genomic DNA was

complete. Total RNA was quantified with a Qubit Fluorometer 3.0 and checked for purity on a Nanodrop spectrophotometer. Complementary DNA was synthesized from 660 ng of total RNA for each sample with iScript Reverse Transcriptase Supermix for RT-qPCR (BioRad). mRNA levels were analyzed with a SsoAdvanced Universal Probes Supermix (BioRad) on a CFX384 machine. Optimal qPCR conditions were determined with temperature gradient and cDNA dilutions for dynamic range of input. Standard curves showed high efficiency of reaction (90–105%) and R^2 was equal to or greater than 0.98 for all primer sets. Control wells with no template or no reverse transcriptase showed no amplification. All primer sets are listed in Table 1 in Chapter 1. The relative mRNA levels were determined as described by Schmittgen & Livak (2008). Target gene expression was normalized to the reference gene *rpL8*, which did not vary significantly across treatment.

Statistical Analysis

Statistical analyses of qPCR data were done with RStudio version 1.1.383 and visualized with ggplot2 (https://ggplot2.tidyverse.org/). Whole body corticosterone content had unequal variance, so data were log transformed. Log-transformed data followed a normal distribution as determined by Q-Q plots and the Shapiro-Wilk test; these data also had equal variance as determined by Levene's test. Dosage-dependent CORT data met the assumptions for a parametric test. Therefore, a one-way ANOVA was used to determine if there were significant differences among groups for both of these datasets, and a Tukey's HSD post-hoc test was used to identify significant differences among treatments. For the *in vivo* CORT and T_3 treatment experiment, data were pooled from four independent experimental replicates. Each experimental replicate came from different clutches. Measures of tail length were normalized to SVL and fitted to a linear model with the formula Tail ~ Treatment, taking into account experimental replicate as a fixed effect. Residuals followed a normal distribution. A Tukey's HSD post-hoc test determined treatments that significantly differed from

each other. For the qPCR experiment, sample size was small (n = 3–4/group). Therefore, a Kruskal-Wallis rank-sum test followed by a post-hoc Dunn's test with the Benjamini-Hochberg correction were used to evaluate differences between all treated groups. Statistical significance was accepted at $\alpha < 0.05$.

RESULTS

Whole body corticosterone content rises at hatching

Whole body CORT content was low at TS stages 10 and 13, then increased 3-fold between TS 13 and 15 and remained at this level 24 hr after hatching (Figure 2.1; $F_{3, 20} = 36.76$, $p < 0.001$). See Appendix B - Table S2.1 for all pairwise comparisons.

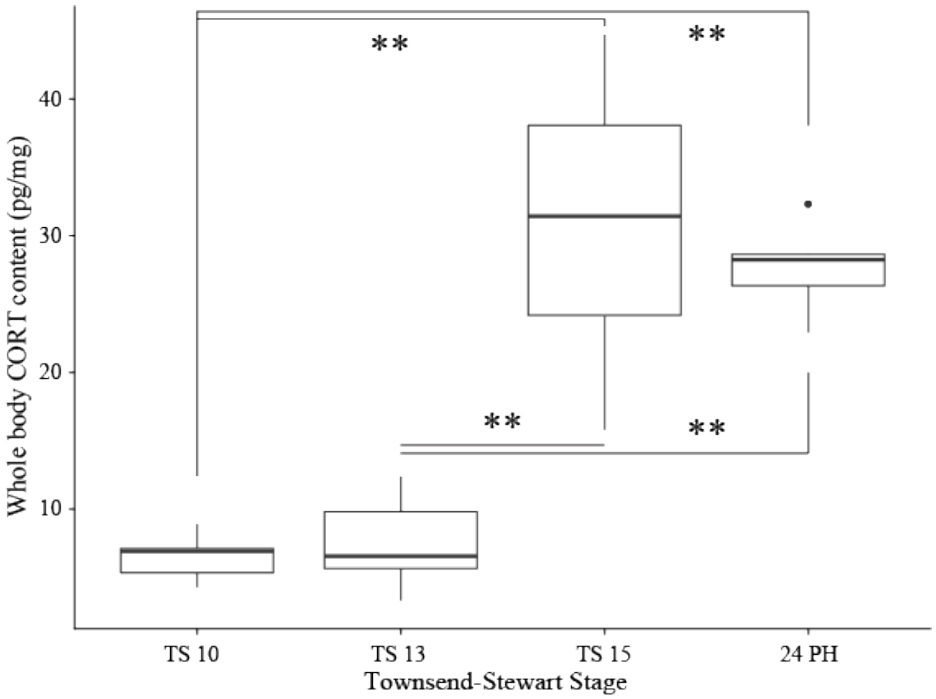

Figure 2.1. Whole body corticosterone content significantly increases in *Eleutherodactylus coqui* embryos between TS stages 10 and 15 (hatching). Boxes and whiskers represent median and range of six biological replicates, respectively. Two asterisks indicate a significant difference at $p < 0.001$ (Tukey's HSD).

Corticosterone has dosage-dependent effects on embryonic morphology

Continuous treatment with 100 nM and 500 nM CORT had dosage-dependent effects on embryo morphology. The effect was statistically significant for the following measured parameters: body size [Figure 2.2A; $F_{2, 28} = 23.22$, $p < 0.001$], ventral width [Figure 2.2A; $F_{2, 28} = 7.16$, $p = 0.003$], distance between the lower jaw tip and the chest suture line [Figure 2.2A; $F_{2, 27} = 11.31$, $p < 0.001$], distance between the snout and the tip of the upper jaw [Figure 2.2A; $F_{2, 27} = 11.82$, $p < 0.001$], relative hind limb length [Figure 2.2B; $F_{2, 27} = 30.34$, $p < 0.001$], femur length-to-width ratio [Figure 2.2C; $F_{2, 28} = 66.86$, $p < 0.001$] and calf length-to-width ratio [Figure 2.2C; $F_{(2, 28)} = 25.52$, $p < 0.001$]. Corticosterone treatment had no significant effect on tail length or tail notochord length. Overall, treatment with 500 nM CORT appeared to significantly affect embryo morphology consistent with a slight developmental delay. Body size and the distance between the lower jaw and suture decreased (Figure 2.2A; Tukey's HSD, $p < 0.001$), ventral width and the distance between the snout and the upper jaw increased (Figure 2.2A, Tukey's HSD, $p = 0.005$, < 0.001, respectively), and hind limbs were relatively shorter (Figure 2.2B, Tukey's HSD, $p < 0.001$) and thicker (Figure 2.2C, $p < 0.001$) after treatment with 500 nM CORT. Treatment with 100 nM CORT had minimal effect. Therefore, a 100 nM CORT dose was chosen to test the hypothesis that CORT and T_3 together have synergistic effects on tail resorption and gene expression. See Appendix B - Table S2.2 for pairwise differences.

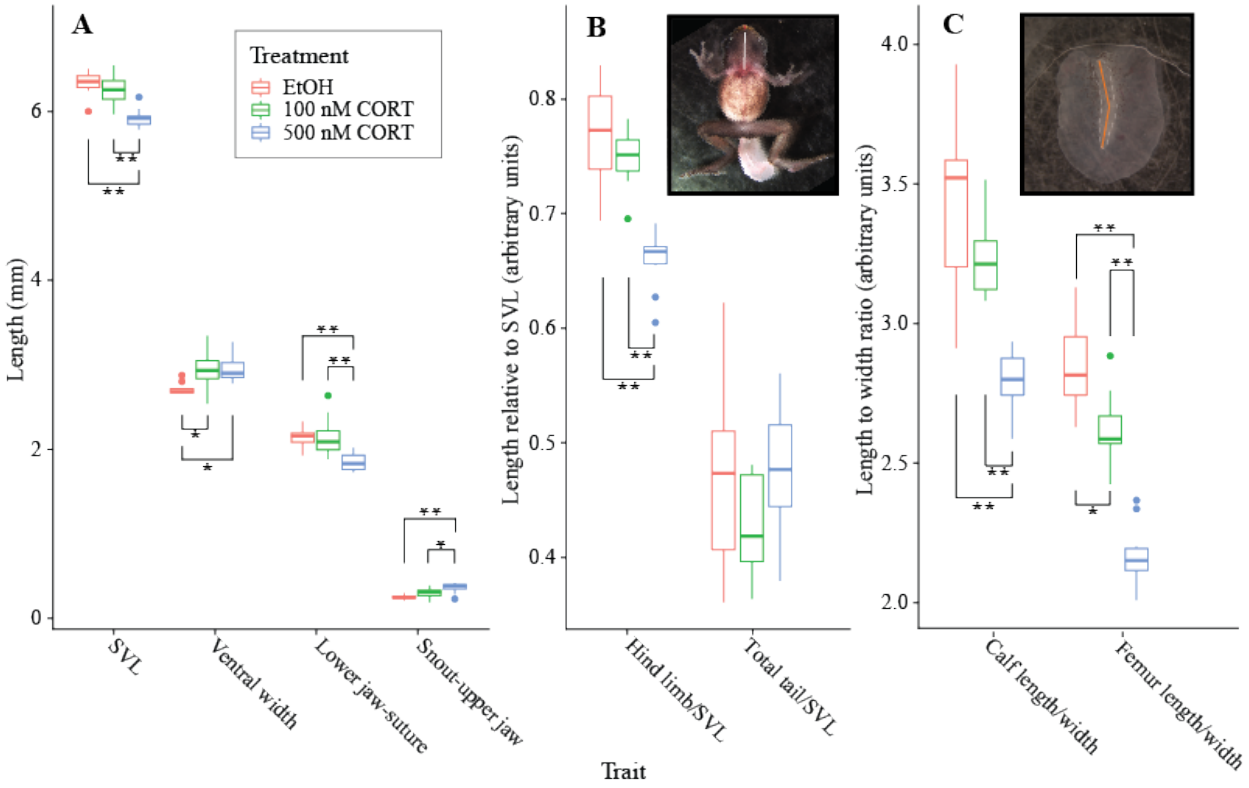

Figure 2.2. Corticosterone treatment affects embryonic morphology in a dosage-dependent manner. Panel A shows absolute size (length) of four features. Panel B shows measurements of hind limb and tail length relative to SVL. Panel C shows ratios of limb length to width. Inset shows how snout-upper jaw (red line) and lower jaw-suture distances (white line) were measured. Boxes and whiskers represent median and range of 9–11 individuals, respectively. One asterisk indicates a significant difference at $p < 0.05$; two asterisks indicate a significant difference at $p < 0.001$ (Tukey's HSD).

Corticosterone and T_3 treatment affect tail resorption and hind limb growth

To determine if CORT could facilitate the effects of T_3, I paired 100 nM CORT, which had little effect on *E. coqui* morphology alone with 50 nM T_3. Hormone treatment did not have any significant effect on embryo body size. Because embryo SVL did vary among experimental replicates

[$F_{3, 68} = 33.40$, $p < 0.001$], measures of tail and limb length were normalized to body size. Hormone treatment significantly affected relative tail area [$F_{3, 68} = 8.033$, $p < 0.001$], relative tail length [$F_{3, 68} = 22.07$, $p < 0.001$], relative tail notochord length [Figure 2.3A; $F_{3, 68} = 23.59$, $p < 0.001$], relative hind limb length [Figure 2.3B; $F_{3, 68} = 9.94$, $p < 0.001$], femur length-to-width ratio [$F_{3, 68} = 19.83$, $p < 0.001$] and calf length-to-width ratio [$F_{3, 68} = 3.24$, $p = 0.027$]. See Appendix B - Table S2.3 for pairwise differences.

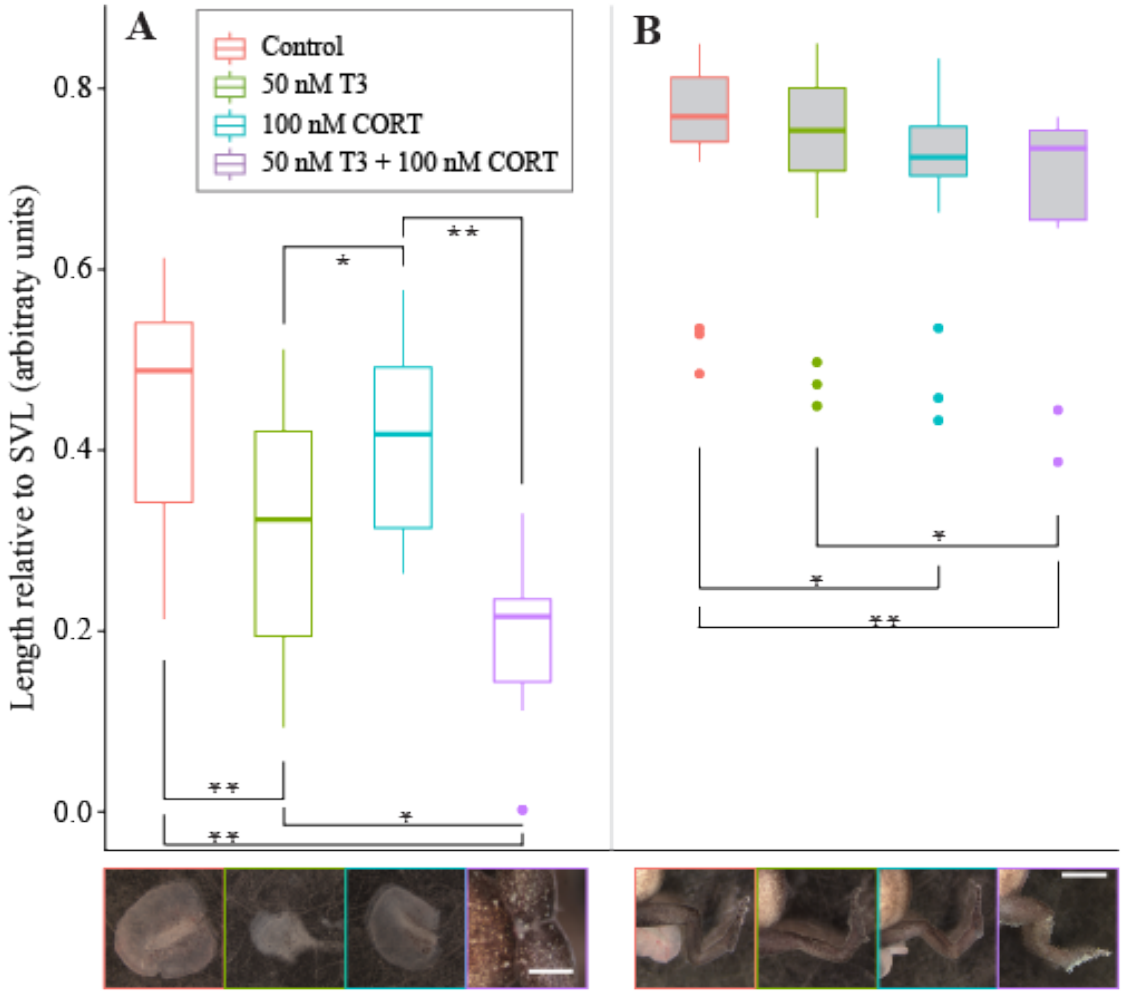

Figure 2.3. Relative tail notochord (white boxes) and limb length (gray boxes) relative to SVL are significantly shorter after treatment with 100 nM CORT and 50 nM T_3 compared to both control embryos and embryos treated with 50 nM T_3 alone. One asterisk indicates a significant difference at $p < 0.05$; two asterisks indicate a significant difference at $p < 0.001$ (Tukey's HSD). Boxes and whiskers represent median and range of 15–21 individuals, respectively. Scale bar is 1 mm.

Corticosterone and T_3 synergistically promote tail resorption

Treatment with either 50 nM T_3 alone or 100 nM CORT plus 50 nM T_3 together decreased all measures of tail size (Table 2.1). However, the magnitude of the decrease after treatment with both hormones was more than the additive effect of each hormone treatment alone. The pattern of tail size across treatments is represented by the relative length of the tail notochord (Figure 2.3A; see Appendix B for plots of other tail measures). The relative length of tail notochords in embryos treated with both hormones was 58% shorter than those of controls (Table 2.1; Tukey's HSD, $p < 0.001$), 55% shorter than those of 100 nM CORT-treated embryos (Table 2.1; Tukey's HSD, $p < 0.001$) and 38% shorter than those of 50 nM T_3-treated embryos (Table 2.1; Tukey's HSD, $p = 0.004$). Embryos treated with 50 nM T_3 also had relative tail notochords lengths that were 32% shorter than control embryos (Tukey's HSD, $p < 0.001$) and 7% shorter than 100 nM CORT-treated embryos (Tukey's HSD, $p = 0.004$).

Table 2.1. Treatment with 50 nM T_3 alone or with 50 nM T_3 and 100 nM CORT together decrease all measures of tail size in *Eleutherodactylus coqui*. Treatment with 100 nM CORT has no effect. Values significantly different from control are set in bold font (Tukey's HSD, $p < 0.05$).

Treatment	**Control**	**50 nM T3**		**100 nM CORT**		**50 nM T3 + 100 nM CORT**	
	Value	Absolute Value	Δ vs. Control	Absolute value	Δ vs. Control	Absolute value	Δ vs. Control
Total tail/SVL	0.573	**0.367**	-0.206	0.589	0.016	**0.299**	-0.274
Tail notochord/SVL	0.438	**0.300**	-0.138	0.407	-0.032	**0.185**	-0.253
Tail area/SVL (mm)	1.222	**0.700**	-0.522	1.046	-0.176	**0.273**	-0.950

Continuous CORT treatment reduces relative hind limb length

Embryos treated with 100 nM CORT until reaching TS stage 15 (6-8 days) had relatively shorter hind limbs than control embryos (Figure 2.3B, Tukey's HSD, $p = 0.006$). Embryos treated with 100 nM CORT plus 50 nM T_3 had hind limbs that were 9% shorter than those of control embryos (Tukey's HSD, $p < 0.001$) and 5% shorter than those of embryos treated with only 50 nM T_3 (Tukey's HSD, $p = 0.017$). Embryos treated with either T_3 alone or CORT and T_3 together often developed flaky layers of skin surrounding the digit tips and tail in the last few days of treatment. I have also observed this flaking during normal development, but only around the resorbing tail (Figure 2.3, T_3-treated tail). Embryos treated with both CORT and T_3 were generally healthy but had higher rates (22%) of edema than other treated embryos (from 0-9.5%). Embryos treated with CORT plus T_3 had 11% wider femurs compared to both 50 nM T_3-treated and control embryos (Appendix B - Table S2.3; Tukey's HSD, $p < 0.001$ for both comparisons). A similar effect was observed in embryos treated with only 100 nM CORT; these embryos had significantly 9% wider femurs than both control embryos and 50 nM T_3-treated embryos (Appendix B - Table S2.3; Tukey's HSD, $p < 0.001$ for each comparison). Calf width was not as strongly affected as femur width; only 100 nM CORT-treated embryos had significantly wider (7%) calves compared to controls (Tukey's HSD, $p = 0.024$).

Treatment with both T_3 and corticosterone increases T_3-response gene mRNA levels

Because CORT and T_3 treatment increased tail resorption more than CORT or T_3 treatment alone, I measured mRNA levels of T_3-response genes to test the hypothesis that the two hormones act synergistically to induce T_3-response genes. Hormone treatment for 46 hr (Figure 2.4A) significantly altered mRNA levels of *dio3* (Kruskal-Wallis, $p = 0.012$), *klf9* (Kruskal-Wallis, $p = 0.004$), *thibz* (Kruskal-Wallis, $p = 0.008$) and *thrb* (Kruskal-Wallis; $p = 0.008$). After 120 hr of

hormone treatment, only levels of *dio3* (Kruskal-Wallis, p = 0.008), *klf9* (Kruskal-Wallis, p = 0.025) and *thibz* (Kruskal-Wallis, p = 0.013) were changed (Figure 2.4B).

Forty-six hr of treatment with 100 nM CORT had no effect on mRNA levels of *dio3*, *klf9*, *thibz* or *thrb* in the tail relative to those of control embryos. Levels of *dio3*, *klf9*, *thibz* and *thrb* increased 1.9-, 40.4-, 144- and 2.6-fold, respectively, after treatment with T_3 for 46 hr. *Krüppel-like factor 9*, *thibz* and *thrb* mRNA also significantly increased after treatment with both T_3 and CORT compared to controls (Figure 2.4A; Dunn's test, p = 0.005, 0.008 and 0.004, respectively). Although mRNA levels in tails of dual-treated embryos were not significantly different from those treated with T_3 alone, CORT and T_3 had synergistic on effects on *thrb*, *klf9* and *thibz* expression: the fold increase in expression relative to expression in control tails was always greater than the additive effect of either CORT or T_3 treatment alone (Table 2.2).

Table 2.2. The magnitude of fold change in T_3-response genes between *Eleutherodactylus coqui* tails treated with T_3 alone (left column for each timepoint) or T_3 and CORT in combination (right column for each time point) and untreated control is always greater when embryos are treated with both hormones together (compare columns within time points). Groups that are significantly different from untreated controls are set in bold font (Dunn's post-hoc test, $p < 0.05$).

	46 hours			120 hours		
Gene	T3 - Control	CORT - Control	T3 + CORT - Control	T3 - Control	CORT - Control	T3 + CORT - Control
dio3	1.91	-1.30	2.17	1.66	-7.31	-3.72
klf9	40.45	12.46	**157.20**	2.72	1.82	**11.56**
thibz	144.35	4.50	**468.17**	3.51	-1.38	**11.37**
thrb	2.56	2.14	**5.68**	1.05	1.01	1.64

Hormone treatment for 120 hr induced the same pattern of *klf9*, *thibz* and *thrb* mRNA expression among treatment groups as did 46 hr of treatment, although the magnitude of change is less (Table 2.2). Moreover, *dio3* mRNA significantly decreased in tails of embryos treated with 100 nM CORT alone or with CORT and T_3 together compared to those treated with T_3 alone (Figure 2.4B; Dunn's test, $p = 0.009$ and 0.043, respectively).

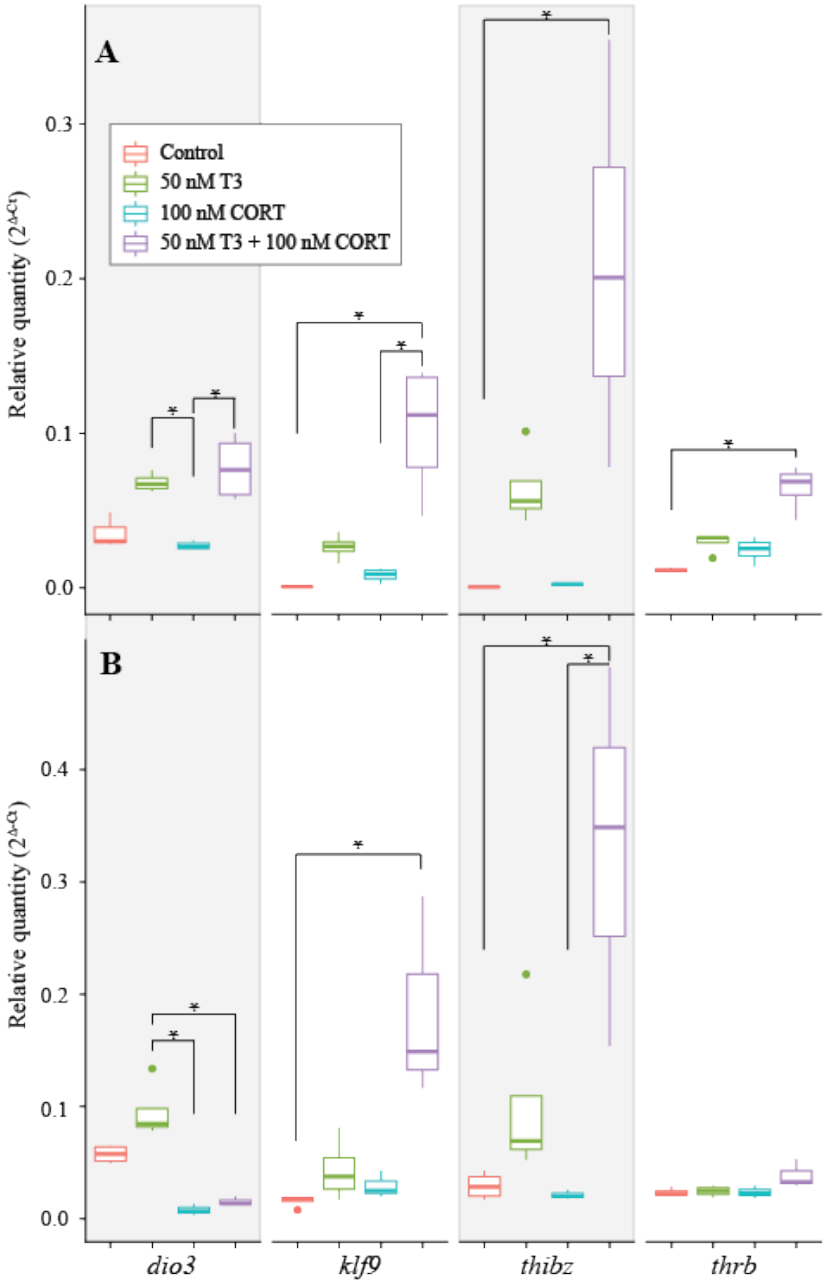

Figure 2.4. Treatment of embryonic tails with 100 nM CORT, 50 nM T_3 or both 100 nM CORT and 50 nM T_3 significantly affects mRNA levels of *deiodinase type III* (*dio3*), *krüppel-like factor 9* (*klf9*), *thyroid hormone induced bZip protein* (*thibz*) and *thyroid hormone receptor β* (*thrb*) after 46 and 120 hr. Asterisks indicate a significant difference at $p < 0.05$ (Tukey's HSD). Boxes and whiskers represent median and range of 3–4 individuals, respectively.

DISCUSSION

In this chapter, I show that the HPI axis activity increases just before hatching in embryos of the direct-developing frog *Eleutherodactylus coqui*, and that CORT and T_3 synergistically promote rapid tail resorption likely via an increase in TH signaling in target tissue. This is similar to what has been reported in metamorphosing frogs. However, the module is expressed at hatching, rather than during the postembryonic metamorphosis that occurs in indirect-developing frogs.

Hypothalamus-pituitary-interrenal axis activity increases prior to hatching in Eleutherodactylus coqui embryos

I report an increase in whole body CORT content prior to hatching in *E. coqui*, suggesting that activity of the HPI axis in *E. coqui* embryos increases at this life history transition. This result is consistent with previous studies that report formation of the median eminence approximately two-thirds of the way through embryonic development (TS stage 10), at approximately the same time as the thyroid gland is first distinguishable histologically (Jennings and Hanken, 1998; Jennings, Evans and Hanken, 2015). At TS stage 10, the *E. coqui* embryo has clearly formed digits and a full, vascularized tail fin.

Many vertebrates experience a peak in GC production coincident with life history transitions: at birth in humans; at hatching in reptiles, some birds and fishes; and during metamorphosis in flatfish and amphibians (Murphy Pearson, 1982; Wada, 2008). Patterns of whole body CORT content have been documented in several frog species; whole body CORT content significantly rises at metamorphic climax (Glennemeier and Denver, 2002; Krain and Denver, 2004).

Glucocorticoids are important mediators of age- and context-dependent life history transitions in vertebrates (Wada, 2008; Denver, 2009; Crespi *et al.*, 2013). An active HPI axis at time of hatching may confer *E. coqui* embryos with some level of plasticity in the timing of hatching in response to environmental stressors, such as predators. While adult male *E. coqui* typically guard egg

clutches, they may abandon the eggs if the nest is disturbed (Michael 1995; Laslo, personal observation). Therefore embryos cannot depend on continuous paternal care, and early hatching in the face of predator attacks and physical disturbances of the clutch may be advantageous (Warkentin 1995).

Finally, GC induce lung morphological development and production of alveolar surfactant in mammals (deLemos *et al.*, 1970; Motoyama *et al.*, 1971; Ballard, 1989; Grier and Halliday, 2004), and the HPI axis is necessary for functional lung development in humans and mice (Muglia *et al.*, 1995; Cole *et al.*, 2001; Saedler and Hochgeschwender, 2011). Additionally, synergistic effects of TH and GC are observed in promoting mammalian lung maturation (Hitchcock, 1979; Gonzalez *et al.*, 1986). In *Xenopus tropicalis* and *Rana catesbeiana*, *glucocorticoid receptor* (*gr*), *thyroid hormone receptor alpha* (*thra*), *thrb* and *klf9* mRNA peak in the lungs during natural metamorphosis (Veldhoen, Stevenson and Helbing, 2015; Shewade *et al.*, 2017), supporting the lungs as a target of GC signaling in frogs. As *E. coqui* development proceeds, the tail shrinks and the froglets likely switch to gas exchange via the lungs, much like metamorphosing frogs switch to lungs as their gills resorb (Burggren and Infantino, 1994). Future studies should examine the likely role of the HPI axis in lung development in *E. coqui*.

Combined CORT and T_3 treatment synergistically promote tail resorption

Eleutherodactylus coqui embryos exhibit tissue-specific responses to combined exogenous T_3 and CORT treatment. Treatment of *E. coqui* embryos with both CORT and T_3 reduces tail size to a greater extent compared to treatment with just T_3 (Table 2.1). These results are consistent with the ability of glucocorticoids to potentiate TH-mediated metamorphosis as described by many researchers. Frieden and Naile (1955) first described such an interaction of glucocorticoids with TH in *Bufo bufo*. Exogenous GC and TH in combination induce morphological changes consistent with TH-mediated metamorphosis in multiple amphibian species (Gray and Janssens, 1990; Wright *et al.*,

1994; Hayes, 1995; Darras *et al.*, 2002; Kühn *et al.*, 2004, 2005; Bonett, Hoopfer and Denver, 2010). Additionally, studies with CORT synthesis inhibitors suggest that endogenous glucocorticoids synergize with TH to increase whole body T_3 content and promote development near metamorphic climax (Glennemeier and Denver 2002; Hayes and Wu 1995).

Exogenous CORT alone inhibits development in premetamorphic tadpoles. In particular, CORT treatment has antagonistic effects on TH-mediated hind limb development (Wright *et al.*, 1994; Hayes and Wu, 1995; Lorenz *et al.*, 2009; Kulkarni and Gramapurohit, 2016). In the present study, treatment with high CORT (500 nM) concentrations alone or with T_3 and CORT in combination resulted in shorter and wider hind limbs in *E. coqui*, a morphology consistent with inhibited growth. Such inhibited growth may have implications for juvenile fitness. For example, both *E. coqui* and *Hylarana indica* froglets with shorter hind limbs cannot jump as far as controls, which presumably affects their ability to escape predators (Buckley, Michael and Irschick, 2005; Kulkarni and Gramapurohit, 2016).

It is also possible that exogenous CORT and T_3 have pharmacological effects on *E. coqui*. However, the concentrations of exogenous T_3 and CORT used in this study are about 2-fold higher than and equal to the maximum whole body content of each endogenous hormone, respectively. Krain and Denver (2004) showed that *X. laevis* tadpoles immersed in CORT and T_3 take up each hormone to a different extent. Therefore, it is possible that the tail may be more exposed to exogenous hormones than other tissues; it is highly vascularized and likely a site of gas exchange.

Combined CORT and T_3 treatment increases TH target gene expression in E. coqui tail

mRNA levels of T_3-response genes in the *E. coqui* tail after treatment with both CORT and T_3 suggest that these hormones increase sensitivity to T_3 and availability of T_3. Increased *thrb* mRNA in the *E. coqui* tail is consistent with results with *X. tropicalis* tail explants (Bonett, Hoopfer and

Denver, 2010) and in *E. coqui* whole embryos after injection with ovine corticotropin-releasing factor (CRF) (Kulkarni, Singamsetty and Buchholz, 2010). *Deiodinase type III* mRNA increased at 46 hr of treatment with both hormones, then decreased after 120 hr, suggesting that conversion of T_3 to biologically inactive forms may also decrease. *Deiodinase type III* mRNA also increases in *X. tropicalis* tail explants, but CRH or DEX (a synthetic corticoid) alone decreases D3 activity in axolotl liver and in *Rana catesbeiana* tadpoles (Galton, 1990; Kühn *et al.*, 2005). Gene expression responses probably differ between tissue and species.

Corticosterone may also directly influence mRNA levels of T_3-response genes, particularly *klf9*, in the *E. coqui* tail. *Krüppel-like factor 9* is directly induced by both TH and CORT individually and together (synergistically) in tadpole and mouse brain (Bonett *et al.*, 2009; Bagamasbad *et al.*, 2012) due to a highly conserved sequence. This highly conserved sequence, called the KLF9 synergy module, is upstream of the KLF9 gene in tadpole and mouse and contains both TR and glucocorticoid receptor response elements (Bagamasbad *et al.*, 2015). *Krüppel-like factor 9* mRNA is also induced by CORT in *X. tropicalis* brain, lung and tail (Shewade *et al.*, 2017). I found this region in the *E. coqui* genome as well (data not shown). Kruppel-like factor 9 also binds to the promotor of TRβ (Bagamasbad *et al.*, 2008), and it promotes TRβ autoinduction and expression of *thibz* and *klf9* mRNA in tadpole brain (Hu, Knoedler and Denver, 2016).

Conclusion

In this chapter, I show that 1) HPI axis activity increases at hatching in the direct-developing frog *E. coqui*, and 2) treatment with CORT and T_3 in combination synergistically induces T_3-response gene expression, including *dio3* and *thrb*, in the *E. coqui* tail. This transcriptional synergy likely underlies the synergistic tail resorption observed after treatment with exogenous CORT and T_3. Experiments with CORT and TH synthesis inhibitors could determine if endogenous CORT

enhances the effects of TH and promotes rapid tail resorption *in vivo*. The synergistic effects of CORT and T_3 on morphology and transcription of T_3-response gene appears to be shared between *E. coqui* and metamorphosing frogs, but tail resorption begins prior to hatching, in contrast to the postembryonic tail resorption characteristic of metamorphosing frogs.

REFERENCES

Bagamasbad, P. *et al.* (2008) 'A role for basic transcription element-binding protein 1 (BTEB1) in the autoinduction of thyroid hormone receptor beta', *The Journal of Biological Chemistry*, 283(4), pp. 2275–85. doi: 10.1074/jbc.M709306200.

Bagamasbad, P. *et al.* (2012) 'Molecular basis for glucocorticoid induction of the Kruppel-like factor 9 gene in hippocampal neurons', *Endocrinology*, 153(11), pp. 5334–45. doi: 10.1210/en.2012-1303.

Bagamasbad, P. D. *et al.* (2015) 'Deciphering the regulatory logic of an ancient, ultraconserved nuclear receptor enhancer module', *Molecular Endocrinology*, 29(6), pp. 856–872. doi: 10.1210/me.2014-1349.

Ballard, P. L. (1989) 'Hormonal regulation of pulmonary surfactant', *Endocrine Reviews*, 10(2), pp. 165–181.

Bonett, R. M. *et al.* (2009) 'Stressor and glucocorticoid-dependent induction of the immediate early gene krüppel-like factor 9: implications for neural development and plasticity', *Endocrinology*, 150(4), pp. 1757–65. doi: 10.1210/en.2008-1441.

Bonett, R. M., Hoopfer, E. D. and Denver, R. J. (2010) 'Molecular mechanisms of corticosteroid synergy with thyroid hormone during tadpole metamorphosis', *General and Comparative Endocrinology*. Elsevier Inc., 168(2), pp. 209–19. doi: 10.1016/j.ygcen.2010.03.014.

Boorse, G. C. and Denver, R. J. (2003) 'Endocrine mechanisms underlying plasticity in metamorphic timing in spadefoot toads', *Integrative and Comparative Biology*, 43(5), pp. 646–57. doi: 10.1093/icb/43.5.646.

Buckley, C. R., Michael, S. F. and Irschick, D. J. (2005) 'Early hatching decreases jumping performance in a direct-developing frog, *Eleutherodactylus coqui*', *Functional Ecology*, pp. 67–72. doi: 10.1111/j.0269-8463.2005.00931.x.

Burggren, W. W. and Infantino, R. L. (1994) 'The respiratory transition from water to air breathing during amphibian metamorphosis', *American Zoologist*, 34(2), pp. 238–246.

Callery, E. M. and Elinson, R. P. (2000) 'Thyroid hormone-dependent metamorphosis in a direct developing frog', *Proceedings of the National Academy of Sciences of the United States of America*, 97(6), pp. 2615–20. doi: 10.1073/pnas.050501097.

Callery, E. M., Fang, H. and Elinson, R. P. (2001) 'Frogs without polliwogs: evolution of anuran direct development', *BioEssays: news and reviews in molecular, cellular and developmental biology*, 23(3), pp. 233–41. doi: 10.1002/1521-1878(200103)23:3<233::AID-BIES1033>3.0.CO;2-Q.

Cole, T. J. *et al.* (2001) 'GRKO mice express an aberrant dexamethasone-binding glucocorticoid receptor, but are profoundly glucocorticoid resistant', *Molecular and Cellular Endocrinology*, 173, pp. 193–202.

Crespi, E. J. *et al.* (2013) 'Life history and the ecology of stress: How do glucocorticoid hormones influence life-history variation in animals?', *Functional Ecology*, 27(1), pp. 93–106. doi: 10.1111/1365-2435.12009.

Darras, V. M. *et al.* (2002) 'Effects of dexamethasone treatment on iodothyronine deiodinase activities and on metamorphosis-related morphological changes in the axolotl (*Ambystoma mexicanum*)', *General and Comparative Endocrinology*, 127(2), pp. 157–164.

deLemos, R. A. *et al.* (1970) 'Acceleration of appearance of pulmonary surfactant in the fetal lamb by administration of corticosteroids', *American Review of Respiratory Disease*, 102(3), pp. 459–461.

Denver, R. J. (1998) 'Hormonal correlates of environmentally induced metamorphosis in the western spadefoot toad, *Scaphiopus hammondii*', *General and Comparative Endocrinology*, 110(3), pp. 326–336.

Denver, R. J. (2009) 'Stress hormones mediate environment-genotype interactions during amphibian development', *General and Comparative Endocrinology*, 164(1), pp. 20–31. doi: 10.1016/j.ygcen.2009.04.016.

Denver, R. J. (2013) 'Neuroendocrinology of amphibian metamorphosis', in Shi, Y. (ed.) *Current Topics in Developmental Biology*. 1st edn. Burlington: Elsevier Inc., pp. 195–227. doi: 10.1016/B978-0-12-385979-2.00007-1.

Frieden, E. and Naile, B. (1955) 'Biochemistry of amphibian metamorphosis: I. enhancement of induced metamorphosis', *Science*, 121(3132), pp. 37–39.

Galton, V. A. (1990) 'Mechanisms underlying the acceleration of thyroid hormone-induced tadpole metamorphosis by corticosterone', *Endocrinology*, 127(6), pp. 2997–3002.

Gao, X. *et al.* (1994) 'Expression of the glucocorticoid receptor gene is regulated during early embryogenesis of *Xenopus laevis*', *Biochimica et Biphysica Acta*, 1218, pp. 194–198.

Glennemeier, K. A. and Denver, R. J. (2002a) 'Developmental changes in interrenal responsiveness in anuran amphibians', *Integrative and Comparative Biology*, 42(3), pp. 565–573.

Glennemeier, K. A. and Denver, R. J. (2002b) 'Role for corticoids in mediating the response of *Rana pipiens* tadpoles to intraspecific competition', *Journal of Experimental Zoology*, 292(1), pp. 32–40. doi: 10.1002/jez.1140.

Gomez-Mestre, I., Kulkarni, S. and Buchholz, D. R. (2013) 'Mechanisms and consequences of developmental acceleration in tadpoles responding to pond drying', *PloS One*, 8(12), p. e84266. doi: 10.1371/journal.pone.0084266.

Gonzalez, L. W. *et al.* (1986) 'Glucocorticoids and thyroid hormones stimulate biochemical and morphological differentiation of human fetal lung in organ culture', *The Journal of Clinical Endocrinology and Metabolism*, 62(4), pp. 678–691.

Gray, K. M. and Janssens, P. A. (1990) 'Gonadal hormones inhibit the induction of metamorphosis by thyroid hormones in *Xenopus laevis* tadpoles *in vivo*, but not *in vitro*', *General and Comparative*

Endocrinology, 77(2), pp. 202–211.

Grier, D. G. and Halliday, H. L. (2004) 'Effects of glucocorticoids on fetal and neonatal lung development', *Treatments in Respiratory Medicine*, 3(5), pp. 295–306.

De Groef, B. *et al.* (2006) 'Role of corticotropin-releasing hormone as a thyrotropin-releasing factor in non-mammalian vertebrates', *General and Comparative Endocrinology*, 146(1), pp. 62–8. doi: 10.1016/j.ygcen.2005.10.014.

Hayes, T. B. (1995) 'Interdependence of corticosterone and thyroid hormones in larval toads (*Bufo boreas*). I. Thyroid hormone-dependent and independent effects of corticosterone on growth and development', *The Journal of Experimental Zoology*, 271(2), pp. 95–102. doi: 10.1002/jez.1402710204.

Hayes, T. B. and Wu, T. H. (1995) 'Interdependence of corticosterone and thyroid hormones in toad larvae (*Bufo boreas*). II. Regulation of corticosterone and thyroid hormones', *The Journal of Experimental Zoology*, 271(2), pp. 103–11. doi: 10.1002/jez.1402710205.

Hitchcock, K. R. (1979) 'Hormones and the lung I. Thyroid hormones and glucocorticoids in lung development', *The Anatomical Record*, 194(1), pp. 15–40.

Hu, F., Knoedler, J. R. and Denver, R. J. (2016) 'A mechanism to enhance cellular responsivity to hormone action: Krüppel-like factor 9 promotes thyroid hormone receptor beta autoinduction during postembryonic brain development', *Endocrinology*, 157(4), pp. 1683–1693. doi: 10.1210/en.2015-1980.

Jaffe, R. C. (1981) 'Plasma concentration of corticosterone during *Rana catesbeiana* tadpole metamorphosis', *General and Comparative Endocrinology*, 44(3), pp. 314–318. doi: 10.1016/0016-6480(81)90007-1.

Jennings, D. H., Evans, B. and Hanken, J. (2015) 'Development of neuroendocrine components of the thyroid axis in the direct-developing frog *Eleutherodactylus coqui*: Formation of the median eminence and onset of pituitary TSH production', *General and Comparative Endocrinology*. Elsevier Inc., 214, pp. 62–67. doi: 10.1016/j.ygcen.2015.01.029.

Jennings, D. H. and Hanken, J. (1998) 'Mechanistic basis of life history evolution in anuran amphibians: thyroid gland development in the direct-developing frog, *Eleutherodactylus coqui*', *General and Comparative Endocrinology*, 111(2), pp. 225–32. doi: 10.1006/gcen.1998.7111.

Kloas, W., Reinecke, M. and Hanke, W. (1997) 'Stage-dependent changes in adrenal steroids and catecholamines during development in *Xenopus laevis*', *General and Comparative Endocrinology*, 108, pp. 416–426.

Krain, L. P. and Denver, R. J. (2004) 'Developmental expression and hormonal regulation of glucocorticoid and thyroid hormone receptors during metamorphosis in *Xenopus laevis*', *The Journal of Endocrinology*, 181(1), pp. 91–104.

Kühn, E. R. *et al.* (2004) 'Low submetamorphic doses of dexamethasone and thyroxine induce complete metamorphosis in the axolotl (*Ambystoma mexicanum*) when injected together', *General and*

Comparative Endocrinology, 137(2), pp. 141–147. doi: 10.1016/j.ygcen.2004.03.005.

Kühn, E. R. *et al.* (2005) 'Corticotropin-releasing hormone-mediated metamorphosis in the neotenic axolotl *Ambystoma mexicanum*: Synergistic involvement of thyroxine and corticoids on brain type II deiodinase', *General and Comparative Endocrinology*, 143, pp. 75–81. doi: 10.1016/j.ygcen.2005.02.022.

Kulkarni, P. S. and Gramapurohit, N. P. (2016) 'Effect of corticosterone on larval growth, antipredator behaviour and metamorphosis of *Hylarana indica*', *General and Comparative Endocrinology*. Elsevier Inc., 251, pp. 21–29. doi: 10.1016/j.ygcen.2016.09.001.

Kulkarni, S. S., Singamsetty, S. and Buchholz, D. R. (2010) 'Corticotropin-releasing factor regulates the development in the direct developing frog, *Eleutherodactylus coqui*', *General and Comparative Endocrinology*, 169(3), pp. 225–30. doi: 10.1016/j.ygcen.2010.09.009.

Lorenz, C. *et al.* (2009) 'Corticosteroids disrupt amphibian metamorphosis by complex modes of action including increased prolactin expression', *Comparative Biochemistry and Physiology, Part C*, 150, pp. 314–321. doi: 10.1016/j.cbpc.2009.05.013.

Michael, S. F. (1995) 'Captive breeding of two species of *Eleutherodactylus* (Anura: Leptodactylidae) from Puerto Rico, with notes on behavior in captivity', *Herpetological Review*, 26(1), pp. 27–28.

Motoyama, E. K. *et al.* (1971) 'Effect of cortisol on the maturaion of fetal rabbit lungs', *Pediatrics*, 48(4), pp. 547–555.

Muglia, L. *et al.* (1995) 'Corticotropin-releasing hormone deficiency reveals major fetal but not adult glucocorticoid need', *Nature*, 373(2), pp. 427–431.

Murphy Pearson, B. E. (1982) 'Human fetal serum cortisol levels related to gestational age: Evidence of a midgestational fall and a steep late gestational rise, independent of sex or mode of delivery', *American Journal of Obstetrics and Gynecology*, 144(3), pp. 276–282.

Niki, K., Yoshizato, K. and Kikuyama, S. (1981) 'Augmentation of nuclear binding capacity for triiodothyroine by aldosterone in tadpole tail', *Proceedings of the Japan Academy*, 57(7), pp. 271–275.

Saedler, K. and Hochgeschwender, U. (2011) 'Impaired neonatal survival of pro-opiomelanocortin null mutants', *Molecular and Cellular Endocrinology*. Elsevier Ireland Ltd, 336(1–2), pp. 6–13. doi: 10.1016/j.mce.2010.12.005.

Shewade, L. H. *et al.* (2017) 'In-vivo regulation of Krüppel-like factor 9 by corticosteroids and their receptors across tissues in tadpoles of *Xenopus tropicalis*', *General and Comparative Endocrinology*. Elsevier Inc., 248, pp. 79–86. doi: 10.1016/j.ygcen.2017.02.007.

Suzuki, M. R. and Kikuyama, S. (1983) 'Corticoids augment nuclear binding capacity for triiodothyronine in bullfrog tadpole tail fins', *General and Comparative Endocrinology*, 52(2), pp. 272–278.

Townsend, D. and Stewart, M. (1985) 'Direct development in *Eleutherodactylus coqui* (Anura: Leptodactylidae): a staging table', *Copeia*, 1985(2), pp. 423–436.

Veldhoen, N., Stevenson, M. R. and Helbing, C. C. (2015) 'Comparison of thyroid hormone-dependent gene responses in vivo and in organ culture of the American bullfrog (*Rana* (*Lithobates*) *catesbeiana*) lung', *Comparative Biochemistry and Physiology - Part D: Genomics and Proteomics*. Elsevier Inc., 16, pp. 99–105. doi: 10.1016/j.cbd.2015.09.001.

Wada, H. (2008) 'Glucocorticoids: mediators of vertebrate ontogenetic transitions', *General and Comparative Endocrinology*, 156(3), pp. 441–53. doi: 10.1016/j.ygcen.2008.02.004.

Warkentin, K. M. (1995) 'Adaptive plasticity in hatching age: A response to predation risk trade-offs', *Proceedings of the National Academy of Sciences of the United States of America*, 92(8), pp. 3507–3510.

Wright, M. L. *et al.* (1994) 'Anterior pituitary and adrenal cortical hormones accelerate or inhibit tadpole hindlimb growth and development depending on stage of spontaneous development or thyroxine concentration in induced metamorphosis', *The Journal of Experimental Zoology*, 270(2), pp. 175–188.

Chapter 3: Evolutionary conservation of gene expression dynamics in *Eleutherodactylus coqui* and *Xenopus tropicalis* hind limb

INTRODUCTION

Direct-developing frogs undergo a cryptic metamorphosis prior to hatching, in contrast to most frogs that undergo a thyroid hormone (TH) dependent postembryonic metamorphosis. This cryptic metamorphosis includes development of adult features, such as limbs, and resorption of larval-specific features, such as gills and tail (Elinson, Pino and Townsend, 1990; Elinson, 2013). Despite multiple independent origins of direct development in frogs (Pough *et al.*, 2015; Feng *et al.*, 2017), only a handful of studies have compared particular features of the cryptic metamorphosis of direct-developing frogs with postembryonic metamorphosis of indirect-developing frogs (Elinson, 2013). The hind limbs of direct-developing frogs are one feature of particular interest because their development differs from that of their metamorphosing counterparts in several ways.

Thyroid hormone (TH) is required for limb development in metamorphosing frogs: tadpoles treated with a TH-synthesis inhibitor develop only a limb bud (Brown *et al.*, 2005). In contrast, direct-developing frogs, in addition to developing limbs *in ovo*, begin to develop limbs prior to histological appearance of thyroid follicles (Townsend and Stewart, 1985; Jennings and Hanken, 1998). This observation initially led to the hypothesis that limb development in direct-developing frogs does not require TH. However, this hypothesis ignores the presence in direct-developing frogs of a large yolk with maternally derived nutrients, including thyroid hormone (Laslo, Denver and Hanken, 2019).

Studies with exogenous triiodothyronine (T_3; the most biologically active TH) and with TH-synthesis inhibitors suggest a partial role for TH in later stages of limb development in direct-developing frogs (Lynn 1948; Lynn & Peadon 1955). In *E. coqui*, for example, exogenous T_3 has little to no effect on limb elongation (Elinson, 1994), but treatment with methimazole, a TH-synthesis inhibitor, inhibits terminal stages of limb development and elongation. However, treatment with exogenous T_3 likely has no effect because of the impermeability of the *E. coqui* integument; treatment

of tissue explants with exogenous hormone induces a robust gene expression response (Laslo, Denver and Hanken, 2019). Moreover, while methimazole treatment does not affect early limb differentiation or digit formation (Callery and Elinson, 2000), this result does not address the possible role of maternally derived TH that is already present at this stage. Future experiments should directly address the role of maternal thyroid hormone in development of a direct-developing frog.

Embryonic *E. coqui* have the requisite TH-signaling components present throughout hind limb development. Thyroid hormone acts by binding to the nuclear thyroid hormone receptors (TRs; designated alpha and beta) and promoting or repressing transcription of T_3-response genes in target tissue (Cheng, Leonard and Davis, 2010). Deiodinase enzymes metabolize iodothyronines into more or less biologically active forms. For example, deiodinase type II converts thyroxine (T_4) into more active iodothyronine T_3, while deiodinase type III metabolizes T_4 and T_3 into the less active rT_3 and T_2, respectively (Galton, 1989; Brown, 2005). *Eleutherodactylus coqui* embryos begin to produce TH about two-thirds of the way through development, but maternally provisioned TH is present prior to embryonic production of TH (Laslo *et al.,* 2019). Additionally, TR and deiodinase mRNA expression dynamics mirror those described in the metamorphosing frog *Xenopus tropicalis* (Laslo, *et al.* 2019).

Studies in metamorphosing frogs suggest that TH activates or represses tissue-specific transcriptional networks. Exogenous T_3 induces a tailfin-specific program in metamorphosing frogs (Brown *et al.*, 1996; Kerdivel *et al.*, 2019). Expression of a dominant-negative TR inhibits limb muscle development, muscle innervation, and cartilage growth in *Xenopus laevis* tadpole hind limbs (Schreiber *et al.*, 2001; Das *et al.*, 2002; Brown *et al.*, 2005). Tissue-specific transcriptional programs have been characterized in metamorphosing frogs with several microarray and RNA-seq studies (Helbing *et al.*, 2003; Das *et al.*, 2006; Buchholz *et al.*, 2007; Wen *et al.*, 2019). These studies provide

several thousand candidate genes that may be regulated by T_3 during hind limb development in *E. coqui*.

In addition to the TRs and the deiodinases, it is likely that *E. coqui* and *X. tropicalis* have similar hind limb gene expression programs during development. Vertebrate limb development is a highly conserved and modular process. Current evidence suggests that relatively small changes in the vertebrate limb developmental modules are responsible for the diversity of vertebrate limbs we see today (Maier *et al.*, 2017; Young and Tabin, 2017). For example, Bmp signaling underlies interdigital cell death that sculpts individual digits in mice and chicken (Zou and Niswander, 1996; Guha *et al.*, 2002). Despite differing functions, the bat wing and the webbing in duck's feet are both maintained through antagonism of Bmp signaling (Merino *et al.*, 1999; Weatherbee *et al.*, 2006).

In this chapter, I test the hypothesis that orthologous genes, and specifically candidate T_3-regulated genes, share expression patterns in the direct-developing *E. coqui* and the metamorphosing frog *X. tropicalis* during hind limb development. I find that 36% of all orthologous genes and 34% of candidate T_3-regulated genes, including several well-characterized players in TH signaling, have the same developmental expression pattern in both species. These data suggest that at least one third of the gene expression program likely underlying hind limb development is conserved in *E. coqui* hind limb development but expressed prior to hatching rather than during a postembryonic metamorphosis.

METHODS

Animal care

Adult *Eleutherodactylus coqui* were field-collected from introduced populations in Hilo, Hawaii, with the permission of the U.S. Fish and Wildlife Service (permits EX-14-06, EX-16-07, and EX 17-11). Embryos were obtained from spontaneous matings between pairs of these frogs in the Hanken

lab breeding colony (IACUC protocol #99-09-03). Embryos were staged according to the normal table of Townsend & Stewart (TS; 1985), which defines 15 stages from fertilization (1) to hatching (15). Following internal fertilization, the adult female deposits embryos at TS stage 1. *Xenopus tropicalis* tadpoles were ordered from Xenopus1 (Ann Arbor) at Nieuwkoop and Faber (1994) stage 48 and kept at 26˚ C in an aerated 5-gallon glass aquarium.

Sample preparation

I sampled three morphologically comparable stages of hind limb development in *Xenopus tropicalis* tadpoles and *E. coqui* embryos: the limb paddle stage ("early," TS 7 and NF 53), the digit formation stage ("middle," TS 10 and NF 56) and the mature limb stage ("late," TS 13 and NF 59). These stages were chosen to capture activation of the thyroid gland: in *E. coqui* whole body TH content begins to increase at TS stage 9 (Laslo *et al.* 2019), whereas in *X. laevis* whole body TH content significantly increases at NF 59 but TH is necessary for hind limb development, including paddle development, prior to NF 59 (Krain and Denver, 2004; Brown *et al.*, 2005). Tadpoles and embryos were terminally anesthetized with neutral-buffered 2% MS-222 in 10% Holtfreter solution until they no longer responded to tail pinches (30–60 sec). Both hind limbs were dissected with forceps and sterile scalpels when needed and immediately put into TriZol (Invitrogen) and homogenized with a TissueLyser LT. One pair of hind limbs from one individual represented a biological replicate; I collected four biological replicates at each stage. Because I wanted to collect samples from the same genetic background (from within the same clutch), homogenized tissue was kept at -20˚ C until all samples from the same clutch reached the appropriate sampling stage. Total RNA was isolated from dissected hind limbs following the manufacturer's protocol. Genomic DNA was removed with an Ambion TURBO DNA-*free* kit (cat. #AM1907). Total RNA was quantified with a Qubit Fluorometer 3.0 and checked for purity on a Nanodrop spectrophotometer. RNA

integrity was determined with a high-sensitivity RNA tape on a TapeStation 2200 (Agilent); only samples with RNA integrity numbers (RIN) greater than 8 were chosen to be prepared as cDNA libraries. Eight hundred nanograms of RNA from each sample were used for library construction, except for *X. tropicalis* NF-53 samples, which only had sufficient RNA to make 300 ng.

cDNA library construction and Illumina sequencing

With the help of Harvard Bauer Core Sequencing staff, I used the intengenX Apollo 324 System and the PrepX™ polyA 48 kit to enrich each sample for mRNA, and the PrepX™ mRNA 48 kit to construct cDNA libraries for each sample. PCR was performed to amplify each library and incorporate sample-specific adapters (Bauer Core, Harvard University) onto the cDNA fragments for multiplex sequencing. Twelve cycles of PCR were performed for all samples except *X. tropicalis* NF-53 samples, which required 15 cycles of PCR due to the lower starting amount of RNA. I used AMPure XP beads and the PrepX mRNA 48 PCR Cleanup protocol. I assessed cDNA library quality with the TapeStation 4200. I quantified cDNA library concentration using qPCR, then pooled all the libraries together at equimolar concentration for multiplexed sequencing. Samples were sequenced as paired-end, 125 base-pair reads in a rapid run flowcell on the Illumina HiSeq 2500 at the Bauer Core Facility at Harvard University.

Data analysis

Adapters and overrepresented sequences were removed from sequencing data with TrimGalore (Krueger, 2015) and a custom script from Harvard Bioinformatics (https://github.com/harvardinformatics/TranscriptomeAssemblyTools/blob/master/RemoveFastqcOverrepSequenceReads.py). I used STAR (Dobin *et al.*, 2013) to align *Xenopus tropicalis* sequencing reads to the *X. tropicalis* genome (xenbase.org, v9.1) and RSEM to calculate gene expression levels. I

used limma voom (Law *et al.*, 2014) in R v1.1.383 to perform differential expression analysis at the gene level.

Eleutherodactylus coqui reads were aligned to a draft genome provided by collaborators (A. Mudd, R. Harland, D. Rokhsar) using HiSat2 (Kim, Langmead and Salzberg, 2015); transcript models were extracted with Scallop (Shao and Kingsford, 2017), and I used Stringtie (Pertea *et al.*, 2015) to identify unique transcripts. Because the draft genome is unannotated, I used *Xenopus* proteins to assign a preliminary annotation to as many *E. coqui* transcripts as possible. I used Transdecoder (http://transdecoder.sourceforge.net/) to predict open reading frames from the transcript models, and then used BLASTp (https://blast.ncbi.nlm.nih.gov/Blast.cgi) against *Xenopus tropicalis* proteins to identify orthologous genes within the *E. coqui* transcripts. This resulted in several classes of *E. coqui* transcripts: transcripts with a single *X. tropicalis* protein match ("unique"); transcripts that had multiple *X. tropicalis* protein matches ("multi"); transcripts that had no *X. tropicalis* protein match ("missing"); and transcripts that had no match but could be grouped with a *X. tropicalis* protein because other transcripts from that gene had unique matches ("rescued"). Some transcripts from different *E. coqui* chromosomes matched a single *X. tropicalis* protein equally well, even though that match was unique for each transcript. See Table 3.1 for quantities of all these transcripts. Sorting transcripts in this way yielded 8,867 of a total of 12,176 annotated genes (73%) that could be identified by a single gene symbol and were found on one chromosome. All transcripts except those designated as "missing" were included in the differential expression analysis. See Appendix C - Table S3.1 for a list of those transcripts that had greater than two *X. tropicalis* protein matches. Genes found on more than one chromosome made up 22% of genes that were significantly differentially expressed between *E. coqui* early/middle and middle/late stage hind limbs. I aligned reads to the genome using Bowtie2, quantified reads with RSEM and analyzed differential expression with limma voom as described above for *X. tropicalis*.

Table 3.1. Numbers of *Eleutherodactylus coqui* transcripts that were either missing, unique, rescued or had hits to multiple *Xenopus tropicalis* proteins ("multi"), and the number of each of these of these categories that was found on a single *E. coqui* chromosome.

	Unique	Rescued	Multi	Missing
Number of transcripts	10532	1251	393	13569
Number on one chromosome	7927	940	361	

Gene ontology analysis

Gene ontology overpresentation analysis was performed using the Gene Ontology Resource (http://geneontology.org/, version 2019-05-09) and PANTHER 14.1 with the biological process setting; significance was set at $\alpha < 0.05$. GO analyses were visualized using ReviGO on the default settings (Supek *et al.*, 2011). I used all the genes that were expressed in all libraries as the background for independent GO analysis; when performing GO analysis on orthologous genes, only the set of orthologous genes was used as a background. Only unique *E. coqui* transcripts with a single identifiable gene symbol found on one chromosome were used for GO analysis, with a background of all unique genes on one chromosome.

Literature search

I searched the literature to identify T_3-response genes in hind limbs and other tissues of metamorphosing frogs. Two studies examined the limb (Das *et al.*, 2006; Helbing *et al.*, 2007) while other studies examined the tail, brain and whole tadpole (Helbing *et al.*, 2003; Das *et al.*, 2009; Kulkarni and Buchholz, 2012; Wen *et al.*, 2019). For studies that looked at multiple time points, I retained genes that consistently were either up- or down-regulated. For example, a gene that was detected and significantly up-regulated at one or all three time points was retained, while a gene that was detected at two time points and significantly down- and then up-regulated was not retained. Altogether, I had 1,088 unique candidate T_3-response genes in the limb, 1,070 in the tail, 3,085 in the brain and 300 in the whole tadpole. Preliminary analyses suggested that a very small percentage of

unique limb T_3-response genes were found in the *E. coqui* dataset (6%); thus I included all candidate T_3-response genes regardless of tissue in further analyses.

RESULTS

Transcriptome analyses & filtering

Illumina sequencing yielded 175 and 203 million raw reads for *Eleutherodactylus coqui* and *Xenopus tropicalis* libraries, respectively. Overrepresented sequences were removed to eliminate contamination from ribosomal RNAs, which resulted in 168 (96% of raw reads) and 193 (95% of raw reads) million reads for *E. coqui* and *X. tropicalis*, respectively. I did not impose any quality filtering on the data, anticipating that low quality reads would be removed during alignment to the genome and aggressive filtering can lead to biased expression estimates (Williams *et al.*, 2016). Overall alignment rates of reads ranged from 64 to 68% for *E. coqui* and from 89 to 91% for *X. tropicalis*. Poor quality of the *E. coqui* draft genome assembly may underlie the low overall alignment rate. Amphibian genomes vary greatly in size and are known to have high proportions of repeat regions (Koepfli *et al.*, 2015), making genome assembly difficult. Bacterial contamination could also reduce the alignment rate. I used Centrifuge, a microbial classification tool (Kim *et al.*, 2016), to spot check libraries for bacterial sequences. *Xenopus tropicalis* and *E. coqui* libraries were highly enriched for sequences of *X. tropicalis* and *Nanorana parkeri* (*E. coqui*'s closest relative for which there are publicly available sequences) and showed no enrichment for bacterial sequences. The low alignment rate for *E. coqui* is most likely due to use of Bowtie2, rather than the splice-aware aligner STAR. Bowtie2 is not splice aware, meaning that reads spanning introns are unlikely to align correctly. Alignment rates for the *X. tropicalis* reads with Bowtie2 range from 60% to 73%, suggesting that even with a well-annotated genome, Bowtie2 incorrectly aligns a significant portion of reads.

Gene expression patterns throughout Eleutherodactylus coqui and Xenopus tropicalis hind limb development

I recovered 12,176 *Eleutherodactylus coqui* genes and 15,716 *Xenopus tropicalis* genes for differential expression analysis. In *E. coqui*, expression of 2,548 genes (20.9%) changed between early and middle limb stages, while expression of 3,811 genes (31.3%) changed between middle and late limb stages. A higher proportion of genes changed at each stage in *X. tropicalis*: expression of 6,011 genes (38.2%) changed between early and middle hind limb stages, while expression of 5,652 genes (36%) changed between the middle and late hind limb stages. Similar proportions of genes consistently increased or decreased throughout development. Almost 7% percent of all *X. tropicalis* genes and 8.4% of all *E. coqui* genes increased significantly at both developmental transitions, while 5.5% of *X. tropicalis* genes and 4.4% of all *E. coqui* genes decreased at both developmental transitions (Table 3.2).

Table 3.2. Numbers of significantly regulated genes in *Xenopus tropicalis* and *Eleutherodactylus coqui* between early and middle stages (NF 53/TS 7 and NF 56/TS 10) and middle and late stages (NF 56/TS 10 and NF 59/TS 13) of hind limb development ($p < 0.01$).

Xenopus tropicalis		Middle-Late			*Eleutherodactylus coqui*		Middle-Late		
		Up	Unregulated	Down			Up	Unregulated	Down
Early-Middle	Up	1066	1462	451	Early-Middle	Up	1021	527	53
	Unregulated	1721	6718	1266		Unregulated	1184	7449	995
	Down	288	1884	860		Down	21	389	537

To understand the function of genes that changed throughout development, I performed a gene ontology (GO) analysis. In *E. coqui*, genes that increased throughout development were significantly over-enriched in categories such as myofibril assembly, skeletal muscle tissue development, system processes and cell adhesion (Figure 3.1A, Appendix C - Table S3.2). Only 537 genes decreased at both developmental stages in *E. coqui*. These genes were over-enriched in GO categories related to DNA replication, cell division, chromatin remodeling and DNA repair (Figure 3.1B, Appendix C - Table S3.3). In *X. tropicalis*, genes that increased consistently were enriched in biological processes such as generation of ATP, plasma membrane organization, skeletal muscle development and cellular homeostasis (Figure 3.1C, Appendix C - Table S3.4). In contrast, genes that decreased consistently throughout development were over-enriched in categories such as chromatin remodeling, cell-cell adhesion, tyrosine kinase signaling pathway, regulation of transcription and nervous system development (Figure 3.1D, Appendix C - Table S3.5).

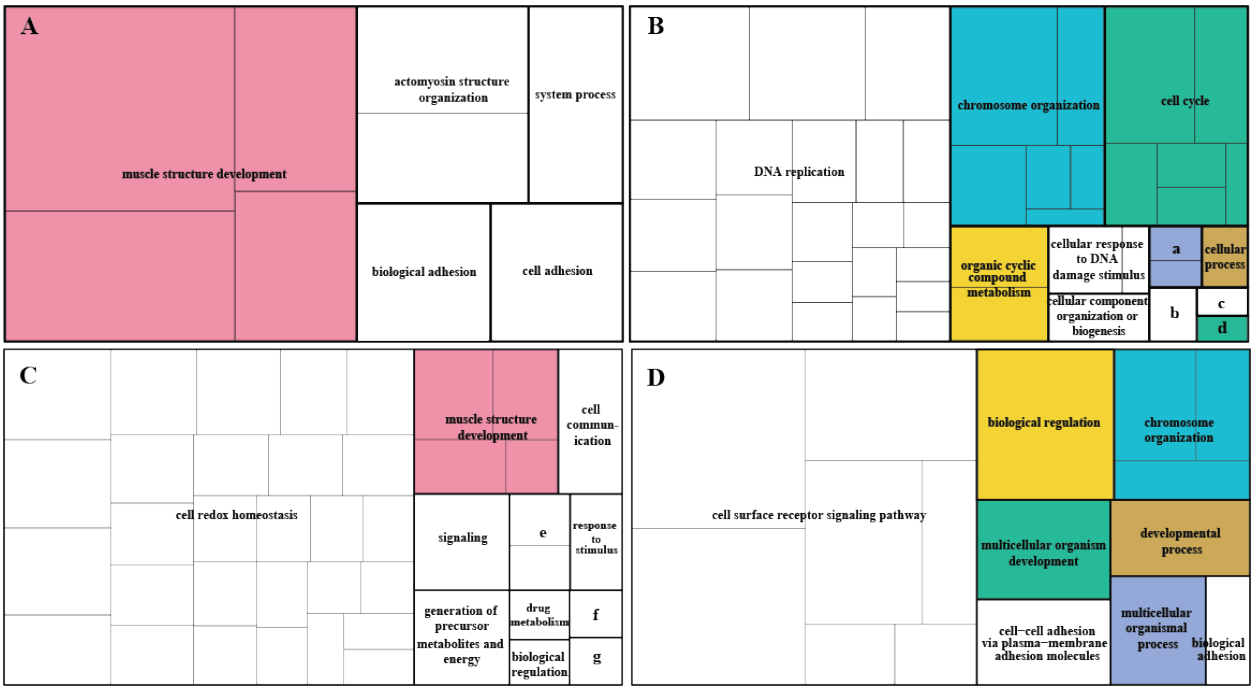

Figure 3.1. Over-enriched gene ontology categories for genes that increased consistently throughout development in *Eleutherodactylus coqui* (A) and *Xenopus tropicalis* (C) and decreased throughout

Figure 3.1 (Continued). development (B) in *E. coqui* and in *X. tropicalis*. Smaller boxes indicate more specific GO categories within the umbrella GO term; all GO terms can be found in Appendix C. Colored boxes highlight similar GO categories present in both species. Labels for small boxes: a, organic substance metabolism; b, nitrogen compound metabolism; c, biological process; d, protein localization to chromosome; e, carbohydrate metabolism; f, carbohydrate catabolism; g, ion transmembrane transport.

A small fraction of the total transcripts detected decreased then increased (*E. coqui*: 0.17%; *X. tropicalis*: 1.8%) or increased then decreased (*E. coqui*: 0.44%; *X. tropicalis*: 2.9%) during hind limb development. Genes with these expression patterns were not over or under-enriched in any GO categories in *E. coqui*. However, genes with these expression patterns in *X. tropicalis* were over-enriched in the GO categories catabolic processes and signal transduction, respectively.

Identifying matching and mismatching gene expression patterns between species

I identified 6,975 shared orthologous genes in *Xenopus tropicalis* and *Eleutherodactylus coqui*. Of these 6,975 genes, 2,578 (36.9%) shared the same expression pattern in both species throughout development (Table 3.3, outlined cells; Figure 3.2A and B). I considered both statistical significance and direction of fold change in determining which genes had matching expression patterns. For example, *myogenic factor 6* (*myf6*) significantly increased between early and middle and between middle and late hind limb stages in both *E. coqui* and *X. tropicalis* (Figure 3.2A; Student's t-test, $p < 0.01$). The remaining 4,379 genes (63.1%) did not have matching expression patterns in both species. Because I considered expression patterns across all three stages of hind limb development, an expression pattern was considered "mismatching" if it differed between species in statistical significance or direction in at least one developmental stage (see Table 3.3).

Table 3.3. Distribution of gene expression patterns between *Xenopus tropicalis* and *Eleutherodactylus coqui*. Expression patterns that match between species are along the top-left-to-bottom-right diagonal (outlined cells). Expression patterns that are the opposite in each species are outlined with dashes. Darker green color in a cell indicates that a higher proportion of genes fall in that category; white cells indicate a low proportion.

Eleutherodactylus coqui		*Xenopus tropicalis*								
	early-middle:	**Down**			**Unregulated**			**Up**		
	middle-late:	**Down**	**Unreg-ulated**	**Up**	**Down**	**Unreg-ulated**	**Up**	**Down**	**Unreg-ulated**	**Up**
early-middle:	middle-late:									
Down	**Down**	**1.41%**	0.95%	0.04%	1.03%	1.53%	0.00%	0.03%	0.06%	**0.01%**
	Unreg-ulated	0.14%	**0.90%**	0.10%	0.52%	1.56%	0.27%	0.01%	0.13%	0.10%
	Up	0.01%	0.01%	**0.00%**	0.00%	0.06%	0.09%	**0.00%**	0.03%	0.03%
Unreg-ulated	**Down**	1.51%	1.43%	0.07%	**1.23%**	3.04%	0.11%	0.16%	0.26%	0.07%
	Unreg-ulated	2.84%	7.67%	1.18%	4.85%	**27.74%**	6.80%	0.89%	5.05%	2.38%
	Up	0.23%	0.66%	0.40%	0.36%	3.53%	**2.42%**	0.13%	1.32%	2.04%
Up	**Down**	0.14%	0.03%	**0.00%**	0.11%	0.04%	0.01%	**0.07%**	0.01%	0.00%
	Unreg-ulated	0.22%	0.20%	0.07%	0.66%	1.46%	0.29%	0.49%	**0.75%**	0.22%
	Up	**0.07%**	0.27%	0.13%	0.36%	1.33%	0.99%	0.40%	1.85%	**2.44%**

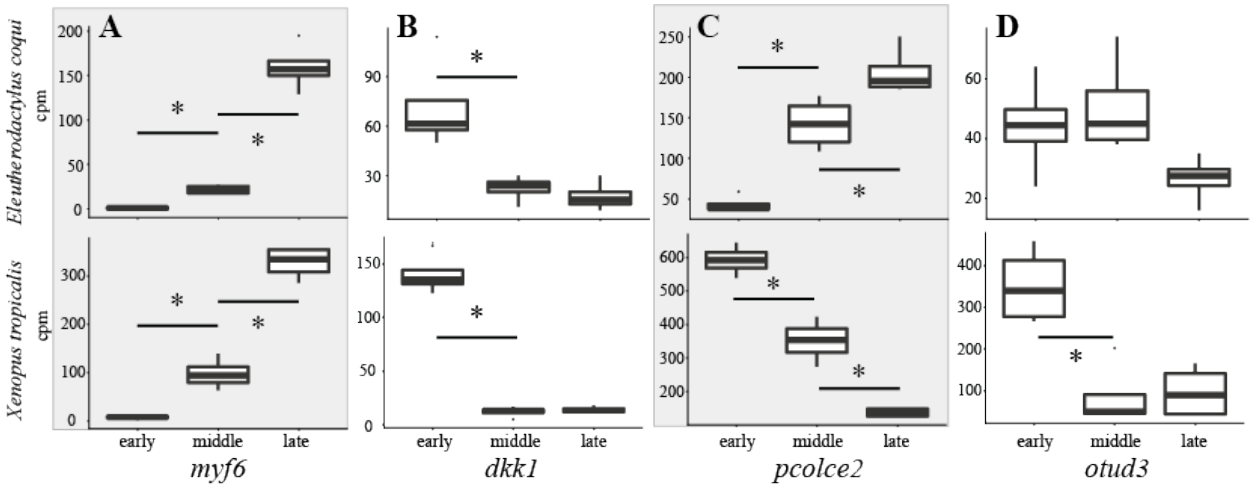

Figure 3.2. Orthologous gene expression patterns in *Eleutherodactylus coqui* and *Xenopus tropicalis* that are representative of matching (A, B), "opposite" mismatching (C) or "unregulated" mismatching expression patterns (D). Each box represents the median and range of four biological replicates.

Genes with shared expression patterns in both Xenopus tropicalis and Eleutherodactylus coqui

Gene ontology analysis of orthologous genes with the same expression pattern in both species showed that genes that increased between at least one developmental stage and did not decrease at any time (Table 3.4, yellow shading) were over-enriched in categories related to skeletal muscle development, carboxylic acid metabolic processes, ion transport and oxidation-reduction processes (Figure 3.3A). In addition to *myf6*, genes in this category include the myogenic factors *myogenic differentiation 1* (*myod1*) and the transcription factor *myocyte enhancer factor 2C* (*mef2c*).

Table 3.4. Nine categories of gene expression pattern that are exact matches between *Xenopus tropicalis* and *Eleutherodactylus coqui*. Gene ontology analysis was performed on genes that increase at one developmental time point (yellow shading) and those that decrease at one developmental time point (green shading).

Matched gene expression patterns		Middle-Late		
		Up	Unregulated	Down
Early-Middle	Up	170	52	5
	Unregulated	169	1935	86
	Down	0	63	98

I also performed GO analysis on genes that decreased at one developmental time point and did not increase (Table 3.4, green shading; Figure 3.2B). This category of genes included several homeodomain transcription factors, such as *lim homeobox 2* (*lhx2*), *even-skipped* (*evx1*), *paired like homeodomain 1* (*pitx1*) and the Wnt antagonist *dickkopf WNT signaling pathway inhibitor 1* (*dkk1*) (Figure 3.2B). These genes were enriched in the GO categories chromosome organization and regulation of DNA-templated transcription (Figure 3.3B).

Gene ontology analysis of the 1,935 genes (27%) that did not change throughout development showed that these genes are over-enriched in translation processes (Figure 3.3C, left side) and under-enriched in GO categories of cell differentiation and tissue development (Figure 3.3C, right side). Only five genes increased and then significantly decreased in both species: *BARX homeobox 1* (*barx1*), *paired box 7* (*pax7*), *creatine kinase brain* (*ckb*), *gap junction protein alpha 5* (*gja5*) and *UTP20 small subunit processome component* (*utp20*).

Figure 3.3. Biological process functional categories for genes shared by *Eleutherodactylus coqui* and *Xenopus tropicalis* that increase throughout development (A), decrease throughout development (B) or are not regulated in either species (C). Right hand side of panel C indicates under-enriched functional categories.

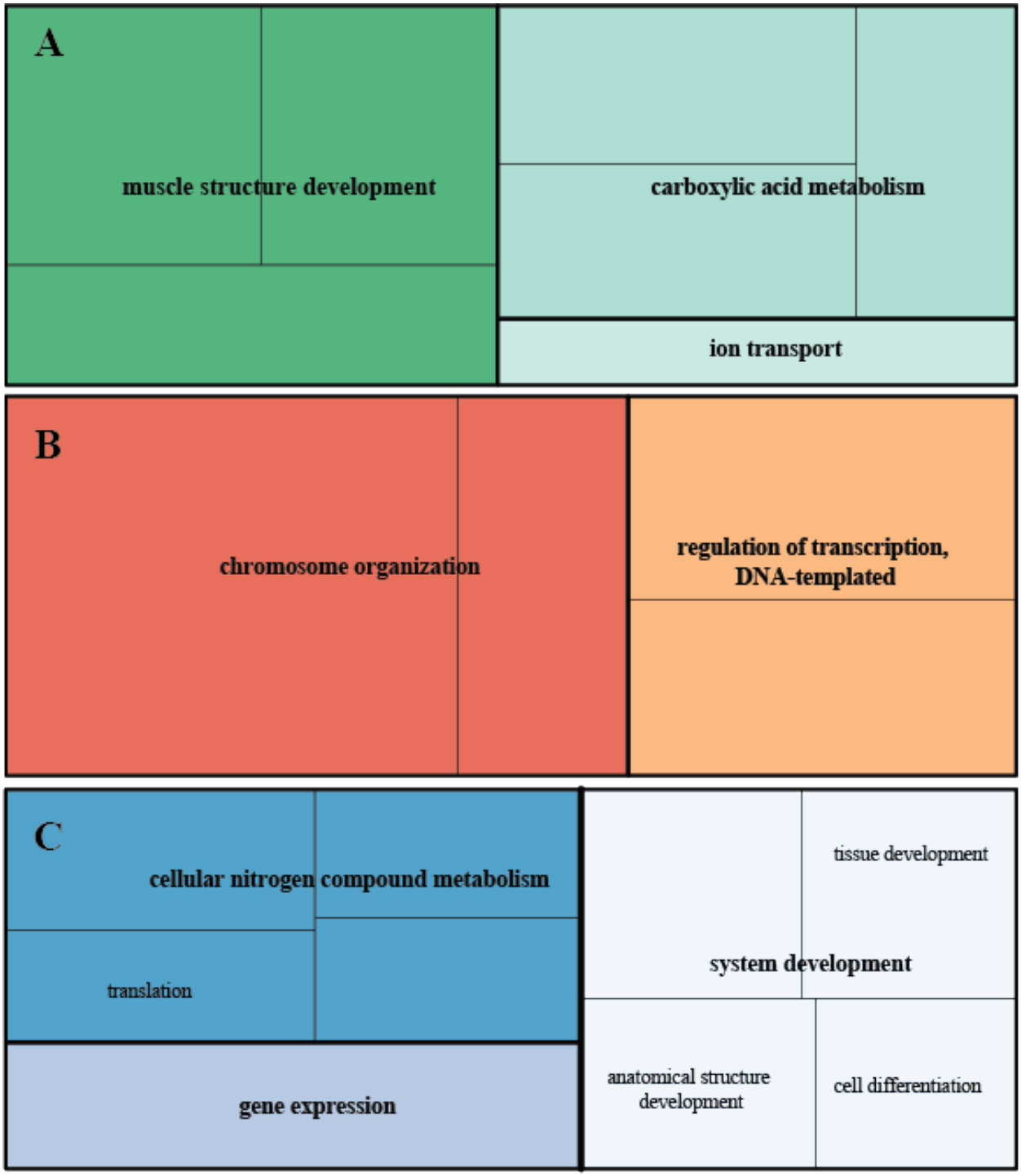
A
muscle structure development
carboxylic acid metabolism
ion transport
B
chromosome organization
regulation of transcription, DNA-templated
C
cellular nitrogen compound metabolism
translation
gene expression
tissue development
system development
anatomical structure development
cell differentiation

Functional categories of genes that do not share expression patterns between species

To better understand how gene expression patterns compare across species, I categorized all genes shared between species into 81 categories based on expression pattern (Table 3.3). In addition to the 36.9% of genes whose expression patterns matched between both species, I considered three overlapping categories of mismatched gene expression patterns for further analysis.

First, I categorized genes that changed in the opposite direction in each species as an "opposite" mismatch. For example, *procollagen C-endopeptidase enhancer 2* (*pcolce2*) significantly increased in *E. coqui* but decreased in *X. tropicalis* throughout development (Figure 3.2C). Second, I looked at genes that had opposing expression patterns between the two species at each developmental transition. This category has some overlap with the first but considers only one developmental stage at a time. For example, this category would include a gene that decreases between the early and middle stage hind limb in *E. coqui* but increases in *X. tropicalis* early to middle hind limb, regardless of the direction or statistical significance of change in the middle to late hind limb. The GO analysis for this category of mismatch had significant overlap with the first category (Appendix C - Tables S3.6 - S3.9). However, these categories account for only 3.4% of the whole data set. Finally, I looked at genes that changed at one or both developmental time points in one species but not the other. For example, *OTU deubiquitinase 3* (*otud3*) did not change in *E. coqui* but significantly decreased between early and middle hind limb stages in *X. tropicalis* (Figure 3.2D; Students t-test, $p < 0.01$). This category of genes with "unregulated" mismatched expression patterns made up 44% of the total data.

Only six genes met the criterion of an opposite mismatch in expression pattern between species: *pcolce2*, *ATP binding cassette subfamily A member 1* (*abca1*), *ATPase Ca++ transporting plasma membrane 2* (*atp2b2*), *fibronectin 1* (*fn1*), *myosin 1D* (*myo1d*) and *glutathione S-transferase omega 2* (*gsto2*)

(Figure 3.2C). Genes that had opposing patterns in *X. tropicalis* and *E. coqui* at one developmental time point were not significantly under- or over-enriched in any GO category.

The largest portion of the data set (44%) that I considered a mismatch in expression pattern between *E. coqui* and *X. tropicalis* were genes that changed once or twice during hind limb development in one species but not the other. These genes were further partitioned into each possible combination of expression patterns between species so that GO analyses could effectively resolve functional categories.

Genes that decreased during at least one developmental transition in *E. coqui* but did not change in *X. tropicalis* are over-enriched in GO categories of cytoskeleton organization involved in mitosis and cell division (Fig 3.4A).

Genes that increased in *X. tropicalis* during hind limb development but did not change in *E. coqui* are over-enriched in aerobic respiration, electron transport chain and translation (Figure 3.4B). Genes that decreased in *X. tropicalis* in the early to middle stage hind limb but are unregulated in *E. coqui* are significantly over-enriched in pattern specification processes, determination of left/right asymmetry and cell projection assembly (Figure 3.4C).

Figure 3.4. Biological process functional categories of genes with different expression patterns in *Eleutherodactylus coqui* and *Xenopus tropicalis*. Panel A represents genes that decrease in *E. coqui* but do not change in *X. tropicalis*; panels B and C represent genes that increase and decrease in *X. tropicalis*, respectively, but do not change in *E. coqui*. Labels for small boxes: a, cellular component organization or biogenesis; b, nitrogen compound metabolism.

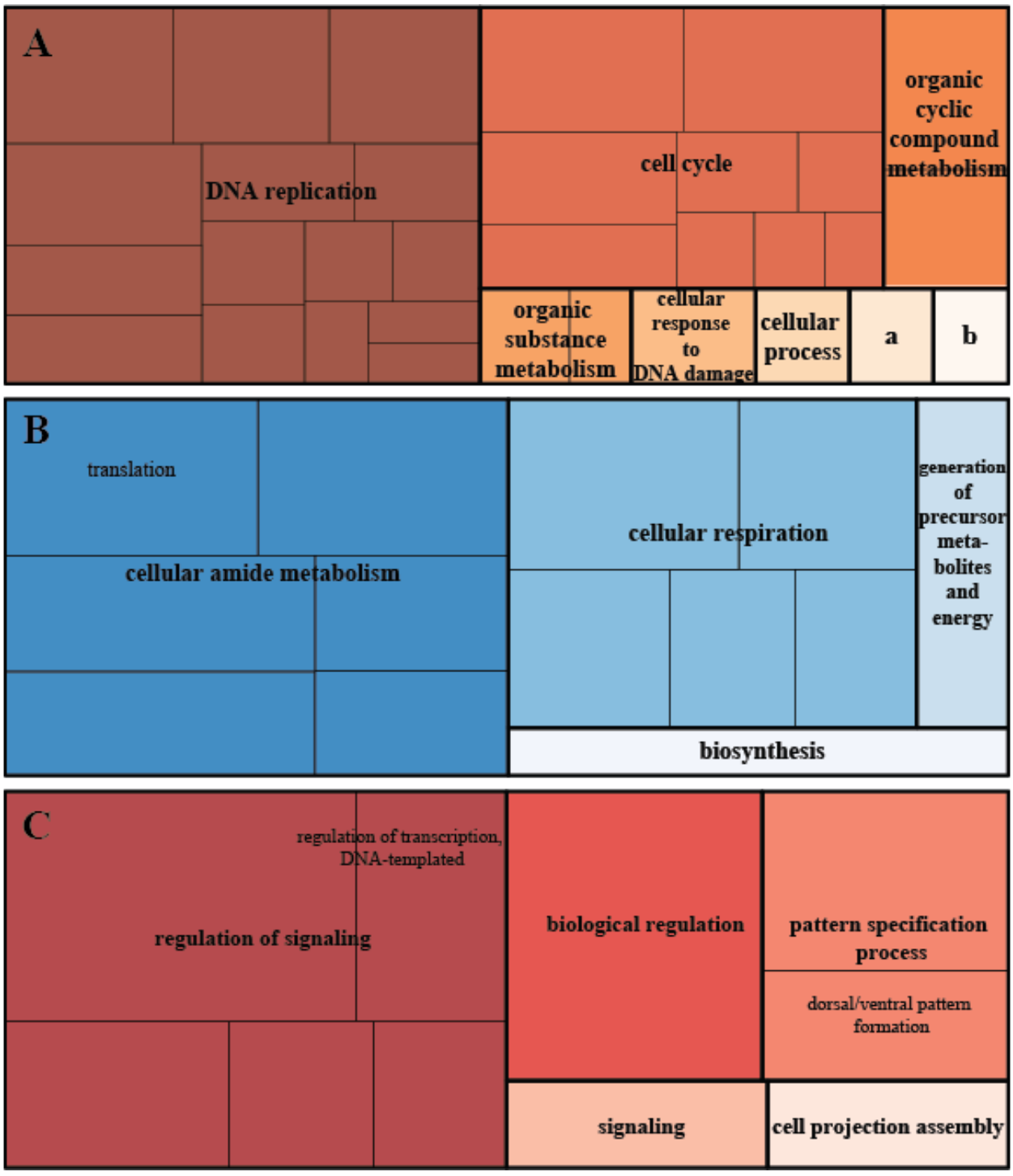
A
DNA replication
cell cycle
organic cyclic compound metabolism
organic substance metabolism
cellular response to DNA damage
cellular process
a
b
B
translation
cellular amide metabolism
cellular respiration
generation of precursor meta-bolites and energy
biosynthesis
C
regulation of transcription, DNA-templated
regulation of signaling
biological regulation
pattern specification process
dorsal/ventral pattern formation
signaling
cell projection assembly

One third of genes regulated in response to exogenous T_3 change during natural development

I searched the literature for candidate genes that are regulated in response to treatment with exogenous T_3. Of the 768 candidate T_3-response genes that are up-regulated in response to exogenous T_3, 75 (9.8%) genes also increased at both developmental time points in the *X. tropicalis* hind limb. When comparing the candidate genes to any genes that increased at one time point in the *X. tropicalis* hind limb (n = 4,249 genes), the proportion of candidate genes that match increased to 36% (n = 205 genes). In contrast, only 6% (n = 35) of the candidate T_3-response genes matched genes that increased at both time points during *E. coqui* hind limb development. Again, expanding the comparison set of genes to those that increased at one developmental time point increased the proportion of matching genes to 19% (n = 103).

Of the 333 candidate T_3-response genes that are down-regulated after treatment with exogenous T_3, 38 (11.4%) are down-regulated throughout development in *X. tropicalis*. When including all genes that decreased at one developmental time point (n = 4,010), the proportion of genes that match the candidate genes increased to 35.8% (n = 119). Similar proportions of candidate T_3 genes match expression patterns in the developing *E. coqui* hind limb: 7.9% (n = 18) of candidate genes consistently decreased and 23.6% (n = 54) decreased at least at one time point.

Conserved T_3-response gene expression patterns between species

I identified 2,405 candidate T_3-response genes in both *Xenopus tropicalis* and *E. coqui*. Candidate T_3-response gene expression patterns between species had the same distribution as all gene expression patterns (Table 3.5). For example, 34.4% (n = 827) of T_3-response genes shared the same pattern across species, including genes known to be mediators of or targets of TH signaling, such as *thyroid hormone receptor β*, *solute carrier family 25, member 23* (*slc25a23*), *nuclear factor 1C* (*nfic*), *krüppel-like factor 4* (*klf4*) and *retinoid X receptor β* (*rxrb*) (Fig 3.5A, B). Genes that have the same

expression pattern in both species are not enriched in any GO category. Of the 65.6% of genes that did not have matching expression patterns in both species, 44.7% were unregulated in one species but regulated in at least one developmental time point in the other ("unregulated" mismatch), while only 1.4% of all genes (*abca1*, *pcolce2*, and *gsto2*) had exact opposing expression patterns in each species ("opposite" mismatch).

Table 3.5. Distribution of gene expression patterns of T_3-respones genes between *Xenopus tropicalis* and *Eleutherodactylus coqui*. Expression patterns that match exactly between species are along the top-left-to-bottom-right diagonal (outlined cells). Expression patterns that are the opposite in each species are outlined with dashes. Darker green color in a cell indicates that a higher proportion of genes fall in that category; white cells indicate a low proportion.

			Xenopus tropicalis								
		early-middle:	**Down**			**Unregulated**			**Up**		
Eleutherodactylus coqui		middle-late:	**Down**	**Unreg-ulated**	**Up**	**Down**	**Unreg-ulated**	**Up**	**Down**	**Unreg-ulated**	**Up**
early-middle:	middle-late:										
Down	**Down**		**1.25%**	1.00%	0.12%	1.12%	1.75%	0.00%	0.04%	0.08%	**0.04%**
	Unregulated		0.04%	**1.00%**	0.04%	0.46%	1.66%	0.33%	0.04%	0.25%	0.04%
	Up		0.00%	0.04%	**0.00%**	0.00%	0.04%	0.04%	**0.00%**	0.04%	0.04%
Unreg-ulated	**Down**		1.54%	1.25%	0.17%	**1.29%**	3.49%	0.25%	0.33%	0.54%	0.12%
	Unregulated		2.58%	7.28%	1.12%	4.12%	**25.86%**	6.53%	0.87%	6.65%	2.91%
	Up		0.29%	0.83%	0.42%	0.46%	3.08%	**2.33%**	0.12%	1.46%	2.04%
Up	**Down**		0.21%	0.04%	**0.00%**	0.08%	0.04%	0.04%	**0.00%**	0.00%	0.00%
	Unregulated		0.25%	0.33%	0.12%	0.79%	1.33%	0.50%	0.54%	**0.83%**	0.25%
	Up		**0.08%**	0.21%	0.25%	0.25%	1.29%	0.75%	0.46%	2.12%	**1.83%**

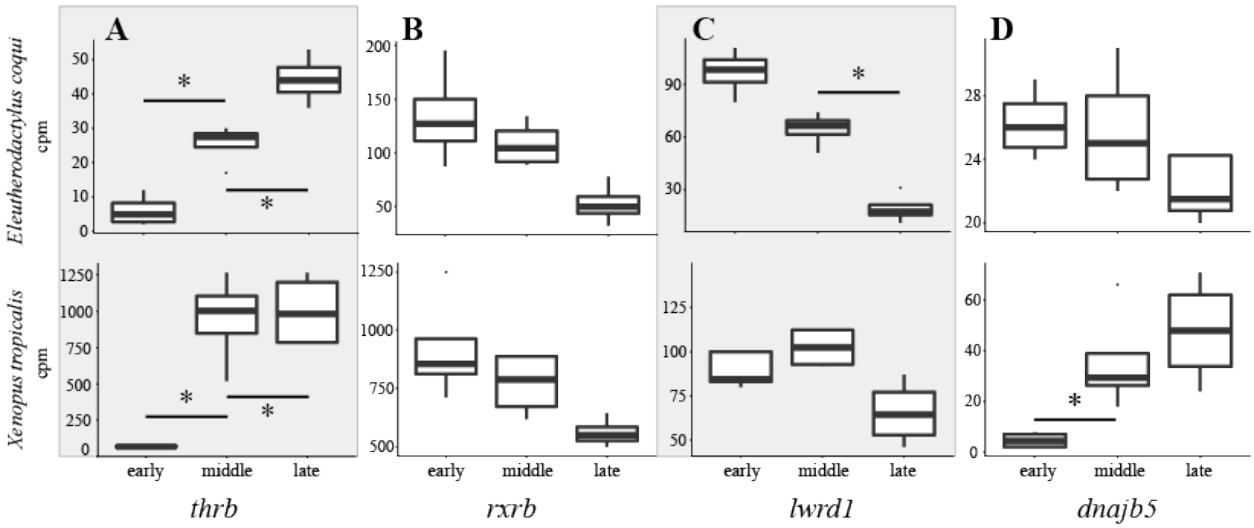

Figure 3.5. Orthologous T_3-response gene expression patterns in *Eleutherodactylus coqui* and *Xenopus tropicalis* that are representative of matching (A, B), "opposite" mismatching (C) or "unregulated" mismatching expression patterns (D). Each box represents the median and range of four biological replicates.

The 1,026 genes (44%) that changed in one species but not the other were enriched in specific functional categories. Genes that decreased in *E. coqui* but did not change in *X. tropicalis*, including the gene *leucine-rich repeats* and *WD repeat domain containing 1* (*lrwd1*, Figure 3.5C), were over-enriched in the GO categories protein localization to chromosome, regulation of ubiquitin protein ligase activity and negative regulation of the mitotic metaphase/anaphase transition. Genes that increased in *E. coqui* but did not change in *X. tropicalis* were not enriched in any GO category. Candidate T_3-response genes that increased in *X. tropicalis* but did not change in *E. coqui* included the gene *DNaJ heat shock protein family (Hsp40) member B5* (*dnajb5*, Figure 3.5D) and were over-enriched in protein folding, cell redox homeostasis, cellular respiration and translation. Genes that decreased in *X. tropicalis* but did not change in *E. coqui* were over-enriched in regulation of cellular process.

DISCUSSION

Data in this chapter suggest that some broad gene expression patterns during hind limb development in the direct-developing frog *Eleutherodactylus coqui* are conserved relative to those in the metamorphosing frog *Xenopus tropicalis*. Approximately one-third of orthologous genes have the same expression patterns in both species. Genes that do not share expression patterns between *E. coqui* and *X. tropicalis* are enriched in a variety of biological processes that suggest there are some differences in relative timing of these processes.

Limitations

There are several caveats to keep in mind when interpreting these data. First, except for *thrb* and *thibz* (Chapter 1), gene expression patterns have not been validated by qPCR.

Second, the currently incomplete annotation of the *E. coqui* genome limits the number of genes that can be used in downstream analysis in two ways. By identifying *E. coqui* genes only via similarity to *X. tropicalis* proteins, this analysis is limited to *E. coqui* transcripts that have not significantly diverged from *X. tropicalis* proteins. *Eleutherodactylus coqui* transcripts that were identified were further filtered after differential expression analysis. Genes on multiple chromosomes or genes that had more than one *X. tropicalis* protein hit were removed prior to GO analysis. Genes found on multiple chromosomes make up 24.2% (n = 2,948) of the entire dataset. Of these genes, 95% (n = 2,801) were found on two chromosomes and the remaining 5% were found on more than two chromosomes. Of the genes found on two or more chromosomes, 15.4% are uncharacterized proteins. It would be interesting to determine if genes found on two or more chromosomes belong to rapidly evolving genes families. If so, it is possible that paralogs exist in *E. coqui*. Genes that had multiple hits to *X. tropicalis* proteins make up 3.2% of the whole dataset. Anecdotally, many of these hits appear closely related; for example, *myosin 9a* and *myosin 9b* and *collagen, type XIV, alpha 1* and

collagen, type XII, alpha 1 both hit to the same two genes in *E. coqui*, respectively. An improved genome annotation via a pipeline such as MAKER2 (Holt and Yandell, 2011) would likely allow confident identification of a higher proportion of genes.

Finally, these data are based entirely on GO analyses. Gene ontology analysis entails comparisons to databases of proteins that are well studied in a small number of model organisms. Therefore, GO analysis alone ignores predicted protein products that differ from well-studied proteins, including novel protein products. In this analysis, 15% of predicted proteins in *E. coqui* and 29% of those in *X. tropicalis* were not assigned any GO identity, suggesting that a significant portion of genes expressed during hind limb development in these two species cannot be easily grouped with well-studied genes. While the present analysis cannot address roles of these uncategorized genes in development, a more complete genome annotation and functional testing could do so. Given the above caveats, this analysis should be regarded as the basis for a more in-depth and functional analysis.

Genes involved in muscle development and regulation of transcription share similar expression patterns

Analysis of *Eleutherodactylus coqui* and *Xenopus tropicalis* gene expression patterns show that genes involved in muscle structure development increase throughout development, while genes involved in chromosome organization and regulation of transcription decrease. Large-scale conservation of gene expression patterns related to these functional categories in both species is consistent with the fact that both species develop muscles over the developmental intervals sampled, which includes the period when processes that specify limb patterning are ending.

In metamorphosing frogs, tadpole limb muscles grow *de novo* (Muntz, 1975; Brown *et al.*, 2005; Satoh *et al.*, 2005). Immature muscle fibers are present in the early *X. tropicalis* limb stage (NF stage 53) and develop to almost fully striated and multinucleate muscle by the late limb stage (NF

stage 59) (Muntz, 1975). Hind limb musculature is not visible in the *E. coqui* TS stage 6 or 9 limb (Elinson and Fang, 1998), two stages that bracket the early hind limb stage sampled for this study. However, cells expressing *ladybird homeobox 1* (*lbx1*), a precursor for muscle development in vertebrates, are found in the early stage *E. coqui* limb (Sabo, Nath and Elinson, 2009). Hind limb muscles are clearly present in *E. coqui* at the middle (TS 10) and late stage (TS 13) sampled (Elinson and Fang, 1998).

Genes involved in processes that specify limb patterns, including axis specification and digit patterning, decrease as the hind limb of both *X. tropicalis* and *E. coqui* develop. Skeletal patterning takes place in the early limb bud stages in *X. tropicalis* and in *E. coqui* (Hanken *et al.*, 2001; Kerney and Hanken, 2008; Gross *et al.*, 2011; Keenan and Beck, 2016). In fact, grafts of *X. laevis* and *E. coqui* limb buds (several stages prior to the early limb stage in this study) develop into a typical hind limb with muscle, skin, and skeletal elements (Tschumi, 1957; Elinson, 1994). This is consistent with genes associated with transcriptional regulation, including homeobox transcription factors, decreasing in both species throughout development.

Genes that do not change significantly at any developmental time point in either *X. tropicalis* or *E. coqui* are related to translation, consistent with the idea that translation is occurring at all stages. Similarly, under-enriched functional categories such as cell differentiation and tissue development suggest these functional processes are occurring during development but not changing significantly from one stage to the next.

Mismatched gene expression patterns between species are basic developmental processes

A large portion of genes shared between species (36%) had the same expression pattern, reflecting the highly conserved vertebrate limb development module. While a few genes had opposing expression patterns, the largest proportion of genes with mismatched expression patterns

(44% of all the data) changed significantly in one species but were unregulated in the other. These genes were over-enriched in common biological processes shared by all animals, such as DNA replication, the cell cycle, translation, cellular respiration, signal transduction and pattern specification. The lack of significant change in genes of these categories suggests that these processes occur at a steady rate in one species but are differentially regulated in the other species. Overall, this result suggests that while each species may regulate specific processes involved in limb development on a different time scale, the processes involved are much the same. The six genes that have opposite expression patterns (*abca1*, *atp2b2*, *fn1*, *pcolce2*, *myo1d* and *gsto2*) do not belong to any single protein category and should be investigated in future studies. In particular, *fn1*, an extracellular glycoprotein, deserves further attention because it is indirectly regulated by T_3 (Brown *et al.*, 1996; Lin *et al.*, 2004). However, *fn1* was not included as a T_3 candidate because it did not meet the criteria of consistent T_3 regulation described in the methods.

Candidate T_3-response gene expression patterns are not consistent with those from previous studies

A slightly smaller proportion of candidate T_3-response genes were identified in *E. coqui* (19%) compared to *X. tropicalis* (36%). This difference is likely due to the smaller total number of *E. coqui* genes considered in the analysis. The *E. coqui* dataset used for the matching analysis did not include any genes found on two or more chromosomes, or any genes that had multiple *X. tropicalis* protein hits during annotation; these criteria removed 27.2% of the data. Future analyses with more thorough annotations should recover these genes.

Studies with exogenous T_3 are useful for exploring how hormones might affect development and gene expression. However, such studies do not address the role of endogenous T_3. Comparisons of studies using exogenous T_3 with studies of natural metamorphosis can be valuable in parsing what proportion of candidate T_3-response genes are regulated by T_3 *in vivo*. Fu and colleagues (2017)

found that 40% of putative T_3-response genes (with TREs upstream of their promoters) in the *X. tropicalis* intestine are regulated during natural metamorphosis. This result is remarkably close to the conservative estimate reported here: a maximum of 36% of candidate T_3-response genes in *X. tropicalis* have an expression pattern consistent with T_3 regulation as described in the literature. The corresponding estimate for *E. coqui* is lower (19–23%), likely due to the poor annotation of the genome and high rate of data filtration. High concentrations of T_3 may induce gene expression artifacts that account for the ~ 60% of candidate T_3-response genes that do not significantly change *in vivo*. Although 10 nM T_3 is estimated to be the plasma concentration of T_3 at metamorphic climax (Niinuma, Hirano and Kikuyama, 1991; Weber *et al.*, 1994), administering this concentration to pre- or prometamorphic tadpoles with low endogenous levels of T_3 does not simulate the gradual natural increase in whole body T_3 content (Krain and Denver 2004).

Candidate T_3-response genes have similar expression patterns in E. coqui and X. tropicalis

Although candidate T_3-response genes with the same expression pattern between species were not enriched for any functional categories, expression patterns of several genes known to be involved in or targets of TH signaling were the same in both *E. coqui* and *X. tropicalis*. *Thyroid hormone receptor β* is a well-characterized direct T_3-response gene in frogs and is autoregulated by TH itself (Ranjan, Wong and Shi, 1994). The parallel rise in whole body content of T_3 with *thrb* expression described here and in chapter 1 is consistent with conserved autoregulation of *thrb* in *E. coqui* hind limb. Although the rise in *thrb* mRNA in *X. tropicalis* between middle and late hind limb stages is not as large as that seen in *E. coqui*, it is of a similar magnitude to some previously reported measures (Yaoita and Brown, 1990; Eliceiri and Brown, 1994) while differing from others (Wang, Matsuda and Shi, 2008). The discrepancies could be due to differences in the tissues sampled (whole tadpole

versus tail), and it is possible that the late hind limb stage could have been sampled prior to the dramatic rise in TH at metamorphic climax (Krain and Denver, 2004).

Other genes reportedly regulated by T_3 also have matching expression patterns in both species: *slc25a23*, *nfic*, *klf4* and *rxrb* (Crump *et al.*, 2002; Das *et al.*, 2009; Kulkarni and Buchholz, 2012; Fu *et al.*, 2017). *Retinoid X receptor β* expression decreases throughout development in both *E. coqui* and *X. tropicalis* but it is surprisingly up-regulated in response to exogenous T_3 (Wang, Matsuda and Shi, 2008; Das *et al.*, 2009). Expression of the pluripotency factor *klf4* increases during development in the frog *Microhyla fissipes* (Zhao *et al.*, 2016). Interestingly, the well described direct T_3-response gene *klf9* does not change significantly in *X. tropicalis* hind limb (data not shown). I did not recover a predicted *klf9* transcript in *E. coqui*.

Two hypotheses could explain shared expression patterns of T_3 response genes between *E. coqui* and *X. tropicalis*. Because whole body TH content profiles in *E. coqui* and *X. tropicalis* are similar throughout embryonic development and metamorphosis, respectively, similar gene expression patterns could reflect T_3 regulation in both species. Alternatively, many of these T_3 response candidates are likely additionally regulated by other developmental factors, which themselves may be maintained because of important roles in multiple signaling cascades. For example, the retinoid X receptors (RXRs) are known to dimerize with both TRβ and the retinoic acid receptor (RAR). Retinoic acid controls expression of HOX genes (Tabin, 1995; Cunningham and Duester, 2015), transcription factors that are important in body patterning.

A large proportion of T_3 candidate gene expression patterns do not match between *E. coqui* and *X. tropicalis*. One of these genes is *lrwd1*, a highly conserved gene implicated in binding of the origin recognition complex to chromatin prior to DNA replication (Shen et al. 2010; Wang et al. 2017). Differential expression patterns of *lrwd1* could reflect species-specific regulation of the cell cycle progression (i.e., each species uses a different mechanism) or a heterochronic shift in when

each species uses this mechanism. Neither species' expression pattern of *lwrd1* is consistent with those reported in published studies, possibly because the initial study used whole tadpole tissue (Das et al. 2009). This could also be the reason that *fn1* expression is inconsistent with the literature; *fn1* expression increases in the *Xenopus* tail in response to exogenous T_3, (Brown *et al.*, 1996; Helbing *et al.*, 2003; Kulkarni and Buchholz, 2012) but decreases through natural hind limb development. Additionally, *fn1* increases in the *E. coqui* hind limb. Fibronectin has a variety of important roles in vertebrate development and is implicated in tadpole cardiac regeneration, intestinal remodeling and tail resorption (Brown *et al.*, 1996; Pankov and Kenneth, 2002; Schreiber, Cai and Brown, 2005; Marshall *et al.*, 2019). It would be interesting to examine the spatial distribution of *fn1* in *E. coqui* and *X. tropicalis* hind limb to determine if differing expression patterns between species is due to species-specific tissue distribution.

Despite the incomplete genome annotation available for *E. coqui*, results presented here suggest that many gene expression programs driving hind limb development in *E. coqui* are conserved relative to those that drive hind limb development in the metamorphosing frog *X. tropicalis*. This is consistent with current knowledge about limb development in vertebrates: limb development is a highly conserved process wherein changes in a relatively small number of genes has a dramatic impact on morphology (Petit *et al.*, 2017; Young and Tabin, 2017). Further research should focus on defining specific developmental pathways that differ between direct- and indirect-developing species.

REFERENCES

Brown, D. D. *et al.* (1996) 'The thyroid hormone-induced tail resorption program during *Xenopus laevis* metamorphosis', *Proceedings of the National Academy of Sciences of the United States of America*, 93(5), pp. 1924–1929.

Brown, D. D. (2005) 'The role of deiodinases in amphibian metamorphosis', *Thyroid: Official Journal of the American Thyroid Association*, 15(8), pp. 815–21. doi: 10.1089/thy.2005.15.815.

Brown, D. D. *et al.* (2005) 'Thyroid hormone controls multiple independent programs required for limb development in *Xenopus laevis* metamorphosis', *Proceedings of the National Academy of Sciences of the United States of America*, 102(35), pp. 12455–12458. doi: 10.1073/pnas.0505989102.

Buchholz, D. R. *et al.* (2007) 'Pairing morphology with gene expression in thyroid hormone-induced intestinal remodeling and identification of a core set of TH-induced genes across tadpole tissues', *Developmental Biology*, 303(2), pp. 576–590. doi: 10.1016/j.ydbio.2006.11.037.

Callery, E. M. and Elinson, R. P. (2000) 'Thyroid hormone-dependent metamorphosis in a direct developing frog', *Proceedings of the National Academy of Sciences of the United States of America*, 97(6), pp. 2615–20. doi: 10.1073/pnas.050501097.

Cheng, S.-Y., Leonard, J. L. and Davis, P. J. (2010) 'Molecular aspects of thyroid hormone actions', *Endocrine reviews*, 31(2), pp. 139–70. doi: 10.1210/er.2009-0007.

Crump, D. *et al.* (2002) 'Exposure to the herbicide acetochlor alters thyroid hormone-dependent gene expression and metamorphosis in *Xenopus laevis*', *Environmental Health Perspectives*, 110(12), pp. 1199–1205.

Cunningham, T. J. and Duester, G. (2015) 'Mechanisms of retinoic acid signalling and its roles in organ and limb development', *Nature Reviews. Molecular Cell Biology* 16(2), pp. 110–123. doi: 10.1038/nrm3932.

Das, B. *et al.* (2002) 'Multiple thyroid hormone-induced muscle growth and death programs during metamorphosis in *Xenopus laevis*', *Proceedings of the National Academy of Sciences of the United States of America*, 99(19), pp. 12230–12235.

Das, B. *et al.* (2006) 'Gene expression changes at metamorphosis induced by thyroid hormone in *Xenopus laevis* tadpoles', *Developmental Biology*, 291(2), pp. 342–355. doi: 10.1016/j.ydbio.2005.12.032.

Das, B. *et al.* (2009) 'Identification of direct thyroid hormone response genes reveals the earliest gene regulation programs during frog metamorphosis', *The Journal of Biological Chemistry*, 284(49), pp. 34167–78. doi: 10.1074/jbc.M109.066084.

Dobin, A. *et al.* (2013) 'STAR: Ultrafast universal RNA-seq aligner', *Bioinformatics*, 29(1), pp. 15–21. doi: 10.1093/bioinformatics/bts635.

Eliceiri, B. and Brown, D. (1994) 'Quantitation of endogenous thyroid hormone receptors α and β during embryogenesis and metamorphosis in *Xenopus laevis*', *Journal of Biological Chemistry*, 269(39), pp. 24459–24465.

Elinson, R. P. (1994) 'Leg development in a frog without a tadpole (*Eleutherodactylus coqui*)', *The Journal of Experimental Zoology*, 270(2), pp. 202–10. doi: 10.1002/jez.1402700209.

Elinson, R. P. (2013) 'Metamorphosis in a frog that does not have a tadpole', in Shi, Y.-B. (ed.) *Current Topics in Developmental Biology*. 1st edn. Elsevier Inc., pp. 259–76. doi: 10.1016/B978-0-12-385979-2.00009-5.

Elinson, R. P. and Fang, H. (1998) 'Secondary coverage of the yolk by the body wall in the direct developing frog, *Eleutherodactylus coqui*: an unusual process for amphibian embryos', *Development Genes and Evolution*, 208(8), pp. 457–66.

Elinson, R., Pino, E. Del and Townsend, D. (1990) 'A practical guide to the developmental biology of terrestrial-breeding frogs', *The Biological Bulletin*, 179, pp. 163–177.

Feng, Y.-J. *et al.* (2017) 'Phylogenomics reveals rapid, simultaneous diversification of three major clades of Gondwanan frogs at the Cretaceous–Paleogene boundary', *Proceedings of the National Academy of Sciences of the United States of America*, 114(29), pp. E5864–E5870. doi: 10.1073/pnas.1704632114.

Fu, L. *et al.* (2017) 'Genome-wide identification of thyroid hormone receptor targets in the remodeling intestine during *Xenopus tropicalis* metamorphosis', *Scientific Reports*. Springer US, (February), pp. 1–11. doi: 10.1038/s41598-017-06679-x.

Galton, V. A. (1989) 'The role of 3,5,3'-triiodothyronine in the physiological action of thyroxine in the premetamorphic tadpole', *Endocrinology*, 124(5), pp. 2427–33.

Gross, J. B. *et al.* (2011) 'Molecular anatomy of the developing limb in the coquí frog, *Eleutherodactylus coqui*', *Evolution & Development*, 13(5), pp. 415–26. doi: 10.1111/j.1525-142X.2011.00500.x.

Guha, U. *et al.* (2002) '*In vivo* evidence that BMP signaling is necessary for apoptosis in the mouse limb', *Developmental Biology*, 249(1), pp. 108–120. doi: 10.1006/dbio.2002.0752.

Hanken, J. *et al.* (2001) 'Limb development in a "nonmodel" vertebrate, the direct-developing frog *Eleutherodactylus coqui*', *The Journal of Experimental Zoology*, 291(4), pp. 375–88.

Helbing, C. C. *et al.* (2003) 'Expression profiles of novel thyroid hormone-responsive genes and proteins in the tail of *Xenopus laevis* tadpoles undergoing precocious metamorphosis', *Molecular Endocrinology*, 17(7), pp. 1395–409. doi: 10.1210/me.2002-0274.

Helbing, C. C. *et al.* (2007) 'Identification of gene expression indicators for thyroid axis disruption in a *Xenopus laevis* metamorphosis screening assay Part 2. Effects on the tail and hindlimb', *Aquatic Toxicology*, 82(4), pp. 215–226. doi: 10.1016/j.aquatox.2007.02.014.

Holt, C. and Yandell, M. (2011) 'MAKER2: an annotation pipeline and genome- database management tool for second- generation genome projects', *BMC Bioinformatics* 12(1), p. 491. doi: 10.1186/1471-2105-12-491.

Jennings, D. H. and Hanken, J. (1998) 'Mechanistic basis of life history evolution in anuran amphibians: thyroid gland development in the direct-developing frog, *Eleutherodactylus coqui*', *General and Comparative Endocrinology*, 111(2), pp. 225–32. doi: 10.1006/gcen.1998.7111.

Keenan, S. R. and Beck, C. W. (2016) '*Xenopus* limb bud morphogenesis', *Developmental Dynamics*, 245(3), pp. 233–243. doi: 10.1002/DVDY.24351.

Kerdivel, G. *et al.* (2019) 'Opposite T3 response of ACTG1 – FOS subnetwork differentiate tailfin fate in *Xenopus* tadpole and post-hatching axolotl', *Frontiers in Endocrinology*, 10(April), pp. 1–17. doi: 10.3389/fendo.2019.00194.

Kerney, R. and Hanken, J. (2008) 'Gene expression reveals unique skeletal patterning in the limb of the direct-developing frog, *Eleutherodactylus coqui*', *Evolution & Development*, 10(4), pp. 439–48. doi: 10.1111/j.1525-142X.2008.00255.x.

Kim, D., Langmead, B. and Salzberg, S. L. (2015) 'HISAT: a fast spliced aligner with low memory requirements', *Nature Methods*, 12(4), pp. 357–360. doi: 10.1038/nmeth.3317.

Kim D., *et al.* (2016) 'Centrifuge: rapid and sensitive classification of metagenomic sequences' *Genome Research*, 26(12), pp. 1721–1729. doi:10.1101/gr.210641.116.

Koepfli, K.-P. *et al.* (2015) 'The Genome 10K Project: A Way Forward', *Annual Review of Animal Biosciences*, 3(1), pp. 57–111. doi: 10.1146/annurev-animal-090414-014900.

Krain, L. P. and Denver, R. J. (2004) 'Developmental expression and hormonal regulation of glucocorticoid and thyroid hormone receptors during metamorphosis in *Xenopus laevis*', *The Journal of Endocrinology*, 181(1), pp. 91–104.

Krueger, F. (2015) 'Trim galore: a wrapper tool around Cutadapt and FastQC to consistently apply quality and adapter trimming to FastQ files'.

Kulkarni, S. S. and Buchholz, D. R. (2012) 'Beyond synergy: Corticosterone and thyroid hormone have numerous interaction effects on gene regulation in *Xenopus tropicalis* tadpoles', *Endocrinology*, 153(11), pp. 5309–5324. doi: 10.1210/en.2012-1432.

Laslo, M., Denver, R. J. and Hanken, J. (2019) 'Evolutionary conservation of thyroid hormone receptor and deiodinase expression dynamics *in ovo* in a direct-developing frog, *Eleutherodactylus coqui*', *Frontiers in Endocrinology*, 10(307), pp. 1–14. doi: 10.3389/fendo.2019.00307.

Law, C. W. *et al.* (2014) 'Voom: Precision weights unlock linear model analysis tools for RNA-seq read counts', *Genome Biology*, 15(2), pp. 1–17. doi: 10.1186/gb-2014-15-2-r29.

Lin, K.-H. *et al.* (2004) 'Regulation of fibronectin by thyroid hormone receptors', *Journal of Molecular Endocrinology*, 33, pp. 445–458. doi: 10.1677/jme.1.01505.

Maier, J. A. *et al.* (2017) 'Transcriptomic insights into the genetic basis of mammalian limb diversity', *BMC Evolutionary Biology*. 17(1), pp. 1–18. doi: 10.1186/s12862-017-0902-6.

Marshall, L. N. *et al.* (2019) 'Stage-dependent cardiac regeneration in *Xenopus* is regulated by thyroid hormone availability', *Proceedings of the National Academy of Sciences of the United States of America*, 116(9), pp. 3614–3623. doi: 10.1073/pnas.1803794116.

Merino, R. *et al.* (1999) 'The BMP antagonist Gremlin regulates outgrowth, chondrogenesis and programmed cell death in the developing limb', *Development*, 126(23), pp. 5515–5522.

Muntz, L. (1975) 'Myogenesis in the trunk and leg during development of the tadpole of *Xenopus laevis* (Daudin 1802)', *Development*, 33(3), pp. 757–774.

Nieuwkoop, P. and Faber, J. (1994) *Normal table of Xenopus laevis (Daudin)*. New York: Garland Publishing Inc. Available at: http://www.xenbase.org/anatomy/alldev.do.

Niinuma, T. M., Hirano, T. and Kikuyama, S. (1991) 'Changes in tissue concentrations of thyroid hormones in metamorphosing toad larvae', *Zoological Science*, 8(2), pp. 345–350.

Pankov, R. and Kenneth, M. (2002) 'Fibronectin at a glance', *Journal of Cell Science*, 115, pp. 3861–3863. doi: 10.1242/jcs.00059.

Pertea, M. *et al.* (2015) 'StringTie enables improved reconstruction of a transcriptome from RNA-seq reads', *Nature Biotechnology*, 33(3), pp. 290–295. doi: 10.1038/nbt.3122.

Petit, F., Sears, K. E. and Ahituv, N. (2017) 'Limb development: a paradigm of gene regulation', *Nature*, 18(4), pp. 245–258. doi: 10.1038/nrg.2016.167.

Pough, F. H. *et al.* (2015) *Herpetology*. 4th edn. Sunderland, MA: Sinauer Associates, Inc.

Ranjan, M., Wong, J. and Shi, Y. B. (1994) 'Transcriptional repression of *Xenopus* TRβ gene is mediated by a thyroid hormone response element located near the start site', *Journal of Biological Chemistry*, 269(40), pp. 24699–24705.

Sabo, M. C., Nath, K. and Elinson, R. P. (2009) 'Lbx1 expression and frog limb development', *Development Genes and Evolution*, 219(11–12), pp. 609–612. doi: 10.1007/s00427-009-0314-8.

Satoh, A. *et al.* (2005) 'Characteristics of initiation and early events for muscle development in the *Xenopus* limb bud', *Developmental Dynamics*, 234(4), pp. 846–857. doi: 10.1002/dvdy.20573.

Schreiber, A. M. *et al.* (2001) 'Diverse developmental programs of *Xenopus laevis* metamorphosis are inhibited by a dominant negative thyroid hormone receptor', *Proceedings of the National Academy of Sciences of the United States of America*, 98(19), pp. 10739–44. doi: 10.1073/pnas.191361698.

Schreiber, A. M., Cai, L. and Brown, D. D. (2005) 'Remodeling of the intestine during metamorphosis of *Xenopus laevis*', *Proceedings of the National Academy of Sciences of the United States of America*, 102(10), pp. 3720–3725.

Shao, M. and Kingsford, C. (2017) 'Scallop enables accurate assembly of transcripts through phasing-preserving graph decomposition', *bioRxiv*. doi: 10.1101/123612.

Supek, F. *et al.* (2011) 'REVIGO summarizes and visualizes long lists of gene ontology terms', *PloS One*, 6(7), p. e21800. doi: 10.1371/journal.pone.0021800.

Tabin, C. (1995) 'The initiation of the limb bud: Growth factors, hox genes, and retinoids', *Cell*, 80(5), pp. 671–674.

Townsend, D. and Stewart, M. (1985) 'Direct development in *Eleutherodactylus coqui* (Anura: Leptodactylidae): a staging table', *Copeia*, 1985(2), pp. 423–436.

Tschumi, P. A. (1957) 'The growth of the hindlimb bud of *Xenopus laevis* and its dependence upon the epidermis', *Journal of Anatomy*, 91(Pt 2), pp. 149–173.

Wang, X., Matsuda, H. and Shi, Y.-B. (2008) 'Developmental regulation and function of thyroid hormone receptors and 9-cis retinoic acid receptors during *Xenopus tropicalis* metamorphosis', *Endocrinology*, 149(11), pp. 5610–8. doi: 10.1210/en.2008-0751.

Weatherbee, S. D. *et al.* (2006) 'Interdigital webbing retention in bat wings illustrates genetic changes underlying amniote limb diversification', *Proceedings of the National Academy of Sciences of the United States of America*, 103(41), pp. 15103–15107.

Weber, G. M. *et al.* (1994) 'Changes in whole-body thyroxine and triiodothyronine concentrations and total content during early development and metamorphosis of the toad *Bufo marinus*', *General and Comparative Endocrinology*, 94, pp. 62–71.

Wen, L. *et al.* (2019) 'Thyroid hormone receptor alpha is required for thyroid hormone-dependent neural cell proliferation during tadpole metamorphosis', *Frontiers in Endocrinology*, 10(June), pp. 1–13. doi: 10.3389/fendo.2019.00396.

Williams C. R., *et al.* (2016) 'Trimming of sequence reads alters RNA-Seq gene expression estimates', *BMC Bioinformatics* 17(1):1–13. doi:10.1186/s12859-016-0956-2.

Yaoita, Y. and Brown, D. D. (1990) 'A correlation of thyroid hormone receptor gene expression with amphibian metamorphosis', *Genes & Development*, 4(11), pp. 1917–1924. doi: 10.1101/gad.4.11.1917.

Young, J. J. and Tabin, J. (2017) 'Saunders's framework for understanding limb development as a platform for investigating limb evolution', *Developmental Biology*, 429, pp. 401–408. doi: 10.1016/j.ydbio.2016.11.005.

Zhao, L. *et al.* (2016) 'Transcriptome profiles of metamorphosis in the ornamented pygmy frog *Microhyla fissipes* clarify the functions of thyroid hormone receptors in metamorphosis', *Scientific Reports*, 6(February), p. 27310. doi: 10.1038/srep27310.

Zou, H. and Niswander, L. (1996) 'Requirement for BMP signaling in interdigital apoptosis and scale formation', *Science*, 272(5262), pp. 1–7.

CONCLUSIONS

Endocrine systems are ancient eukaryotic signaling systems. In amphibians, they are likely targets of selection that could facilitate the evolution of dramatic shifts in life history, including direct development. The evolution of direct development in the lineage leading to *Eleutherodactylus coqui* resulted in both limb development and tail resorption occurring prior to hatching rather than during a postembryonic metamorphosis, as in metamorphosing frogs such as *Xenopus tropicalis*. Despite this drastic difference in life history between these two species, numerous key features of thyroid hormone (TH)-dependent tail resorption and limb development have been retained, including TH receptor and deiodinase enzyme mRNA expression dynamics, whole-body TH and corticosteroid (CORT) content profiles, maternally derived TH, and tissue sensitivity to exogenous hormones. The presence of these endocrine components (and conserved expression dynamics) in a direct-developing frog is not surprising given the presence of TH and glucocorticoid signaling components across the animal kingdom. Analogous signaling systems in plants speaks to the importance of these hormones in regulating eukaryote biology.

Comparing hormonal control of development across species with different life histories is a crucial step in building our knowledge of these endocrine systems and understanding how endocrine systems themselves evolve. Understanding hormonal mediation of development in the direct-developing frog *E. coqui* can therefore shed light on how endocrine axes evolve over time. Future studies of direct-developing species have the potential to address exciting questions at the intersection of evolution, development, and endocrinology.

Evolutionary origins of TH and CORT signaling

Descriptions of TH and CORT signaling components in diverse animal groups paint a picture as to how these signaling systems may have evolved. Both TH and CORT act via binding to

a nuclear receptor (NR), a signaling system that probably originated at the base of the Metazoa (Owen and Zelent, 2000). Phylogenetic analysis suggests that the ancestral NR could homodimerize and that the ability to heterodimerize with other NRs arose only once (Laudet, 1997). A vertebrate-specific genome duplication gave rise to NR paralogs, a phenomenon observed for other families of paralogous genes such as HOX genes. The ability to heterodimerize with related NRs expanded the toolkit for transcriptional regulation.

The hypothalamus-pituitary-interrenal (HPI) axis interprets environmental signals and translates them into a physiological response via changes in transcription. Components of the HPI axis were likely present in the earliest vertebrates (Denver, 2009). Phylogenetic analysis suggests that the glucorticoid receptor (GR) lineage arose from a large genome expansion that occurred in gnathostomes around 450 million years ago (Bridgham et al., 2006). Differentiated tissue that can produce corticosteroids is found in all major vertebrate groups examined so far (reviewed in Denver 2009). The ability to synthesize corticosteroids probably arose prior to the gnathostome lineage, as both hagfish and lamprey can produce corticosteroids (Weisbart *et al.*, 1980; Close *et al.*, 2010). The HPI axis and glucocorticoid signaling cascade components have likely been maintained because of their integral role in allowing organisms to respond to environmental stimuli.

Selection has likely maintained TH signaling components because of the pleiotropic roles of TH in numerous developmental processes. Several pieces of evidence suggest that TH signaling arose early in Metazoa as an environmental sensor: 1) TR exists as an orphan receptor in tunicates, 2) TH influences development in animals that cannot produce TH (to our knowledge), and 3) iodinated compounds exist in algae, a common marine food source. Although treatment with TH accelerates metamorphosis in tunicates, the tunicate TR ortholog is very divergent from vertebrate TRs and no known TH derivatives can regulate transcription via this TR (Carosa *et al.*, 1998). Treatment with TH and TH-like compounds accelerates metamorphosis and larval settlement in

several echinoderm species (Heyland et al., 2004; Heyland *et al.*, 2006; Johnson and Cartwright, 2019). Although a TR ortholog has been identified in the sea urchin genome (Tu *et al.*, 2012; Taylor, 2017), there has been no formal demonstration of TH binding to the TR ortholog. Finally, tunicates and most echinoderms do not seem capable of endogenously synthesizing TH. Algae contain iodine; marine larvae could get iodine, the essential component of TH, via ingestion of algae (Miller and Heyland, 2010). Altogether, this evidence supports the hypothesis that TH signaling arose as a method of assessing sufficient food availability. Under this hypothesis, the presence of TH would indicate high food availability and promote development; the ability to endogenously synthesize TH arose subsequently.

Over evolutionary time, thyroid hormone and glucocorticoid signaling have increased in complexity. Thyroid hormone and glucocorticoid signaling together impact reproduction, metabolism, physiology, and development in living animals. These pleiotropic effects go hand in hand with modularity. The modularity of NR signaling and hormone metabolism and action allow for gain or loss of hormone-regulated transcription without substantial changes in other aspects of the system. Indeed, because of the modularity inherent in these signaling systems, small changes can have dramatic effects on life history.

Insects and echinoderms: parallel studies to understanding developmental mechanisms of life history evolution

Like amphibians, insects and echinoderms have diverse developmental modes, and they too have been the target of study by scientists wanting to understand the basis of life history evolution. Holometabolous insects, those characterized by a complete metamorphosis, likely evolved once from a direct-developing ancestor (Whiting *et al.*, 1997). Direct development, the loss of the free-living larva, has evolved several times independently in sea urchins (Raff, 1987). Studies in each of these two groups highlight themes of evolutionary changes in life history modes, respectively:

modularity of hormone signaling pathways, and the idea that multiple trajectories can be taken to achieve one evolutionary end.

There are several functional and structural similarities between hormonal control of metamorphosis in amphibians and insects. Juvenile hormone (JH) and 20-hydroxy-ecdysone (20E) control insect development, metamorphosis, and life history transitions (Flatt, Tu and Tatar, 2005; Truman and Riddiford, 2007). Both TH and JH/20E have pleiotropic roles in development, reproduction, physiology, and metabolism, although I discuss only the developmental role here. In insects, if both JH and 20E are present, the insect molts to the same stage as the previous one. Low concentrations of JH, but high concentrations of ecdysone (the precursor of 20E) induce metamorphosis to the adult form. As such, JH and 20E can be viewed as having antagonistic actions towards each other: JH maintains the "status quo" while 20E promotes development of adult features (Truman and Riddiford, 2007; Liu *et al.*, 2018). In amphibian metamorphosis, TH and the peptide hormone prolactin may have a similar relationship (Denver, 2009). It is very clear that TH promotes metamorphosis, while prolactin can inhibit T_3-induced metamorphoric changes (Kikuyama *et al.*, 1993), suggesting that prolactin may antagonize TH action.

Structural similarities of TH and JH/20E signaling extend to the receptors and downstream target genes. Thyroid hormone and 20E each bind to a nuclear receptor, the TR and the ecdysone receptor (EcR), respectively. Interestingly, both TR and EcR share a dimerization partner, RXR, and its insect homolog, USP (Hall and Thummel, 1998). Molecular analyses suggest that the DNA binding motifs for both TR and EcR likely shared a common ancestor. Few changes in the nucleotide sequence of each receptor's DNA binding motif are required to convert each to a functional binding sequence of the opposite type (Martinez, Givel and Wahli, 1991). Finally, similar proteins interact with both the TR/RXR and EcR/USP complex to activate or repress transcription.

For example, the vertebrate protein Alien and the *Drosophila* ortholog of Alien both repress transcription in the absence of TH (Dressel *et al.*, 1999; Flatt *et al.*, 2006).

Structural and functional similarities between JH-20E and TH signaling include similar regulation of metamorphosis by multiple hormones with pleiotropic effects and regulation of transcription via NRs and similar proteins. These similarities suggest that evolutionary changes in insect hormone signaling may also underlie the evolution of metamorphosis. This conservation of fundamental aspects of hormonal signaling during development suggests that components of the hormone signaling pathway can be "switched out" and replaced with functionally similar components without negatively disrupting development. Again, this modularity characteristic of hormone signaling pathways could circumvent developmental constraints and facilitate evolution of diverse life histories.

There are several parallels in the evolution of direct development in echinoderms and anurans. First, the ancestral state for both echinoderms and anurans included a free-living and likely feeding larva (Raff, 1987; Schoch, 2009). Facultatively feeding larvae also exist within both groups (Emlet, 1986; Crump, 1989). Secondly, as in anurans and insects, hormones and, specifically, THs are implicated in evolution of developmental mode. Thyroid hormone treatment can shift developmental mode of an obligatory feeding larva to a facultatively feeding larva, and THs are hypothesized to regulate phenotypic plasticity observed in another species of sand dollars (Heyland and Hodin, 2004; Heyland, Reitzel and Hodin, 2004).

More broadly, we can infer similar steps that occurred in the evolution of direct development in both echinoderms and anurans. In urchins, specific cell lineages give rise to larval or adult structures only, or contribute to both larval and adult structures. Raff (1987) makes several explicit predictions about the fate of these cell types in the evolution of direct development: larval-specific cell types should be lost, differentiation of adult-specific cell types should be accelerated,

and lineages giving rise to both larval and adult structures should experience both of the changes listed above. Accumulating evidence supports these predictions in both echinoderms and frogs. In the direct-developing frog *E. coqui*, larval specific features such as tadpole-specific cartilages and muscle are lost (Hanken *et al.*, 1992, 1997). In the direct-developing urchin, *Heliocidaris erythrogramma*, the skeletogenic precursor cells do not migrate or proliferate as they do in species with indirect development (Parks *et al.*, 1988). Additionally, the gene regulatory network that underlies larval skeletal specification is at least greatly reduced, if not totally absent (Israel *et al.*, 2016; Edgar *et al.*, 2019). In contrast, development of adult features is accelerated in direct-developing frogs and echinoderms. In frogs, these accelerated adult features include jaw muscles, limbs, and the retinotectal system (Townsend and Stewart, 1985; Hanken *et al.*, 1997; Schlosser and Roth, 1997; Gross *et al.*, 2011). The formation of the left coelom, which gives rise to adult features, forms and differentiates a few hours post-fertilization in contrast to indirect developing urchin which form the left coelom only after a few weeks of feeding (Smith, Zigler and Raff, 2007).

Finally, development of some direct-developing sea urchins is similar to that in some direct-developing frogs in that it is described as a simple acceleration of adult features, which develop in the same order as they do in indirect-developing species. However, in several urchin species the relative order of developmental events is also shifted, as is observed in direct-developing frogs (Raff, 1987).

The parallel changes observed in the evolution of direct-developing echinoderms and frogs suggest that there are multiple ways to achieve one evolutionary end (the formation of the adult), but that certain pathways to achieve that end may be taken more often than others. The fact that we observe similar changes in these two distantly related groups (loss of larval specific features and acceleration of adult development) suggests that development may constrain the paths available for modification. Hormone signaling may be both a particular target for modification to evolve direct

development, but also a constraint due to the pleiotropy of endocrine systems. Data presented here supports the hypothesis that developmental modules in frogs, such as limb development, are internally constrained but can still be disassociated from each other, often observed in heterochronies (Alberch *et al.*, 1979). Studying closely related animals with different developmental modes allows us to understand how the same goal (an adult form) is achieved through different means and begin to disentangle developmental and genetic mechanisms.

Increased maternal investment as a preadaptation for direct development

An additional parallel of direct development in frogs and echinoderms is increased maternal investment in direct-developing species. The lack of a free-living and feeding larval stage is associated with larger egg size in both animal groups (Elinson 2013; Raff 1987). Several researchers have proposed that an increased maternal investment is the first step in the evolution of direct development (Wray & Raff 1981; Smith, Zigler, Raff 1991). Once the larva has access to greater energy resources via the maternal nutrients in the yolk, the larval feeding structures can be lost, followed by subsequent changes in larval morphology.

In a direct-developing echinoderm or frog, egg yolk contains all the nutrients necessary for either settlement or development into a juvenile. Hormones are also sequestered into the eggs during vitellogenesis or pass through the placenta (in mammals). The importance of maternal TH in early development was first noticed in humans: Children of hypothyroid mothers are characterized by neurological deficits and bone abnormalities (Bernal, 2007; Waung, Bassett and Williams, 2012). Maternal glucocorticoids are also implicated in human health. *In utero* exposure to high levels of GCs programs the fetal stress axis and may predispose those individuals for disease later in life (Amiel-Tison *et al.*, 2004; Ward *et al.*, 2004; Denver and Crespi, 2006).

The importance of maternal GCs and THs is also recognized in oviparous vertebrates. Thyroid hormones have been found in yolk or fertilized eggs of birds (Prati, Calvo and de Escobar, 1992), frogs (Weber *et al.*, 1994; Laslo, Denver and Hanken, 2019), sharks (McComb *et al.*, 2005), and several species of bony fish (de Jesus, Hirano and Inui, 1991; Weber *et al.*, 1992; Ayson and Lam, 1993), while GCs have been measured in eggs of several fish species (Hwang *et al.*, 1992; Eriksen *et al.*, 2006; Gagliano and McCormick, 2009), several bird species (Hayward and Wingfield, 2004; Rubolini *et al.*, 2005; Almasi *et al.*, 2012), and reptiles (Painter *et al.*, 2002). Experimental manipulation of maternal TH in fish and birds suggests that maternal thyroid hormone (TH) provisioning impacts body size, development and growth rate, and survival (Brown *et al.*, 1989; Wilson and McNabb, 1997; Kang and Chang, 2004; Urbinati *et al.*, 2008). Emerging evidence suggests that maternal TH is important in tadpole brain development, as it is in humans (Fini *et al.*, 2012). Thyroid hormones have been detected in yolk and gastrulating embryos of five anuran species—*Bufo marinus* (Weber *et al.*, 1994), *Rana catesbeiana* (Fujikara and Suzuki, 1991), *Bombina orientalis* (Jennings, 1997), *Xenopus laevis* (Fini *et al.*, 2012), and *Eleutherodactylus coqui* (Laslo, Denver and Hanken, 2019), while GCs have not been measured at all. Given all that we know about the powerful effects of hormone signaling on anuran life history, and the role of maternal hormone in vertebrate development, future work should focus on the role of maternal hormones, particularly TH, in frog life history.

Several approaches could shed light on the role of maternal TH in both direct and indirect development. Inhibition of the mother's thyroid axis could decrease the TH deposited in the egg, but would also likely change nutrient content, even if normal vitellogenesis did occur. Yolk removal could also reveal impacts of maternal provisioning on life history, although not specifically the effects of maternal TH. Yolk removal in *Ambystoma maculatum* salamanders induced early hatching and affected hatchling body size (Landberg, 2014). Blocking the action of TRs with an antagonist

such as NH-3 is perhaps the most elegant experiment. The antagonist NH-3 was used to determine that yolk TH affected tadpole brain development (Fini *et al.*, 2012). Antagonizing the TRs in a direct-developing frog prior to production of embryonic TH would allow inference of the impact of maternal TH only. Gene editing technologies like CRISPR may also be a method to investigate the role of maternal TH or the TRs in early development. Thyroid hormone receptor knockouts in *E. coqui* could clarify their function and determine if TR regulation of transcription is conserved in direct-developing frogs.

Case studies of specific organisms as described above coupled with efforts to correlate measures of endocrine physiology with life history traits across anuran taxa will connect proximate developmental mechanisms with ultimate evolutionary patterns. For example, a phylogenetic analysis of egg size and developmental mode could explicitly address the hypothesis that maternal investment increases in direct-developing species and determine how increased maternal investment correlates with time to and size at metamorphosis in frogs. A similar study in echinoderms suggests that, counter to what has been assumed for decades, increased maternal investment does not decrease time to metamorphosis (Levitan, 2000). Measures of endocrine physiology like maternal TH contributions could be included in a phylogenetic study. Comparison of TH concentrations across species is currently difficult: the methodology for collection, measurement, and reporting units varies, and conclusions that can be drawn from this single value are limited. Standard hormone measurement methods should be developed and examined across a broad range of species. Museum collections could be used to measure physical traits such as pituitary, interrenal, and thyroid gland size. Phylogenetic studies like these, combined with a better understanding of species-specific endocrinology can better determine the role of maternal hormones in amphibian life history evolution and reveal important patterns in amphibian life history evolution.

Summary

This dissertation is a valuable contribution to the field of comparative endocrinology. Despite the 150 million years since *Eleutherodactylus coqui* and *Xenopus tropicalis* shared a common ancestor (Feng *et al.*, 2017), two fundamental aspects of TH signaling appear to be the same in both species: whole body content profiles of TH, and the temporal dynamics of TR and deiodinase mRNAs. The conservation of these features suggests that TH signaling acts via TRs to regulate limb development in *E. coqui*, much as it does in metamorphosing species. These results are consistent with the evolutionary conservation of TH signaling components in animals, and suggest that modularity of these pleiotropic signaling systems may contribute to diversity of developmental modes. Although the whole body TH content profiles are similar during limb development in both *E. coqui* and metamorphosing species, TH present during early limb development is maternally derived. An increased maternal investment or contribution of TH could be a crucial step in the evolution of direct development and should be the focus of future studies.

REFERENCES

Alberch, P. *et al.* (1979) 'Size and shape in ontogeny and phylogeny', *Paleobiology*, 5(3), pp. 296–317.

Almasi, B. *et al.* (2012) 'Maternal corticosterone is transferred into the egg yolk', *General and Comparative Endocrinology*. Elsevier Inc., 178(1), pp. 139–144. doi: 10.1016/j.ygcen.2012.04.032.

Amiel-Tison, C. *et al.* (2004) 'Fetal adaptation to stress: Part II. Evolutionary aspects; stress-induced hippocampal damage; long-term effects on behavior; consequences on adult health.', *Early Human Development*, 78(2), pp. 81–94. doi: 10.1016/j.earlhumdev.2004.03.007.

Ayson, F. G. and Lam, T. J. (1993) 'Thyroxine injection of female rabbitfish (*Siganus guttatus*) broodstock: changes in thyroid hormone levels in plasma, eggs, and yolk-sac larvae, and its effect on larval growth and survival', *Aquaculture*, 109(1), pp. 83–93.

Bernal, J. (2007) 'Thyroid hormone receptors in brain development and function', *Nature Clinical Practice: Endocrinology & Metabolism*, 3(3), pp. 249–259.

Bridgham, J. T., Carroll, S. M. and Thornton, J. W. (2006) 'Evolution of hormone-receptor complexity by molecular exploitation', *Science*, 312(5770), pp. 97–102.

Brown, C. L. *et al.* (1989) 'Enhanced survival in striped bass fingerlings after maternal triiodothyronine treatment', *Fish Physiology and Biochemistry*, 7(1–6), pp. 295–9. doi: 10.1007/BF00004720.

Carosa, E. *et al.* (1998) '*Ciona intestinalis* nuclear receptor 1: A member of steroid/thyroid hormone receptor family', *Proceedings of the National Academy of Sciences of the United States of America*, 95(19), pp. 11152–11157.

Close, D. A. *et al.* (2010) '11-Deoxycortisol is a corticosteroid hormone in the lamprey', *Proceedings of the National Academy of Sciences of the United States of America*, 107(31), pp. 13942–13947. doi: 10.1073/pnas.0914026107/-/DCSupplemental.www.pnas.org/cgi/doi/10.1073/pnas.0914026107.

Crump, M. L. (1989) 'Life history consequences of feeding versus non-feeding in a facultatively non-feeding toad larva', *Oecologia*, 78(4), pp. 486–489. doi: 10.1007/BF00378738.

Denver, R.J. (2009) 'Endocrinology of Complex Life Cycles: Amphibians', in R.J. Denver (ed.) *Hormones, Brain, and Behavior*, pp. 707–744.

Denver, Robert John (2009) 'Structural and functional evolution of vertebrate neuroendocrine stress systems.', *Annals of the New York Academy of Sciences*, 1163, pp. 1–16. doi: 10.1111/j.1749-6632.2009.04433.x.

Denver, R. J. and Crespi, E. J. (2006) 'Stress hormones and human developmental plasticity: Lessons From tadpoles', *NeoReviews*, 7(4), pp. e183–e188. doi: 10.1542/neo.7-4-e183.

Dressel, U. *et al.* (1999) 'Alien, a highly conserved protein with characteristics of a corepressor for members of the nuclear hormone receptor superfamily', *Molecular and Cellular Biology*, 19(5), pp. 3383–3394.

Edgar, A. *et al.* (2019) 'Evolution of abbreviated development in *Heliocidaris erythrogramma* dramatically re-wired the highly conserved sea urchin developmental gene regulatory network to decouple signaling center function from ultimate fate', *bioRxiv*.

Emlet, R. B. (1986) 'Facultative planktotrophy in the tropicalis echinoid *Clypeaster rosaceus* and a comparison with obligate planktotrophy in *Clypeaster subdepressus* (Gray) (Clypeasteroida: Echinoidea)', *Journal of Experimental Marine Biology and Ecology*, 95, pp. 183–202.

Eriksen, M. S. *et al.* (2006) 'Prespawning stress in farmed Atlantic salmon *Salmo salar*: Maternal cortisol exposure and hyperthermia during embryonic development affect offspring survival, growth and incidence of malformations', *Journal of Fish Biology*, 69(1), pp. 114–129. doi: 10.1111/j.1095-8649.2006.01071.x.

Feng, Y.-J. *et al.* (2017) 'Phylogenomics reveals rapid, simultaneous diversification of three major clades of Gondwanan frogs at the Cretaceous–Paleogene boundary', *Proceedings of the National Academy of Sciences of the United States of America*, 114(29), pp. E5864–E5870. doi: 10.1073/pnas.1704632114.

Fini, J. B. *et al.* (2012) 'Thyroid hormone signaling in the *Xenopus laevis* embryo is functional and susceptible to endocrine disruption', *Endocrinology*, 153(10), pp. 5068–5081. doi: 10.1210/en.2012-1463.

Flatt, T. *et al.* (2006) 'Comparing thyroid and insect hormone signaling', *Integrative and Comparative Biology*, 46(6), pp. 777–794. doi: 10.1093/icb/icl034.

Flatt, T., Tu, M.-P. and Tatar, M. (2005) 'Hormonal pleiotropy and the juvenile hormone regulation of Drosophila development and life history', *BioEssays*, 27, pp. 999–1010. doi: 10.1002/bies.20290.

Fujikara, K. and Suzuki, S. (1991) 'Thyroxine and thyroglobulin in eggs and embryos of bullfrog', *Zoological Science*, 8(6), p. 1166.

Gagliano, M. and McCormick, M. I. (2009) 'Hormonally mediated maternal effects shape offspring survival potential in stressful environments', *Oecologia*, 160(4), pp. 657–665. doi: 10.1007/s00442-009-1335-8.

Gross, J. B. *et al.* (2011) 'Molecular anatomy of the developing limb in the coquí frog, *Eleutherodactylus coqui*', *Evolution & Development*, 13(5), pp. 415–26. doi: 10.1111/j.1525-142X.2011.00500.x.

Hall, B. L. and Thummel, C. S. (1998) 'The RXR homolog Ultraspiracle is an essential component of the *Drosophila* ecdysone receptor', *Development*, 125, pp. 4709–4717.

Hanken, J. *et al.* (1992) 'Cranial ontogeny in the direct-developing frog, *Eleutherodactylus coqui* (Anura: Leptodactylidae), analyzed using whole-mount immunohistochemistry', *Journal of Morphology*, 211(1), pp. 95–118. doi: 10.1002/jmor.1052110111.

Hanken, J. *et al.* (1997) 'Jaw muscle development as evidence for embryonic repatterning in direct-developing frogs', *Proceedings: Biological sciences / The Royal Society*, 264(1386), pp. 1349–54. doi: 10.1098/rspb.1997.0187.

Hayward, L. S. and Wingfield, J. C. (2004) 'Maternal corticosterone is transferred to avian yolk and may alter offspring growth and adult phenotype', *General and Comparative Endocrinology*, 135(3), pp. 365–371. doi: 10.1016/j.ygcen.2003.11.002.

Heyland, A. *et al.* (2006) 'Thyroid hormone metabolism and peroxidase function in two non-chordate animals', *Journal of Experimental Biology*, 306(6), pp. 551–566. doi: 10.1002/jez.b.

Heyland, A. and Hodin, J. (2004) 'Heterochronic developmental shift caused by thyroid hormone in larval sand dollars and its implications for phenotypic plasticity and the evolution of nonfeeding development', *Evolution*, 58(3), pp. 524–538. doi: 10.1111/j.0014-3820.2004.tb01676.x.

Heyland, A., Reitzel, A. M. and Hodin, J. (2004) 'Thyroid hormones determine developmental mode in sand dollars (Echinodermata: Echinoidea)', *Evolution & Development*, 6, pp. 382–392. doi: 10.1111/j.1525-142X.2004.04047.x.

Hwang, P. P. *et al.* (1992) 'Cortisol content of eggs and larvae of teleosts', *General and Comparative Endocrinology*, 86(2), pp. 189–196. doi: 10.1016/0016-6480(92)90101-O.

Israel, J. W. *et al.* (2016) 'Comparative developmental transcriptomics reveals rewiring of a highly conserved gene regulatory network during a major life history switch in the sea urchin genus *Heliocidaris*', *PLOS Biology*, 14(3), pp. 1–28. doi: 10.5061/dryad.cr0mb.

Jennings, D. H. (1997) *Evolution of endocrine control of development in direct-developing amphibians*. University of Colorado, Boulder.

de Jesus, E. G. T., Hirano, T. and Inui, Y. (1991) 'Changes in cortisol and thyroid hormone concentrations during early development and metamorphosis in the Japanese flounder *Paralichthys olivaceus*', *General and Comparative Endocrinology*, 376(82), pp. 369–376.

Johnson, L. G. and Cartwright, C. M. (2019) 'Thyroxine-accelerated larval development in the crown-of-thorns starfish, *Acanthaster planci*', *Biological Bulletin*, 190(3), pp. 299–301.

Kang, D. Y. and Chang, Y. J. (2004) 'Effects of maternal injection of 3,5,3-triiodo-L-thyronine (T3) on growth of newborn offspring of rockfish, *Sebastes schlegeli*', *Aquaculture*, 234(December), pp. 641–655. doi: 10.1016/j.aquaculture.2004.01.011.

Kikuyama, S. *et al.* (1993) 'Aspects of amphibian metamorphosis: hormonal control.', *International Review of Cytology*, 145, pp. 105–148.

Landberg, T. (2014) 'Embryonic yolk removal affects a suite of larval salamander life history traits', *Journal of Experimental Zoology Part B Molecular and Developmental Evolution*, 322(1), pp. 45–53. doi: 10.1002/jez.b.22544.

Laslo, M., Denver, R. J. and Hanken, J. (2019) 'Evolutionary conservation of thyroid hormone receptor and deiodinase expression dynamics *in ovo* in a direct-developing frog, *Eleutherodactylus coqui*', *Frontiers in Endocrinology*, 10(307), pp. 1–14. doi: 10.3389/fendo.2019.00307.

Laudet, V. (1997) 'Evolution of the nuclear receptor superfamily: early diversification from an ancestral orphan receptor', *Journal of Molecular Endocrinology*, 19(3), pp. 207–226.

Levitan, D. R. (2000) 'Optimal egg size in marine invertebrates: Theory and phylogenetic analysis of the critical relationship between egg size and development time in echinoids', *The American Naturalist*, 156(2), pp. 175–192.

Liu, S. *et al.* (2018) 'Antagonistic actions of juvenile hormone and 20-hydroxyecdysone within the ring gland determine developmental transitions in Drosophila', *Proceedings of the National Academy of Sciences of the United States of America*, 115(1), pp. 139–144. doi: 10.1073/pnas.1716897115.

Martinez, E., Givel, F. and Wahli, W. (1991) 'A common ancestor DNA motif for invertebrate and vertebrate hormone response elements', *The EMBO Journal*, 10(2), pp. 263–268. doi: 10.1002/j.1460-2075.1991.tb07946.x.

McComb, D. M. *et al.* (2005) 'Comparative thyroid hormone concentration in maternal serum and yolk of the bonnethead shark (*Sphyrna tiburo*) from two sites along the coast of Florida', *General and Comparative Endocrinology*, 144(2), pp. 167–173. doi: 10.1016/j.ygcen.2005.05.005.

Miller, A. E. M. and Heyland, A. (2010) 'Endocrine interactions between plants and animals: Implications of exogenous hormone sources for the evolution of hormone signaling', *General and Comparative Endocrinology*, 166(3), pp. 455–461. doi: 10.1016/j.ygcen.2009.09.016.

Owen, G. I. and Zelent, A. (2000) 'Origins and evolutionary diversification of the nuclear receptor superfamily', *Celluluar and Molecular Life Sciences*, 57, pp. 809–827.

Painter, D., Jennings, D. H. and Moore, M. C. (2002) 'Placental buffering of maternal steroid hormone effects on fetal and yolk hormone levels: a comparative study of a viviparous lizard, *Sceloporus jarrovi*, and an oviparous lizard, *Sceloporus graciosus*', *General and Comparative Endocrinology*, 127(2), pp. 105–116. doi: 10.1016/S0016-6480(02)00075-8.

Parks, A. L. *et al.* (1988) 'Molecular analysis of heterochronic changes in the evolution of direct developing sea urchins', *Journal of Evolutionary Biology*, 44, pp. 27–44.

Prati, M., Calvo, R. and de Escobar, G. M. (1992) 'L-thyroxine and 3,5,3'-triiodothyronine concentrations in the chicken egg and in the embryo before and after the onset of thyroid function', *Endocrinology*, 130(5), pp. 2651–2659.

Raff, R. A. (1987) 'Constraint, flexibility, and phylogenetic history in the evolution of direct development in sea urchins', *Developmental Biology*, 119, pp. 6–19.

Rubolini, D. *et al.* (2005) 'Effects of elevated egg corticosterone levels on behavior, growth, and immunity of yellow-legged gull (*Larus michahellis*) chicks', *Hormones and behavior*, 47(5), pp. 592–605. doi: 10.1016/j.yhbeh.2005.01.006.

Schlosser, G. and Roth, G. (1997) 'Development of the retina is altered in the directly developing frog *Eleutherodactylus coqui* (Leptodactylidae)', *Neuroscience Letters*, 224(3), pp. 153–156. doi: 10.1016/S0304-3940(97)00174-2.

Schoch, R. R. (2009) 'Evolution of life cycles in early amphibians', *Annual Review of Earth and Planetary Sciences*, 37(May), pp. 135–62. doi: 10.1146/annurev.earth.031208.100113.

Smith, M. S., Zigler, K. S. and Raff, R. A. (2007) 'Evolution of direct-developing larvae: selection vs loss', *BioEssays*, (13), pp. 566–571. doi: 10.1002/bies.20579.

Taylor, E. (2017) *Thyroid hormones accelerate larval skeletogenesis in sea urchins (Strongylocentrotus purpuratus) through a membrane receptor-mediated MAPK signalling cascade*. University of Guelph.

Townsend, D. and Stewart, M. (1985) 'Direct development in *Eleutherodactylus coqui* (Anura: Leptodactylidae): a staging table', *Copeia*, 1985(2), pp. 423–436.

Truman, J. W. and Riddiford, L. M. (2007) 'The morphostatic actions of juvenile hormone', *Insect Biochemistry and Molecular Biology*, 37, pp. 761–770. doi: 10.1016/j.ibmb.2007.05.011.

Tu, Q. *et al.* (2012) 'Gene structure in the sea urchin *Strongylocentrotus purpuratus* based on transcriptome analysis', pp. 2079–2087. doi: 10.1101/gr.139170.112.22.

Urbinati, E. C. *et al.* (2008) 'Larval performance of matrinxã, *Brycon amazonicus* (Spix & Agassiz 1829), after maternal triiodothyronine injection or egg immersion', *Aquaculture Research*, 39(13), pp. 1355–1359. doi: 10.1111/j.1365-2109.2008.02002.x.

Ward, A. M. V *et al.* (2004) 'Fetal programming of the hypothalamic-pituitary-adrenal (HPA) axis: low birth weight and central HPA regulation', *The Journal of Clinical Endocrinology and Metabolism*, 89(3), pp. 1227–33. doi: 10.1210/jc.2003-030978.

Waung, J. A., Bassett, J. H. D. and Williams, G. R. (2012) 'Thyroid hormone metabolism in skeletal development and adult bone maintenance', *Trends in Endocrinology and Metabolism*, 23(4), pp. 155–161. doi: 10.1016/j.tem.2011.11.002.

Weber, G. M. *et al.* (1992) 'Patterns of thyroxine and triiodothyronine in serum and follicle-bound oocytes of the tilapia, *Oreochromis mossambicus*, during oogenesis', *Gen Comp Endocrinol*, 85(3), pp. 392–404.

Weber, G. M. *et al.* (1994) 'Changes in whole-body thyroxine and triiodothyronine concentrations and total content during early development and metamorphosis of the toad *Bufo marinus*', *General and Comparative Endocrinology*, 94, pp. 62–71.

Weisbart, M. *et al.* (1980) 'The presence of steroids in the sera of the pacific hagfish *Eptatretus stouti*, and the sea lamprey, *Petromyzon marinus*', *General and Comparative Endocrinology*, 41(4), pp. 506–519.

Whiting, M. F. *et al.* (1997) 'The strepsiptera problem: Phylogeny of the holometabolous insect orders inferred from 18S and 28S ribosomal DNA sequences and morphology', *Systematic Biology*, 46(l), pp. 1–68.

Wilson, C. M. and McNabb, F. M. (1997) 'Maternal thyroid hormones in Japanese quail eggs and their influence on embryonic development', *General and Comparative Endocrinology*, 107(2), pp. 153–65. doi: 10.1006/gcen.1997.6906.

APPENDIX A – Supplementary Materials for Chapter 1

Please find all supplementary information for Chapter 1 under "Supplementary Material"

at the link provided below:

https://www.frontiersin.org/articles/10.3389/fendo.2019.00307/full#supplementary-material

APPENDIX B – Supplementary Materials for Chapter 2

Supplementary Table 2.1. Pairwise comparisons for morphological measurements in CORT dosage experiment. Significant p-values are set in bold font (Tukey's HSD, $p < 0.05$). Upper and lower denote a 95% confidence interval.

Stage	Difference	Lower	Upper	Adj. p-value
13-10	0.035	-0.204	0.275	0.976
15-10	0.665	0.425	0.905	**0.000**
24ph-10	0.640	0.401	0.880	**0.000**
15-13	0.630	0.390	0.870	**0.000**
24ph-13	0.605	0.365	0.845	**0.000**
24ph-15	-0.025	-0.265	0.215	0.991

Supplementary Figure 2.2. Pairwise comparisons for morphological measurements in CORT dosage experiment. Significant p-values are set in bold font (Tukey's HSD, $p < 0.05$).

SVL	Difference	Lower	Upper	Adj. p-value
100nM CORT-EtOH	-0.076	-0.235	0.083	0.472
500nM CORT-EtOH	-0.411	-0.570	-0.252	**0.000**
500nM CORT-100nM CORT	-0.335	-0.494	-0.176	**0.000**
Ventral width	Difference	Lower	Upper	Adj. p-value
100nM CORT-EtOH	0.227	0.048	0.406	**0.011**
500nM CORT-EtOH	0.253	0.070	0.437	**0.005**
500nM CORT-100nM CORT	0.027	-0.152	0.206	0.929
Lower jaw - suture	Difference	Lower	Upper	Adj. p-value
100nM CORT-EtOH	-0.002	-0.182	0.178	1.000
500nM CORT-EtOH	-0.300	-0.480	-0.120	**0.001**
500nM CORT-100nM CORT	-0.298	-0.479	-0.118	**0.001**
Snout - upper jaw	Difference	Lower	Upper	Adj. p-value
100nM CORT-EtOH	0.047	-0.011	0.104	0.132
500nM CORT-EtOH	0.113	0.055	0.170	**0.000**
500nM CORT-100nM CORT	0.066	0.008	0.124	**0.022**
Tail length/SVL	Difference	Lower	Upper	Adj. p-value
100nM CORT-EtOH	-0.044	-0.119	0.031	0.325
500nM CORT-EtOH	0.006	-0.067	0.079	0.975
500nM CORT-100nM CORT	0.050	-0.025	0.125	0.235
Tail notochord length/SVL	Difference	Lower	Upper	Adj. p-value
100nM CORT-EtOH	-0.046	-0.113	0.022	0.232
500nM CORT-EtOH	-0.011	-0.077	0.055	0.908
500nM CORT-100nM CORT	0.035	-0.033	0.102	0.423
Hind limb length/SVL	Difference	Lower	Upper	Adj. p-value
100nM CORT-EtOH	-0.021	-0.058	0.016	0.346
500nM CORT-EtOH	-0.110	-0.147	-0.073	**0.000**
500nM CORT-100nM CORT	-0.089	-0.126	-0.052	**0.000**
Femur length : width	Difference	Lower	Upper	Adj. p-value
100nM CORT-EtOH	-0.239	-0.387	-0.091	**0.001**
500nM CORT-EtOH	-0.696	-0.848	-0.545	**0.000**
500nM CORT-100nM CORT	-0.457	-0.606	-0.309	**0.000**
Calf length : width	Difference	Lower	Upper	Adj. p-value
100nM CORT-EtOH	-0.200	-0.424	0.024	0.086
500nM CORT-EtOH	-0.646	-0.875	-0.417	**0.000**
500nM CORT-100nM CORT	-0.446	-0.670	-0.221	**0.000**

Supplementary Table 2.3. Pairwise comparisons for morphological measurements and experimental replicates in dual treatment experiment. All models are x ~ Treatment + Date of experimental replicate. Significant values are set in bold font (Tukey's HSD, $p < 0.05$).

SVL				
$Treatment	Difference	Lower	Upper	Adj. p-value
50nM T3-Control	0.018	-0.196	0.233	0.996
100nM CORT-Control	-0.131	-0.348	0.086	0.392
50nM T3 + 100nM CORT-Control	-0.143	-0.377	0.091	0.382
100nM CORT-50nM T3	-0.149	-0.361	0.063	0.258
50nM T3 + 100nM CORT-50nM T3	-0.161	-0.390	0.068	0.260
50nM T3 + 100nM CORT-100nM CORT	-0.012	-0.243	0.220	0.999
$Date of experimental replicate	Difference	Lower	Upper	Adj. p-value
Feb-Dec	-0.100	-0.342	0.143	0.702
Jan-Dec	0.712	0.502	0.922	**0.000**
Nov-Dec	0.271	0.071	0.471	**0.004**
Jan-Feb	0.811	0.549	1.074	**0.000**
Nov-Feb	0.370	0.116	0.625	**0.002**
Nov-Jan	-0.441	-0.665	-0.218	**0.000**

Tail area/SVL				
$Treatment	Difference	Lower	Upper	Adj. p-value
50nM T3-Control	-0.522	-1.028	-0.016	**0.040**
100nM CORT-Control	-0.176	-0.688	0.336	0.802
50nM T3 + 100nM CORT-Control	-0.950	-1.501	-0.398	**0.000**
100nM CORT-50nM T3	0.346	-0.153	0.845	0.270
50nM T3 + 100nM CORT-50nM T3	-0.427	-0.967	0.113	0.169
50nM T3 + 100nM CORT-100nM CORT	-0.774	-1.319	-0.228	**0.002**
$Date of experimental replicate	Difference	Lower	Upper	Adj. p-value
Feb-Dec	-0.351	-0.923	0.220	0.375
Jan-Dec	0.278	-0.217	0.772	0.456
Nov-Dec	-0.691	-1.162	-0.220	**0.001**
Jan-Feb	0.629	0.011	1.247	**0.045**
Nov-Feb	-0.340	-0.940	0.260	0.448
Nov-Jan	-0.969	-1.496	-0.442	**0.000**

Supplementary Table 2.3 (Continued).

Total tail length/SVL				
$Treatment	Difference	Lower	Upper	Adj. p-value
50nM T3-Control	-0.206	-0.316	-0.097	**0.000**
100nM CORT-Control	0.016	-0.095	0.127	0.982
50nM T3 + 100nM CORT-Control	-0.274	-0.394	-0.154	**0.000**
100nM CORT-50nM T3	0.222	0.114	0.331	**0.000**
50nM T3 + 100nM CORT-50nM T3	-0.068	-0.185	0.050	0.432
50nM T3 + 100nM CORT-100nM CORT	-0.290	-0.408	-0.172	**0.000**
$Date of experimental replicate	Difference	Lower	Upper	Adj. p-value
Feb-Dec	-0.104	-0.228	0.020	0.131
Jan-Dec	0.010	-0.097	0.118	0.994
Nov-Dec	0.079	-0.023	0.181	0.184
Jan-Feb	0.114	-0.020	0.248	0.122
Nov-Feb	0.183	0.053	0.313	**0.002**
Nov-Jan	0.069	-0.046	0.183	0.394

Tail notochord/SVL				
$Treatment	Difference	Lower	Upper	Adj. p-value
50nM T3-Control	-0.138	-0.219	-0.057	**0.000**
100nM CORT-Control	-0.032	-0.113	0.050	0.741
50nM T3 + 100nM CORT-Control	-0.253	-0.342	-0.165	**0.000**
100nM CORT-50nM T3	0.107	0.027	0.186	**0.004**
50nM T3 + 100nM CORT-50nM T3	-0.115	-0.202	-0.029	**0.004**
50nM T3 + 100nM CORT-100nM CORT	-0.222	-0.309	-0.134	**0.000**
$Date of experimental replicate	Difference	Lower	Upper	Adj. p-value
Feb-Dec	-0.065	-0.156	0.026	0.248
Jan-Dec	0.074	-0.005	0.153	0.076
Nov-Dec	0.132	0.056	0.207	**0.000**
Jan-Feb	0.139	0.040	0.238	**0.002**
Nov-Feb	0.197	0.101	0.293	**0.000**
Nov-Jan	0.058	-0.026	0.142	0.277

Relative hind limb length				
$Treatment	Difference	Lower	Upper	Adj. p-value
50nM T3-Control	**-0.029**	**-0.058**	**0.001**	**0.056**
100nM CORT-Control	-0.038	-0.068	-0.009	**0.006**

Supplementary Table 2.3 (Continued).

50nM T3 + 100nM CORT-Control	-0.065	-0.097	-0.033	**0.000**
100nM CORT-50nM T3	-0.009	-0.038	0.020	0.827
50nM T3 + 100nM CORT-50nM T3	-0.036	-0.068	-0.005	**0.016**
50nM T3 + 100nM CORT-100nM CORT	-0.027	-0.059	0.005	0.122
$Date of experimental replicate	Difference	Lower	Upper	Adj. p-value
Feb-Dec	-0.260	-0.294	-0.227	**0.000**
Jan-Dec	-0.002	-0.031	0.027	0.997
Nov-Dec	0.068	0.041	0.096	**0.000**
Jan-Feb	0.258	0.222	0.294	**0.000**
Nov-Feb	0.329	0.294	0.363	**0.000**
Nov-Jan	0.070	0.040	0.101	**0.000**

Femur length: width ratio				
$Treatment	Difference	Lower	Upper	Adj. p-value
50nM T3-Control	-0.012	-0.142	0.117	0.994
100nM CORT-Control	-0.254	-0.385	-0.123	**0.000**
50nM T3 + 100nM CORT-Control	-0.316	-0.458	-0.175	**0.000**
100nM CORT-50nM T3	-0.242	-0.370	-0.114	**0.000**
50nM T3 + 100nM CORT-50nM T3	-0.304	-0.442	-0.165	**0.000**
50nM T3 + 100nM CORT-100nM CORT	-0.062	-0.202	0.078	0.649
$Date of experimental replicate	Difference	Lower	Upper	Adj. p-value
Feb-Dec	-1.292	-1.438	-1.145	**0.000**
Jan-Dec	0.936	0.809	1.063	**0.000**
Nov-Dec	0.507	0.386	0.628	**0.000**
Jan-Feb	2.228	2.070	2.387	**0.000**
Nov-Feb	1.799	1.645	1.952	**0.000**
Nov-Jan	-0.429	-0.564	-0.294	**0.000**

Calf length: width ratio				
$Treatment	Difference	Lower	Upper	Adj. p-value
50nM T3-Control	-0.063	-0.284	0.158	0.877
100nM CORT-Control	-0.248	-0.472	-0.024	**0.024**
50nM T3 + 100nM CORT-Control	-0.153	-0.394	0.088	0.347
100nM CORT-50nM T3	-0.185	-0.403	0.033	0.124
50nM T3 + 100nM CORT-50nM T3	-0.090	-0.326	0.146	0.747
50nM T3 + 100nM CORT-100nM CORT	0.095	-0.143	0.333	0.721

Supplementary Table 2.3 (Continued).

$Date of experimental replicate	Difference	Lower	Upper	Adj. p-value
Feb-Dec	-2.225	-2.475	-1.976	**0.000**
Jan-Dec	-0.685	-0.902	-0.469	**0.000**
Nov-Dec	-0.027	-0.232	0.179	0.986
Jan-Feb	1.540	1.270	1.810	**0.000**
Nov-Feb	2.199	1.937	2.461	**0.000**
Nov-Jan	0.659	0.429	0.889	**0.000**

Supplementary Table 2.4. Pairwise comparisons between different sets of qPCR data. a = control, b = 50 nM T3, c = 100 nM CORT, d = 50 nM T3 + 100 nM CORT. Significant values are set in bold font (Dunn's post-hoc test, $p < 0.05$).

46 hours					**120 hours**			
dio3					*dio3*			
	a	**b**	**c**			**a**	**b**	**c**
b	0.107	-	-		**b**	0.264	-	-
c	0.593	**0.022**	-		**c**	0.107	**0.009**	-
d	0.107	1	**0.022**		**d**	0.276	**0.043**	0.495
klf9					*klf9*			
	a	**b**	**c**			**a**	**b**	**c**
b	0.056	-	-		**b**	0.192	-	-
c	0.306	0.247	-		**c**	0.241	0.896	-
d	**0.005**	0.247	**0.034**		**d**	**0.014**	0.192	0.192
thibz					*thibz*			
	a	**b**	**c**			**a**	**b**	**c**
b	0.069	-	-		**b**	0.114	-	-
c	0.38	0.289	-		**c**	0.715	0.089	-
d	**0.008**	0.289	0.069		**d**	**0.032**	0.434	**0.032**
thrb					*thrb*			
	a	**b**	**c**			**a**	**b**	**c**
b	0.135	-	-		**b**	0.938	-	-
c	0.197	0.635	-		**c**	0.938	0.938	-
d	**0.005**	0.145	0.098		**d**	0.081	0.081	0.081

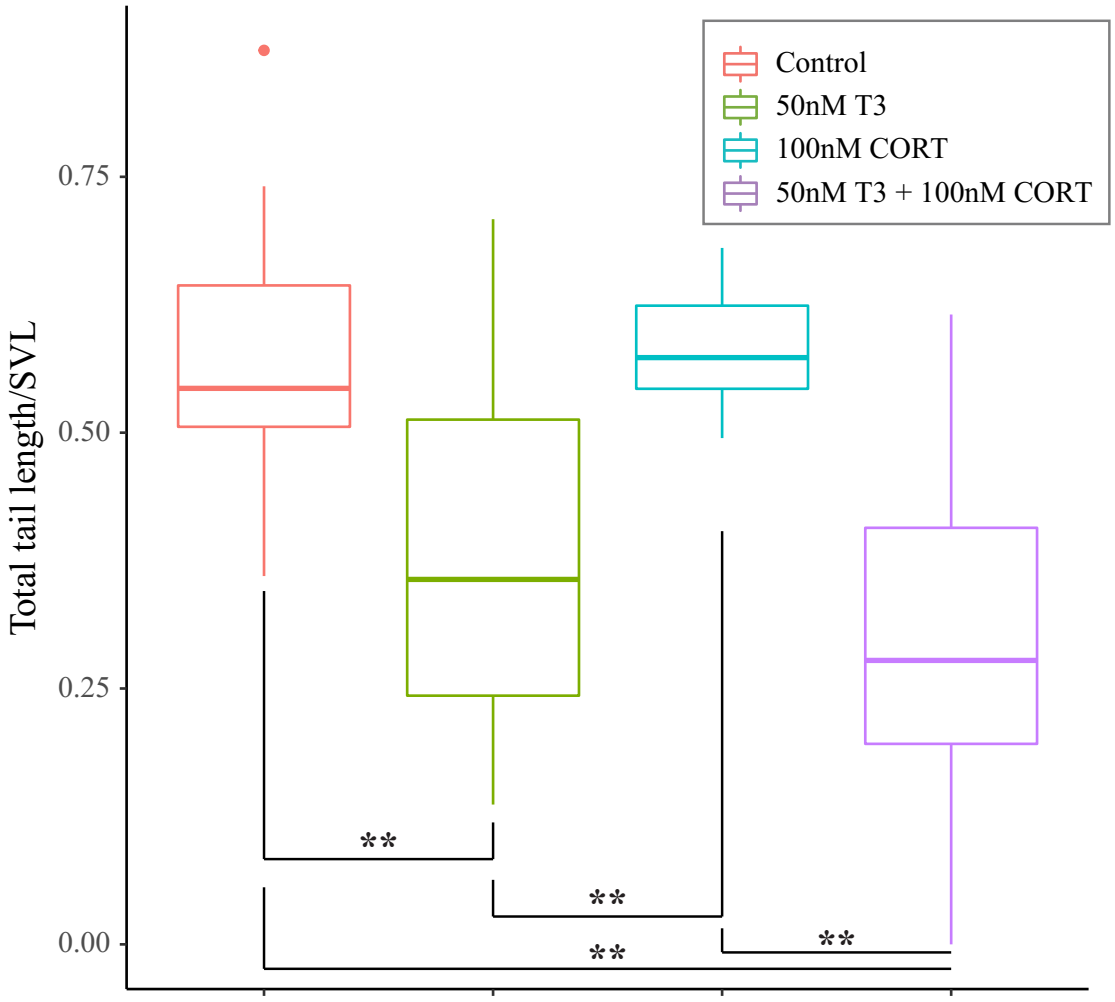

Supplementary Figure 2.1. Treatment with CORT and T_3 significantly affects *Eleutherodactylus coqui* total relative tail length. One asterisk indicates a significant difference at $p < 0.05$; two asterisks indicate a significant difference at $p < 0.001$ (Tukey's HSD). Boxes and whiskers represent median and range of 15-21 individuals.

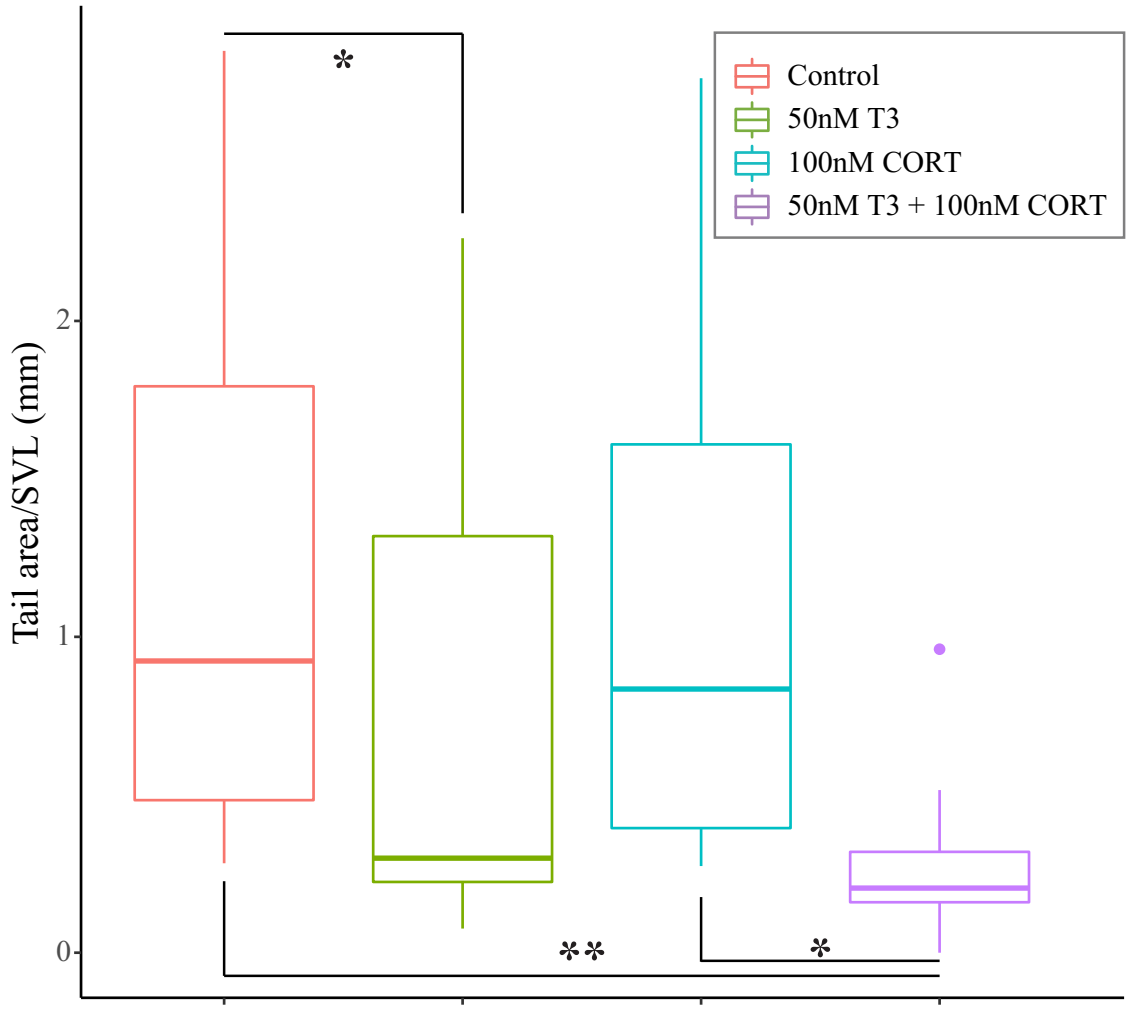

Supplementary Figure 2.2. Treatment with CORT and T_3 significantly affects *Eleutherdactylus coqui* total relative tail area. One asterisk indicates a significant difference at $p < 0.05$; two asterisks indicates a significant difference at $p < 0.05$; two asterisks indicate a significant difference at $p < 0.001$ (Tukey's HSD). Boxes and whiskers represent median and range of 15-21 individuals.

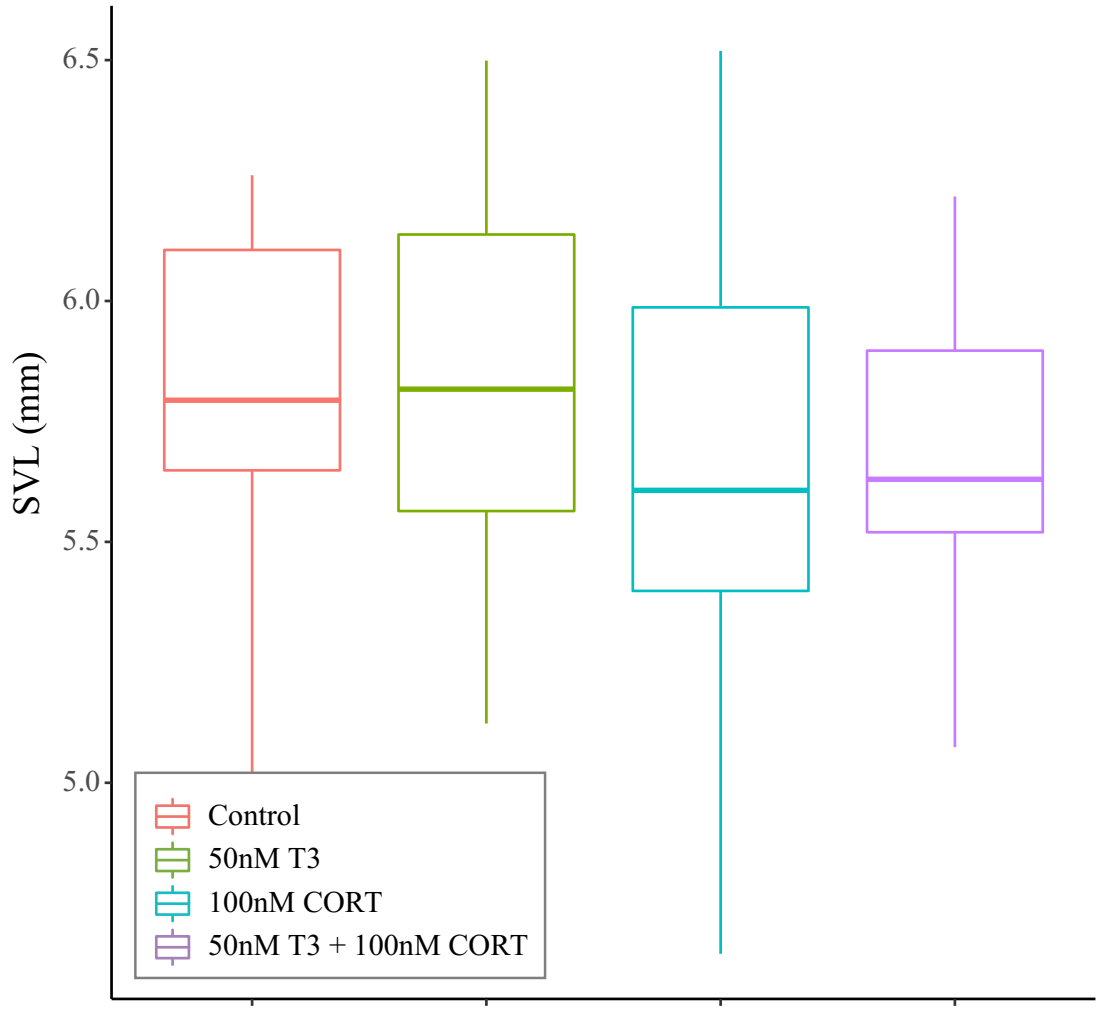

Supplementary Figure 2.3. Treatment with CORT and T_3 does not affect *Eleutherodactylus coqui* body size. Boxes and whiskers represent median and range of 15-21 individuals.

APPENDIX C – Supplementary Materials for Chapter 3

Supplementary Table 3.1. *Eleutherodactylus coqui* transcripts that have more than one *Xenopus tropicalis* protein hit.

E. coqui transcript ID	*Xenopus tropicalis* protein match 1	*Xenopus tropicalis* protein match 2	*Xenopus tropicalis* protein match 3	*Xenopus tropicalis* protein match 4	num_chrom
MSTRG.29572.2	aadacl4	XENTR_v90029431mg			1
MSTRG.21418.1	abca10	abca8			1
MSTRG.22120.2	abcb9	abcb10			1
MSTRG.4354.2	acpp	acp2			1
MSTRG.23628.2	actb	actg1			1
MSTRG.26950.2	ada2	XENTR_v900286571mg			1
MSTRG.7412.1	adgre5	hmcn2			1
MSTRG.12866.1	adgrg6	XENTR_v90028112mg			1
MSTRG.4622.5	agap1	agap2			1
MSTRG.1573.2	ago4	ago3	EIF2C3		1
MSTRG.12128.2	ank2	ank3			1
MSTRG.13111.1	ankrd13b	ankrd13a			1
MSTRG.31893.1	ankrd50	XENTR_v90026746mg			1
MSTRG.6030.1	ano5	XENTR_v900270511mg			1
MSTRG.11223.1	anpep	lvrn			1
MSTRG.12680.3	ap4b1	ap2b1			1
MSTRG.17070.2	arhgap33	XENTR_v90028380mg			1
MSTRG.16568.1	arhgef6	plekhn1			1

Supplementary Table 3.1 (Continued).

MSTRG.293.2	atp6v0d2	atp6v0d1			1
MSTRG.8457.3	auh	Unchar.protein_F6ZTW0_XENTR			1
MSTRG.24085.2	brpf3	Unchar.protein.(Fragment)_F7D1S7_XENTR			1
MSTRG.28800.4	c4bpa	Unchar.protein.(Fragment)_F7ECP3_XENTR	Unchar.protein_F7ECQ0_XENTR		1
MSTRG.20757.1	cat1	XENTR_v900302601mg			1
MSTRG.4999.1	ccdc102a	nedd4l			1
MSTRG.7314.1	chmp7	Unchar.protein.(Fragment)_F7AF33_XENTR			1
MSTRG.21891.3	chtop	LOC496726	XENTR_v900267012mg		1
MSTRG.26304.3	cntrl	XENTR_v900260383mg			1
MSTRG.22598.2	col14a1	col12a1			1
MSTRG.26131.1	col21a1	col14a1			1
MSTRG.31443.2	cps1	XENTR_v90030749mg			1
MSTRG.8161.1	csnk1g3	csnk1g1			1
MSTRG.30567.1	cul9	XENTR_v900277965mg			1
MSTRG.21459.2	cxxc1	XENTR_v90028034mg			1
MSTRG.29894.2	cyb5r2	cyb5r1			1
MSTRG.24679.2	cyp2c8.1	loc100145695.Sca2360			2
MSTRG.27378.1	cyp2c8.1	loc100145695.Sca4043			2

Supplementary Table 3.1 (Continued).

MSTRG.27467.2	dab2ip	XENTR_v900260505mg			1
MSTRG.26245.1	dck.2	dmgdh			1
MSTRG.26684.2	dctn1	mst1r			1
MSTRG.15939.2	ddhd2	Unchar.protein.(Fragment)_F7AM03_XENTR	sec23ip		1
MSTRG.25562.8	ddx39b	ddx39a			1
MSTRG.20656.1	ddx5	XENTR_v900263352mg			1
MSTRG.376.1	dip2a	dip2b			1
MSTRG.890.2	dock9	dock11			1
MSTRG.12438.1	dpf2	kat7			1
MSTRG.27996.2	dpysl4	dpysl3			1
MSTRG.2452.5	dst	plec			1
MSTRG.11896.4	ebf3	ebf2	coe2		1
MSTRG.24526.2	elk1	XENTR_v900280211mg			1
MSTRG.20522.2	ephb1	ephb4			1
MSTRG.20139.2	fam122c	fam122a	Unchar.protein.(Fragment)_F7E6H8_XENTR		1
MSTRG.21724.2	fam208a	XENTR_v90029071mg			1
MSTRG.14711.1	fam98b	LOC100145158	fam98a		1
MSTRG.8120.1	fan1	Unchar.protein_F6XT43_XENTR			1

Supplementary Table 3.1 (Continued).

MSTRG.5176.3	fanca	znf276			1
MSTRG.3840.2	fastkd1	XENTR_v900278881mg			1
MSTRG.30935.3	gal3st4.1	XENTR_v90028994mg	gal3st4		1
MSTRG.2932.3	gigyf2	gigyf1			1
MSTRG.26188.1	gli2	XENTR_v90029134mg			1
MSTRG.11971.2	gsto2	tlr12	LOC100498493		1
MSTRG.22239.4	gstp1	Unchar.protein_F6TAT2_XENTR.Sca1472			2
MSTRG.27574.5	gstp1	Unchar.protein_F6TAT2_XENTR.Sca421			2
MSTRG.29427.3	hadhb	XENTR_v90028292mg			1
MSTRG.823.4	herc1	Unchar.protein_F6RP89_XENTR			1
MSTRG.16923.1	hmbs	Unchar.protein.(Fragment)_F6QS06_XENTR			1
MSTRG.16865.2	hsph1	hyou1			1
MSTRG.27674.2	il12rb2	il6st			1
MSTRG.24839.3	ipo7	ipo8			1
MSTRG.21863.1	jmjd7-pla2g4b	pla2g4f			1
MSTRG.20826.1	kctd6	XENTR_v90030770mg			1
MSTRG.1877.2	keap1	klhl12	LOC100127776		1
MSTRG.7142.2	kif3b	XENTR_v900278093mg			1
MSTRG.16067.1	kmt5b	Unchar.protein_F6Q5B0_XENTR			1

Supplementary Table 3.1 (Continued).

MSTRG.23941.2	kpna2	TEgg002b07.1-001	XENTR_v90027576mg		1
MSTRG.506.2	kpna4	kpna3			1
MSTRG.2061.2	lama4	lama5			1
MSTRG.17739.3	larp1b	larp1			1
MSTRG.26533.1	lhfpl5	lhfpl3			1
MSTRG.20495.3	limk2	tesk2	XENTR_v90027114mg		1
MSTRG.30943.1	LOC100135188	Unchar.protein_F6YU25_XENTR			1
MSTRG.20842.2	LOC100145164	XENTR_v900278351mg			1
MSTRG.21947.1	LOC100216020	Unchar.protein.(Fragment)_F7B9I6_XENTR			1
MSTRG.14647.1	LOC100216123	LOC100037903			1
MSTRG.20722.1	LOC100488227	LOC100487918	cyp4b1.2		1
MSTRG.11640.2	LOC100490503	XENTR_v90029900mg			1
MSTRG.29557.2	loc100492245	Unchar.protein.(Fragment)_F7D5K2_XENTR			1
MSTRG.23436.2	loc100492245	XENTR_v90029342mg	Unchar.protein.(Fragment)_F7D5K2_XENTR	Unchar.protein_K9J8C4_XENTR	1
MSTRG.27366.1	loc548390	LOC100145000			1
MSTRG.27190.4	loxl2	loxl4			1
MSTRG.4134.1	map3k2	XENTR_v90028119mg			1
MSTRG.2681.4	map4k4	tnik			1

Supplementary Table 3.1 (Continued).

MSTRG.30440.2	mapk8	mapk10			1
MSTRG.13511.1	mcoln3	mcoln2			1
MSTRG.2700.1	mecom	XENTR_v90025893mg			1
MSTRG.10765.1	med15	XENTR_v90030391mg			1
MSTRG.17742.2	mfsd10	Unchar.protein_F6R9P9_XENTR			1
MSTRG.25474.3	MGC145244	Unchar.protein_F6YAK3_XENTR			1
MSTRG.25475.3	MGC145244	Unchar.protein.(Fragment)_F6PM71_XENTR	Unchar.protein_F6SD19_XENTR		1
MSTRG.31957.1	MGC145244	Unchar.protein.(Fragment)_F6Z3V8_XENTR			1
MSTRG.7734.3	MGC145518	Unchar.protein_F7CLZ7_XENTR			1
MSTRG.12547.3	mitf	tfeb			1
MSTRG.15575.3	map4k (EC.2.7.11.1)	map4k3			1
MSTRG.52.4	mtmr2	mtmr1			1
MSTRG.2516.1	mul1	XENTR_v900282611mg			1
MSTRG.31167.1	mvp	XENTR_v90028945mg			1
MSTRG.29582.2	myh13	myh3	myh2	myh4	1
MSTRG.9833.4	myo9b	myo9a			1
MSTRG.753.2	naa16	naa15			1
MSTRG.25713.1	nlk.2	XENTR_v900271632mg			1

Supplementary Table 3.1 (Continued).

MSTRG.25689.4	npr1	XENTR_v90030081mg	XENTR_v90029985mg		1
MSTRG.21281.2	nr2c2	nr2c1	dor2		1
MSTRG.11998.1	nrdc	ide			1
MSTRG.14297.2	nt5dc2	XENTR_v90030173mg			1
MSTRG.26005.1	obscn	ttn			1
MSTRG.1675.3	pabpc1	pabpc4			1
MSTRG.23291.2	parp10	XENTR_v90026815mg	XENTR_v900304162mg		1
MSTRG.31242.1	pde4dip	lamb2			1
MSTRG.21102.2	pfkm	pfkp			1
MSTRG.14146.2	phf2	phf8			1
MSTRG.16468.2	prr12	XENTR_v90027146mg			1
MSTRG.24935.2	ptpn23	XENTR_v90028544mg			1
MSTRG.22539.3	pyurf	pigy	prey	znf106	1
MSTRG.25746.2	r3hdm1	r3hdm2			1
MSTRG.21310.3	racgap1	Unchar.protein.(Fragment)_F7AHX8_XENTR			1
MSTRG.20822.1	rpp14	XENTR_v90030774mg			1
MSTRG.12916.2	rps6ka1	rps6ka2			1
MSTRG.11645.1	rusc2	XENTR_v90030511mg			1

Supplementary Table 3.1 (Continued).

MSTRG.15120.4	rybp	enah			1
MSTRG.27442.5	scamp2	BC067960.1-001	scamp1		1
MSTRG.20863.11	scrib	XENTR_v900304252mg	XENTR_v90026700mg		1
MSTRG.20433.1	sgo1	XENTR_v90030419mg			1
MSTRG.31536.2	slc12a9	Unchar.protein.(Fragment)_F6SEH8_XENTR			1
MSTRG.5259.2	slc22a31	cdh15			1
MSTRG.4428.4	slc4a7	slc4a8			1
MSTRG.29029.1	slc6a12	Transporter			1
MSTRG.17428.2	slc7a2.1	slc7a1			1
MSTRG.4140.2	smarcal1	harp	XENTR_v90028124mg		1
MSTRG.30224.3	smpd1	XENTR_v90030947mg	smpd1.(EC.3.1.4.12)		1
MSTRG.10948.1	snrnp70	ppil4	LOC733774		1
MSTRG.3518.1	snx30	snx4			1
MSTRG.16998.1	spen	XENTR_v900287892mg			1
MSTRG.27242.2	sptbn2	XENTR_v900303596mg			1
MSTRG.17266.1	stim2	XENTR_v900300383mg	XENTR_v900300382mg		1
MSTRG.14645.3	sult6b1	LOC100037903			1
MSTRG.1754.1	syncrip	hnrnpr			1
MSTRG.25634.1	tfcp2	tfcp2l1			1
MSTRG.10235.1	tjp2	tjp1			1

Supplementary Table 3.1 (Continued).

MSTRG.10302.1	tle1	tle4			1
MSTRG.26955.1	tmem248	XENTR_v90027925mg			1
MSTRG.22005.1	TNeu062j22.1-001	XENTR_v90030629mg	tial1		1
MSTRG.7978.3	trpm3	trpm6			1
MSTRG.1050.1	Transmembrane.protein.131	Unchar.protein.(Fragment)_F6V325_XENTR			1
MSTRG.26004.1	ttn	obsl1			1
MSTRG.20855.1	tuba1b	Tubulin.alpha.chain.(Fragment)			1
MSTRG.22137.2	tulp3	XENTR_v90030765mg			1
MSTRG.22912.2	twf1	twf2			1
MSTRG.16854.1	ube4a	XENTR_v90028817mg			1
MSTRG.7100.1	uck2	uprt			1
MSTRG.10891.3	Unc-51.like.autophagy.activating.kinase.2	ulk1			1
MSTRG.28281.2	Unchar.protein_F6PJN5_XENTR	Unchar.protein_F6SY01_XENTR			1
MSTRG.25059.1	Unchar.protein_F6PNQ1_XENTR	XENTR_v90025901mg			1
MSTRG.1157.1	Unchar.protein_F6Q1E4_XENTR	Unchar.protein_F6XGM5_XENTR	morf4l1		1
MSTRG.17034.1	Unchar.protein_F6Q604_XENTR	XENTR_v90027221mg			1
MSTRG.23922.1	Unchar.protein_F6QWB2_XENTR	XENTR_v900273345mg			1
MSTRG.10314.3	Unchar.protein_F6RCZ7_XENTR	rmi1			1

Supplementary Table 3.1 (Continued).

MSTRG.27233.2	Unchar.protein_F6RYC2_XENTR	loc100036663			1
MSTRG.25153.2	Unchar.protein_F6S9B6_XENTR	XENTR_v90028287mg			1
MSTRG.3849.2	Unchar.protein_F6SI93_XENTR	ubr1			1
MSTRG.20726.2	Unchar.protein_F6SY01_XENTR	Unchar.protein_F6Y5U3_XENTR			1
MSTRG.30260.7	Unchar.protein_F6TSQ2_XENTR	Unchar.protein_K9J8C4_XENTR			1
MSTRG.20672.1	Unchar.protein_F6TSQ2_XENTR	Unchar.protein.(Fragment)_F6WAQ7_XENTR			1
MSTRG.22111.1	Unchar.protein_F6TSQ2_XENTR	znf717	Unchar.protein_K9J8C4_XENTR		1
MSTRG.9391.1	Unchar.protein_F6UX26_XENTR	Unchar.protein.(Fragment)_F6SL28_XENTR			1
MSTRG.9397.2	Unchar.protein_F6UXV0_XENTR	XENTR_v90029680mg			1
MSTRG.13182.10	Unchar.protein_F6VNK4_XENTR	ubc			1
MSTRG.9421.1	Unchar.protein_F6WRG4_XENTR	Unchar.protein_F6UVA7_XENTR			1
MSTRG.11871.3	Unchar.protein_F6WSL3_XENTR	ndst2	hs3st4	hs3st3a1	1
MSTRG.30563.7	Unchar.protein_F6WWX4_XENTR	XENTR_v90026860mg			1
MSTRG.22307.2	Unchar.protein_F6X2H7_XENTR	LOC100488817			1
MSTRG.24707.2	Unchar.protein_F6X2H7_XENTR	Unchar.protein_F6TSQ2_XENTR	XENTR_v90028954mg		1
MSTRG.23915.1	Unchar.protein_F6X2H7_XENTR	Unchar.protein_F6WUZ5_XENTR			1
MSTRG.23487.1	Unchar.protein_F6X2H7_XENTR	Unchar.protein_F7CN80_XENTR			1
MSTRG.26244.3	Unchar.protein_F6X2H7_XENTR	Unchar.protein_K9J8C4_XENTR			1

Supplementary Table 3.1 (Continued).

MSTRG.24749.2	Unchar.protein_F6X2H7_XENTR	Unchar.protein.(Fragment)_F6WAQ7_XENTR			1
MSTRG.20994.1	Unchar.protein_F6X2H7_XENTR	Unchar.protein.(Fragment)_F7D5K2_XENTR			1
MSTRG.29988.2	Unchar.protein_F6X2H7_XENTR	Unchar.protein.(Fragment)_K9J7Y4_XENTR	XENTR_v90028824mg		1
MSTRG.4645.2	Unchar.protein_F6X2H7_XENTR	Unchar.protein.(Fragment)_K9J8E1_XENTR			1
MSTRG.29534.1	Unchar.protein_F6X2H7_XENTR	XENTR_v900267802mg			1
MSTRG.27915.1	Unchar.protein_F6X2H7_XENTR	XENTR_v90029328mg			1
MSTRG.29532.1	Unchar.protein_F6X2H7_XENTR	XENTR_v90029342mg			1
MSTRG.29254.1	Unchar.protein_F6X2H7_XENTR	XENTR_v90030623mg			1
MSTRG.20783.2	Unchar.protein_F6X2H7_XENTR	XENTR_v90030623mg	XENTR_v900267802mg	Unchar.protein.(Fragment)_F7D5K2_XENTR	1
MSTRG.3231.3	Unchar.protein_F6X2H7_XENTR	XENTR_v90030623mg	XENTR_v90029329mg		1
MSTRG.862.2	Unchar.protein_F6YAR4_XENTR	dzip1			1
MSTRG.6158.3	Unchar.protein_F6YJ44_XENTR	notum			1
MSTRG.27443.4	Unchar.protein_F6ZHD2_XENTR	fam189a1	MGC146654		1
MSTRG.29064.4	Unchar.protein_F6ZYP3_XENTR	XENTR_v900282391mg	XENTR_v90028237mg		1
MSTRG.13377.3	Unchar.protein_F7AGI7_XENTR	son			1
MSTRG.29990.2	Unchar.protein_F7BHV2_XENTR	XENTR_v90029323mg			1
MSTRG.19898.2	Unchar.protein_F7BWA1_XENTR	Unchar.protein_K9J8C4_XENTR			1
MSTRG.25269.1	Unchar.protein_F7CN80_XENTR	Unchar.protein.(Fragment)_L7N389_XENTR			1

Supplementary Table 3.1 (Continued).

MSTRG.21464.1	Unchar.protein_F7CN80_XENTR	XENTR_v900267802mg.Sca1239			2
MSTRG.23863.2	Unchar.protein_F7CN80_XENTR	XENTR_v900267802mg.Sca20			2
MSTRG.25569.3	Unchar.protein_K9J7M3_XENTR	XENTR_v90030623mg			1
MSTRG.4611.2	Unchar.protein_K9J7V2_XENTR	znf630			1
MSTRG.24613.2	Unchar.protein_K9J881_XENTR	Unchar.protein_K9J8C4_XENTR			1
MSTRG.31845.1	Unchar.protein_K9J881_XENTR	Unchar.protein.(Fragment)_F7D5K2_XENTR			1
MSTRG.22966.2	Unchar.protein_K9J881_XENTR	XENTR_v900267802mg			1
MSTRG.30575.2	Unchar.protein_K9J881_XENTR	znf717			1
MSTRG.22891.2	Unchar.protein.(Fragment)_F6QX31_XENTR	Unchar.protein.(Fragment)_F7B9I6_XENTR			1
MSTRG.22167.2	Unchar.protein.(Fragment)_F6RSU3_XENTR	XENTR_v900298221mg			1
MSTRG.28253.2	Unchar.protein.(Fragment)_F6TA52_XENTR	Unchar.protein.(Fragment)_F7EUW0_XENTR			1
MSTRG.7735.1	Unchar.protein.(Fragment)_F6VVC1_XENTR	LOC496795			1
MSTRG.27273.1	Unchar.protein.(Fragment)_F6VVC1_XENTR	Unchar.protein_K9J7M3_XENTR			1
MSTRG.21425.1	Unchar.protein.(Fragment)_F6VVC1_XENTR	Unchar.protein.(Fragment)_K9J7Y4_XENTR			1
MSTRG.16339.1	Unchar.protein.(Fragment)_F6VVC1_XENTR	XENTR_v90027410mg	XENTR_v90027165mg		1
MSTRG.22778.2	Unchar.protein.(Fragment)_F6VVC1_XENTR	zkscan7			1
MSTRG.24487.1	Unchar.protein.(Fragment)_F6VVC1_XENTR	znf180	MGC147120		1
MSTRG.22311.1	Unchar.protein.(Fragment)_F6VVC1_XENTR	Unchar.protein_K9J8C4_XENTR.Sca1491			2

Supplementary Table 3.1 (Continued).

MSTRG.23535.2	Unchar.protein.(Fragment)_F6VVC1_XENTR	Unchar.protein_K9J8C4_XENTR.Sca1885			2
MSTRG.26248.2	Unchar.protein.(Fragment)_F6Y098_XENTR	Unchar.protein.(Fragment)_F7D5K2_XENTR			1
MSTRG.28500.2	Unchar.protein.(Fragment)_F6YM55_XENTR	XENTR_v90026658mg			1
MSTRG.1552.1	Unchar.protein.(Fragment)_F6Z2I2_XENTR	khdrbs1			1
MSTRG.17043.10	Unchar.protein.(Fragment)_F7CIW9_XENTR	XENTR_v900284251mg	ubr4		1
MSTRG.25331.3	Unchar.protein.(Fragment)_F7D5K2_XENTR	Unchar.protein_F6PSR7_XENTR	Unchar.protein_K9J8C4_XENTR		1
MSTRG.31010.5	Unchar.protein.(Fragment)_F7D5K2_XENTR	znf717	Unchar.protein_K9J8C4_XENTR		1
MSTRG.15174.3	Unchar.protein.(Fragment)_F7D5K2_XENTR	Unchar.protein_K9J8C4_XENTR.Chr5			3
MSTRG.29492.2	Unchar.protein.(Fragment)_F7D5K2_XENTR	Unchar.protein_K9J8C4_XENTR.Sca611			3
MSTRG.31671.2	Unchar.protein.(Fragment)_F7D5K2_XENTR	Unchar.protein_K9J8C4_XENTR.Sca91			3
MSTRG.20065.2	Unchar.protein.(Fragment)_F7DNY4_XENTR	znf180	MGC147120		1
MSTRG.25767.4	Unchar.protein.(Fragment)_F7E9I5_XENTR	XENTR_v90027770mg			1
MSTRG.24625.1	Unchar.protein.(Fragment)_F7E9Z0_XENTR	arhgef17	XENTR_v90028168mg		1
MSTRG.28087.2	Unchar.protein.(Fragment)_F7E9Z0_XENTR	des.1			1
MSTRG.2342.1	Unchar.protein.(Fragment)_F7EI10_XENTR	znf292			1
MSTRG.26076.2	Unchar.protein.(Fragment)_K9J7Y3_XENTR	XENTR_v90030384mg			1
MSTRG.8899.1	usp44	usp49			1
MSTRG.21042.2	usp9x	usp24			1

Supplementary Table 3.1 (Continued).

MSTRG.4998.2	utp6	XENTR_v900289171mg			1
MSTRG.25212.1	vav2	XENTR_v90026874mg			1
MSTRG.4059.2	wdr5	vps8			1
MSTRG.22849.1	wdr91	XENTR_v900265572mg			1
MSTRG.26800.4	wnk1	nrbp1			1
MSTRG.26617.2	XENTR_v90025770mg	XENTR_v90025764mg			1
MSTRG.16969.4	XENTR_v90025816mg	znf362			1
MSTRG.2695.1	XENTR_v90025892mg	mynn			1
MSTRG.26799.3	XENTR_v900258941mg	Unchar.protein_F6VUL1_XENTR	Unchar.protein.(Fragment)_F6PK90_XENTR		1
MSTRG.27244.2	XENTR_v90025942mg	Unchar.protein.(Fragment)_F6XML6_XENTR			1
MSTRG.29324.1	XENTR_v90025993mg	Unchar.protein_F6V7I2_XENTR			1
MSTRG.21844.2	XENTR_v900261241mg	Farnesyl-diphosphate.farnesyltransferase.1			1
MSTRG.29431.1	XENTR_v900261671mg	XENTR_v900261521mg			1
MSTRG.20616.2	XENTR_v90026186mg	dmtn			1
MSTRG.11626.2	XENTR_v900262953mg	vwa5a			1
MSTRG.4568.3	XENTR_v900265661mg	malsu1	LOC548894	Unchar.protein.(Fragment)_F7D7Y8_XENTR	1
MSTRG.6053.1	XENTR_v900265661mg	mical2			1
MSTRG.26747.1	XENTR_v90026601mg	Unchar.protein_F6QG95_XENTR			1

Supplementary Table 3.1 (Continued).

MSTRG.14107.1	XENTR_v900266351mg	magi1			1
MSTRG.30073.1	XENTR_v90026770mg	Unchar.protein_K9J8C4_XENTR			1
MSTRG.28062.1	XENTR_v90026770mg	Unchar.protein.(Fragment)_F7D5K2_XENTR			1
MSTRG.26041.1	XENTR_v90026770mg	znf300			1
MSTRG.29227.3	XENTR_v900267791mg	Unchar.protein_K9J8C4_XENTR			1
MSTRG.4705.3	XENTR_v900267791mg	Unchar.protein.(Fragment)_K9J8E1_XENTR			1
MSTRG.32054.1	XENTR_v900267802mg	zkscan7			1
MSTRG.22770.1	XENTR_v900267802mg	Unchar.protein_K9J8C4_XENTR.Sca1622			2
MSTRG.24111.4	XENTR_v900267802mg	Unchar.protein_K9J8C4_XENTR.Sca2099			2
MSTRG.25422.1	XENTR_v90026850mg	XENTR_v90026799mg			1
MSTRG.30871.1	XENTR_v900268651mg	slc2a8			1
MSTRG.31358.2	XENTR_v90026878mg	hhipl2	XENTR_v90029712mg	XENTR_v90030406mg	1
MSTRG.24464.2	XENTR_v90026887mg	Unchar.protein.(Fragment)_F6XML6_XENTR	XENTR_v90025738mg	Unchar.protein.(Fragment)_F6TMI4_XENTR	1
MSTRG.31779.1	XENTR_v900269721mg	Unchar.protein_F6TSQ2_XENTR			1
MSTRG.31784.2	XENTR_v900269721mg	Unchar.protein_F6X2H7_XENTR			1
MSTRG.30329.1	XENTR_v900269721mg	Unchar.protein_K9J8C4_XENTR			1
MSTRG.31785.3	XENTR_v900269721mg	Unchar.protein.(Fragment)_F6VVC1_XENTR			1
MSTRG.24312.1	XENTR_v900269721mg	XENTR_v900288722mg			1

Supplementary Table 3.1 (Continued).

MSTRG.27430.1	XENTR_v900269721mg	XENTR_v90029342mg	Unchar.protein_F6WUZ5_XENTR		1
MSTRG.22983.2	XENTR_v900269721mg	XENTR_v90030623mg			1
MSTRG.23700.3	XENTR_v900269721mg	XENTR_v90030623mg	Unchar.protein_F6WUZ5_XENTR		1
MSTRG.28314.2	XENTR_v900269721mg	XENTR_v900267802mg.Sca491			2
MSTRG.31880.1	XENTR_v900269721mg	XENTR_v900267802mg.Sca9494			2
MSTRG.29357.2	XENTR_v90027044mg	ctr9	sh2bp1		1
MSTRG.21475.1	XENTR_v90027094mg	iqcb1			1
MSTRG.6741.2	XENTR_v90027123mg	dtx3			1
MSTRG.25511.1	XENTR_v900271992mg	XENTR_v90027910mg			1
MSTRG.18173.1	XENTR_v90027235mg	XENTR_v90030353mg			1
MSTRG.26319.2	XENTR_v90027291mg	XENTR_v90030617mg			1
MSTRG.6037.3	XENTR_v900273181mg	nav2			1
MSTRG.18791.1	XENTR_v900273435mg	dtnb			1
MSTRG.27668.2	XENTR_v90027400mg	nasp	Unchar.protein.(Fragment)_F6W717_XENTR		1
MSTRG.30940.3	XENTR_v90027410mg	znf628	Unchar.protein_F6Q247_XENTR		1
MSTRG.7292.4	XENTR_v90027439mg	XENTR_v900263022mg	XENTR_v90027291mg		1
MSTRG.4873.2	XENTR_v900274461mg	vill			1
MSTRG.31526.1	XENTR_v90027490mg	Unchar.protein_F7ASL6_XENTR			1

Supplementary Table 3.1 (Continued).

MSTRG.23348.2	XENTR_v90027513mg	pip5k1a			1
MSTRG.27217.1	XENTR_v90027549mg	XENTR_v900297601mg			1
MSTRG.28186.2	XENTR_v90027562mg	mon1a			1
MSTRG.5597.10	XENTR_v90027590mg	Unchar.protein.(Fragment)_F6ZV90_XENTR			1
MSTRG.16826.1	XENTR_v90027592mg	XENTR_v90030297mg			1
MSTRG.24231.2	XENTR_v900276042mg	stk11ip			1
MSTRG.30157.4	XENTR_v90027624mg	XENTR_v90026593mg	XENTR_v90030063mg		1
MSTRG.29614.1	XENTR_v900276991mg	cgn			1
MSTRG.29618.1	XENTR_v900277043mg	snx27			1
MSTRG.24130.1	XENTR_v900277961mg	cul9			1
MSTRG.24127.3	XENTR_v900277967mg	cul9			1
MSTRG.22085.1	XENTR_v90027846mg	Transmembrane.protein.8B			1
MSTRG.23267.5	XENTR_v900281393mg	mroh1			1
MSTRG.23270.2	XENTR_v90028141mg	Unchar.protein_F6TK99_XENTR			1
MSTRG.20647.2	XENTR_v90028232mg	iah1			1
MSTRG.24848.2	XENTR_v90028370mg	ctu1	atpbd3	ncs6	1
MSTRG.26090.2	XENTR_v90028417mg	dbn1			1
MSTRG.31690.4	XENTR_v900284801mg	XENTR_v90029225mg			1

Supplementary Table 3.1 (Continued).

MSTRG.26455.2	XENTR_v90028486mg	fkbp15			1
MSTRG.6682.1	XENTR_v900284962mg	rapgefl1			1
MSTRG.22503.1	XENTR_v90028662mg	XENTR_v90028659mg			1
MSTRG.22500.2	XENTR_v900286638mg	Voltage-dependent.L-type.calcium.channel.subunit.alpha			1
MSTRG.28710.2	XENTR_v900287352mg	ptpn4			1
MSTRG.26444.2	XENTR_v90028808mg	dock6			1
MSTRG.23626.2	XENTR_v90028834mg	Unchar.protein_F7EQ60_XENTR			1
MSTRG.30074.2	XENTR_v900288722mg	Unchar.protein_F7CN80_XENTR			1
MSTRG.26218.7	XENTR_v900288722mg	XENTR_v90029329mg	XENTR_v900267802mg		1
MSTRG.25264.1	XENTR_v90028954mg	Unchar.protein_F7CN80_XENTR			1
MSTRG.24690.2	XENTR_v90029030mg	glipr2			1
MSTRG.26689.1	XENTR_v90029032mg	ccn1			1
MSTRG.12925.2	XENTR_v900290671mg	XENTR_v90025925mg			1
MSTRG.24789.2	XENTR_v900291112mg	Unchar.protein_F6PSR7_XENTR			1
MSTRG.29803.2	XENTR_v90029305mg	prpf4			1
MSTRG.28474.1	XENTR_v90029323mg	Unchar.protein_F6TD83_XENTR			1
MSTRG.23841.2	XENTR_v90029329mg	XENTR_v900267802mg.Sca20			2
MSTRG.24489.1	XENTR_v90029329mg	XENTR_v900267802mg.Sca22630			2

Supplementary Table 3.1 (Continued).

MSTRG.31520.1	XENTR_v90029331mg	Unchar.protein_K9J8C4_XENTR			1
MSTRG.9672.2	XENTR_v900294811mg	ttll1			1
MSTRG.17011.1	XENTR_v900294842mg	fbxo42			1
MSTRG.11856.1	XENTR_v90029490mg	Unchar.protein_F6Y0P2_XENTR			1
MSTRG.28544.4	XENTR_v90029603mg	XENTR_v90029604mg			1
MSTRG.20621.2	XENTR_v90029613mg	XENTR_v90029612mg			1
MSTRG.24850.3	XENTR_v90029733mg	gon4l	XENTR_v90029730mg		1
MSTRG.9204.1	XENTR_v900298633mg	RBR-type.E3.ubiquitin.transferase.(EC.2.3.2.31)			1
MSTRG.22349.4	XENTR_v900299102mg	pdxk			1
MSTRG.28284.2	XENTR_v90029926mg	Unchar.protein_F6PSR7_XENTR			1
MSTRG.23328.1	XENTR_v90029926mg	Unchar.protein_K9J8C4_XENTR			1
MSTRG.31991.1	XENTR_v90029926mg	zfp1			1
MSTRG.28293.1	XENTR_v90029928mg	nucb1	nucb2		1
MSTRG.21036.2	XENTR_v900299741mg	RNF8			1
MSTRG.22097.2	XENTR_v900299921mg	traf2			1
MSTRG.23285.1	XENTR_v900302683mg	XENTR_v90029815mg			1
MSTRG.20528.8	XENTR_v90030362mg	tpm2	tpm1	XENTR_v90026674mg	1
MSTRG.28344.2	XENTR_v900303931mg	helz			1

Supplementary Table 3.1 (Continued).

MSTRG.7138.1	XENTR_v90030503mg	XENTR_v90025819mg			1
MSTRG.14814.6	XENTR_v90030530mg	XENTR_v90029001mg			1
MSTRG.28807.1	XENTR_v90030539mg	XENTR_v900269861mg			1
MSTRG.27734.2	XENTR_v90030612mg	XENTR_v90027511mg			1
MSTRG.30783.2	XENTR_v90030617mg	ddx18			1
MSTRG.30075.3	XENTR_v90030623mg	Unchar.protein_F6PSR7_XENTR			1
MSTRG.23370.2	XENTR_v90030623mg	Unchar.protein_F7A1U1_XENTR	XENTR_v90028824mg		1
MSTRG.30853.1	XENTR_v90030623mg	XENTR_v90029342mg			1
MSTRG.18203.2	XENTR_v90030623mg	znf41			1
MSTRG.26403.2	XENTR_v90030623mg	XENTR_v900267791mg.Sca33411			2
MSTRG.31670.2	XENTR_v90030623mg	XENTR_v900267791mg.Sca91			2
MSTRG.24306.3	XENTR_v90030623mg	XENTR_v900267802mg.Sca2187			2
MSTRG.25730.1	XENTR_v90030623mg	XENTR_v900267802mg.Sca2946			2
MSTRG.29326.2	XENTR_v90030623mg	XENTR_v90029329mg.Sca5926			2
MSTRG.31800.1	XENTR_v90030623mg	XENTR_v90029329mg.Sca934			2
MSTRG.25256.2	XENTR_v90030623mg	Unchar.protein_K9J8C4_XENTR.Sca27			3
MSTRG.27916.2	XENTR_v90030623mg	Unchar.protein_K9J8C4_XENTR.Sca4500			3
MSTRG.31887.2	XENTR_v90030623mg	Unchar.protein_K9J8C4_XENTR.Sca951			3

Supplementary Table 3.1 (Continued).

MSTRG.24126.1	XENTR_v90030731mg	pacs2			1
MSTRG.20795.3	XENTR_v90030762mg	emilin1			1
MSTRG.30172.9	XENTR_v90030765mg	XENTR_v900259232mg			1
MSTRG.4849.1	XENTR_v90030822mg	XENTR_v900265921mg			1
MSTRG.29769.1	zan	XENTR_v90030941mg			1
MSTRG.1535.1	zbtb8a	Unchar.protein_F6ZSA7_XENTR			1
MSTRG.19401.2	zbtb9	matr3			1
MSTRG.7098.2	zfat	Unchar.protein.(Fragment)_F6T6P1_XENTR			1
MSTRG.30069.2	znf205	XENTR_v90026781mg	XENTR_v900267802mg		1
MSTRG.31676.3	znf205	XENTR_v90026781mg	znf208		1
MSTRG.31899.2	znf347	XENTR_v90028950mg			1
MSTRG.6368.2	znf420	Unchar.protein_F6Q247_XENTR			1
MSTRG.4633.1	znf605	Unchar.protein.(Fragment)_F6YSY1_XENTR			1
MSTRG.20743.1	znf630	Unchar.protein_F7D9V7_XENTR			1
MSTRG.23344.1	znf687	XENTR_v90029363mg			1
MSTRG.20477.1	znf717	Unchar.protein_K9J8C4_XENTR.Sca1005			3
MSTRG.21028.2	znf717	Unchar.protein_K9J8C4_XENTR.Sca1128			3
MSTRG.31942.1	znf717	Unchar.protein_K9J8C4_XENTR.Sca9609			3

Supplementary Table 3.1 (Continued).

MSTRG.25368.3	znf721	Unchar.protein.(Fragment)_F6ZVX9_XENTR	Unchar.protein.(Fragment)_K9J8E1_XENTR	Unchar.protein.(Fragment)_F7D5K2_XENTR	1
MSTRG.25271.5	znf721	XENTR_v90026770mg	XENTR_v90030623mg		1
MSTRG.24709.2	znf721	XENTR_v90030623mg	XENTR_v90029342mg		1
MSTRG.21991.2	znf721	XENTR_v90030623mg.Sca140			3
MSTRG.22768.1	znf721	XENTR_v90030623mg.Sca1622			3
MSTRG.28064.1	znf721	XENTR_v90030623mg.Sca4649			3

Supplementary Table 3.2. Gene ontology categories significantly enriched in genes that are consistently up-regulated throughout *Eleutherodactylus coqui* hind limb development. Values > 1 indicate overenrichment; values < 1 indicate underenrichment.

Biological Process	GO ID	Fold Enrichment	p-value	Reg. direction
myofibril assembly	GO:0030239	6.7	1.39E-02	up_up
cellular component assembly involved in morphogenesis	GO:0010927	5.99	2.13E-02	up_up
actomyosin structure organization	GO:0031032	5.27	2.13E-02	up_up
skeletal muscle organ development	GO:0060538	5.06	2.45E-02	up_up
skeletal muscle tissue development	GO:0007519	4.95	4.80E-02	up_up
muscle organ development	GO:0007517	4.54	5.94E-03	up_up
striated muscle cell development	GO:0055002	4.52	3.57E-03	up_up
muscle cell development	GO:0055001	4.48	1.37E-03	up_up
striated muscle tissue development	GO:0014706	4.32	8.86E-03	up_up
muscle tissue development	GO:0060537	4.32	8.39E-03	up_up
striated muscle cell differentiation	GO:0051146	4.13	4.30E-03	up_up
muscle cell differentiation	GO:0042692	4.07	1.83E-03	up_up
muscle structure development	GO:0061061	4	5.34E-05	up_up
supramolecular fiber organization	GO:0097435	3.07	3.93E-02	up_up
system process	GO:0003008	2.93	2.07E-02	up_up
cell adhesion	GO:0007155	2.87	2.17E-02	up_up
biological adhesion	GO:0022610	2.87	2.08E-02	up_up
organic substance metabolic process	GO:0071704	0.76	3.87E-02	up_up
primary metabolic process	GO:0044238	0.75	2.14E-02	up_up
nitrogen compound metabolic process	GO:0006807	0.74	3.90E-02	up_up
macromolecule metabolic process	GO:0043170	0.7	1.18E-02	up_up
cellular metabolic process	GO:0044237	0.64	5.80E-05	up_up
cellular protein metabolic process	GO:0044267	0.64	4.47E-02	up_up
cellular macromolecule metabolic process	GO:0044260	0.59	8.61E-04	up_up
cellular aromatic compound metabolic process	GO:0006725	0.39	1.11E-04	up_up
organic cyclic compound metabolic process	GO:1901360	0.38	5.74E-05	up_up
nucleobase-containing compound metabolic process	GO:0006139	0.36	6.33E-05	up_up
heterocycle metabolic process	GO:0046483	0.35	1.61E-05	up_up
cellular nitrogen compound metabolic process	GO:0034641	0.33	3.27E-07	up_up
RNA metabolic process	GO:0016070	0.28	1.88E-03	up_up
nucleic acid metabolic process	GO:0090304	0.24	7.70E-06	up_up
gene expression	GO:0010467	0.24	8.68E-06	up_up
protein modification by small protein conjugation or removal	GO:0070647	0.22	2.92E-02	up_up
chromosome organization	GO:0051276	0.18	2.15E-02	up_up

Supplementary Table 3.2 (Continued).

RNA processing	GO:0006396	0.11	3.07E-03	up_up
cellular response to DNA damage stimulus	GO:0006974	0.09	4.72E-02	up_up
protein ubiquitination	GO:0016567	0.08	2.07E-02	up_up
DNA metabolic process	GO:0006259	0.07	1.18E-02	up_up
protein modification by small protein conjugation	GO:0032446	0.07	1.17E-02	up_up
DNA repair	GO:0006281	< 0.01	2.64E-02	up_up

Supplementary Table 3.3. Gene ontology categories significantly enriched in genes that are consistently down-regulated throughout *Eleutherodactylus coqui* hind limb development. Values > 1 indicate overenrichment; values < 1 indicate underenrichment.

Biological Process	GO ID	Fold Enrichment	p-value	Reg. direction
DNA unwinding involved in DNA replication	GO:0006268	20.46	1.74E-02	down_down
regulation of DNA-dependent DNA replication initiation	GO:0030174	20.46	1.72E-02	down_down
regulation of DNA-dependent DNA replication	GO:0090329	17.9	2.42E-04	down_down
regulation of DNA replication	GO:0006275	16.37	7.88E-05	down_down
DNA replication initiation	GO:0006270	16.37	7.70E-05	down_down
regulation of G2/M transition of mitotic cell cycle	GO:0010389	16.37	2.73E-02	down_down
negative regulation of cell cycle G2/M phase transition	GO:1902750	13.64	4.09E-02	down_down
DNA-dependent DNA replication	GO:0006261	13.64	1.04E-06	down_down
protein localization to chromosome	GO:0034502	13.64	4.06E-02	down_down
regulation of cell cycle G2/M phase transition	GO:1902749	12.28	4.06E-03	down_down
negative regulation of mitotic cell cycle phase transition	GO:1901991	11.93	1.31E-03	down_down
negative regulation of cell cycle phase transition	GO:1901988	11.69	4.19E-04	down_down
regulation of cytokinesis	GO:0032465	11.02	1.84E-03	down_down
DNA replication	GO:0006260	10.23	5.35E-15	down_down
mitotic cell cycle checkpoint	GO:0007093	10.23	8.02E-03	down_down
negative regulation of cell cycle process	GO:0010948	10.23	7.52E-05	down_down
regulation of mitotic cell cycle phase transition	GO:1901990	10.23	2.46E-04	down_down
negative regulation of mitotic cell cycle	GO:0045930	10.23	8.36E-04	down_down
regulation of cell cycle phase transition	GO:1901987	9.79	3.00E-05	down_down
mitotic sister chromatid segregation	GO:0000070	8.61	1.84E-03	down_down
sister chromatid segregation	GO:0000819	8.18	2.40E-03	down_down
histone lysine methylation	GO:0034968	8.01	1.02E-03	down_down
regulation of mitotic cell cycle	GO:0007346	7.67	6.64E-05	down_down
regulation of cell cycle process	GO:0010564	7.52	4.16E-07	down_down
DNA biosynthetic process	GO:0071897	7.44	3.81E-03	down_down
regulation of cell division	GO:0051302	7.16	1.19E-02	down_down
histone methylation	GO:0016571	7.06	8.44E-04	down_down
cell cycle checkpoint	GO:0000075	6.82	6.05E-03	down_down
DNA packaging	GO:0006323	6.82	3.47E-02	down_down
peptidyl-lysine methylation	GO:0018022	6.82	2.42E-03	down_down
nuclear chromosome segregation	GO:0098813	6.82	5.97E-03	down_down
DNA conformation change	GO:0071103	6.68	5.69E-06	down_down

Supplementary Table 3.3 (Continued).

chromosome segregation	GO:0007059	6.43	6.45E-04	down_down
mitotic nuclear division	GO:0140014	6.39	1.52E-03	down_down
mitotic cell cycle	GO:0000278	6.02	2.07E-08	down_down
negative regulation of cell cycle	GO:0045786	5.99	4.59E-04	down_down
chromatin remodeling	GO:0006338	5.97	2.58E-02	down_down
DNA geometric change	GO:0032392	5.85	1.26E-02	down_down
DNA duplex unwinding	GO:0032508	5.73	3.08E-02	down_down
mitotic cell cycle process	GO:1903047	5.72	2.79E-06	down_down
nuclear division	GO:0000280	5.53	3.73E-03	down_down
cell cycle	GO:0007049	5.37	1.05E-13	down_down
DNA metabolic process	GO:0006259	5.35	1.13E-14	down_down
cell cycle process	GO:0022402	5.33	1.25E-07	down_down
organelle fission	GO:0048285	5.25	5.22E-03	down_down
protein methylation	GO:0006479	5.23	2.51E-03	down_down
protein alkylation	GO:0008213	5.23	2.48E-03	down_down
chromosome organization	GO:0051276	5.09	1.98E-16	down_down
cell division	GO:0051301	4.68	2.65E-05	down_down
chromatin organization	GO:0006325	4.21	3.75E-07	down_down
macromolecule methylation	GO:0043414	3.84	1.20E-02	down_down
histone modification	GO:0016570	3.78	1.01E-03	down_down
covalent chromatin modification	GO:0016569	3.78	9.92E-04	down_down
peptidyl-lysine modification	GO:0018205	3.75	8.45E-03	down_down
cellular response to DNA damage stimulus	GO:0006974	3.73	5.86E-06	down_down
nucleic acid phosphodiester bond hydrolysis	GO:0090305	3.67	5.93E-03	down_down
regulation of cell cycle	GO:0051726	3.6	1.29E-04	down_down
microtubule cytoskeleton organization	GO:0000226	3.46	3.86E-02	down_down
DNA repair	GO:0006281	3.3	9.97E-04	down_down
microtubule-based process	GO:0007017	3.17	1.59E-03	down_down
cellular response to stress	GO:0033554	3.03	1.03E-04	down_down
peptidyl-amino acid modification	GO:0018193	2.72	5.98E-03	down_down
nucleic acid metabolic process	GO:0090304	2.68	6.23E-11	down_down
organelle organization	GO:0006996	2.43	1.24E-07	down_down
nucleobase-containing compound metabolic process	GO:0006139	2.24	6.65E-08	down_down
regulation of cellular macromolecule biosynthetic process	GO:2000112	2.24	9.58E-07	down_down
regulation of nucleobase-containing compound metabolic process	GO:0019219	2.21	9.27E-07	down_down
regulation of macromolecule biosynthetic process	GO:0010556	2.19	1.08E-06	down_down
regulation of transcription, DNA-templated	GO:0006355	2.18	1.11E-05	down_down
heterocycle metabolic process	GO:0046483	2.15	3.28E-07	down_down

Supplementary Table 3.3 (Continued).

regulation of cellular biosynthetic process	GO:0031326	2.15	1.97E-06	down_down
regulation of biosynthetic process	GO:0009889	2.15	1.96E-06	down_down
response to stress	GO:0006950	2.14	1.22E-02	down_down
cellular aromatic compound metabolic process	GO:0006725	2.13	3.90E-07	down_down
regulation of RNA biosynthetic process	GO:2001141	2.12	1.89E-05	down_down
regulation of nucleic acid-templated transcription	GO:1903506	2.12	1.84E-05	down_down
regulation of gene expression	GO:0010468	2.1	3.82E-06	down_down
organic cyclic compound metabolic process	GO:1901360	2.1	4.27E-07	down_down
regulation of RNA metabolic process	GO:0051252	2.1	1.02E-05	down_down
regulation of macromolecule metabolic process	GO:0060255	2.03	4.13E-07	down_down
cellular component organization	GO:0016043	1.98	4.08E-06	down_down
regulation of nitrogen compound metabolic process	GO:0051171	1.95	5.85E-06	down_down
regulation of metabolic process	GO:0019222	1.95	1.59E-06	down_down
cellular component organization or biogenesis	GO:0071840	1.93	7.47E-06	down_down
regulation of primary metabolic process	GO:0080090	1.92	1.05E-05	down_down
regulation of cellular metabolic process	GO:0031323	1.9	9.39E-06	down_down
cellular macromolecule biosynthetic process	GO:0034645	1.86	1.88E-02	down_down
macromolecule biosynthetic process	GO:0009059	1.85	1.93E-02	down_down
cellular nitrogen compound metabolic process	GO:0034641	1.76	1.92E-04	down_down
cellular macromolecule metabolic process	GO:0044260	1.69	2.76E-06	down_down
macromolecule metabolic process	GO:0043170	1.58	2.75E-06	down_down
nitrogen compound metabolic process	GO:0006807	1.4	1.90E-03	down_down
cellular metabolic process	GO:0044237	1.37	3.19E-03	down_down
organic substance metabolic process	GO:0071704	1.32	1.20E-02	down_down
primary metabolic process	GO:0044238	1.3	3.21E-02	down_down
cellular process	GO:0009987	1.27	1.01E-03	down_down
biological_process	GO:0008150	1.13	3.04E-02	down_down
Unclassified	UNCLASSIFIED	0.76	3.07E-02	down_down
organonitrogen compound biosynthetic process	GO:1901566	0.26	1.41E-02	down_down
regulation of signal transduction	GO:0009966	0.2	2.62E-02	down_down
regulation of cell communication	GO:0010646	0.2	1.95E-02	down_down
regulation of signaling	GO:0023051	0.19	1.96E-02	down_down
cellular amide metabolic process	GO:0043603	0.09	2.14E-02	down_down
peptide metabolic process	GO:0006518	< 0.01	8.34E-03	down_down
peptide biosynthetic process	GO:0043043	< 0.01	1.18E-02	down_down
translation	GO:0006412	< 0.01	1.18E-02	down_down

Supplementary Table 3.4. Gene ontology categories significantly enriched in genes that are consistently up-regulated throughout *Xenopus tropicalis* hind limb development. Values > 1 indicate overenrichment; values < 1 indicate underenrichment.

Biological Process	GO ID	Fold Enrichment	p-value	Reg. direction
ribonucleoside diphosphate metabolic process	GO:0009185	7.03	1.58E-03	up_up
purine ribonucleoside diphosphate metabolic process	GO:0009179	7.03	1.51E-03	up_up
purine nucleoside diphosphate metabolic process	GO:0009135	7.03	1.44E-03	up_up
ADP metabolic process	GO:0046031	6.7	3.83E-03	up_up
ATP generation from ADP	GO:0006757	6.62	1.83E-02	up_up
glycolytic process	GO:0006096	6.62	1.79E-02	up_up
pyruvate metabolic process	GO:0006090	5.92	2.86E-02	up_up
myofibril assembly	GO:0030239	5.75	1.78E-02	up_up
plasma membrane organization	GO:0007009	5.36	4.04E-02	up_up
carbohydrate catabolic process	GO:0016052	5.36	3.98E-02	up_up
ATP metabolic process	GO:0046034	5.28	3.66E-03	up_up
cell redox homeostasis	GO:0045454	5.28	6.59E-04	up_up
cellular component assembly involved in morphogenesis	GO:0010927	5.28	2.56E-02	up_up
actomyosin structure organization	GO:0031032	5.16	8.56E-03	up_up
muscle fiber development	GO:0048747	5.06	2.94E-02	up_up
skeletal muscle tissue development	GO:0007519	5.02	1.84E-02	up_up
nucleoside diphosphate metabolic process	GO:0009132	4.99	1.03E-02	up_up
striated muscle cell development	GO:0055002	4.78	4.71E-04	up_up
nucleotide phosphorylation	GO:0046939	4.69	4.12E-02	up_up
nucleoside diphosphate phosphorylation	GO:0006165	4.69	4.06E-02	up_up
skeletal muscle organ development	GO:0060538	4.54	2.87E-02	up_up
muscle cell development	GO:0055001	4.52	4.81E-04	up_up
striated muscle cell differentiation	GO:0051146	4.38	3.88E-04	up_up
striated muscle tissue development	GO:0014706	4.33	1.76E-03	up_up
muscle tissue development	GO:0060537	4.33	1.69E-03	up_up
muscle organ development	GO:0007517	4.31	2.95E-03	up_up
electron transport chain	GO:0022900	4.06	1.28E-02	up_up
muscle cell differentiation	GO:0042692	4.02	5.05E-04	up_up
generation of precursor metabolites and energy	GO:0006091	4.02	9.49E-06	up_up
muscle structure development	GO:0061061	3.62	1.12E-04	up_up
energy derivation by oxidation of organic compounds	GO:0015980	3.52	4.01E-02	up_up
drug metabolic process	GO:0017144	3.3	2.28E-02	up_up
purine nucleotide metabolic process	GO:0006163	3.29	7.64E-03	up_up
supramolecular fiber organization	GO:0097435	3.26	1.77E-03	up_up

Supplementary Table 3.4 (Continued).

Purine ribonucleotide metabolic process	GO:0009150	3.23	1.27E-02	up_up
purine-containing compound metabolic process	GO:0072521	3.05	1.47E-02	up_up
cellular homeostasis	GO:0019725	3.03	3.76E-03	up_up
ribonucleotide metabolic process	GO:0009259	2.95	2.59E-02	up_up
ribose phosphate metabolic process	GO:0019693	2.92	2.83E-02	up_up
actin filament-based process	GO:0030029	2.88	1.81E-03	up_up
actin cytoskeleton organization	GO:0030036	2.86	2.90E-03	up_up
organic acid metabolic process	GO:0006082	2.69	6.86E-05	up_up
oxoacid metabolic process	GO:0043436	2.69	6.10E-05	up_up
carboxylic acid metabolic process	GO:0019752	2.67	8.83E-05	up_up
nucleobase-containing small molecule metabolic process	GO:0055086	2.6	5.79E-03	up_up
cellular amino acid metabolic process	GO:0006520	2.55	3.38E-02	up_up
nucleotide metabolic process	GO:0009117	2.46	3.96E-02	up_up
carbohydrate metabolic process	GO:0005975	2.44	1.82E-02	up_up
nucleoside phosphate metabolic process	GO:0006753	2.42	4.16E-02	up_up
small molecule metabolic process	GO:0044281	2.35	4.13E-06	up_up
oxidation-reduction process	GO:0055114	2.14	5.55E-06	up_up
ion transmembrane transport	GO:0034220	1.84	4.11E-02	up_up
biological regulation	GO:0065007	0.79	3.10E-02	up_up
regulation of biological process	GO:0050789	0.76	1.79E-02	up_up
macromolecule metabolic process	GO:0043170	0.75	3.14E-02	up_up
regulation of cellular process	GO:0050794	0.7	7.33E-04	up_up
regulation of metabolic process	GO:0019222	0.64	3.36E-02	up_up
regulation of nitrogen compound metabolic process	GO:0051171	0.63	4.14E-02	up_up
regulation of cellular metabolic process	GO:0031323	0.62	2.83E-02	up_up
regulation of primary metabolic process	GO:0080090	0.62	2.92E-02	up_up
response to stimulus	GO:0050896	0.61	1.65E-03	up_up
regulation of cellular biosynthetic process	GO:0031326	0.58	4.33E-02	up_up
regulation of biosynthetic process	GO:0009889	0.58	4.18E-02	up_up
regulation of RNA metabolic process	GO:0051252	0.56	3.78E-02	up_up
regulation of RNA biosynthetic process	GO:2001141	0.55	4.11E-02	up_up
regulation of nucleic acid-templated transcription	GO:1903506	0.55	4.05E-02	up_up
regulation of nucleobase-containing compound metabolic process	GO:0019219	0.54	2.40E-02	up_up
regulation of transcription, DNA-templated	GO:0006355	0.54	4.12E-02	up_up
cellular response to stimulus	GO:0051716	0.51	6.01E-05	up_up
signaling	GO:0023052	0.42	8.57E-06	up_up

Supplementary Table 3.4 (Continued).

cell communication	GO:0007154	0.42	7.15E-06	up_up
signal transduction	GO:0007165	0.41	6.48E-06	up_up
nucleic acid metabolic process	GO:0090304	0.35	1.09E-04	up_up
cell surface receptor signaling pathway	GO:0007166	0.26	3.12E-03	up_up
RNA processing	GO:0006396	0.2	8.51E-03	up_up
chromosome organization	GO:0051276	0.16	4.83E-03	up_up
cellular response to DNA damage stimulus	GO:0006974	0.15	4.07E-02	up_up
DNA repair	GO:0006281	0.01	1.16E-02	up_up
DNA metabolic process	GO:0006259	0.01	6.66E-04	up_up

Supplementary Table 3.5. Gene ontology categories significantly enriched in genes that are consistently down-regulated through *Xenopus tropicalis* hind limb development. Values > 1 indicate overenrichment; values < 1 indicate underenrichment.

Biological Process	GO ID	Fold Enrichment	p-value	Reg. direction
chromatin remodeling	GO:0006338	5.57	1.83E-02	down_down
cell-cell adhesion via plasma-membrane adhesion molecules	GO:0098742	5.13	5.04E-04	down_down
homophilic cell adhesion via plasma membrane adhesion molecules	GO:0007156	4.86	2.49E-03	down_down
cell-cell adhesion	GO:0098609	4.15	1.59E-03	down_down
enzyme linked receptor protein signaling pathway	GO:0007167	3.16	2.47E-03	down_down
transmembrane receptor protein tyrosine kinase signaling pathway	GO:0007169	3.05	4.06E-02	down_down
cell adhesion	GO:0007155	2.42	4.11E-02	down_down
biological adhesion	GO:0022610	2.42	4.04E-02	down_down
cell surface receptor signaling pathway	GO:0007166	2.42	3.04E-06	down_down
chromatin organization	GO:0006325	2.31	2.88E-02	down_down
chromosome organization	GO:0051276	2.28	2.37E-03	down_down
regulation of transcription, DNA-templated	GO:0006355	2.28	9.92E-10	down_down
regulation of RNA biosynthetic process	GO:2001141	2.18	2.40E-09	down_down
regulation of nucleic acid-templated transcription	GO:1903506	2.18	1.92E-09	down_down
regulation of RNA metabolic process	GO:0051252	2.14	2.35E-09	down_down
regulation of nucleobase-containing compound metabolic process	GO:0019219	2.1	3.59E-09	down_down
regulation of cellular macromolecule biosynthetic process	GO:2000112	2.1	5.24E-09	down_down
regulation of gene expression	GO:0010468	2.1	2.63E-09	down_down
regulation of macromolecule biosynthetic process	GO:0010556	2.01	4.00E-08	down_down
regulation of cellular biosynthetic process	GO:0031326	1.98	7.14E-08	down_down
regulation of biosynthetic process	GO:0009889	1.98	7.10E-08	down_down
nervous system development	GO:0007399	1.84	2.22E-02	down_down
regulation of signaling	GO:0023051	1.78	2.77E-02	down_down
regulation of macromolecule metabolic process	GO:0060255	1.77	9.69E-07	down_down
regulation of nitrogen compound metabolic process	GO:0051171	1.76	2.96E-06	down_down
regulation of cell communication	GO:0010646	1.76	3.71E-02	down_down

Supplementary Table 3.5 (Continued).

regulation of primary metabolic process	GO:0080090	1.75	3.15E-06	down_down
regulation of cellular metabolic process	GO:0031323	1.73	4.14E-06	down_down
regulation of metabolic process	GO:0019222	1.71	3.13E-06	down_down
multicellular organism development	GO:0007275	1.61	1.40E-04	down_down
anatomical structure development	GO:0048856	1.56	4.44E-04	down_down
developmental process	GO:0032502	1.53	8.41E-04	down_down
multicellular organismal process	GO:0032501	1.51	1.03E-03	down_down
regulation of cellular process	GO:0050794	1.5	1.45E-08	down_down
system development	GO:0048731	1.47	4.77E-02	down_down
regulation of biological process	GO:0050789	1.46	4.39E-08	down_down
biological regulation	GO:0065007	1.39	1.04E-06	down_down
nitrogen compound metabolic process	GO:0006807	0.73	1.12E-02	down_down
primary metabolic process	GO:0044238	0.71	1.47E-03	down_down
organic substance metabolic process	GO:0071704	0.7	5.71E-04	down_down
cellular metabolic process	GO:0044237	0.7	9.02E-04	down_down
metabolic process	GO:0008152	0.63	1.44E-08	down_down
cellular nitrogen compound metabolic process	GO:0034641	0.51	1.22E-03	down_down
gene expression	GO:0010467	0.49	4.33E-02	down_down
cellular biosynthetic process	GO:0044249	0.44	2.35E-03	down_down
organic substance biosynthetic process	GO:1901576	0.43	1.25E-03	down_down
biosynthetic process	GO:0009058	0.42	4.90E-04	down_down
cellular nitrogen compound biosynthetic process	GO:0044271	0.35	9.87E-03	down_down
organonitrogen compound biosynthetic process	GO:1901566	0.34	5.59E-03	down_down
oxidation-reduction process	GO:0055114	0.25	4.60E-04	down_down
small molecule metabolic process	GO:0044281	0.23	1.30E-03	down_down
translation	GO:0006412	0.14	2.28E-02	down_down
peptide biosynthetic process	GO:0043043	0.14	1.66E-02	down_down
peptide metabolic process	GO:0006518	0.13	8.75E-03	down_down
amide biosynthetic process	GO:0043604	0.13	9.07E-03	down_down
cellular amide metabolic process	GO:0043603	0.11	1.29E-03	down_down

Supplementary Table 3.6. Significantly over- and underenriched gene ontology categories for genes that significantly increase between NF stages 53 and 56 *Xenopus tropicalis* hind limbs. Values > 1 indicate overenrichment; values < 1 indicate underenrichment.

Biological Process	GO ID	Fold Enrichment	p-value	Reg. direction
muscle organ development	GO:0007517	2.76	1.27E-02	up
muscle structure development	GO:0061061	2.33	2.57E-03	up
carboxylic acid metabolic process	GO:0019752	1.81	3.93E-03	up
organic acid metabolic process	GO:0006082	1.8	3.82E-03	up
oxoacid metabolic process	GO:0043436	1.8	3.66E-03	up
cation transport	GO:0006812	1.6	2.56E-02	up
small molecule metabolic process	GO:0044281	1.56	3.54E-03	up
ion transport	GO:0006811	1.49	1.13E-02	up
transmembrane transport	GO:0055085	1.48	7.83E-03	up
regulation of macromolecule metabolic process	GO:0060255	0.67	3.83E-04	up
regulation of metabolic process	GO:0019222	0.67	4.33E-04	up
regulation of nitrogen compound metabolic process	GO:0051171	0.67	5.11E-04	up
regulation of cellular metabolic process	GO:0031323	0.66	3.60E-04	up
regulation of biosynthetic process	GO:0009889	0.66	3.08E-03	up
regulation of primary metabolic process	GO:0080090	0.66	3.72E-04	up
regulation of cellular macromolecule biosynthetic process	GO:2000112	0.66	4.04E-03	up
regulation of cellular biosynthetic process	GO:0031326	0.66	2.67E-03	up
regulation of gene expression	GO:0010468	0.66	2.65E-03	up
regulation of macromolecule biosynthetic process	GO:0010556	0.66	2.70E-03	up
regulation of transcription, DNA-templated	GO:0006355	0.65	4.54E-03	up
regulation of RNA biosynthetic process	GO:2001141	0.64	2.85E-03	up
regulation of nucleic acid-templated transcription	GO:1903506	0.64	2.69E-03	up
regulation of RNA metabolic process	GO:0051252	0.64	1.67E-03	up
nucleic acid metabolic process	GO:0090304	0.62	2.92E-03	up
regulation of nucleobase-containing compound metabolic process	GO:0019219	0.62	4.99E-04	up
cellular response to stress	GO:0033554	0.42	9.03E-03	up
cell cycle	GO:0007049	0.31	6.99E-04	up

Supplementary Table 3.6 (Continued).

cellular response to DNA damage stimulus	GO:0006974	0.27	1.06E-03	up
mitotic cell cycle	GO:0000278	0.24	2.51E-02	up
DNA metabolic process	GO:0006259	0.23	1.66E-04	up
chromatin organization	GO:0006325	0.22	3.94E-04	up
chromosome organization	GO:0051276	0.21	1.04E-06	up
cilium assembly	GO:0060271	0.2	2.30E-02	up
plasma membrane bounded cell projection assembly	GO:0120031	0.2	1.29E-02	up
cilium organization	GO:0044782	0.19	1.23E-02	up
cell projection assembly	GO:0030031	0.19	1.19E-02	up
DNA repair	GO:0006281	0.17	3.61E-04	up
regulation of cell population proliferation	GO:0042127	0.13	2.07E-02	up
DNA conformation change	GO:0071103	0.01	1.32E-02	up
determination of left/right symmetry	GO:0007368	2.32	1.01E-02	down
histone modification	GO:0016570	2.24	5.14E-04	down
covalent chromatin modification	GO:0016569	2.24	4.99E-04	down
determination of bilateral symmetry	GO:0009855	2.15	3.68E-02	down
specification of symmetry	GO:0009799	2.15	3.61E-02	down
pattern specification process	GO:0007389	2.15	1.10E-04	down
chromatin organization	GO:0006325	2.14	2.72E-05	down
cilium assembly	GO:0060271	2	4.42E-02	down
cell-cell signaling	GO:0007267	1.92	1.83E-02	down
chromosome organization	GO:0051276	1.9	4.50E-05	down
cell surface receptor signaling pathway	GO:0007166	1.63	5.04E-04	down
regulation of transcription, DNA-templated	GO:0006355	1.62	2.45E-07	down
regulation of RNA metabolic process	GO:0051252	1.59	3.52E-07	down
regulation of RNA biosynthetic process	GO:2001141	1.59	2.46E-07	down
regulation of nucleic acid-templated transcription	GO:1903506	1.59	2.05E-07	down
regulation of nucleobase-containing compound metabolic process	GO:0019219	1.57	3.02E-07	down
regulation of cellular macromolecule biosynthetic process	GO:2000112	1.57	2.64E-07	down
regulation of gene expression	GO:0010468	1.55	2.06E-07	down
regulation of macromolecule biosynthetic process	GO:0010556	1.54	4.74E-07	down
regulation of cellular biosynthetic process	GO:0031326	1.53	8.86E-07	down

Supplementary Table 3.6 (Continued).

regulation of biosynthetic process	GO:0009889	1.52	1.06E-06	down
regulation of primary metabolic process	GO:0080090	1.38	6.18E-05	down
anatomical structure morphogenesis	GO:0009653	1.38	4.16E-02	down
regulation of nitrogen compound metabolic process	GO:0051171	1.38	9.08E-05	down
regulation of cellular metabolic process	GO:0031323	1.37	7.81E-05	down
regulation of macromolecule metabolic process	GO:0060255	1.36	1.13E-04	down
regulation of metabolic process	GO:0019222	1.35	1.61E-04	down
multicellular organism development	GO:0007275	1.35	1.10E-04	down
anatomical structure development	GO:0048856	1.31	7.35E-04	down
developmental process	GO:0032502	1.3	6.66E-04	down
multicellular organismal process	GO:0032501	1.3	7.16E-04	down
regulation of cellular process	GO:0050794	1.25	5.44E-06	down
regulation of biological process	GO:0050789	1.21	6.12E-05	down
biological regulation	GO:0065007	1.17	7.99E-04	down
metabolic process	GO:0008152	0.87	1.27E-02	down
macromolecule biosynthetic process	GO:0009059	0.64	1.84E-02	down
cellular macromolecule biosynthetic process	GO:0034645	0.64	1.80E-02	down
biosynthetic process	GO:0009058	0.62	6.81E-05	down
organic substance biosynthetic process	GO:1901576	0.6	5.74E-05	down
cellular biosynthetic process	GO:0044249	0.6	5.85E-05	down
cellular nitrogen compound biosynthetic process	GO:0044271	0.56	1.33E-03	down
oxidation-reduction process	GO:0055114	0.52	1.75E-04	down
small molecule metabolic process	GO:0044281	0.5	4.90E-04	down
organonitrogen compound biosynthetic process	GO:1901566	0.49	2.73E-05	down
cellular amide metabolic process	GO:0043603	0.4	2.02E-04	down
translation	GO:0006412	0.3	6.98E-05	down
peptide metabolic process	GO:0006518	0.3	2.75E-05	down
peptide biosynthetic process	GO:0043043	0.29	4.48E-05	down
amide biosynthetic process	GO:0043604	0.29	1.81E-05	down
generation of precursor metabolites and energy	GO:0006091	0.09	1.75E-04	down
energy derivation by oxidation of organic compounds	GO:0015980	0.01	3.70E-02	down

Supplementary Table 3.7. Significantly over- and underenriched gene ontology categories for genes that significantly increase between NF stages 56 and 59 *Xenopus tropicalis* hind limbs. Values > 1 indicate overenrichment; values < 1 indicate underenrichment.

Biological Process	GO ID	Fold Enrichment	p-value	Reg. direction
aromatic amino acid family metabolic process	GO:0009072	4.5	2.20E-02	up
tricarboxylic acid cycle	GO:0006099	3.99	3.75E-03	up
pyruvate metabolic process	GO:0006090	3.85	1.38E-02	up
ATP metabolic process	GO:0046034	3.81	2.67E-04	up
ribonucleoside diphosphate metabolic process	GO:0009185	3.76	8.10E-03	up
purine ribonucleoside diphosphate metabolic process	GO:0009179	3.76	7.98E-03	up
purine nucleoside diphosphate metabolic process	GO:0009135	3.76	7.87E-03	up
ATP generation from ADP	GO:0006757	3.73	3.46E-02	up
glycolytic process	GO:0006096	3.73	3.44E-02	up
ADP metabolic process	GO:0046031	3.71	1.20E-02	up
aerobic respiration	GO:0009060	3.65	7.04E-03	up
cellular respiration	GO:0045333	3.56	2.70E-04	up
carbohydrate catabolic process	GO:0016052	3.48	2.55E-02	up
cellular amino acid catabolic process	GO:0009063	3.39	2.21E-02	up
electron transport chain	GO:0022900	3.36	1.25E-04	up
energy derivation by oxidation of organic compounds	GO:0015980	3.35	9.97E-05	up
generation of precursor metabolites and energy	GO:0006091	3.2	1.17E-09	up
cell redox homeostasis	GO:0045454	2.92	7.13E-03	up
nucleoside diphosphate metabolic process	GO:0009132	2.83	4.24E-02	up
organic acid catabolic process	GO:0016054	2.75	2.59E-02	up
carboxylic acid catabolic process	GO:0046395	2.75	2.57E-02	up
drug metabolic process	GO:0017144	2.66	1.27E-03	up
alpha-amino acid metabolic process	GO:1901605	2.66	5.79E-03	up
small molecule catabolic process	GO:0044282	2.62	7.98E-03	up
proton transmembrane transport	GO:1902600	2.48	1.07E-02	up
cellular amino acid metabolic process	GO:0006520	2.48	1.39E-05	up
carboxylic acid metabolic process	GO:0019752	2.41	1.34E-09	up
organic acid metabolic process	GO:0006082	2.39	1.44E-09	up
oxoacid metabolic process	GO:0043436	2.39	1.26E-09	up
oxidation-reduction process	GO:0055114	2.3	3.26E-21	up
purine-containing compound metabolic process	GO:0072521	2.23	7.69E-03	up

Supplementary Table 3.7 (Continued).

Carbohydrate metabolic process	GO:0005975	2.2	9.37E-05	up
purine ribonucleotide metabolic process	GO:0009150	2.17	2.51E-02	up
purine nucleotide metabolic process	GO:0006163	2.15	2.22E-02	up
monocarboxylic acid metabolic process	GO:0032787	2.14	2.61E-02	up
ribonucleotide metabolic process	GO:0009259	2.05	4.81E-02	up
cellular homeostasis	GO:0019725	2.01	2.01E-02	up
small molecule metabolic process	GO:0044281	2	2.35E-10	up
nucleobase-containing small molecule metabolic process	GO:0055086	1.94	4.81E-03	up
small molecule biosynthetic process	GO:0044283	1.9	3.56E-02	up
nucleotide metabolic process	GO:0009117	1.87	2.95E-02	up
nucleoside phosphate metabolic process	GO:0006753	1.84	4.21E-02	up
inorganic cation transmembrane transport	GO:0098662	1.7	3.52E-02	up
inorganic ion transmembrane transport	GO:0098660	1.68	2.55E-02	up
cation transmembrane transport	GO:0098655	1.62	4.39E-02	up
cellular amide metabolic process	GO:0043603	1.61	6.66E-03	up
amide biosynthetic process	GO:0043604	1.58	2.84E-02	up
ion transmembrane transport	GO:0034220	1.57	8.93E-03	up
organic substance catabolic process	GO:1901575	1.47	4.60E-02	up
catabolic process	GO:0009056	1.44	4.89E-02	up
transmembrane transport	GO:0055085	1.37	4.65E-02	up
organonitrogen compound biosynthetic process	GO:1901566	1.37	4.58E-02	up
metabolic process	GO:0008152	1.19	9.93E-06	up
macromolecule metabolic process	GO:0043170	0.83	5.37E-03	up
cellular macromolecule metabolic process	GO:0044260	0.81	1.02E-02	up
multicellular organismal process	GO:0032501	0.79	3.37E-02	up
developmental process	GO:0032502	0.77	1.06E-02	up
anatomical structure development	GO:0048856	0.77	1.20E-02	up
macromolecule modification	GO:0043412	0.77	1.38E-02	up
biological regulation	GO:0065007	0.75	4.61E-09	up
multicellular organism development	GO:0007275	0.75	5.88E-03	up
response to stimulus	GO:0050896	0.74	2.62E-04	up
cellular component organization	GO:0016043	0.74	9.64E-03	up
heterocycle metabolic process	GO:0046483	0.73	2.43E-02	up

Supplementary Table 3.7 (Continued).

cellular component organization or biogenesis	GO:0071840	0.73	4.85E-03	up
regulation of biological process	GO:0050789	0.73	1.38E-09	up
regulation of cellular process	GO:0050794	0.71	2.55E-10	up
cellular response to stimulus	GO:0051716	0.68	7.04E-06	up
organelle organization	GO:0006996	0.67	8.72E-03	up
nucleobase-containing compound metabolic process	GO:0006139	0.67	2.10E-03	up
regulation of metabolic process	GO:0019222	0.67	3.11E-05	up
regulation of cellular metabolic process	GO:0031323	0.67	5.56E-05	up
regulation of primary metabolic process	GO:0080090	0.66	5.47E-05	up
regulation of response to stimulus	GO:0048583	0.66	3.39E-02	up
regulation of macromolecule metabolic process	GO:0060255	0.63	3.42E-06	up
regulation of signaling	GO:0023051	0.63	2.57E-02	up
regulation of nitrogen compound metabolic process	GO:0051171	0.63	6.10E-06	up
protein phosphorylation	GO:0006468	0.62	2.97E-02	up
regulation of cell communication	GO:0010646	0.62	1.72E-02	up
signaling	GO:0023052	0.6	1.46E-07	up
cell communication	GO:0007154	0.59	8.44E-08	up
regulation of signal transduction	GO:0009966	0.59	8.72E-03	up
nervous system development	GO:0007399	0.59	1.22E-02	up
regulation of cellular biosynthetic process	GO:0031326	0.59	6.34E-06	up
signal transduction	GO:0007165	0.59	1.53E-07	up
regulation of biosynthetic process	GO:0009889	0.59	6.18E-06	up
regulation of macromolecule biosynthetic process	GO:0010556	0.59	6.06E-06	up
regulation of cellular macromolecule biosynthetic process	GO:2000112	0.58	8.41E-06	up
regulation of gene expression	GO:0010468	0.57	1.09E-06	up
regulation of RNA biosynthetic process	GO:2001141	0.55	2.30E-06	up
regulation of nucleic acid-templated transcription	GO:1903506	0.55	2.18E-06	up
regulation of transcription, DNA-templated	GO:0006355	0.55	3.83E-06	up
regulation of RNA metabolic process	GO:0051252	0.54	3.69E-07	up
regulation of nucleobase-containing compound metabolic process	GO:0019219	0.52	6.03E-08	up
RNA metabolic process	GO:0016070	0.46	2.89E-06	up
regulation of cell cycle	GO:0051726	0.43	3.62E-02	up

Supplementary Table 3.7 (Continued).

Cellular response to DNA damage stimulus	GO:0006974	0.43	2.45E-02	up
nucleic acid metabolic process	GO:0090304	0.41	1.16E-10	up
locomotion	GO:0040011	0.4	1.19E-02	up
cell surface receptor signaling pathway	GO:0007166	0.4	5.73E-06	up
DNA repair	GO:0006281	0.4	3.40E-02	up
cell projection organization	GO:0030030	0.39	2.35E-03	up
plasma membrane bounded cell projection organization	GO:0120036	0.37	2.36E-03	up
movement of cell or subcellular component	GO:0006928	0.35	1.90E-04	up
cell cycle	GO:0007049	0.34	5.96E-04	up
microtubule-based process	GO:0007017	0.34	2.42E-03	up
cell cycle process	GO:0022402	0.34	2.91E-02	up
DNA metabolic process	GO:0006259	0.32	4.40E-04	up
cilium assembly	GO:0060271	0.3	4.57E-02	up
RNA processing	GO:0006396	0.29	1.74E-06	up
mRNA metabolic process	GO:0016071	0.29	7.04E-04	up
plasma membrane bounded cell projection assembly	GO:0120031	0.29	3.57E-02	up
cilium organization	GO:0044782	0.28	2.75E-02	up
cell projection assembly	GO:0030031	0.28	2.72E-02	up
microtubule cytoskeleton organization	GO:0000226	0.27	4.44E-02	up
nucleic acid-templated transcription	GO:0097659	0.26	1.22E-02	up
transcription, DNA-templated	GO:0006351	0.26	1.20E-02	up
RNA biosynthetic process	GO:0032774	0.25	9.78E-03	up
histone modification	GO:0016570	0.25	5.85E-03	up
covalent chromatin modification	GO:0016569	0.25	5.75E-03	up
mRNA processing	GO:0006397	0.25	1.42E-03	up
chromatin organization	GO:0006325	0.24	7.60E-05	up
chromosome organization	GO:0051276	0.22	9.10E-08	up
RNA splicing	GO:0008380	0.18	2.35E-03	up
enzyme linked receptor protein signaling pathway	GO:0007167	0.09	9.60E-05	up
mRNA splicing, via spliceosome	GO:0000398	0.07	8.84E-03	up
RNA splicing, via transesterification reactions with bulged adenosine as nucleophile	GO:0000377	0.07	8.72E-03	up
RNA splicing, via transesterification reactions	GO:0000375	0.07	8.82E-03	up
DNA replication	GO:0006260	0.07	4.76E-03	up
transmembrane receptor protein tyrosine kinase signaling pathway	GO:0007169	0.06	1.08E-03	up
neuron projection guidance	GO:0097485	0.01	2.55E-02	up
axon guidance	GO:0007411	0.01	2.53E-02	up

Supplementary Table 3.7 (Continued).

DNA-dependent DNA replication	GO:0006261	3.59	2.33E-02	down
transmembrane receptor protein tyrosine kinase signaling pathway	GO:0007169	2.58	8.35E-04	down
cell-cell adhesion via plasma-membrane adhesion molecules	GO:0098742	2.58	4.34E-02	down
peptidyl-tyrosine phosphorylation	GO:0018108	2.55	1.55E-02	down
enzyme linked receptor protein signaling pathway	GO:0007167	2.52	7.39E-05	down
DNA replication	GO:0006260	2.52	4.47E-03	down
peptidyl-tyrosine modification	GO:0018212	2.47	2.83E-02	down
cell surface receptor signaling pathway	GO:0007166	1.86	8.54E-07	down
chromosome organization	GO:0051276	1.86	1.77E-04	down
tissue morphogenesis	GO:0048729	1.74	4.94E-02	down
regulation of transcription, DNA-templated	GO:0006355	1.73	8.97E-10	down
embryonic morphogenesis	GO:0048598	1.69	2.51E-02	down
regulation of RNA biosynthetic process	GO:2001141	1.68	4.17E-09	down
regulation of nucleic acid-templated transcription	GO:1903506	1.68	3.79E-09	down
regulation of nucleobase-containing compound metabolic process	GO:0019219	1.67	8.09E-10	down
regulation of RNA metabolic process	GO:0051252	1.67	2.22E-09	down
regulation of gene expression	GO:0010468	1.66	7.83E-10	down
tube development	GO:0035295	1.65	4.66E-02	down
regulation of cellular macromolecule biosynthetic process	GO:2000112	1.65	4.03E-09	down
regulation of macromolecule biosynthetic process	GO:0010556	1.6	2.67E-08	down
nervous system development	GO:0007399	1.6	9.27E-04	down
regulation of biosynthetic process	GO:0009889	1.59	2.62E-08	down
regulation of cellular biosynthetic process	GO:0031326	1.59	3.16E-08	down
regulation of macromolecule metabolic process	GO:0060255	1.52	6.01E-09	down
regulation of signal transduction	GO:0009966	1.51	6.82E-03	down
regulation of metabolic process	GO:0019222	1.51	6.14E-09	down
regulation of nitrogen compound metabolic process	GO:0051171	1.51	5.49E-08	down
regulation of signaling	GO:0023051	1.5	6.41E-03	down
regulation of primary metabolic process	GO:0080090	1.5	4.58E-08	down
tissue development	GO:0009888	1.5	1.46E-02	down

Supplementary Table 3.7 (Continued).

regulation of cell communication	GO:0010646	1.5	7.40E-03	down
regulation of cellular metabolic process	GO:0031323	1.5	4.16E-08	down
cell communication	GO:0007154	1.47	3.99E-07	down
anatomical structure morphogenesis	GO:0009653	1.46	4.58E-03	down
signal transduction	GO:0007165	1.46	2.13E-06	down
signaling	GO:0023052	1.45	1.37E-06	down
cell differentiation	GO:0030154	1.42	1.54E-02	down
multicellular organism development	GO:0007275	1.42	1.99E-06	down
system development	GO:0048731	1.42	4.78E-05	down
regulation of response to stimulus	GO:0048583	1.42	3.64E-02	down
regulation of cellular process	GO:0050794	1.41	4.64E-16	down
regulation of biological process	GO:0050789	1.4	1.95E-16	down
cellular developmental process	GO:0048869	1.4	2.16E-02	down
anatomical structure development	GO:0048856	1.39	7.21E-06	down
developmental process	GO:0032502	1.37	1.30E-05	down
biological regulation	GO:0065007	1.36	3.67E-15	down
multicellular organismal process	GO:0032501	1.35	4.73E-05	down
animal organ development	GO:0048513	1.34	3.66E-02	down
cellular response to stimulus	GO:0051716	1.33	1.49E-04	down
response to stimulus	GO:0050896	1.27	1.15E-03	down
organic substance metabolic process	GO:0071704	0.86	3.86E-02	down
cellular metabolic process	GO:0044237	0.85	2.17E-02	down
metabolic process	GO:0008152	0.79	3.02E-07	down
establishment of localization	GO:0051234	0.76	4.33E-02	down
cellular nitrogen compound metabolic process	GO:0034641	0.69	9.35E-04	down
cellular biosynthetic process	GO:0044249	0.68	9.58E-03	down
organic substance biosynthetic process	GO:1901576	0.66	2.59E-03	down
biosynthetic process	GO:0009058	0.65	8.50E-04	down
macromolecule localization	GO:0033036	0.57	1.07E-02	down
gene expression	GO:0010467	0.52	1.01E-05	down
organic substance transport	GO:0071702	0.52	3.51E-04	down
protein localization	GO:0008104	0.51	7.30E-03	down
cellular nitrogen compound biosynthetic process	GO:0044271	0.48	3.87E-05	down
nitrogen compound transport	GO:0071705	0.45	1.12E-04	down
organonitrogen compound biosynthetic process	GO:1901566	0.42	5.70E-07	down
protein transport	GO:0015031	0.41	5.31E-04	down
amide transport	GO:0042886	0.41	2.37E-04	down
peptide transport	GO:0015833	0.41	4.08E-04	down

Supplementary Table 3.7 (Continued).

small molecule metabolic process	GO:0044281	0.41	7.07E-06	down
establishment of protein localization	GO:0045184	0.4	3.28E-04	down
organic acid metabolic process	GO:0006082	0.35	1.49E-03	down
oxoacid metabolic process	GO:0043436	0.35	1.47E-03	down
oxidation-reduction process	GO:0055114	0.35	4.32E-09	down
carboxylic acid metabolic process	GO:0019752	0.33	8.44E-04	down
peptide metabolic process	GO:0006518	0.13	3.63E-09	down
cellular amide metabolic process	GO:0043603	0.13	6.81E-11	down
amide biosynthetic process	GO:0043604	0.13	2.47E-09	down
translation	GO:0006412	0.12	5.59E-09	down
peptide biosynthetic process	GO:0043043	0.12	4.48E-09	down
generation of precursor metabolites and energy	GO:0006091	0.1	6.66E-04	down
cellular amino acid metabolic process	GO:0006520	0.09	1.59E-04	down
drug metabolic process	GO:0017144	0.09	3.35E-02	down
tRNA metabolic process	GO:0006399	0.06	4.10E-04	down
mitochondrion organization	GO:0007005	0.01	3.75E-02	down

Supplementary Table 3.8. Significantly over- and underenriched gene ontology categories for genes that significantly increase and decrease between TS7 and TS 10 *Eleutherdactylus coqui* hind limbs. Values > 1 indicate overenrichment; values < 1 indicate underenrichment.

Biological Process	GO ID	Fold Enrichment	p-value	Reg. direction
skeletal muscle tissue development	GO:0007519	4.77	2.93E-03	up
skeletal muscle organ development	GO:0060538	4.7	1.91E-03	up
myofibril assembly	GO:0030239	4.61	3.38E-02	up
muscle organ development	GO:0007517	4.22	2.24E-04	up
striated muscle tissue development	GO:0014706	4.02	3.62E-04	up
muscle tissue development	GO:0060537	4.02	3.51E-04	up
calcium ion transport	GO:0006816	3.18	3.40E-02	up
muscle structure development	GO:0061061	3.18	1.18E-04	up
striated muscle cell development	GO:0055002	3.17	1.67E-02	up
muscle cell development	GO:0055001	3.1	9.66E-03	up
cell adhesion	GO:0007155	3.03	1.10E-04	up
biological adhesion	GO:0022610	3.03	1.04E-04	up
striated muscle cell differentiation	GO:0051146	2.88	2.59E-02	up
muscle cell differentiation	GO:0042692	2.8	2.52E-02	up
supramolecular fiber organization	GO:0097435	2.61	2.19E-02	up
circulatory system development	GO:0072359	1.91	1.47E-02	up
response to chemical	GO:0042221	1.89	2.31E-03	up
cell surface receptor signaling pathway	GO:0007166	1.8	1.45E-02	up
tissue development	GO:0009888	1.74	4.23E-03	up
anatomical structure morphogenesis	GO:0009653	1.66	2.81E-03	up
signal transduction	GO:0007165	1.62	1.35E-04	up
cell communication	GO:0007154	1.6	1.63E-04	up
signaling	GO:0023052	1.59	2.21E-04	up
cell differentiation	GO:0030154	1.56	2.08E-02	up
cellular developmental process	GO:0048869	1.56	2.21E-02	up
system development	GO:0048731	1.43	9.93E-03	up
response to stimulus	GO:0050896	1.4	1.51E-03	up
developmental process	GO:0032502	1.4	3.45E-03	up
multicellular organismal process	GO:0032501	1.39	4.48E-03	up
anatomical structure development	GO:0048856	1.38	7.68E-03	up
multicellular organism development	GO:0007275	1.35	2.75E-02	up
cellular response to stimulus	GO:0051716	1.35	4.16E-02	up
metabolic process	GO:0008152	0.8	1.72E-03	up

Supplementary Table 3.8 (Continued).

organic substance metabolic process	GO:0071704	0.76	4.02E-04	up
primary metabolic process	GO:0044238	0.73	1.07E-04	up
nitrogen compound metabolic process	GO:0006807	0.72	1.03E-04	up
macromolecule metabolic process	GO:0043170	0.7	1.44E-04	up
cellular protein metabolic process	GO:0044267	0.68	7.76E-03	up
cellular metabolic process	GO:0044237	0.65	1.18E-08	up
cellular macromolecule metabolic process	GO:0044260	0.61	5.52E-06	up
organic substance biosynthetic process	GO:1901576	0.56	2.75E-03	up
biosynthetic process	GO:0009058	0.56	1.74E-03	up
cellular biosynthetic process	GO:0044249	0.54	1.20E-03	up
organonitrogen compound biosynthetic process	GO:1901566	0.47	7.74E-03	up
macromolecule biosynthetic process	GO:0009059	0.41	2.32E-04	up
cellular macromolecule biosynthetic process	GO:0034645	0.39	1.60E-04	up
cellular nitrogen compound biosynthetic process	GO:0044271	0.32	1.61E-05	up
organic cyclic compound metabolic process	GO:1901360	0.32	2.08E-11	up
cellular aromatic compound metabolic process	GO:0006725	0.32	2.41E-11	up
nucleobase-containing compound metabolic process	GO:0006139	0.29	1.06E-11	up
heterocycle metabolic process	GO:0046483	0.28	7.84E-13	up
cellular nitrogen compound metabolic process	GO:0034641	0.26	2.39E-17	up
chromatin organization	GO:0006325	0.22	2.30E-02	up
RNA metabolic process	GO:0016070	0.19	7.05E-09	up
nucleic acid metabolic process	GO:0090304	0.19	4.39E-13	up
amide biosynthetic process	GO:0043604	0.19	3.83E-04	up
cellular amide metabolic process	GO:0043603	0.17	7.47E-05	up
peptide biosynthetic process	GO:0043043	0.16	3.19E-04	up
gene expression	GO:0010467	0.16	1.24E-13	up
cellular response to DNA damage stimulus	GO:0006974	0.16	4.27E-03	up
peptide metabolic process	GO:0006518	0.16	1.38E-04	up
chromosome organization	GO:0051276	0.15	7.91E-05	up
mRNA processing	GO:0006397	0.14	2.18E-02	up
translation	GO:0006412	0.12	1.05E-04	up
mRNA metabolic process	GO:0016071	0.11	2.23E-03	up
RNA processing	GO:0006396	0.1	2.95E-06	up

Supplementary Table 3.8 (Continued).

cell cycle	GO:0007049	0.1	2.31E-04	up
DNA metabolic process	GO:0006259	0.09	1.13E-04	up
RNA splicing	GO:0008380	0.09	3.97E-02	up
ncRNA metabolic process	GO:0034660	0.06	1.51E-03	up
DNA repair	GO:0006281	0.06	1.53E-03	up
mitotic cell cycle	GO:0000278	< 0.01	7.74E-03	up
mitotic cell cycle process	GO:1903047	< 0.01	4.88E-02	up
ribonucleoprotein complex biogenesis	GO:0022613	< 0.01	7.70E-03	up
ncRNA processing	GO:0034470	< 0.01	7.61E-03	up
cell cycle process	GO:0022402	< 0.01	1.83E-03	up
cell division	GO:0051301	< 0.01	7.56E-03	up
regulation of DNA-dependent DNA replication	GO:0090329	11.49	1.06E-03	down
regulation of DNA replication	GO:0006275	10.34	5.93E-04	down
DNA replication initiation	GO:0006270	10.34	5.82E-04	down
DNA-dependent DNA replication	GO:0006261	9.58	2.24E-06	down
regulation of cell cycle G2/M phase transition	GO:1902749	8.04	1.28E-02	down
DNA replication	GO:0006260	6.9	4.87E-13	down
negative regulation of mitotic cell cycle phase transition	GO:1901991	6.7	2.52E-02	down
mitotic sister chromatid segregation	GO:0000070	6.65	9.76E-04	down
negative regulation of cell cycle phase transition	GO:1901988	6.57	1.25E-02	down
regulation of cell cycle phase transition	GO:1901987	6.5	2.54E-04	down
regulation of mitotic cell cycle phase transition	GO:1901990	6.38	2.77E-03	down
sister chromatid segregation	GO:0000819	6.32	1.28E-03	down
regulation of cytokinesis	GO:0032465	6.19	3.46E-02	down
microtubule cytoskeleton organization involved in mitosis	GO:1902850	6.13	1.66E-02	down
DNA duplex unwinding	GO:0032508	5.98	4.51E-04	down
mitotic cell cycle phase transition	GO:0044772	5.75	4.61E-02	down
cell cycle phase transition	GO:0044770	5.75	4.57E-02	down
cytokinesis	GO:0000910	5.75	4.52E-02	down
DNA geometric change	GO:0032392	5.75	2.98E-04	down
nuclear chromosome segregation	GO:0098813	5.75	1.16E-03	down
spindle assembly	GO:0051225	5.75	4.48E-02	down
negative regulation of cell cycle process	GO:0010948	5.75	5.11E-03	down
mitotic nuclear division	GO:0140014	5.75	7.69E-05	down
negative regulation of mitotic cell cycle	GO:0045930	5.75	2.20E-02	down
mitotic cell cycle	GO:0000278	5.68	4.12E-13	down

Supplementary Table 3.8 (Continued).

DNA conformation change	GO:0071103	5.63	2.72E-07	down
chromosome segregation	GO:0007059	5.58	5.63E-05	down
mitotic cell cycle process	GO:1903047	5.58	4.99E-10	down
spindle organization	GO:0007051	5.47	6.74E-03	down
nuclear division	GO:0000280	5.28	8.30E-05	down
DNA packaging	GO:0006323	5.11	3.73E-02	down
cell cycle process	GO:0022402	5.03	7.67E-12	down
organelle fission	GO:0048285	5.01	1.30E-04	down
histone lysine methylation	GO:0034968	5	1.17E-02	down
regulation of cell cycle process	GO:0010564	4.93	1.38E-05	down
cell cycle checkpoint	GO:0000075	4.79	1.42E-02	down
histone methylation	GO:0016571	4.76	4.24E-03	down
cell cycle	GO:0007049	4.67	3.11E-17	down
regulation of mitotic cell cycle	GO:0007346	4.67	2.61E-03	down
cell division	GO:0051301	4.57	2.57E-08	down
DNA recombination	GO:0006310	4.53	3.23E-03	down
peptidyl-lysine methylation	GO:0018022	4.26	2.71E-02	down
DNA metabolic process	GO:0006259	4.14	1.06E-14	down
double-strand break repair	GO:0006302	3.96	4.07E-02	down
negative regulation of cell cycle	GO:0045786	3.92	5.50E-03	down
chromosome organization	GO:0051276	3.83	1.79E-15	down
microtubule cytoskeleton organization	GO:0000226	3.71	3.20E-04	down
cellular response to DNA damage stimulus	GO:0006974	3.49	1.83E-08	down
protein methylation	GO:0006479	3.47	2.22E-02	down
protein alkylation	GO:0008213	3.47	2.20E-02	down
DNA repair	GO:0006281	3.24	6.35E-06	down
histone modification	GO:0016570	3.12	4.69E-04	down
covalent chromatin modification	GO:0016569	3.12	4.60E-04	down
macromolecule methylation	GO:0043414	3.05	1.24E-02	down
microtubule-based process	GO:0007017	3.03	3.28E-05	down
chromatin organization	GO:0006325	3.02	1.10E-05	down
cellular response to stress	GO:0033554	2.86	9.00E-07	down
nucleic acid phosphodiester bond hydrolysis	GO:0090305	2.8	1.31E-02	down
peptidyl-lysine modification	GO:0018205	2.75	2.89E-02	down
regulation of cell cycle	GO:0051726	2.67	1.15E-03	down
methylation	GO:0032259	2.49	2.51E-02	down
nucleic acid metabolic process	GO:0090304	2.29	8.59E-12	down
macromolecule catabolic process	GO:0009057	2.27	5.42E-03	down
cellular macromolecule catabolic process	GO:0044265	2.22	1.16E-02	down
protein catabolic process	GO:0030163	2.22	4.71E-02	down
mRNA metabolic process	GO:0016071	2.18	3.48E-02	down
organonitrogen compound catabolic process	GO:1901565	2.16	2.36E-02	down

Supplementary Table 3.8 (Continued).

organelle organization	GO:0006996	2.04	1.81E-07	down
peptidyl-amino acid modification	GO:0018193	2.04	4.76E-02	down
response to stress	GO:0006950	2	1.67E-03	down
nucleobase-containing compound metabolic process	GO:0006139	1.95	1.77E-08	down
cellular aromatic compound metabolic process	GO:0006725	1.91	2.48E-08	down
heterocycle metabolic process	GO:0046483	1.9	4.41E-08	down
organic cyclic compound metabolic process	GO:1901360	1.86	8.14E-08	down
regulation of nucleobase-containing compound metabolic process	GO:0019219	1.75	7.57E-05	down
regulation of cellular macromolecule biosynthetic process	GO:2000112	1.74	1.33E-04	down
regulation of macromolecule biosynthetic process	GO:0010556	1.73	1.07E-04	down
regulation of cellular biosynthetic process	GO:0031326	1.71	1.69E-04	down
regulation of biosynthetic process	GO:0009889	1.7	1.70E-04	down
regulation of transcription, DNA-templated	GO:0006355	1.7	9.08E-04	down
regulation of RNA biosynthetic process	GO:2001141	1.69	9.14E-04	down
regulation of nucleic acid-templated transcription	GO:1903506	1.69	8.99E-04	down
regulation of macromolecule metabolic process	GO:0060255	1.69	7.50E-06	down
regulation of RNA metabolic process	GO:0051252	1.68	5.97E-04	down
RNA metabolic process	GO:0016070	1.67	1.78E-02	down
regulation of gene expression	GO:0010468	1.67	3.64E-04	down
cellular component organization	GO:0016043	1.66	5.43E-05	down
regulation of nitrogen compound metabolic process	GO:0051171	1.64	6.92E-05	down
regulation of metabolic process	GO:0019222	1.62	5.69E-05	down
cellular component organization or biogenesis	GO:0071840	1.62	1.10E-04	down
regulation of primary metabolic process	GO:0080090	1.61	1.30E-04	down
cellular nitrogen compound metabolic process	GO:0034641	1.61	5.98E-05	down
regulation of cellular metabolic process	GO:0031323	1.57	4.32E-04	down
cellular macromolecule metabolic process	GO:0044260	1.56	2.29E-07	down

Supplementary Table 3.8 (Continued).

macromolecule metabolic process	GO:0043170	1.48	1.24E-07	down
nitrogen compound metabolic process	GO:0006807	1.36	5.36E-05	down
cellular metabolic process	GO:0044237	1.34	1.08E-04	down
organic substance metabolic process	GO:0071704	1.29	8.01E-04	down
primary metabolic process	GO:0044238	1.27	2.94E-03	down
cellular process	GO:0009987	1.25	6.32E-06	down
metabolic process	GO:0008152	1.19	4.62E-02	down
biological_process	GO:0008150	1.11	1.29E-02	down
Unclassified	UNCLASSIFIED	0.8	1.28E-02	down
localization	GO:0051179	0.56	1.83E-03	down
establishment of localization	GO:0051234	0.52	1.16E-03	down
transport	GO:0006810	0.49	2.87E-04	down
organonitrogen compound biosynthetic process	GO:1901566	0.38	4.07E-03	down
ion transport	GO:0006811	0.31	6.66E-03	down
transmembrane transport	GO:0055085	0.28	1.20E-03	down
ion transmembrane transport	GO:0034220	0.23	2.13E-02	down

Supplementary Table 3.9. Significantly over- and underenriched gene ontology categories for genes that significantly increase and decrease between TS 10 and TS 13 *Eleutherodactylus coqui* hind limbs. Values > 1 indicate overenrichment; values < 1 indicate underenrichment.

Biological Process	GO ID	Fold Enrichment	p-value	Reg. direction
muscle cell development	GO:0055001	2.61	2.92E-02	up
muscle cell differentiation	GO:0042692	2.42	3.72E-02	up
muscle structure development	GO:0061061	2.31	1.30E-02	up
oxidation-reduction process	GO:0055114	1.71	2.92E-04	up
ion transmembrane transport	GO:0034220	1.69	3.37E-02	up
ion transport	GO:0006811	1.57	2.51E-02	up
transmembrane transport	GO:0055085	1.57	1.39E-02	up
cellular process	GO:0009987	0.87	4.03E-03	up
organic substance metabolic process	GO:0071704	0.83	1.21E-02	up
primary metabolic process	GO:0044238	0.83	1.61E-02	up
nitrogen compound metabolic process	GO:0006807	0.8	4.93E-03	up
cellular metabolic process	GO:0044237	0.77	7.15E-05	up
macromolecule metabolic process	GO:0043170	0.71	1.74E-06	up
organic substance biosynthetic process	GO:1901576	0.68	3.17E-02	up
cellular biosynthetic process	GO:0044249	0.68	3.86E-02	up
cellular macromolecule metabolic process	GO:0044260	0.67	6.66E-06	up
regulation of RNA metabolic process	GO:0051252	0.67	3.11E-02	up
regulation of gene expression	GO:0010468	0.67	2.12E-02	up
regulation of macromolecule biosynthetic process	GO:0010556	0.66	2.33E-02	up
regulation of cellular biosynthetic process	GO:0031326	0.66	1.87E-02	up
regulation of biosynthetic process	GO:0009889	0.66	1.65E-02	up
regulation of nucleobase-containing compound metabolic process	GO:0019219	0.65	1.69E-02	up
regulation of cellular metabolic process	GO:0031323	0.64	6.25E-04	up
regulation of macromolecule metabolic process	GO:0060255	0.64	5.72E-04	up
regulation of nitrogen compound metabolic process	GO:0051171	0.64	5.81E-04	up
regulation of metabolic process	GO:0019222	0.64	2.34E-04	up
regulation of primary metabolic process	GO:0080090	0.63	2.61E-04	up

Supplementary Table 3.9 (Continued).

organic cyclic compound metabolic process	GO:1901360	0.5	9.09E-08	up
cellular macromolecule biosynthetic process	GO:0034645	0.5	3.71E-04	up
macromolecule biosynthetic process	GO:0009059	0.49	2.97E-04	up
cellular aromatic compound metabolic process	GO:0006725	0.49	8.38E-08	up
cellular nitrogen compound biosynthetic process	GO:0044271	0.46	1.73E-04	up
heterocycle metabolic process	GO:0046483	0.46	8.11E-09	up
cellular nitrogen compound metabolic process	GO:0034641	0.45	3.75E-12	up
nucleobase-containing compound metabolic process	GO:0006139	0.45	4.94E-09	up
peptide metabolic process	GO:0006518	0.41	2.01E-02	up
amide biosynthetic process	GO:0043604	0.41	1.59E-02	up
cellular response to stress	GO:0033554	0.39	1.40E-02	up
peptide biosynthetic process	GO:0043043	0.3	8.11E-04	up
ncRNA metabolic process	GO:0034660	0.3	2.87E-02	up
regulation of cell cycle	GO:0051726	0.29	2.88E-02	up
RNA metabolic process	GO:0016070	0.28	2.51E-09	up
gene expression	GO:0010467	0.28	6.18E-13	up
translation	GO:0006412	0.27	4.63E-04	up
chromosome organization	GO:0051276	0.24	3.50E-05	up
nucleic acid metabolic process	GO:0090304	0.24	2.05E-16	up
cell cycle process	GO:0022402	0.22	2.94E-02	up
cell cycle	GO:0007049	0.2	1.74E-04	up
mRNA processing	GO:0006397	0.18	3.72E-03	up
RNA splicing	GO:0008380	0.18	2.59E-02	up
mRNA metabolic process	GO:0016071	0.15	2.01E-04	up
cell division	GO:0051301	0.13	1.23E-02	up
mitotic cell cycle	GO:0000278	0.12	8.49E-03	up
RNA processing	GO:0006396	0.11	3.48E-09	up
cellular response to DNA damage stimulus	GO:0006974	0.11	7.92E-06	up
DNA metabolic process	GO:0006259	0.09	2.70E-07	up
DNA repair	GO:0006281	0.08	4.52E-05	up
ribonucleoprotein complex biogenesis	GO:0022613	0.06	2.70E-03	up
ncRNA processing	GO:0034470	0.06	1.77E-03	up
RNA modification	GO:0009451	< 0.01	2.32E-02	up
regulation of DNA replication	GO:0006275	6.87	9.39E-03	down
regulation of DNA-dependent DNA replication	GO:0090329	6.67	4.58E-02	down
DNA replication initiation	GO:0006270	6.1	3.13E-02	down
DNA-dependent DNA replication	GO:0006261	5.51	2.01E-03	down

Supplementary Table 3.9 (Continued).

DNA replication	GO:0006260	5.47	9.15E-12	down
ATP-dependent chromatin remodeling	GO:0043044	5.28	2.99E-02	down
negative regulation of cell cycle phase transition	GO:1901988	4.9	4.16E-02	down
negative regulation of mitotic cell cycle	GO:0045930	4.77	2.64E-02	down
DNA geometric change	GO:0032392	4.36	1.96E-03	down
DNA duplex unwinding	GO:0032508	4.27	6.21E-03	down
regulation of mitotic cell cycle phase transition	GO:1901990	4.24	4.58E-02	down
negative regulation of cell cycle process	GO:0010948	4.2	3.00E-02	down
chromatin remodeling	GO:0006338	4.13	1.26E-02	down
DNA conformation change	GO:0071103	4.05	2.02E-05	down
histone lysine methylation	GO:0034968	3.98	2.55E-02	down
regulation of cell cycle phase transition	GO:1901987	3.98	2.52E-02	down
DNA biosynthetic process	GO:0071897	3.81	4.81E-02	down
histone methylation	GO:0016571	3.68	1.65E-02	down
nuclear transport	GO:0051169	3.41	8.39E-03	down
chromosome organization	GO:0051276	3.37	3.18E-16	down
regulation of mitotic cell cycle	GO:0007346	3.34	3.15E-02	down
nucleocytoplasmic transport	GO:0006913	3.3	1.66E-02	down
regulation of cell cycle process	GO:0010564	3.11	6.42E-03	down
chromatin organization	GO:0006325	3.08	8.77E-09	down
mRNA splicing, via spliceosome	GO:0000398	2.97	7.09E-03	down
RNA splicing, via transesterification reactions with bulged adenosine as nucleophile	GO:0000377	2.97	6.98E-03	down
RNA splicing, via transesterification reactions	GO:0000375	2.91	8.48E-03	down
histone modification	GO:0016570	2.82	2.45E-04	down
covalent chromatin modification	GO:0016569	2.82	2.38E-04	down
mitotic cell cycle process	GO:1903047	2.8	4.58E-03	down
mitotic cell cycle	GO:0000278	2.78	7.72E-04	down
ribonucleoprotein complex biogenesis	GO:0022613	2.76	1.16E-03	down
cell cycle process	GO:0022402	2.7	6.93E-04	down
peptidyl-lysine modification	GO:0018205	2.69	6.51E-03	down
cell cycle	GO:0007049	2.67	7.29E-07	down
cell division	GO:0051301	2.67	2.36E-03	down
DNA metabolic process	GO:0006259	2.66	2.07E-07	down
retina development in camera-type eye	GO:0060041	2.58	1.67E-02	down

Supplementary Table 3.9 (Continued).

macromolecule methylation	GO:0043414	2.5	4.94E-02	down
mRNA processing	GO:0006397	2.43	1.60E-03	down
camera-type eye development	GO:0043010	2.4	1.52E-02	down
RNA splicing	GO:0008380	2.37	2.11E-02	down
mRNA metabolic process	GO:0016071	2.34	1.07E-03	down
RNA processing	GO:0006396	2.31	1.70E-06	down
nucleic acid metabolic process	GO:0090304	2.16	8.21E-14	down
regulation of cell cycle	GO:0051726	2.14	1.26E-02	down
eye development	GO:0001654	2.08	4.55E-02	down
visual system development	GO:0150063	2.08	4.50E-02	down
microtubule-based process	GO:0007017	2.01	4.49E-02	down
cellular response to DNA damage stimulus	GO:0006974	2.01	2.08E-02	down
RNA metabolic process	GO:0016070	2	1.88E-07	down
regulation of nucleobase-containing compound metabolic process	GO:0019219	1.93	3.84E-10	down
regulation of transcription, DNA-templated	GO:0006355	1.9	9.96E-09	down
regulation of RNA metabolic process	GO:0051252	1.88	4.78E-09	down
regulation of RNA biosynthetic process	GO:2001141	1.87	1.09E-08	down
regulation of nucleic acid-templated transcription	GO:1903506	1.87	1.04E-08	down
regulation of cellular macromolecule biosynthetic process	GO:2000112	1.87	6.07E-09	down
organelle organization	GO:0006996	1.85	7.52E-08	down
nucleobase-containing compound metabolic process	GO:0006139	1.85	9.79E-10	down
regulation of macromolecule biosynthetic process	GO:0010556	1.85	6.75E-09	down
regulation of gene expression	GO:0010468	1.85	3.35E-09	down
regulation of cellular biosynthetic process	GO:0031326	1.83	7.30E-09	down
regulation of biosynthetic process	GO:0009889	1.82	9.31E-09	down
heterocycle metabolic process	GO:0046483	1.78	6.18E-09	down
cellular aromatic compound metabolic process	GO:0006725	1.77	7.15E-09	down
organic cyclic compound metabolic process	GO:1901360	1.76	6.52E-09	down
regulation of macromolecule metabolic process	GO:0060255	1.72	2.88E-09	down
cellular component organization or biogenesis	GO:0071840	1.71	6.29E-09	down
regulation of nitrogen compound metabolic process	GO:0051171	1.68	5.83E-08	down

Supplementary Table 3.9 (Continued).

regulation of metabolic process	GO:0019222	1.67	1.37E-08	down
regulation of primary metabolic process	GO:0080090	1.66	9.92E-08	down
cellular component biogenesis	GO:0044085	1.64	1.50E-02	down
cellular component organization	GO:0016043	1.64	5.49E-07	down
regulation of cellular metabolic process	GO:0031323	1.64	1.86E-07	down
cellular nitrogen compound metabolic process	GO:0034641	1.48	1.68E-04	down
animal organ development	GO:0048513	1.46	2.54E-02	down
system development	GO:0048731	1.37	4.48E-02	down
multicellular organism development	GO:0007275	1.35	2.47E-02	down
macromolecule metabolic process	GO:0043170	1.34	1.16E-05	down
anatomical structure development	GO:0048856	1.33	3.62E-02	down
cellular macromolecule metabolic process	GO:0044260	1.31	3.60E-03	down
cellular metabolic process	GO:0044237	1.19	4.93E-02	down
establishment of localization	GO:0051234	0.62	3.88E-03	down
transport	GO:0006810	0.62	4.24E-03	down
small molecule metabolic process	GO:0044281	0.42	4.72E-03	down
transmembrane transport	GO:0055085	0.39	1.50E-03	down
ion transport	GO:0006811	0.33	7.08E-04	down
organonitrogen compound biosynthetic process	GO:1901566	0.31	4.32E-06	down
oxidation-reduction process	GO:0055114	0.29	1.26E-05	down
ion transmembrane transport	GO:0034220	0.27	3.82E-03	down
amide biosynthetic process	GO:0043604	0.26	2.92E-03	down
translation	GO:0006412	0.24	2.56E-03	down
cation transmembrane transport	GO:0098655	0.24	4.73E-02	down
peptide biosynthetic process	GO:0043043	0.24	2.58E-03	down
cellular amide metabolic process	GO:0043603	0.23	2.42E-04	down
peptide metabolic process	GO:0006518	0.23	1.06E-03	down
carbohydrate metabolic process	GO:0005975	0.07	6.53E-03	down